DIRECTOR DE LA TESIS

Dr. Francisco López Almansa
Universidad Politécnica de Cataluña

TUTOR DE LA TESIS

Dr. Lluís Pujades Beneit
Universidad Politécnica de Cataluña

TRIBUNAL DE LA TESIS

Presidente

Secretario

Vocal

El éxito es un 1% inspiración y un 99% transpiración

Thomas A. Edison

Universitat Politècnica de Catalunya
Escola Tècnica Superior d'Enginyers de Camins, Canals i Ports de Barcelona
Departament d'Enginyeria del Terreny, Cartogràfica i Geofísica

Seismic vulnerability analysis of mid-height steel buildings in Bogotá

Miguel Ángel Montaña Peña

A mi padre (†), mi madre, mis hermanos y mi esposa Mónica

Acknowledgements

First, the author wants to express special thanks to his thesis supervisor, Dr. Francesc López Almansa. As well, the strong help from his tutor, Dr. Lluís G. Pujades, is gratefully acknowledged.

This author also wishes to express his gratitude to their close Colombian friends Javier Jesús Cabarique, Néstor Eduardo Mendoza, Natalia Cuevas (†) and Guillermo Cuevas.

Thanks to the people who accompanied me, offered their help in different ways on the road, and offered their hands when mine were not enough. My gratitude to all my friends, Diego Andrés Bravo, Ahmet Utku Yazgan, David Domínguez, Helbert Gonzales, Hugo Araníbar, Juan Carlos Castro, Edgar Segués, Sebastiá Miquel, Carlos Mario Piscal and Alireza Kharazian.

Last but foremost, the author wholeheartedly wishes to thank his parents, Miguel Ángel Montaña (†) & Digna Cecilia Peña, his sister Olga Cecilia Montaña and his brother Carlos Andrés Montaña for their years of help and support.

Resumen

Una serie de edificios de acero a media altura se han erigido recientemente en Bogotá; su riesgo sísmico puede ser excesivo, dada la nueva microzonificación de Bogotá y la falta de estudios previos; notablemente, los factores de reducción de respuesta se obtienen comúnmente de recomendaciones generales que no tienen en cuenta las características de cada edificio. El objetivo de este trabajo es investigar el comportamiento sísmico de estos edificios. Este estudio se lleva a cabo en dieciocho edificios-prototipo representativos de la mayor parte de los existentes. Todos estos edificios tienen simetría en planta y son uniformes a lo largo de su altura. Los dieciocho edificios-prototipo se generan mediante la combinación de los valores de los tres parámetros: luces en ambas direcciones (6 y 8 m), número de plantas (5, 10 y 15) y sistemas de resistencia a los terremotos (pórticos de nudos rígidos, pórticos arriostrados concéntricamente y pórticos arriostrados excéntricamente). Las estructuras de cada uno de estos dieciocho edificios-prototipo han sido proyectadas de acuerdo con la normativa sismorresistente de Colombia, en particular la microzonificación sísmica de Bogotá. Las propiedades estructurales de los edificios diseñados con códigos los colombianos actuales y con los previos se comparan para investigar las repercusiones prácticas de la nueva regulación. La vulnerabilidad de estos edificios ha sido evaluada por análisis "push-over" bidimensionales. El principal objetivo de estos análisis es determinar el factor de reducción de respuesta; los valores obtenidos se comparan con las recomendaciones del actual código colombiano de diseño sísmico. Así mismo, se compara el comportamiento sísmico de los tres sistemas de resistencia a los terremotos.

Summary

A number of mid-height steel buildings have been erected recently in Bogotá. Their seismic risk might be high, given the new microzonation of Bogotá and the lack of comprehensive previous studies; noticeably, the response reduction factors were commonly obtained only from general recommendations. The objective of this work is to investigate the seismic performance of these buildings. This study is carried out on eighteen representative prototype buildings. All these edifices have plan symmetry and are uniform along their height. The eighteen considered prototype buildings are generated by combining the values of three parameters: span-length (6 and 8 m), number of floors (5, 10 and 15) and earthquake-resistant systems (moment-resistant frames, concentrically-braced frames and eccentrically-braced frames –using chevron braces–). The structures of each of these eighteen prototype buildings have been designed according to the former and to the current Colombian seismic design codes; in the former code two seismic zones are considered, and in the current code, such zones are roughly subdivided in three and in five zones, respectively. The structural properties of the buildings designed with the former and the current Colombian codes are compared to investigate the practical repercussions of the new regulation. The vulnerability of these buildings has been evaluated by 2-D "push-over" analyses. The main objective of these analyses is to determine the response reduction factor; the obtained values are compared with the recommendations of the current Colombian seismic design code. As well, the seismic performance of the three considered earthquake-resistant systems are compared.

List of Figures

List of Tables

List of symbols

Latin alphabet. Lower case

a: Acceleration. Ratio between the web area and the total section area. Parameter of moment-rotation laws [FEMA 356 2000].
b, b_f: Width of a section, width of the flange of a section. Parameter of moment-rotation laws [FEMA 356 2000].
c: Damping. Parameter of moment-rotation laws [FEMA 356 2000].
d: Displacement. Height of a section
d_y: Yielding displacement
e: Length of the link segment of a beam of a EBF (Eccentric Braced Frame)
f: Flange of a section
f_y: Yielding stress
f_u: Ultimate stress
g: Acceleration of gravity
h: Depth (height) of a section
h_i: Height of the i-th story
i, j: Subindexes
k: Stiffness. Exponent of the height of a story in the distribution of the shear force among all the stories [NSR-10 2010]
m: Mass
m_i^*: Equivalent mass of the i-th mode.
n: Number of years. Ratio between the demanding axial force and the plastic resistance of a section. Number of stories
p_n: Probability of exceedance of the determined seismic action in n years
q: Ductility factor (EC-8), distributed force
d: Displacement. Height of a section
s: Separation between the stiffeners of the link segment of a beam of a EBF (Eccentric Braced Frame)
t_f, t_w: Thickness of the flange/web of a section
v_s, $v_{s,30}$: Shear-wave velocity, shear-wave velocity averaged along to top 30 m of soil
w: Web of a section
x: Absolute displacement
$\ddot{x}$: Absolute acceleration
y: Relative displacement between the structure and the ground. Strong (major) axis of a section
z: Weak (minor) axis of a section
z_g: Ground displacement
$\ddot{z}_g$: Ground acceleration

Latin alphabet. Upper case

A: Sectional area
A_{eff}: Effective area for sections of class 4
A_a/A_v: Effective peak accelerations [Decreto 523 2010]
A_m/A_n: Maximum/nominal acceleration [Decreto 196 2006]
A_v: Shear area
C_m: Equivalent modal mass participation factor of the first mode
C_t: Coefficient for the empirical expression of the fundamental period [NSR-98 1998; NSR-10 2010]
CP: Target drift "Collapse Prevention"
CSS: Circular Square Section

D: Displacement of the upper floor of the building relative to the ground. Park & Ang Damage index. Dead load
E: Energy. Modulus of elasticity. Seismic forces
E_D: Energy that contributes to damage
E_H: Hysteretic energy
E_I: Energy introduced to the structure by a given register (input energy)
E_s: Elastic strain energy. Modulus of elasticity of steel
F/F_i: Force (Equivalent force) / on the i-th story
F_a/F_v: Acceleration/velocity amplification factors for short/intermediate periods [Decreto 523 2010]
F_e, F_u, F_y: Design elastic, ultimate and yielding strength
F_{ye}: Design expected strength [FEMA 356 2000]
HSS: Hollow Square Section
H: Height of a building
I: Importance factor in the Colombian regulations
IO: Target drift "Immediate Occupancy"
L, L_r: Live load, roof live load
LS: Target drift "Life Safety"
Q: Restoring force
Q_y: Yielding value of the restoring force
M: Bending moment
M_{CE}: Expected flexural strength [FEMA 356 2000]
M_{el}, M_{pl}: Elastic, plastic bending moment
M_n/M_u: Nominal/ultimate bending moment in the American regulations
M_y: Yielding moment
N: Axial force
N_{pl}: Plastic axial force
P_n/P_u: Nominal/ultimate axial force in the American regulations
P_r/P_c: Demand and strength values of axial the compressive force in the American regulations
R: Response reduction factor
R_c: Corrected value of the response reduction factor [NSR-98 1998]
R_d: Response reduction factor for elastic vs. collapse
R_y: Factor linking the lower and the expected values of the steel strength [FEMA 356 2000]
R_0: Basic value of the response reduction factor [NSR-98 1998; NSR-10 2010]
S: Soil coefficient
S_a: Acceleration response spectrum (absolute)
S_d: Displacement response spectrum (relative)
S_{pv}: Pseudo-velocity response spectrum (relative)
S_v: Velocity response spectrum (relative)
S_y: First moment of area of the part of the section that is situated above the neutral axis
T: Natural (fundamental) vibration period of the structure. Return period of the earthquake. Torque
T_a: Approximate value of the fundamental period [NSR-98 1998; NSR-10 2010]
T_e: Equivalent period
T_i: Period of the mode i
T_x, T_y: Fundamental periods in the x and y directions
T_A, T_B: Periods used at the design spectrum of the Spanish code
T_A, T_B, T_C, T_D: Periods used at the design spectrum of eurocode 8
T_0/T_C: Left/right corner periods of the plateau of the NSR-98 design code and the former seismic microzonation of Bogotá
T_1: Natural period (fundamental) of the first mode of vibration of the structure
V: Earthquake force (base shear). Shear force
V_{CE}: Expected shear strength [FEMA 356 2000]
V_D: Energy that contributes to the damage expressed as equivalent velocity
V_E: Input energy expressed as equivalent velocity

V_n/V_u: Nominal/ultimate shear force in the American regulations
V_{pl}: Plastic shear force
V_y: Yielding value of the base shear
W: Weight of the building. Section modulus. Wind forces
W_{el}, W_{pl}: Elastic, plastic section modulus
W_u: Energy absorption capacity

Greek alphabet. Lower case

α: Coefficient, thermal expansion coefficient, exponent of the empirical expression for the fundamental period
α_u: Coefficient corresponding to collapse (Eurocode 8)
α_1: Coefficient corresponding to yielding (Eurocode 8)
β: Empirical coefficient at the Park & Ang index
χ: Strength reduction coefficient because of buckling (Eurocode 3)
δ: Displacement
ε: Strain
ε_y, ε_u: Yielding/ultimate strain
ϕ: Sectional strength reduction factor in the American regulations
ϕ_a, ϕ_p, ϕ_r: In the expression for the response reduction factor, factors accounting for the lack of elevation uniformity, the plan asymmetry and the structural redundancy [NSR-98 1998; NSR-10 2010]
γ: Unit weight. Shear strain
η: Cumulated ductility. Correction coefficient of the spectra according to the damping (eurocode).
λ_i: Weighting coefficient of the Park & Ang damage indices
μ: Ductility. Displacement ductility
ν: Correction coefficient of the spectra according to the damping (Spanish code)
θ: Rotation angle
ρ: Importance factor of the building. Reduction factor in the interaction between axial force, shear force and bending moment
σ: Normal stress
σ_I, σ_{II}, σ_{III}: Normal stresses
τ: Time (auxiliary variable). Shear stress
ω: Frequency (rad/s)
ω_d: Natural frequency of the system with damping
ω_0: Natural frequency of the system without damping
ψ: Shape factor
ζ: Damping factor

Greek alphabet. Upper case

Δ: Displacement
Δ_C/Δ_T: Axial deformation at the expected buckling load/yielding tensile load [FEMA 356 2000]
Ω: Over-strength factor

1 INTRODUCTION

1.1 Background and motivation

A number of mid-height steel buildings have been erected in the last years in Colombia, principally in Bogotá. The seismic risk of these buildings might be high, given that a new microzonation of Bogotá has been recently released and that no comprehensive theoretical studies about their vulnerability have been carried out; in particular, the values of the response reduction factor are commonly obtained only from general recommendations that do not account for the individual characteristics of each building. Moreover, given that Bogotá belongs to the intermediate seismicity region of Colombia, the seismic design codes do not enforce any prescription aming to fulfill the "strong column-wak beam" condition. The concern of this researcher for this subject arises from his former consultancy activities in Colombia; looking for improving his knowledge about earthquake-resistant design of building and other constructions, inscribed in October 2006 in the Master Program "Earthquake Engineering and Structural Dynamics", taught at the Technical University of Catalonia at Barcelona. In February 2010, this researcher concluded his Master studies; his Master Thesis ("Análisis push-over de edificios con pórticos de acero en Bogotá") was carried out under the supervision of Prof. F. López Almansa. In March 2010 this student started his PhD Thesis, also under the supervision of Prof. López Almansa.

The objective of this work is to investigate the seismic performance of these buildings in order to provide more accurate estimates of the response reduction factor and to be able to formulate design criteria; these recommendations might be incorporated to the Colombian seismic design code. As well, retrofit strategies will be proposed in further studies.

This study is carried out on a number of representative prototype buildings with 5, 10 and 15 stories and 4 bays in each direction. Three earthquake-resistant systems have been considered: moment-resistant frames, concentrically braced frames and eccentrically braced frames; in these last two cases, chevron braces are contemplated. The structure of each prototype building is designed for ten seismic zones in Bogotá; two of them correspond to the former microzonation and the remaining eight belong to the current microzonation. The seismic vulnerability of these buildings has been evaluated, in the framework of the Performance-Based Design, by static nonlinear analyses (push-over). The Target Drifts (Performance Points) are determined, for each performance objective IO, LS and CP. The results of the push-over analyses provide estimates of the response reduction factor.

1.2 Objectives

1.2.1 Main objective

The main goal of this study is **TO INVESTIGATE NUMERICALLY THE SEISMIC PERFORMANCE OF MID-HEIGHT STEEL BUILDINGS IN BOGOTÁ**. As well, it is expected that the obtained conclusions can be broadly generalized to other regions of Colombia and other close countries with similar seismicity.

1.2.2 Specific objectives

To reach the aforementioned main goal, these specific targets are pursued:

- To select a number of representative prototype buildings.
- To develop numerical models of the structural behavior of the prototype buildings.
- To carry out push-over analyses using the above numerical models.
- To obtain the Target Drifts corresponding to each of the considered performance objectives.
- To decide the acceptability of each Target Drift.
- To determine the actual value of the response reduction factor for each prototype building.
- To issue overall conclusions about the seismic performance of the prototype buildings.
- To identify further research needs.

1.3 Methodology

This section describes in more detail the investigation carried out to achieve each of the above specific objectives.

Selection of prototype buildings. Eighteen prototype buildings are selected to represent the vast majority of the mid-rise steel edifices in Bogotá. All these buildings have plan symmetry and are uniform along their height. The main carrying-load system is composed of steel columns and of steel decks topped with a concrete layer. The prototype buildings are distinguished by the span-length (in both directions), by the number of floors and by the type of earthquake-resistant system (alike in both directions). Two span-lengths and three numbers of floors are considered: 6 – 8 m and 5 –10 – 15, respectively. Three earthquake-resistant systems have been considered: moment-resistant frames (MRF), concentrically braced frames (CBF) and eccentrically braced frames (EBF). All the buildings have four bays in each direction.

Numerical models of the structural behavior of the prototype buildings. The structural behavior of the selected buildings is described with 2-D finite element models with frame elements. The cooperation of the non-seismic frames is neglected; as well, given the absence of shear studs in the seismic frames, the cooperation of the top concrete layer is neglected. The hysteretic behavior of the plastic hinges is described by multi-linear moment-curvature laws derived from the structural parameters of the steel and the geometrical parameters of the members and of the connections.

Push-over analyses. The 2-D nonlinear static (push-over) analyses of the buildings are carried out from the structural models that correspond to the previous objective. In the push-over analyses, two vertical distributions of the pushing horizontal forces are considered: uniform pattern and modal pattern (e.g. shaped as the first mode of vibration). Second-order analyses are performed; however, in most of the cases the differences with the first-order analyses are small. Given the rather lateral flexibility of these buildings, the soil-structure interaction is not accounted for. The progression of damage is investigated by analyzing the progression of plastic hinges in the structures; the collapse mechanism is studied as well.

Target Drifts. To determine the Target Drifts, the demanding spectra are obtained from the former and current Colombian design codes and from the previous and the recently issued microzonation for Bogotá. For LS (Life Safety) such spectra are intended to correspond to 475 years return period, and for IO (Immediate Occupancy) and CP (Collapse Prevention) they correspond to 225 and 2475 years, respectively. The target drifts are determined by intersecting the capacity curves and the demand spectra.

Acceptability of each Target Drift. For each capacity curve, the damage intervals suggested by the research project RISK-UE are adopted. For a proper seismic behavior, Target Drifts for IO,

LS and CP should correspond to SD (Slight Damage), MD (Moderate Damage), and ED (Extended Damage), respectively.

Response reduction factor. Following the classic equal-displacement approach, the ductility is determined as the ratio between the collapse and the yielding displacements. The obtained values are compared to those considered in the design.

Conclusions. Both overall and particular conclusions are issued.

Further research. Taking profit of the results of this research, new research fields are identified and discussed.

1.4 Organization of this document

This document is organized in six chapters and an appendix, where the first chapter is this introduction. The second chapter is the state of the art, which contains a review of the seismic design methodologies and of the seismic design and performance of steel constructions. The third chapter describes the seismicity of Colombia and of Bogotá, emphasizing its seismic microzonation. The fourth chapter presents the selected prototype buildings and their numerical modeling; chapter 5 describes the push-over analyses and discusses their main results. Chapter 6 presents the overall conclusions of the research and the future investigations. A list of the consulted bibliography is included after chapter 6. Appendix A lists the publications generated during this research.

2 STATE OF THE ART

2.1 Earthquake-Resistant Design Methods

This section presents a brief introduction and a concise historical review of earthquake-resistant design strategies of structures. Although this study has a general context, it is especially applicable for the buildings subjected to horizontal seismic inputs. Formulations for other situations (e.g. vertical inputs or structures other than buildings) are basically similar.

The first seismic analysis methods appear on the year 1923 in Japan (after the earthquake in Kanto [Ohashi 1993]) and can be included within the package of so-called *Earthquake Analysis Methods Based on Resistance.* These procedures were intended to provide buildings with lateral (horizontal) resistance; it was believed that if the structure of the building had enough lateral resistance it should be capable to survive the design earthquake. This resistance is guaranteed by designing the structure to be able to withstand horizontal forces applied at each floor level and in each direction of the building (usually two orthogonal directions). Figure 2-1 illustrates this concept.

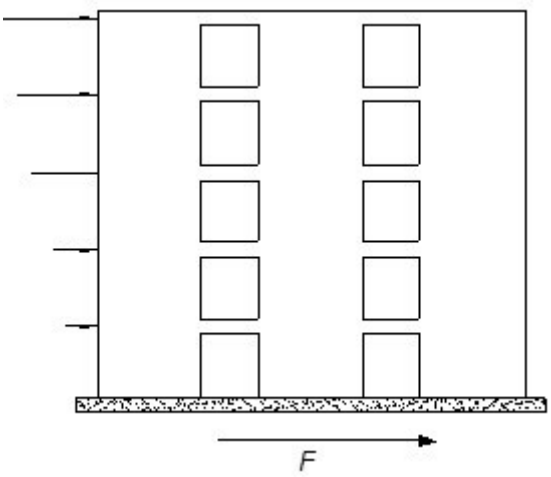

Figure 2-1. Lateral forces that are equivalent to a seismic input

In Figure 2-1, F is the sum of the forces acting at each floor level; in other words, the horizontal interaction force between the ground and the building. F is also known as base shear. Obviously, the value of F quantifies the severity of the earthquake effect on the building.

In the firstly developed earthquake-resistant design methods, horizontal forces represented in Figure 2-1 were obtained by multiplying the weight of each floor by a constant coefficient. This ratio between the horizontal and vertical forces was called seismic coefficient and in the first 1923 Japanese Seismic Code [Ohashi 1993] it was estimated as 0.1. This value gradually increased as it was experienced that structures designed with this resistance value failed when an earthquake stronger than expected occurred. This ratio took to the values of 0.10, 0.15 and 0.20 until, thanks

to the development of computers and by having more and more seismic experiences, it was concluded that structures that had been designed with a certain lateral resistance, did not reach collapse but could suffer damage in the case of a larger earthquake. After that, resistance was not the primary goal and everybody started paying more attention to the ductility; it can be roughly defined as the ability of a given structure to resist after the onset of damage. The ductility of a given building can be estimated from observed damages or by numerical simulation. The regulations began to introduce the concept of ductility by quantifying it with a *response reduction factor*, which reduces the equivalent lateral forces (Figure 2-1); it was mentioned in the 1957 American design code [Housner 1990]. Thus, this approach has been incorporated to the current worldwide regulations. In summary, most of the earthquake-resistant regulations require to provide buildings with a certain level of lateral resistance. This resistance is obtained by dividing the resistance that a given building should have to remain in the elastic range under the design input by the aforementioned response reduction factor. This factor should obviously be equal to or greater than the unity. This coefficient is represented by different symbols in each standard; in the case of Spain [NCSE-02 2002] it is termed μ, in the European standard [EN-1998 2004] it is named q, in the United States [IBC 2000] it is known as R. It is remarkable that, in fact, this ratio does not take into account only the ductile behavior of the structure but also includes the over-resistance of the building due to the conservative considerations that are regularly considered (safety factors, among others) and the increase of the material resistance under dynamic inputs ("strain rate effect").

In any case, it should be kept in mind that in these methods the effect of the earthquake on the structure is characterized by means of equivalent static forces (Figure 2-1); they are determined as those that generate a lateral displacement equal to the maximum one that would occur along the duration of the earthquake. However, another possible strategy is to represent the seismic action by a much more direct way: as input accelerograms. In this case, dynamic analysis must be performed to determine the time-history responses; then, the maximum values will be selected, they would represent the design demands. This formulation is often referred to as *earthquake-resistant design based on dynamic calculations*. This strategy seems appropriate and has apparently shown to be quite capable of simulating the actual seismic behavior of structures with great accuracy and reliability; however, there are some drawbacks that hinder the use of such formulations: (1) the information about the earthquakes that may occur for a particular structure during its lifetime is limited, which severely impairs the accuracy of the study, (2) for economic reasons, structures are designed to behave nonlinearly during the design earthquake (the most severe earthquake expected with a reasonable probability) and, hence, nonlinear dynamic analyses are a must. Dynamic analyses in the nonlinear regime are much more complex than the, already complex, dynamic linear calculations. Currently the most common way of characterizing the dynamic effect of earthquakes is by equivalent static forces (or other non-dynamic quantities, e.g. not forming part of a dynamic calculation) obtained from elastic response spectra. Next section explains how to determine these values using response spectra.

2.1.1 Earthquake-resistant design based on spectra

In general terms, these methods are based on estimating the equivalent static forces (which characterize the effect of the seismic action) in terms of the fundamental period of the structure. This is done by using response spectra; they are plots whose ordinates are certain response magnitudes and whose abscissas are the natural periods of SDOF systems that represent the structure. Up to date, three types of spectra have been basically proposed: absolute acceleration, relative displacement, and energy spectra. In the absolute acceleration spectra, the ordinates are the ratio between the maximum absolute acceleration in the top of the building and the maximum input acceleration in the base of the building. In the relative displacement spectra, the ordinates are the ratio between the maximum relative displacement between the top and the base of the building and the maximum input relative displacement. In the energy spectra, the ordinates are the input energy introduced by the seismic input in the building. These three types of spectra are described next in this subsection; applications to earthquake-resistant design are described in the

three following subsections, respectively. It is noteworthy that each of these three spectra considers a meaningful response magnitude: the relative displacement is an indicator of the apparent structural damage level (i.e. not cumulative), the absolute acceleration is related the human perception of the motion and the damage to the facilities (and, more generally, to all the non-structural elements) and the energy reports on the accumulated structural damage.

The energy spectra are usually expressed in terms of equivalent velocity, which is the square root of the ratio between the double of the input energy and the mass.

Linear spectra plot the ratio between the maximum values of the response of an elastic single-degree-of-freedom system and of the input acceleration. Figure 2-2 shows an elastic model of a single-degree-of freedom system undergoing a horizontal ground motion z_g.

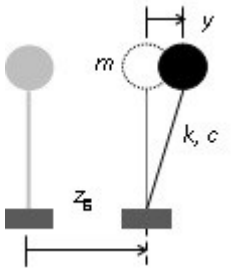

Figure 2-2. Elastic single-degree-of-freedom systems

In Figure 2-2, m, c and k are the mass, damping and stiffness coefficients, respectively, y is the relative displacement between the mass and the base (degree-of-freedom) and z_g is the displacement of the ground. Yet this formulation is commonly applied to horizontal motion, can be also considered for vertical vibrations.

The equation of motion of the system described in Figure 2-2 is given by

$$m\ddot{y} + c\dot{y} + ky = -m\ddot{z}_g \tag{2-1}$$

By dividing both sides by m, relation (2-1) becomes

$$\ddot{y} + 2\zeta\omega_0\dot{y} + \omega_0^2 y = -\ddot{z}_g \tag{2-2}$$

In this relationship, ω_0 is the undamped natural frequency of the system and ζ is the critical damping factor. These coefficients are given by

$$\omega_0 = \sqrt{\frac{k}{m}} \qquad \zeta = \frac{c}{2m\omega_0} \tag{2-3}$$

The damped natural frequency ω_d is related to ω_0 and to ζ by

$$\omega_d = \omega_0\sqrt{1-\zeta^2} \tag{2-4}$$

It is remarkable that, unless the damping ζ takes extremely high values, ω_0 and ω_d are nearly coincident.

The acceleration, velocity and displacement spectra are obtained, for each input $z_g(t)$, as the maximum values of the absolute acceleration $\ddot{x}$ (where $\ddot{x} = \ddot{y} + \ddot{z}_g$), relative velocity $\dot{y}$ and relative displacement y. They depend on the natural period T ($T = 2\,\pi/\,\omega_0$) and on the damping factor ζ. These quantities are obtained by the following linear relationships [Clough, Penzien 1993; García Reyes 1998; Chopra 2001]:

$$y(t) = -\frac{1}{m\omega_d}\int_0^t m\,\ddot{z}_g(\tau)\sin\omega_d(t-\tau)e^{-\zeta\omega_0(t-\tau)}d\tau \tag{2-5}$$

$$\dot{y}(t) = \int_0^t \ddot{z}_g(\tau)\cos\omega_d(t-\tau)e^{-\zeta\omega_0(t-\tau)}d\tau - \frac{\zeta\omega_0}{\omega_d}\int_0^t \ddot{z}_g(\tau)\sin\omega_d(t-\tau)e^{-\zeta\omega_0(t-\tau)}d\tau \tag{2-6}$$

$$\ddot{x}(t) = \left(\frac{2\zeta^2\omega_0^2}{\omega_d} - \frac{\omega_0^2}{\omega_d}\right)\int_0^t \ddot{z}_g\cos\omega_d(t-\tau)e^{-\zeta\omega_0(t-\tau)}d\tau - -2\zeta\omega_0\int_0^t \ddot{z}_g(\tau)\cos\omega_d(t-\tau)e^{-\zeta\omega_0(t-\tau)}d\tau \tag{2-7}$$

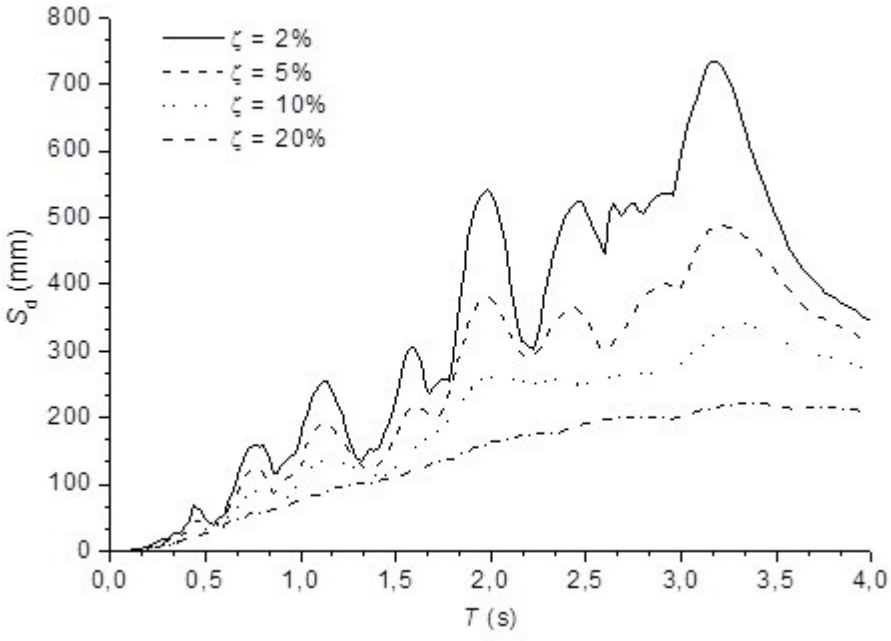

Figure 2-3. Relative displacement spectra

Figure 2-3, Figure 2-4 and Figure 2-5 show, relative displacement, relative velocity and absolute acceleration spectra, respectively. Such spectra correspond to the accelerogram registered in the ICA2 station (E-W component) during the Pisco earthquake, 15 august 2007.

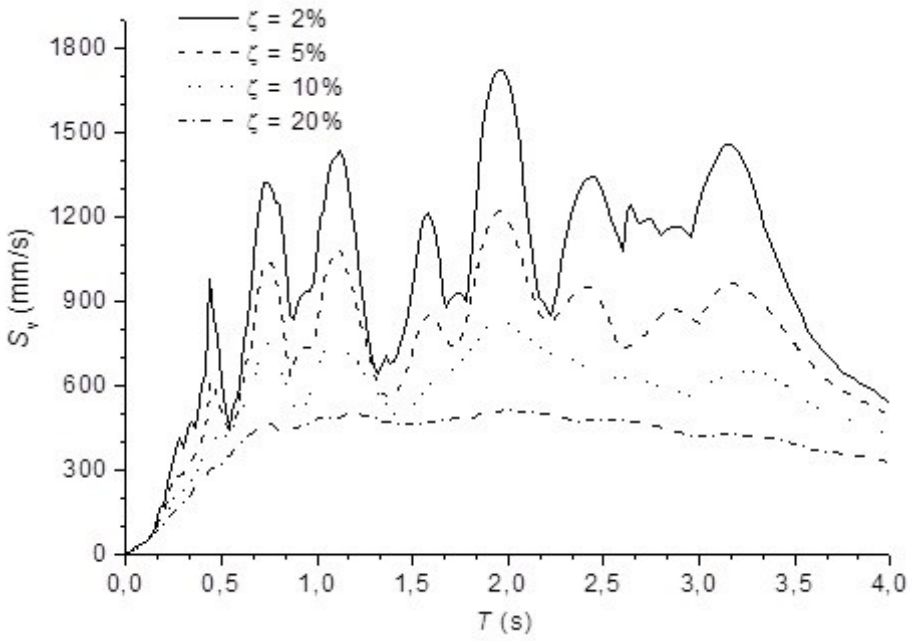

Figure 2-4. Relative velocity spectra

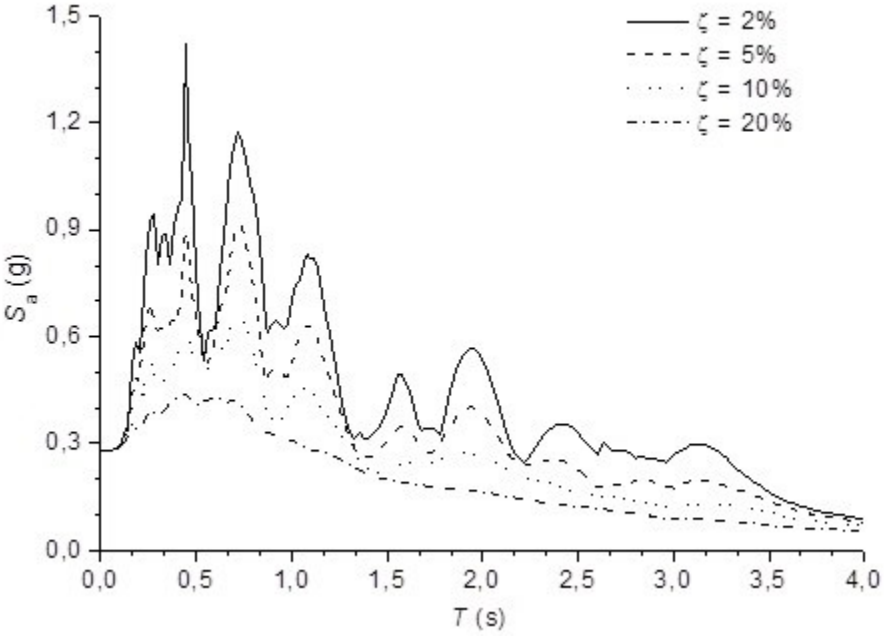

Figure 2-5. Absolute acceleration spectra

Figure 2-3, Figure 2-4 and Figure 2-5 show that the spectral ordinates decrease with the increasing damping ratio; this shows that damping has a beneficial effect, since it contributes to reduce relevant response magnitudes (relative displacement, relative velocity and absolute acceleration). Moreover, the spectrum corresponding to zero damping exhibits sharper peaks than the spectra for non-zero damping; it means damping contributes to smoothen the spectra, e.g. making it less sensitive to small period changes.

It has been demonstrated [Chopra 2001] that for small values of damping and not too long periods (under 10 seconds), the velocity spectra are obtained by multiplying the acceleration spectra by $T / 2\pi$ and that the displacement spectra are obtained in the same way from the velocity ones:

$$S_v = S_a \ (T / 2\,\pi) \quad S_d = S_v \ (T / 2\,\pi) = S_a \,(T / 2\,\pi) \tag{2-8}$$

These relationships among the three types of spectra allows an easy shifting among them. At this point it should be clarified that, in fact, in order to satisfy these relationships it is necessary to modify slightly the spectra of velocity and acceleration; hence, they should be termed in a more correct way pseudo-velocity and pseudo-acceleration spectra [Clough, Penzien 1993; García Reyes 1998; Chopra 2001]. In this thesis, we will usually replace these names by velocity and acceleration spectra.

Figure 2-3, Figure 2-4 and Figure 2-5 correspond to the spectrum of a single input, and consequently are not applicable for the earthquake-resistant design of a particular structure as it would not be reasonable to design it only to support that single input. In fact, different accelerograms should be considered and then the spectrum envelope should be taken. The earthquake-resistant design standards propose different spectra whose shape is similar to those of Figure 2-3, Figure 2-4 and Figure 2-5, although they are significantly smoother. As an example, the spectrum of the Spanish code [NCSE-02 2002] is shown in Figure 2-6.

2.1.2 Absolute acceleration response spectra

As discussed in the previous subsection, the absolute acceleration response spectra are curves that represent, in ordinates, the ratio between the maximum values of the absolute acceleration of the SDOF system that represents the dynamic behavior of the structure in a given vibration mode and the ground acceleration. The design spectra are smoothed envelopes obtained from a number of individual records.

Figure 2-6 shows, the design spectrum of the Spanish regulation [NCSE-02 2002].

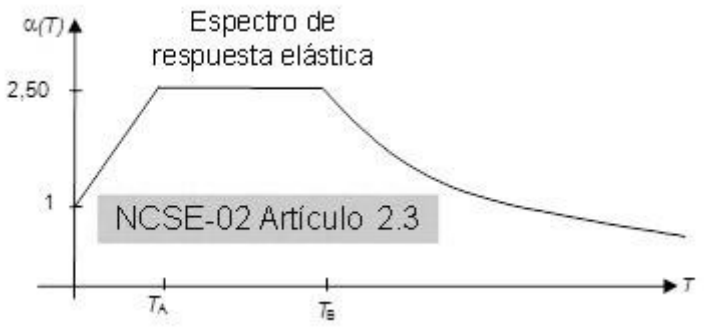

Figure 2-6. Design acceleration spectrum [NCSE-02 2002]

The spectrum shown in Figure 2-6 consists of three branches: a linearly increasing one (e.g. with exponent 1), a constant one (e.g. with exponent 0) and a hyperbolically decreasing one (e.g. with exponent −1). Periods T_A and T_B depend on the characteristics of the soil, being higher as it has less stiffness; in some codes, the spectral ordinate (e.g. the height of spectrum) also grows as the flexibility of the soil does. The interpretation of each of these branches in terms of the effect of the earthquake on the structure is quite clear: (1) short-period structures are very rigid (usually they are low-rise) and tend to behave as the surrounding soil, but its motion is amplified as its rigidity decreases, (2) in the medium period range, the ground motion reaches its highest amplification inside the building and, (3) in the long periods range, structures are flexible enough so that its stiffness is not capable of overcoming the high inertia forces. This interpretation helps us to understand the influence of the soil stiffness in T_A and T_B: for stiff soil the range of building periods whose motion is highly amplified (in between T_A and T_B) is narrow, while this range widens and encompasses higher rise buildings as the soil becomes less stiff.

This spectrum is commonly presented in dimensionless form (the ordinates S_a are dimensionless); in this way the base shear is determined as the product of the weight of the building (W), the soil coefficient (S), the importance factor (ρ) and the peak ground acceleration (a_{max}), divided by the ductility factor R:

$$F = S_a(T_1)\ W\ S\ \rho\ a_{max} / R \tag{2-9}$$

In this relation W is the weight of the building; obviously it depends on the percentage of live load that is simultaneous with the design earthquake, each code specifies this percentage in terms of the use of the building. S is the soil coefficient; for hard soil (rock and stiff soil) its value is usually 1 and it takes higher values for softer soils (S rarely reaches values greater than 1.50, except on very soft soils). The importance factor ρ is a coefficient that quantifies the severity of the consequences of the collapse of the building; in buildings of normal importance (such as residential constructions) is $\rho = 1$ and for more important buildings is $\rho > 1$. a_{max} is the design peak ground acceleration expressed in "g". The values of a_{max} are specified by the seismic design codes; usually each country is divided into distinct zones, each of them with its own value of a_{max}. In the Spanish seismic regulations, the values of a_{max} range from 0.04 g (minimum considered value) and 0.25 g (for some municipalities in the province of Granada). The Spanish regulations quantify a_{max} as the expected seismic acceleration on stiff soil (not rock) for an earthquake with 500 years return period. It is remarkable that this criterion does not coincide with those considered in most countries; normally it is considered as the expected seismic acceleration in rock for a return period of 475 years. Finally, the response reduction factor R (*ductility* behavior factor) represents the ability of the structure to undergo plastic deformation until failure; in other words, it represents the safety margin of the structure after the onset of plastification. The current design standards estimate the values of R in a rather empirical way; these values basically depend on the type of structure and of the structural detailing, especially the connections among members. In the Spanish code [NCSE-02 2002], this coefficient is denoted by μ and four situations are considered: $\mu = 1$ (no ductility), $\mu = 2$ (low ductility), $\mu = 3$ (high ductility) and $\mu = 4$ (very high ductility); other codes often consider higher values for this coefficient. Figure 2-6 shows that $S_a(0) = 1$; replacing this result in equation (2-9) we conclude that for structures of high horizontal stiffness when $S = \rho = 1$, the equivalent static force is equal to $a_{max}\ W / R$. Consequently, since the acceleration in the base and the top of this type of structures should be virtually alike regardless of ductility, it follows that R should tend to 1 when T approaches zero.

In multi-story buildings, F represents the sum of the forces acting on each floor; in other words, it is the horizontal interaction force between the ground and the building (Figure 2-1). This force has to be distributed among the floors proportion to their masses and modal amplitudes (for the considered vibration mode of the building). The forces acting at the each level represent the equivalent seismic effect; hence, they can be used to obtain the lateral resistance to be provided to the building.

In single-degree-of-freedom systems (typically, used to describe single-story buildings), the interpretation of the abscissa of the spectrum is very clear, as it represents the natural period of the system. In actual structures (typically multi-story buildings), multi-degree-of-freedom models should be considered. In this case, the application of this method is carried out usually in modal coordinates; in each *i-th* mode, its natural period T_i is considered. The structure should be decomposed in different vibration modes, the maximum response for each mode is calculated and then such responses are combined by using empirical rules (SRSS "Square Root of the Sum of the Squares", CQC "Complete Quadratic Combination" [NCSE-02 2002], among others). Typically, the combinations are set in terms of the shear forces at each floor, in other words, the sum of shear forces on the columns and walls of each floor. For each mode, the situation is similar to that described in Figure 2-1; the main difference is that the interaction force F has to be distributed among the different floors in proportion to their masses and modal amplitudes corresponding to the considered mode. The regulations usually specify the number r of modes to

be included in the calculation, two types of criteria are generally provided: empirical ones and criteria that are more complex and are based on the distribution of equivalent modal masses [Clough, Penzien 1993; García Reyes 1998; Chopra 2001]. The empirical criteria often link the value of *r* with the fundamental period of the building and its plan symmetry; *r* generally ranges from 1 (for symmetrical buildings of small to medium height) and 4 (for high-rise buildings asymmetric). The criteria based on the equivalent mass of each mode often recommends a value of *r* such that the sum of the equivalent masses of the modes included in the combinations reach at least 90% of the total mass of the building, in some cases [EN-1998 2004] also reports that should include all modes whose equivalent modal mass exceed 5% of the total mass of the building.

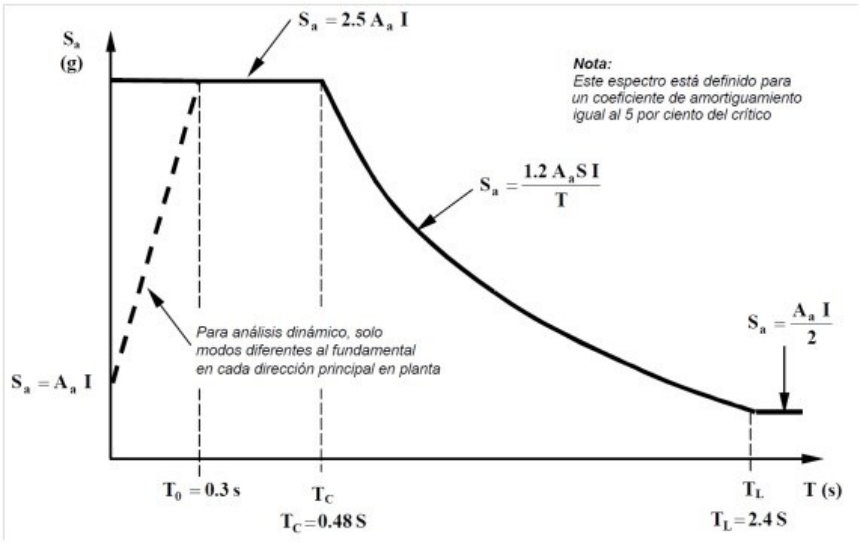

Figure 2-7. Design acceleration response spectrum [NSR-98 1998]

It should be emphasized that equation (2-9) represents, with minor modifications, the approach suggested by almost all the current earthquake-resistant regulations.

Figure 2-7 shows another example of design acceleration spectrum, obtained from the Colombian standard [NSR-98 1998]. Figure 2-7 shows, similarly to Figure 2-6, a typical absolute acceleration spectrum, which is divided into four segments: (1) short periods ($T < T_0$), the spectrum presents a linearly increasing branch, (2) medium periods ($T_0 < T < T_C$), the spectrum shows a horizontal branch (commonly known as plateau), (3) long periods ($T_C < T < T_L$), the spectrum usually decreases hyperbolically (with exponent -1) and (4) very long periods ($T_L < T$), the spectrum is again horizontal but with lower height than the medium periods plateau. Similarly to what happens in Figure 2-6 with periods T_A and T_B, the values of the periods T_0, T_C and T_L depend on the characteristics of the soil, being higher as the soil is more flexible. In the very long periods, the reduction of the spectral ordinate is interrupted not to minimize in excess the effect on tall buildings.

It is remarkable that in some cases [EN-1998 2004] in the very long periods, instead of levelling the height of the spectrum, there is a sharper decrease of spectral ordinate. This fact is shown in Figure 2-8. In the two decreasing branches in Figure 2-8 (between T_C and T_D periods and beyond period T_D) the exponents usually take values close to – 1 and – 2, respectively (hence, the branch between T_C and T_D periods is hyperbolic).

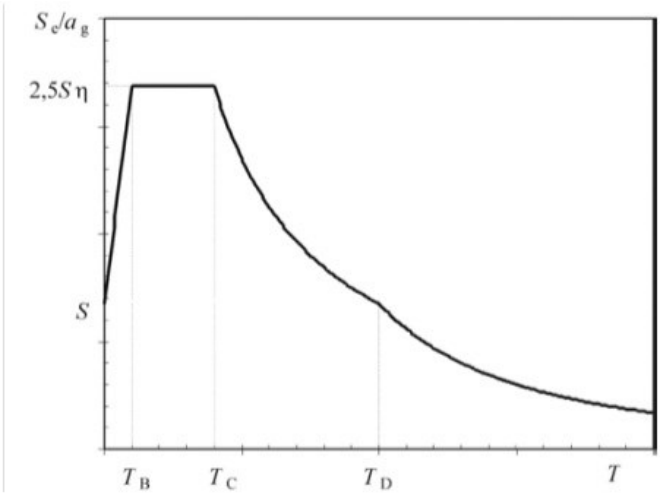

Figure 2-8. Design acceleration response spectrum [EN-1998 2004]

The spectral ordinates grow as the damping of the structure decreases; this is consistent with Figure 2-3, Figure 2-4 and Figure 2-5 with the interpretation that damping reduces the response of the structure. The spectra proposed by the codes correspond generally to damping 5% since most of buildings correspond to this level of damping. The regulations generally incorporate correction coefficients for other levels of damping; for example, the Spanish standard includes a coefficient given by $\nu = (5 / \Omega)^{0.4}$ where Ω is the damping factor expressed in percentage and the European standard [EN-1998 2004] includes a similar expression given by $\eta = [10 / (5 + \zeta)]^{0.5}$ where ζ is the damping factor expressed in percentage. For example, for a damping factor 4%, the Spanish legislation proposes a coefficient $\nu = (5 / 4)^{0.4} = 1.09$ and European standard proposes a coefficient $\eta = [10 / (5 + 4)]^{0.5} = 1.054$; for a damping factor of 6%, $\nu = (5 / 6)^{0.4} = 0.93$ y $\eta = [10 / (5 + 6)]^{0.5} = 0.953$. It is remarkable that, since the damping exerts a beneficial effect of reducing the structural response, the adoption of damping factors greater than 0.05 needs adequate justification.

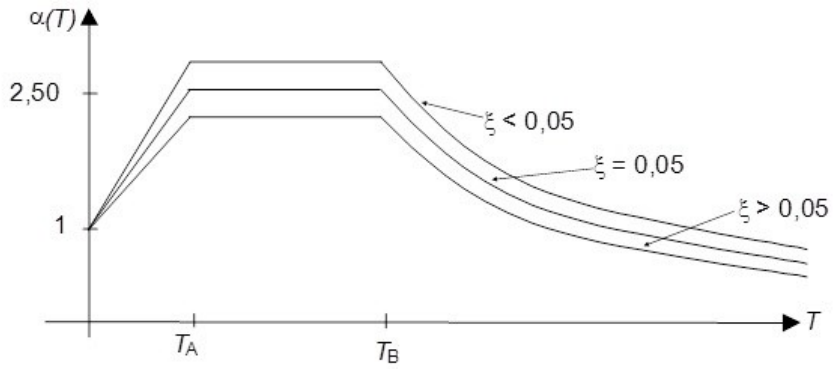

Figure 2-9. Design acceleration response spectra for different values of damping

The damping correction of the design spectra is usually done by multiplying it by the corresponding coefficient (ν or η in the above examples) but keeping the initial value $S_a = 1$ for $T = 0$ (what is consistent with Figure 2-5). Figure 2-9 shows the spectrum of Figure 2-6 with the adjusted values of damping above and below 5%.

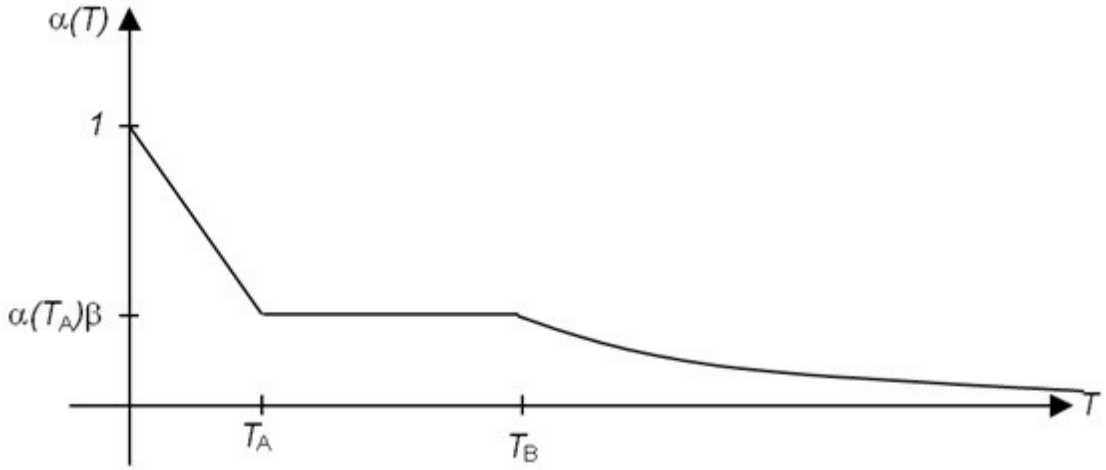

Figure 2-10. Nonlinear Design Acceleration Spectrum

The codes consider the ductility by reducing the force F, it is divided by the ductility coefficient (response reduction factor). In some cases, this operation is carried out of the spectrum, as shown in equation (2-9), but often it is incorporated into the spectrum by dividing their ordinates by that coefficient. In that way, there are two types of spectra, those in which the ordinates are not divided by any factor and those in which they have been divided by it. The first spectra are termed linear (or elastic) spectra and the second spectra are termed nonlinear. Obviously, the spectra shown in Figure 2-3 to Figure 2-9 are linear; Figure 2-10 shows a nonlinear spectrum obtained essentially dividing the spectrum of Eurocode 8 in Figure 2-8 by the ductility coefficient (q).

Remarkably, since the normalized spectral ordinate of the plateau is usually equal to 2.5, if the ductility factor is higher than that value, the initial branch is decreasing instead of increasing; this fact is reflected in the spectrum of Figure 2-10.

It should be noted that the absolute response acceleration spectra characterize the dynamic effect of a group of earthquakes in terms of forces (as represented in Figure 2-6 to Figure 2-10). This involves several drawbacks, first of all (and possibly one of the most important) the quantification of the severity of an earthquake in terms of the force F is only meaningful when the structure is maintained in elastic regime, since the more severe the earthquake, the greater the response acceleration and the internal forces; therefore, this is directly related to the resistance that must be provided to the structure. However, when the structure yields, the lateral force F is maintained essentially constant, hence, the internal forces are kept constant; therefore, the force ceases to be a valid parameter to characterize the dynamic effect of the earthquake. For example, even if the peak ground acceleration and/or the duration of a given input accelerogram is several times larger and/or longer than another one, if both earthquakes are severe enough to induce an inelastic response of the structure, both will produce approximately the same lateral force on the structure, while the response in terms of maximum displacements and damage can be completely different. The more severe the earthquake, the higher the structural damage and the maximum displacements; therefore, the damage cannot be characterized in terms of forces. In other words, there is a more direct correlation between damage and displacement comparing to the existing correlation between damage and force. The following subsection describes the relative displacement spectra discussing how avoiding this drawback.

2.1.3 Relative displacement response spectra

The dynamic effect of the seismic action is characterized through relative displacement spectra. As discussed previously, they consist of representations of maximum relative displacement of a SDOF system that represents the response of the structure in a given vibration mode (in ordinates)

as a function of its period (in abscissas). Equation (2-8) indicates that these diagrams can be obtained from the absolute acceleration spectra by multiplying them by $(T / 2\ \pi)^2$. Figure 2-11 shows an example of design displacement spectra obtained from the reference [Priestley, Calvi, Kowalski 2007] and corresponding to the acceleration spectrum of the European code [EN-1998 2004]. The horizontal axis contains the natural period of the mode under consideration and the vertical axis contains the relative displacement between the mass of the equivalent SDOF system and its base. These spectra correspond to the envelope of the maximum values of equation (2-5) for the expected accelerograms. In other words, they are the envelopes of individual spectra as those represented in Figure 2-3. The comparison with Figure 2-8 confirms that these spectra can be obtained by multiplying the acceleration spectra by $(T / 2\ \pi)^2$. Equation (2-5) shows that the displacement spectra are dependent on damping, as the acceleration spectra (as described in the preceding paragraph).

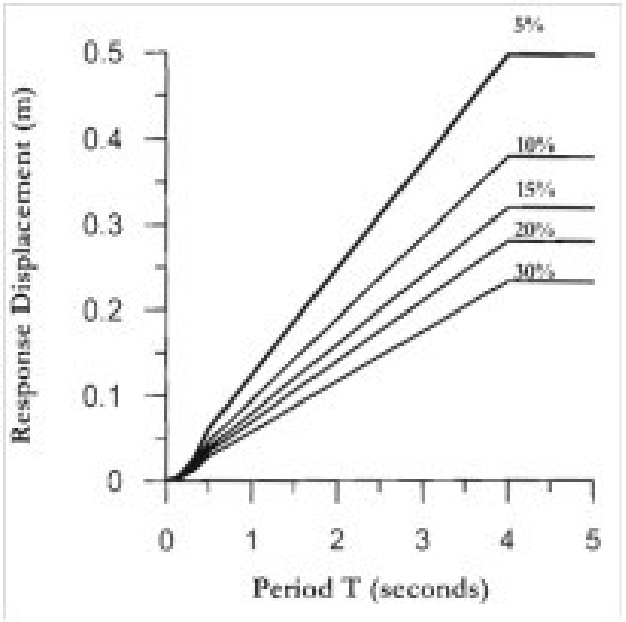

Figure 2-11. Design displacement spectra [Priestley, Calvi, Kowalski 2007]

This strategy (based on displacements) constitutes an advance compared to the methods based on forces since beyond the linear range, it is more reasonable to quantify the input as an imposed motion than as an equivalent force. To characterize the effect of the seismic action through forces is appropriate as long as the structure remains elastic, but is no longer valid as the structure yields.

While the behavior of the structure is linear (in other words, there is no any damage) the force is a fairly reliable index of the damage. However, once the structure yields, it rapidly loses its rigidity and the displacement increase significantly faster than the forces (assuming a positive post-yield stiffness), so that a small variation of forces can generate a significant change in displacement and therefore in structural damage. Since there is a strong correlation between the displacement and the damage, "Displacement Based Design" is usually identified with "Performance Based Design" (described in subsection 2.1.5) [Priestley, Calvi, Kowalski 2007].

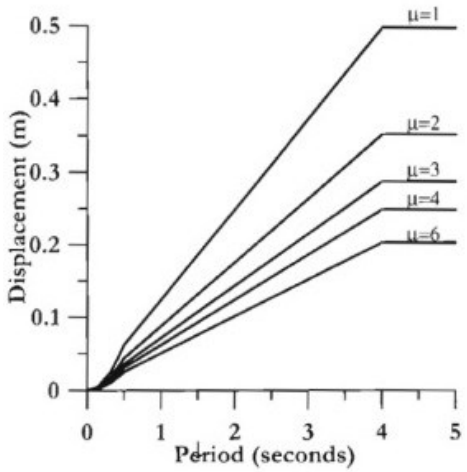

Figure 2-12. Design displacement spectra for different levels of ductility [Priestley, Calvi, Kowalski 2007]

The nonlinear behavior of structures can be represented in terms of an equivalent viscous damping coefficient. Alternatively, similarly to the seismic design methods based on forces, a ductility coefficient can be considered. Figure 2-12 represents displacement spectra for different values of the displacement ductility factor μ (ratio between the maximum displacement d_{max} and the yielding displacement d_y: $\mu = d_{max} / d_y$). It is remarkable that the influence of μ is not linear; the reference [Priestley, Calvi, Kowalski 2007] provides procedures to quantify it.

2.1.4 Input energy response spectra

This formulation consists basically of characterizing the dynamic effect of the seismic action by energy spectra; they are representations of the energy introduced into the structure by the earthquake (E_I) (in ordinates) in function of the period of an SDOF system that represents the structure in a given vibration mode (in abscissas). Typically, the energy is expressed in terms of equivalent velocity (V_E) by the relation

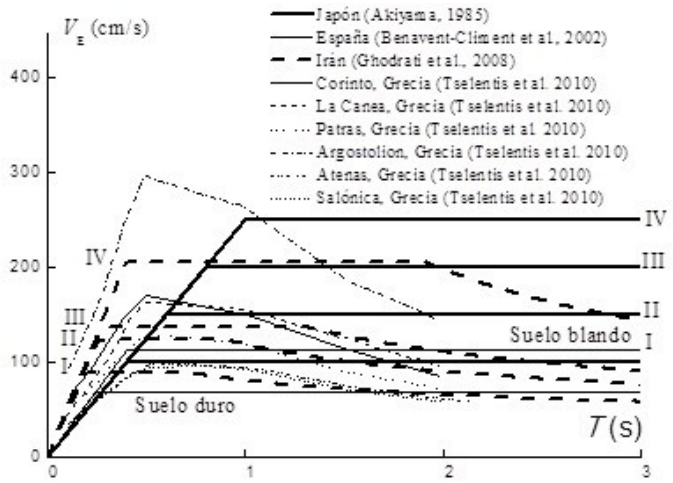

Figure 2-13. Examples of design energy spectra (in terms of velocity) proposed for Japan, Greece, Spain and Iran

$$V_E = \sqrt{2E_I / m} \tag{2-10}$$

In this expression, m is the mass of the structure. Figure 2-13 shows an example of energy spectra in terms of equivalent velocity.

Most of the spectra that are represented in Figure 2-13 are bilinear with an initial branch starting from the origin and a horizontal branch; as well, in some spectra decreasing branches are observed for long periods. Comparing the bilinear spectra represented in Figure 2-13 with the acceleration spectrum in Figure 2-6 confirms that, except in the short period range, these spectra (velocity) may be obtained approximately by multiplying the acceleration by $T / 2\pi$, as indicated by equations (2-8). In this case, the period T_B in Figure 2-6 corresponds to the intersection between both branches. In fact, the increasing branch between $T = 0$ and $T = T_A$ in the velocity spectrum corresponds to a parabolic segment, but in practice it resembles a straight line, whereby the energy spectra in terms of velocity generally have a linearly increasing branch in the range of periods between 0 and T_B. Moreover, comparing the spectra with decreasing branches represented in Figure 2-13 with the acceleration spectrum in Figure 2-8 shows that these branches correspond to the periods higher than T_D in Figure 2-8. Figure 2-13 illustrates the energy levels in terms of equivalent velocity (equation (2-10)) for different soil types: type I corresponds to hard rock or very hard conglomerates where the shear velocity v_s is higher than 750 m/s, type II corresponds to hard packed sand and gravel with $375 \leq v_s < 750$ m/s, type III corresponds to intermediate soils like sands and gravels semi-compact with $175 \leq v_s < 375$ m/s, and type IV is soft soil with $v_s < 175$ m/s. The characterization of very soft ground (with $v_s < 175$ m/s) requires special studies as there are important differences among the existing types.

The methods that are based on energy spectra are the basis for this study. The seismic input is not characterized in terms of forces (as in the methods based on acceleration spectra) nor in terms of displacement (as in the methods based on displacement spectra) but in terms of the product of both quantities (force per displacement), in other words, in terms of energy.

The main advantages of the methods based on energy spectra are:

- The ability to quantify the amount of energy that the design earthquake introduces in a given structure provides conceptual clarity and allows representing the effect of the seismic input by a simple scalar quantity.

- We can define from the design stage how do we want the structure dissipates the energy: deforming plastically, storing it temporarily (along the input duration) as elastic vibration energy and allowing then it to dissipate by the natural damping of the structure or by a combination of both.

- Damage can be quantified in the structure after an earthquake, by means of cumulated plastic deformation energy.

The methods based on energy balance (also known as methods based on the energy balance-Housner-Akiyama) have their origins in the work of George Housner [Housner 1956], Tanahashi [Tanahashi 1956], Berg and Thomaides [Berg, Thomaides 1960], Kato and Akiyama [Kato, Akiyama 1975], Housner and Jennings [Housner, Jennings 1977], Uang and Bertero [Uang, Bertero 1988; Uang, Bertero 1990], McCabe and Hall [McCabe , Hall 1989], Fajfar et al. [Fajfar et al. 1992], Zhu and Tsu [Zhu, Tsu 1992], Wang and Bruneau [Bruneau, Wang 1996], Chapman [Chapman 1999] and Chou and Uang [Chou, Uang 2000], among others. Housner died in 2008, having been one of the most productive and successful researchers in earthquake engineering, especially in energy methods. The wrong idea that Housner's concept of energy was inherited by Veletsos and Newmark [Veletsos, Newmark 1960] has hindered the development of energy-based methods. During many years, it was wrongly understood that the concept of energy proposed by

Housner had been continued in the work of Veletsos and Newmark. However, Veletsos and Newmark were not interested in calculating the energy that an earthquake introduced into the structure, they used the energy stored/dissipated by elastic/elastoplastic SDOF systems under monotonic loading up to the maximum displacement (not the total energy input during the cyclic loading reversals), to relate the maximum displacements in a given range of periods.

One of the greatest contributions to this methodology is due to Professor Hiroshi Akiyama, whose investigations are an important part of its current theoretical framework. Akiyama [Akiyama 1985] showed that the amount of energy introduced by an earthquake in a given structure is a highly stable quantity with respect to the structural resistance, the distribution of its rigidity and mass, the damping level and the hysteretic behavior of the structural elements; it depends basically on the fundamental period of vibration of the structure and its mass. This conclusion has also been verified experimentally by dynamic tests on earthquake simulators [Uang, Bertero 1990]. Moreover, the dependence of the energy on the mass is proportional; in consequence, the energy expressed in equivalent velocity (V_E) is independent of the mass, as expressed by the relationship (2-10). These circumstances provide a significant advantage when interpreting the effect of the earthquake on the structure in terms of energy instead of forces; the advantage is that the problem of assessing the seismic force induced by the earthquake and the problem of estimating the resistance of the structure (the term resistance is understood in a broad sense) can be uncoupled, in other words, can be treated separately.

However, it should be noted that the independence between the energy E_I and the properties of strength, stiffness, damping and hysteretic behavior of the structure has some exceptions, among these are the quasi-harmonic motion, in other words, a narrow frequency content. For example, the energy introduced by a harmonic motion in an undamped system can reach infinite values if the frequency of excitation corresponds to the natural frequency of the structure (in this case, resonance occurs if the duration of excitation is sufficient); consequently it is strongly dependent on the damping of the structure. In summary, in narrow-band inputs (typical of soft soil) the energy introduced by the earthquake E_I depends heavily on the properties of the structure. This is a limitation of the seismic design methods based on energy

In the seismic design methodology based on energy balance, the effect of the earthquake on the structure is expressed in terms of the energy introduced by the earthquake and the strength of the structure is measured by its limit capacity for energy absorption W_u. The condition for the structure to survive the earthquake can be written as follows:

$$W_u > E_I \tag{2-11}$$

This relationship is the basic criterion of energy balance for checking the suitability of the structure to withstand the design earthquake by accepting a certain level of damage. However, it should be noted that in fact it is not true that a certain structure has a single value of energy dissipation capacity; in fact, it depends on the type of excitation and, specially, on the history of loading [Chai 1995; Chai 2004; Erberik, Sucuoğlu 2004; Sucuoğlu, Erberik 2004; Benavent 2007]. This makes the evaluation of the ultimate energy dissipation capacity of structures a cumbersome issue that, for design purposed, can be addressed by using lower bound values. On the other hand, obviously, the energy absorption capacity of a structure depends on its general characteristics, and consequently analyses for different types of most common structural systems (concrete frames, concrete walls, steel frames, steel braced frames, masonry buildings, wooden buildings, buildings with base isolation, energy dissipation buildings, etc.) must be carried out. The usual strategy [Akiyama 1999] is first, to define the regions of the structure where plastic strain energy is expected to be released (plastic hinges), second, to determine the capacity of each floor and, third, to analyze the distribution of damage among the different floors. The third part is the most important and cumbersome one, and at the same time one of the main advantages of energy-based seismic methods, because the susceptibility of a structure to damage concentration

in given stories can be addressed, controlled and foreseen. For this purpose a damage concentration coefficient n is defined, in the reference [Akiyama 2003] it is described the calculation of this coefficient from dynamic analyses. The applicability of this study is limited because it is based on an excessively low number of earthquakes. For the purpose of further studies, the hysteretic models described in references [Erberik, Sucuoğlu 2004; Sucuoğlu, Erberik 2004] can be useful as they relate the degradation of stiffness and strength to the energy consumption.

The capacity of each floor (or the whole structure) can be estimated mainly in two ways: from its hysteretic behavior (subsection 2.1.6.4), or from the results of nonlinear dynamic analyses of the structure under seismic actions. The first procedure is described in [Akiyama 1985] and basically consists of identifying the damage with the cumulated ductility η. The second procedure is based on determining the values of damage indices that quantify the damage to the structure; the values of these indices are obtained from the dynamic analyses. Different indices to assess structural damage have been proposed in the literature [Lybas, Sozen 1977; Banon, Veneciano 1982; Park, Ang 1985; Soo et al. 1989]. Among them, the Park & Ang index [Park, Ang 1985] is one of the most used for reinforced concrete structures and has the advantage of being calibrated experimentally, so that the values adopted may be related to damage levels observed in real structures. The index of Park & Ang damage referred to a particular structural component is defined by the following expression:

$$D = \frac{\delta_M}{\delta_u} + \frac{\beta}{Q_y \delta_u} \int dE_H \tag{2-12}$$

δ_M is the maximum strain response (in absolute value) and δ_u is the ultimate deformation capacity under monotonic forces. Q_y is the yield strength and β is an empirical calibration factor ranging between 0.03 and 1.2, with an average value of 0.15. In the reference [Cosenza et al. 1990], it is shown that β = 0.15 provides a good correlation with other indices of damage. Importantly, the term δ_M of the above formula includes the elastic deformation. Accordingly, in cases where the structural element is kept within the elastic domain (i.e. without structural damage) the index value of Park & Ang can be different from zero. The index of Park & Ang of a part or of all the structure can be estimated by the weighting average of the damage indices of the components:

$$D = \sum \lambda_i D_i \tag{2-13}$$

The summation extends along all the involved structural components. D_i is the damage index of the structural component i and λ_i is a weighting factor defined as the ratio of the plastic energy in the structural component i and the plastic energy in all the structural components of the story or in the whole structure. The index of Park & Ang damage has been calibrated by many researchers from the observation of damage to actual structures under past earthquakes [Park et al. 1987; Gunturi 1992; Stone, Taylor 1994] and its correlation with these are indicated in Table 2-1.

Table 2-1 Correlation between the Park & Ang index and the observed damage

Observed damage	Damage index Park & Ang
Small damage	0.1 – 0.2
Medium damage	0.2 – 0.5
Severe damage	0.5 – 1
Collapse	> 1

In general, the collapse of the structure is defined as the state in which one of the structural elements (mainly beam or column) loses its restoring force. One of the main shortcomings of the Park and Ang indexes of damage is that they do not consider the influence of the loading path (i.e. history of loading) followed by the structure. An alternative index that takes into account the

loading path was proposed by Benavent-Climent [Benavent-Climent 2007] in the context of steel structures.

2.1.5 Performance-based earthquake-resistant design

The objective of the current seismic design codes is to prepare the structure to resist the design seismic input only under ultimate limit state; in other words, the structure is intended to resist the design earthquake with an acceptable level of serious damage but without collapse (in other words, avoiding at all costs the loss of human lives). Remarkably, that approach does not include any requirement about the behavior under seismic actions with lower or higher level of severity; this contrasts with the usual strategy against other type of actions (gravity, for example) where two types of limit states (ultimate and service) are considered. This approach is broadly valid and has been used for decades but was in shortage especially after the Northridge earthquake in 1994 and Kobe in 1995; after these highly severe earthquakes it was found that some structures, even those relatively new and that had been designed with the latest seismic standards, did not collapse (and in them there were no human casualties), but the damage to buildings (both structural and non-structural) was very serious. In the Kobe earthquake, some hospitals had been so intensely reinforced that effectively its structure did not collapse but absolute accelerations in the building were so high that it damaged the installations and were unusable at the time of greatest need (a few hours after the earthquake). After these events, the earthquake engineering was directed not only to prevent loss of human lives but also to quantify, reduce and prevent the damage. Depending on the damage, we are able to accept when an earthquake occurs, different solutions can be proposed. This strategy is commonly known as "Performance Based Design"; it is mainly described in the references [SEAOC 1995], [EERC 1995], [Bertero et al. 1996], [Hamburger 1998], [FEMA 350 2000], [FEMA 356 2000], [FEMA 349 2000] and [ATC-58 2002]. These documents present different seismic design methodologies oriented to control and to quantify the level of structural damage due to seismic action and to design structures that do not exceed the corresponding level.

Based on structural and non-structural damage the following four levels of performance ("Performance States") [SEAOC 1995] are defined:

Based on structural and non-structural damage defines the following four levels of performance ("Performance States") [SEAOC 1995]:

- **Fully Operational**. Uninterrupted service. Negligible structural and non-structural damage.

- **Operational**. Most of the activities can be resumed immediately. The structure is safe and can be inhabited. The essential activities are maintained while the non-essential ones are interrupted. Repairs are necessary to resume the non-essential activities. Slight damage.

- **Life Safe**. Moderate damage, the structure remains safe. Some elements or components of the building may be protected to avoid damage. The risk of loss of life is low. The building may need to be evacuated after the earthquake. The repair is possible, but can be economically unfeasible.

- **Near Collapse**. Severe damage, but without risk of collapse. Possible fall of non-structural elements.

More recently, another similar classification is considered [ATC-40 1996; FEMA 350 2000; FEMA 356 2000; FEMA 349 2000]:

- **Immediate Occupancy**. Occupants' safety. Important services are not uninterrupted. Negligible structural damage. The global damage is minor. The period of lack of functionality ("down time") is about 14 hours.

- **Damage Control**. Slight structural damage. Achievable occupants' safety. The essential activities are repairable. Moderate overall damage. The period of lack of functionality ("down time") is about 2 or 3 weeks.

- **Life Safety**. Probable structural damage but no collapse. No risk from falling non-structural elements. The evacuation of the occupants can be done without risk. Possibility of irreparable building.

- **Collapse Prevention**. Severe structural damage, with risk of collapse. Likely fall of non-structural elements. The evacuation of the occupants may involve risk. Building likely irreparable.

These four levels are often represented by their initials: IO, DC, LS and CP. The three levels IO, LS and CP are the most commonly used for seismic design; Figure 2-14 presents a graphical and easily understandable way, the practical significance of these levels and their relationship with the percentage of damage. The case "operational" in this case refers to a building without any damage

For each structural type, more precise definitions of these levels have been developed depending on the type of experienced structural damage.

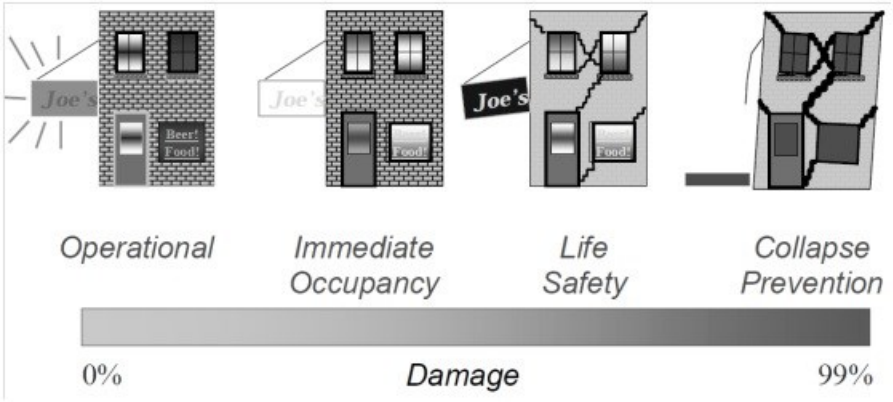

Figure 2-14. Damage levels [Hamburger 1998]

Regarding the seismic action, four levels of severity as defined as specified in Table 2-2.

Table 2-2 Severity levels of the seismic inputs

Design Earthquake	Return Periods (years)	Probability of Occurrence
Frequent	43	50% in 30 years
Occasional	72	50% in 50 years
Rare	475	10% in 50 years
Very rare	970	10% in 100 years

Table 2-2 shows that the severity of the earthquakes is quantified in terms of their return period; it is understood as the average of the elapsed time among earthquakes with the same magnitude or, almost equivalently, as the inverse of the probability of occurrence in one year. In some cases, seismic actions more severe than those contained in Table 2-2 are considered; the so-called MCE ("Maximum Considered Earthquake") [Malhotra 2006] corresponds to a return period of about 2475 years. The relationship between the return period T and the probability p_n of being exceeded n years is given by the expression $T = -n/ln(1 - p_n)$; it is often used to indicate the severity of

an earthquake by the probability p_{50} to be exceeded in 50 years, for example, in the case of MCE is $p_{50} = 1 - e^{-\frac{50}{2475}} = 0.02$ and in the case of an earthquake "Rare" is $p_{50} = 1 - e^{-\frac{50}{475}} = 0.10$.

Table 2-3 shows the demand levels of for each of the four performance levels previously described [SEAOC 1995], when the earthquakes that have the probability of occurrence specified in Table 2-2 occur.

Table 2-3 shows three levels of protection (expressed by the three represented diagonals): less intense for systems of moderate importance ("Basic Facilities"), more intense for major facilities ("Essential / Hazardous Facilities") and even more intense for crucial facilities ("Safety critical Facilities"). For example, in "Essential / Hazardous Facilities" (diagonal terms) it is required that for an earthquake of return period of 75 years the building remains fully operational, for an earthquake of return period of 475 years the building keeps operating in its major functions and for a return period of 970 years the building is able to preserve the lives of its occupants.

Table 2-3 Required levels of protection for each severity level of the seismic action [SEAOC 1995]

Levels of the expected earthquake	Level of required behavior			
	Full Functionality	Functionality	Life Safety	Near Collapse
Frequent (43 years)			Unacceptable Behavior	
Occasional (72 years)				
Rare (475 years)				
Very Rare (970 years)				

2.1.6 Nonlinear static analyses ("push-over")

2.1.6.1 Capacity curves

The method of earthquake-resistant design based on displacements consists basically of comparing the capacity of the structure, characterized by a curve representing its behavior under incremental forces, with the effect of the design earthquake, characterized by a demand curve. The intersection between both curves is termed as "target drift" (or displacement) or "performance point", in other words, that point indicates the effect produced by the earthquake on the structure [ATC-40 1996]. The capacity curve is usually expressed by representing on the ordinates the interaction force *F* between the building and the base (Figure 2-1) and on the abscissas the displacement of the top floor [Kircher et al. 1997; Krawinkler 1998]. The analysis that generates this curve is static and obviously nonlinear, being commonly known as push-over. Figure 2-15 shows an example of a capacity curve obtained from a push-over analysis.

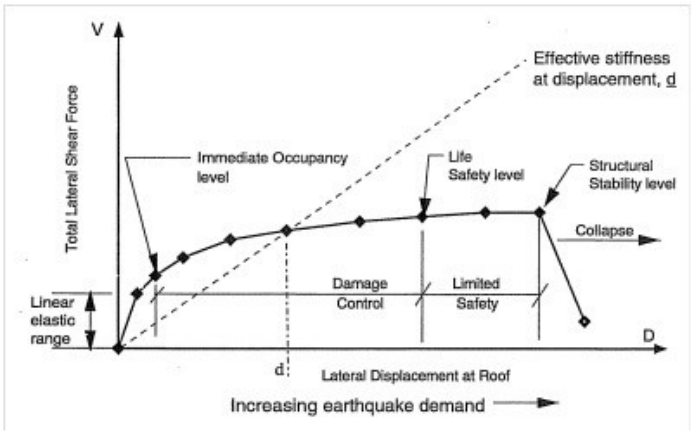

Figure 2-15. Capacity curve obtained from push-over analyses [ATC-40 1996]

In Figure 2-15 *V* represents the interaction force between the building and the ground (base shear force) and *D* is the displacement of the upper floor. The correspondence between the values of *D* and the aforementioned performance levels is also indicated.

In the push-over analyses the base shear force is distributed along the floors according to certain patterns; the most commonly used are the first modal shape, uniform or linear ("triangular") distributions. The push-over analyses are made incrementally, in other words, the lateral forces are increased progressively. For small values of *F,* the behavior of the structure is linear and as *F* increases, the structure is becoming gradually more damaged; the stiffness of the structure decreases and its capacity curve becomes more flat. The smallest slope of the capacity curve with the increasing displacement illustrates clearly the elongation of the natural period of the structure.

Some researchers [Fajfar, Fischinger 1988; Bracci et al. 1997; Gupta, Kunnath 2000] have proposed techniques to modify the distribution of the lateral forces among the floors to take into account the variation of the modal properties (mainly the first mode modal vector) by the increasing degradation of the structure. Other studies have proposed techniques to take into account the contribution of the higher modes [Paret et al. 1996; Sasaki, Freeman, Parent 1998; Gupta, Kunnath 2000; Kunnath, Gupta 2000; Matsumori et al. 2000], also [Chopra 2001; Goel, Chopra 2002; Chintanapakdee, Chopra 2003] have proposed a new formulation known as Modal Push-Over Analysis.

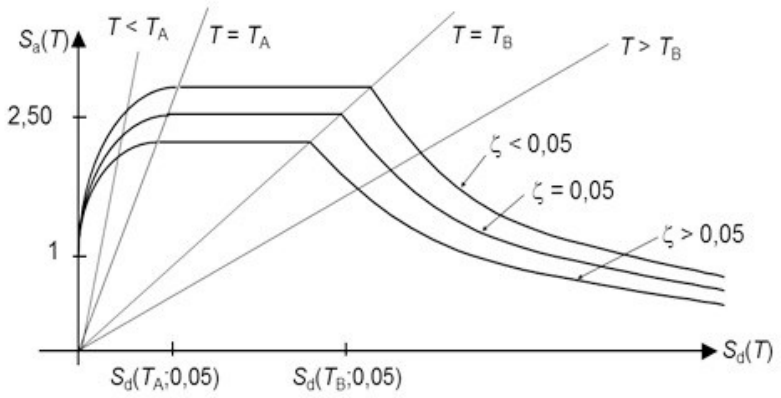

Figure 2-16. Acceleration spectra vs. displacement spectra

2.1.6.2 Target displacement

The demand is characterized by the design spectrum for the considered level of seismic action (Table 2-2); to be able to intersect it with the capacity curve, it is represented as the absolute

acceleration spectrum S_a (vertical axis) vs. the relative displacement spectrum S_d (horizontal axis). This type of representation is commonly known as "Acceleration-Displacement Response Spectra" (SARD). Figure 2-16 shows a spectrum from Figure 2-9 plotted using these coordinates.

The methods mostly used to obtain the target displacements are:

- Capacity Spectrum Method [ATC-40 1996]
- Displacement Coefficient Method [FEMA 356 2000]
- Equivalent linearization method [FEMA 440 2005]
- Modified displacement coefficient method [FEMA 440 2005]
- Modified Capacity Spectrum [ATC-40 1996]

Capacity Spectrum Method

In order to intersect the curves as shown in Figure 2-14 and Figure 2-15, they must be represented in the same coordinates. In this strategy [ATC-40 1996], the capacity curve is modified as (Figure 2-14): the ordinate is divided by the part of the building mass that corresponds to its first mode (in other words, the equivalent modal mass divided by the total mass) [Clough, Penzien 1993; García Reyes 1998; Chopra 2001] and the abscissa is multiplied by the modal participation factor of the first mode [Clough, Penzien 1993; García Reyes 1998; Chopra 2001]. The capacity curve expressed in these coordinates is usually termed as capacity spectrum. Obtaining a target displacement for each level of damage (characterized by design displacement, horizontal axis of the spectrum of Figure 2-16) is performed in an iterative way according to the following process:

- To select the desired value for the design displacement and to find the corresponding acceleration determined by the spectrum in Figure 2-16.
- To determine, from the capacity curve, the horizontal force (on the vertical axis) that corresponds to the selected displacement. An equivalent bilinear plot will replace the curve between the origin and this point. The first branch of this plot coincides with the linear part of the capacity curve (from the origin) but extends beyond it. The second branch of this plot is similar to the actual capacity curve; it is selected with the provision that the areas bounded by the bilinear plot and the actual capacity curve (until the design displacement) are equal. Figure 2-17 shows an example of this process. Once the bilinear plot is generated, the equivalent damping viscous damping ζ_{eq} is determined; ζ_{eq} is selected (as usual, [Clough, Penzien 1993; García Reyes 1998; Chopra 2001]) by equaling the areas of the hysteresis loops for the bilinear plot and with viscous damping. This damping is added to the inherent damping in the structure, whose value is usually 5%.
- The acceleration-displacement spectrum is corrected to fit the value of ζ_{eq} obtained in the previous stage. The intersection between the corrected spectrum and the capacity curve (in the coordinates according to the formulation given in [ATC-40 1996]) is determined. If the abscissa of this intersection is close to the selected displacement (with a predetermined tolerance), the point corresponds to the target displacement. Otherwise, the process has to be repeated iteratively until a sufficient approximation is reached.

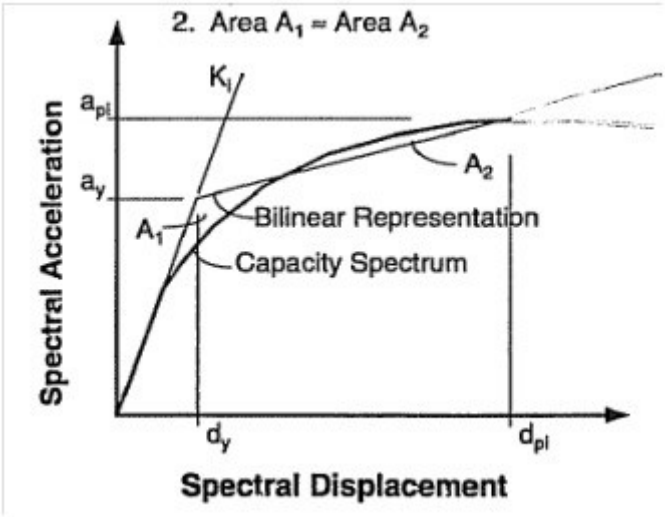

Figure 2-17. Bilinear approximation of the capacity curve [ATC-40 1996]

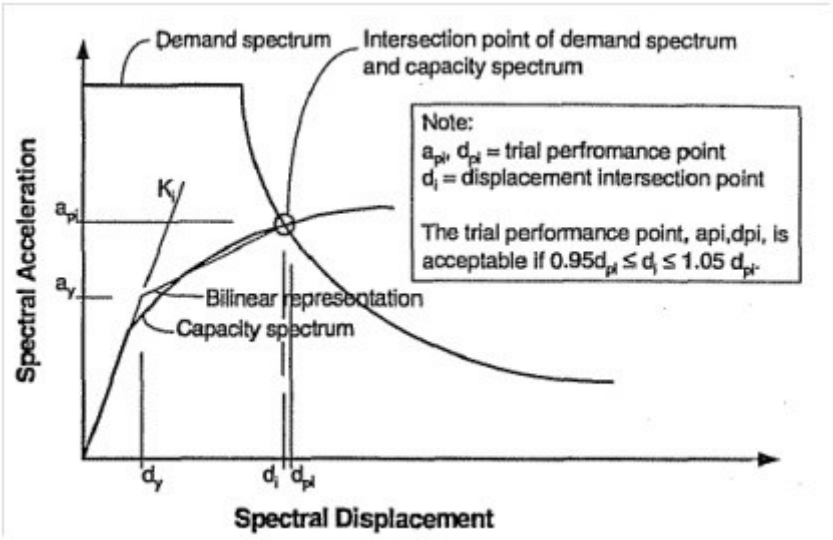

Figure 2-18. Obtaining the target displacement [ATC-40 1996]

Figure 2-18 describes the iterative process for obtaining the target displacement.

Displacement Coefficient Method

This method uses the following empirical formula for calculating the target displacement:

$$\delta_t = C_0 C_1 C_2 C_3 S_a \frac{T_e^2}{4\pi^2} g \tag{2-14}$$

T_e is the effective fundamental period of the equivalent SDOF system, calculated using the bilinear approximation of the capacity curve (Figure 2-19):

$$T_e = T_i \sqrt{\frac{K_i}{K_e}} \tag{2-15}$$

T_i is the fundamental period calculated by an elastic dynamic analysis and K_i is the lateral stiffness. K_e is the effective lateral stiffness that is taken as the secant stiffness corresponding to a base shear force equal to 60% of the effective yield strength of the structure.

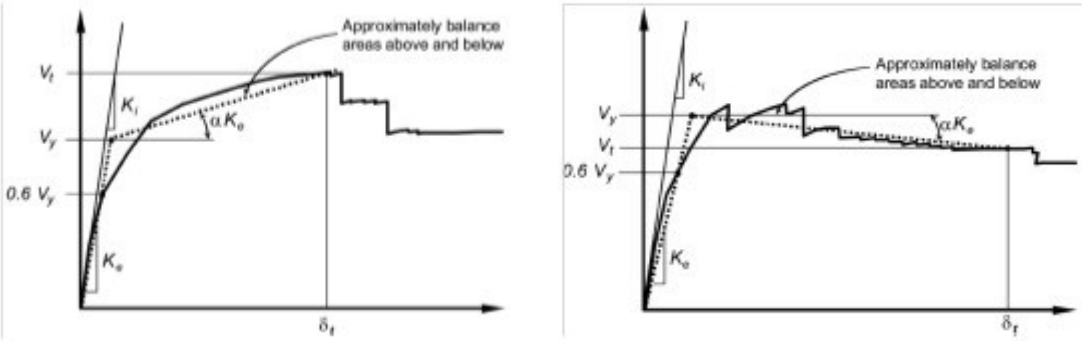

(a) Positive post-yielding slope (b) Negative post-yielding slope

Figure 2-19. Idealized force – displacement curves [FEMA 356 2000]

C_0 is a coefficient that relates the displacement of an equivalent single-degree-of-freedom system with the displacement on the roof of the building. Table 2-4 presents a way to obtain the values of C_0 [FEMA 356 2000] as a function of the number of stories of the structure, the building type and variation of the forces through the height obtained from the push-over analysis.

Table 2-4 Values for the modification factor C_0 [FEMA 356 2000]

Table 3-2 Values for Modification Factor C_0 [1]

	Shear Buildings[2]		Other Buildings
Number of Stories	**Triangular Load Pattern (1.1, 1.2, 1.3)**	**Uniform Load Pattern (2.1)**	**Any Load Pattern**
1	1.0	1.0	1.0
2	1.2	1.15	1.2
3	1.2	1.2	1.3
5	1.3	1.2	1.4
10+	1.3	1.2	1.5

1. Linear interpolation shall be used to calculate intermediate values.
2. Buildings in which, for all stories, interstory drift decreases with increasing height.

In equation (2-14) C_1 is a modification factor that relates the expected inelastic displacements with those calculated for the linear elastic response: for $T_e \geq T_s$ is $C_1 = 1$ and for $T_e \geq T_s$ is $C_1 = [1 + (R - 1)T_S / T_e] / R$. T_s is the characteristic period of the response spectrum (transition between the branches of constant acceleration and constant velocity) and R is the ratio between the elastic and inelastic demands calculated by $R = [S_a / (V_y / W) / C_m]$ where V_y is the yield strength obtained from the idealized capacity curve, W is the weight of the building and C_m is the equivalent modal mass participation factor of the first mode; alternately [FEMA 356 2000] proposes a table ("Table 3.1") with approximate values

In equation (2-14) C_2 is a modification factor representing the effect of the shape of the hysteresis loops. Table 2-5 presents the values of C_2 [FEMA 356 2000] depending on the level of damage, the type of frame and the fundamental period of the building.

Table 2-5 Values for the modification factor C_2 [FEMA 356 2000]

Table 3-3 Values for Modification Factor C_2

	$T \leq 0.1$ second[3]		$T \geq T_S$ second[3]	
Structural Performance Level	Framing Type 1[1]	Framing Type 2[2]	Framing Type 1[1]	Framing Type 2[2]
Immediate Occupancy	1.0	1.0	1.0	1.0
Life Safety	1.3	1.0	1.1	1.0
Collapse Prevention	1.5	1.0	1.2	1.0

1. Structures in which more than 30% of the story shear at any level is resisted by any combination of the following components, elements, or frames: ordinary moment-resisting frames, concentrically-braced frames, frames with partially-restrained connections, tension-only braces, unreinforced masonry walls, shear-critical, piers, and spandrels of reinforced concrete or masonry.
2. All frames not assigned to Framing Type 1.
3. Linear interpolation shall be used for intermediate values of T.

In equation (2-14) C_3 is a modification factor that represents the increment of displacement due to the second order effects. For buildings with positive post-yield stiffness Figure 2-19(b)), C_3 is equal to 1 and for buildings with negative post-yield stiffness (Figure 2-19 (a)) C_3 is calculated as $C_3 = 1 + [|\alpha| (R - 1)^{3/2}] / T_e$. α is the ratio of post-yield stiffness to the effective elastic rigidity, with the relation of force-displacement (capacity curve) represented by a bilinear approximation (Figure 2-19).

These operations must be carried out iteratively:

- Estimate a (Δ) value for the displacement. Make a bilinear approximation. Get K_e, T_e and the ductility factor μ.
- Check the response spectra S_a (for a damping factor 5%) with the period T_e.
- From S_a obtain $H(m, S_a)$ and the displacement Δ.
- Get factors C_1, C_2 and C_3 and the scaled displacement Δ C_1 C_2 C_3.
- Compare the scaled displacement Δ with its initial value, the iteration should continue until both are equal (with a prescribed tolerance).

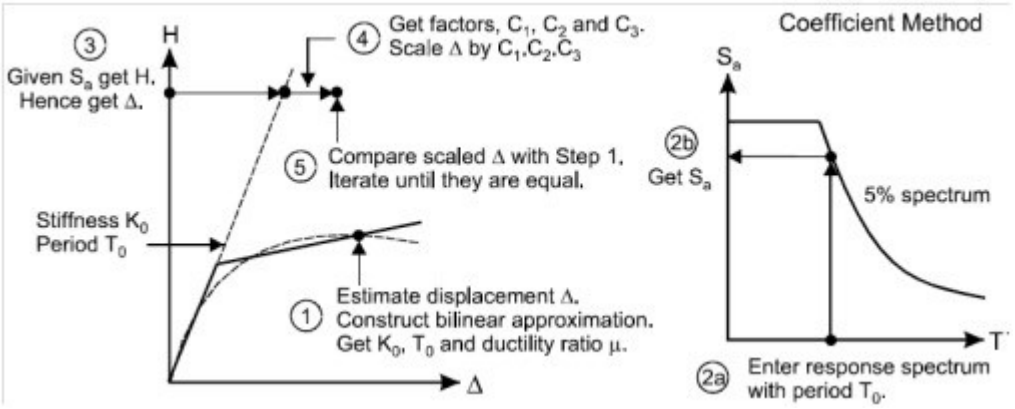

Figure 2-20. Iterative operations in the displacement coefficient method

Linearization Method

The following operations should be performed iteratively (Figure 2-21):

- Estimate an initial value (Δ) for the displacement. Make a bilinear approximation. Get K_e, K_h, T_e and the ductility factor μ.

- From K_e, K_h, T_e and μ obtain the effective stiffness K_{eff}, the effective period T_{eff} and the damping factor B_{eff}.
- Obtain the S_a ordinate of the response spectrum with the period T_e and the damping B_{eff}.
- From S_a obtain H (m S_a) and displacement Δ.
- Compare the scaled displacement Δ to the initial value; the iteration should continue until both are equal (with a prescribed tolerance).

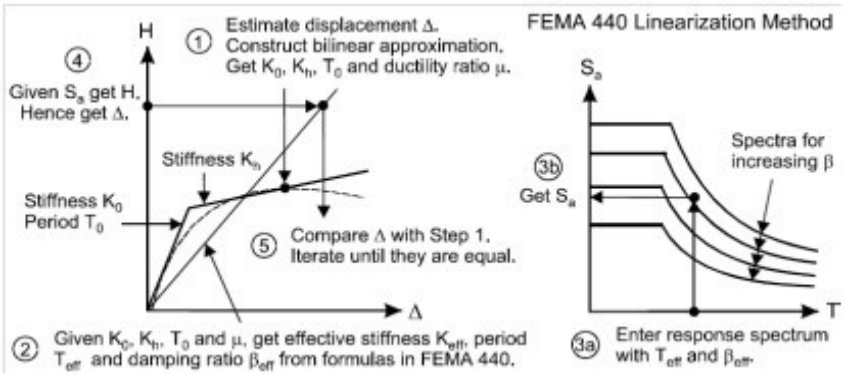

Figure 2-21. Iterative operations in the method of linearization

Modified Displacement Coefficient Method

In [FEMA 440 2005] modification of the displacement coefficient method, it is to propose new expressions for the coefficients C_1 and C_2 and eliminate the coefficient C_3 and replace it with a limitation of the maximum value of the resistance to avoid dynamic instability.

Modified Capacity Spectrum

The improved capacity spectrum method [ATC-40 1996] determines the equivalent linear parameters, effective period T_{eff} and effective damping B_{eff}, by a statistical analysis that minimizes the extreme differences among the maximum response of an actual single-degree-of-freedom inelastic system and their equivalent linear counterpart [Guyader, Iwan 2006].

2.1.6.3 Obtaining the response reduction factor

In the earthquake-resistant design method based on forces (through absolute acceleration response spectra) the values of the design equivalent horizontal forces (Figure 2-1) are obtained by dividing the elastic forces F_e by a reduction coefficient provided by the linear design response spectra, usually represented by R (Figure 2-10). This subsection describes the determination of this coefficient from capacity curves.

Early studies [Veletsos and Newmark 1960] proposed to determine the value of R from the displacement ductility μ (obtained from the capacity curves). Their proposal consists of three expressions: $R = 1$ for $T = 0$, $R = \sqrt{2\mu - 1}$ for $0 \le T < 0.5$ s and $R = \mu$ for $T \ge 0.5$ s. The first expression arises from the obvious consideration that the static response should not be affected by the ductility, the second expression comes from finding that energies in this range of periods corresponding to elastic and inelastic behavior are basically the same and the third expression is obtained assuming that the maximum displacements of elastic and inelastic systems are basically the same ("Equal displacement approach"). The dependence of the coefficient of reduction of the overall ductility and the structural period has prevailed in the design codes, although recent

research has shown that applying these factors is unsafe for low periods and excessively conservative for intermediate and long periods, [Ordaz and Pérez-Rocha 1998].

The capacity curves usually show an ultimate strength greater than the yield value F_y (Figure 2-15). This on-resistance is usually quantified by an over-strength dimensionless coefficient Ω, ratio of ultimate strength to yield strength ($\Omega = F_u / F_y$); in actual structures, the values of this coefficient usually range between 1 and 2. By using this ratio, the response reduction factor is usually expressed as

$$R = R_d \, \Omega = (F_e / F_u) \, (F_u / F_y) = F_e / F_y \tag{2-16}$$

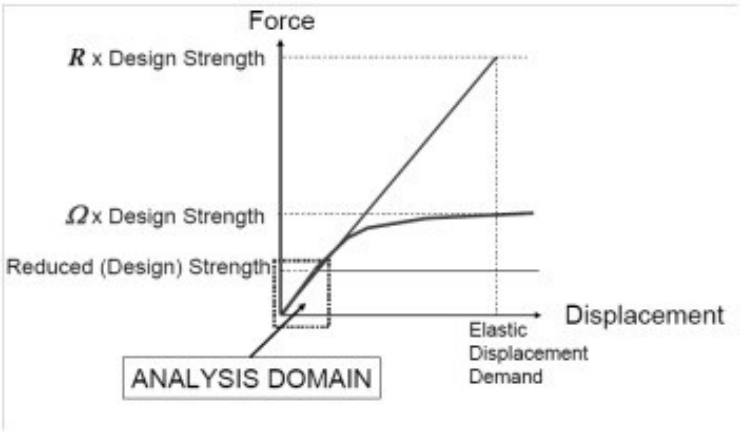

Figure 2-22. Factors contained in the response reduction factor [FEMA 450 2003]

Figure 2-22 illustrates the meaning of this expression. Some relevant studies related to the response reduction factor are [Newmark, Hall 1973; Miranda, Bertero 1994], among others.

2.1.6.4 Limitations of the push-over analyses

The main limitations of earthquake design methods based on displacement are described next. The analysis push-over characterizes the nonlinear dynamic behavior of the structure by means of increasing static forces. The main drawback of this strategy is that the response of the structure to a given input is not incremental but cyclical and the push-over analyses cannot take into account the accumulated plastic strain, in other words, the cumulated damage. Therefore, we cannot establish a clear relationship between the maximum displacement of the structure and the energy stored during plastic deformation cycles. When the structure enters the inelastic range, deterioration occurs by the accumulation of plastic incursions; that can produce the complete breakdown of structural elements for deformations smaller than those that could be resisted under monotonic forces. This type of failure is called low cycle fatigue or plastic fatigue [Teran-Gilmore, Jirsa 2007] (as opposed to the fatigue caused by a high number of cycles, which does not involve plastic deformations). Fajfar [Fajfar 1992] proposed a method to take into account the effect of cumulated damage in which the ductility of the structure is reduced by a dimensionless parameter that represents a normalization of the energy. Recently, Teran-Gilmore and Jirsa [Teran-Gilmore, Jirsa 2005] have used the correlation between energy and the response reduction factor, *R*, to propose two simple calculation procedures for low cycle fatigue; the energy demand is indirectly controlled through the concept of ductility. However, the disadvantages of the calculation procedures based on forces already have been previously pointed out; those disadvantages are closely related to the fact that equivalent forces representing the effect of the input depend on the elastic and plastic characteristics of the structure, which in its own turn regulate the structural strength. This coupling between the effect of the earthquake and strength of the structure makes the seismic calculation more complex and cumbersome. Furthermore, the concept of ductility allows determining only indirectly the cumulative fatigue damage for low

number of cycles, and requires the use of large numbers of empirical parameters. The main reason to address indirectly the accumulated damage through the concept of equivalent ductility factor is that it provides a calculation process that can adapt easily to the current codes and practices. Since designers are reluctant to change radically their state of practice, new procedures are more likely to be accepted if they represent only a small change in a concept, such as ductility factor, which is well understood and has been widely used in practice. The calculation procedures based on displacements solve several of the drawbacks of the procedures based on forces, but are also incapable of dealing with the effects of cumulated damage in a simple and satisfactory manner.

Another drawback of the earthquake design strategy based on displacements is that the hysteretic behavior is interpreted as an equivalent viscous damping (ζ_{eq}); this introduces a relevant error, especially for significant levels of damping. Moreover, such identification is not based on any physical principle that justifies, in inelastic systems, the existence of a direct relationship between the energy corresponding to the maximum displacement and the equivalent viscous damping.

Another strategy to bypass that the push-over analysis cannot take into account the cumulated deformations is to use energy spectra. The main motivation that has inspired its development is that the plastic deformation energy is fairly accurate to quantify the damage in the structure. These procedures exploit the difference between ductility μ, which expresses essentially the relationship between maximum deformation δ_{max} and the yield deformation δ_y, and the accumulated η ductility. The meaning of μ and η is described in Figure 2-23 [Benavent-Climent et al. 2001].

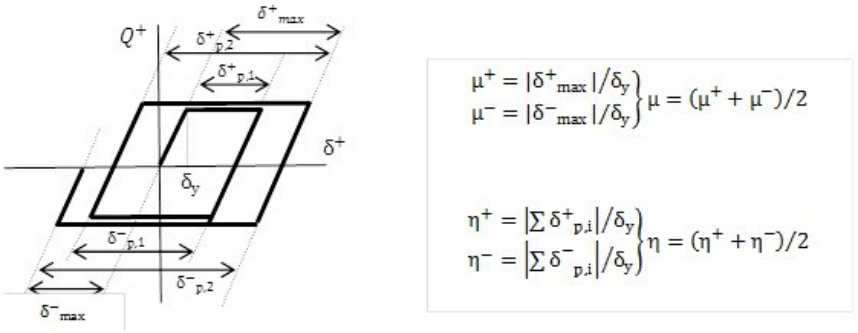

Figure 2-23. Meaning of the coefficients of ductility μ and η [Benavent-Climent et al. 2001]

Figure 2-23 shows that the ductility μ is defined as the average of the positive and negative values of displacement δ; each of them is calculated as the ratio between the maximum displacement (in other words, measured from the beginning of the yield) and the yielding displacement δ_y. The cumulative ductility η is also defined as the average of the values corresponding to positive and negative displacements; each of them is calculated by dividing the sum of the displacements of each plastic branch (horizontal in Figure 2-23) and the yielding displacement δ_y.

The limitations and disadvantages of earthquake-resistant design methods based on displacements are avoided in energy-based methods, which are described in the following subsection. Moreover, these procedures are quite appropriate in buildings with energy dissipation devices.

2.1.7 Dynamic analyses

This procedure evaluates the effect of earthquakes on buildings based on determining the dynamic response (commonly known as "time history") to the expected accelerograms. The most relevant response quantities are the maximum relative displacements (along the duration of the earthquake) in between consecutive floors (inter-story drifts) and the maximum absolute accelerations thereof; the maximum relative displacements report about the experienced level of structural damage and the maximum absolute accelerations are directly correlated with the non-structural damage (for facilities and non-structural elements) and the human comfort conditions.

Since the dynamic calculations take into account the performance of buildings under seismic inputs in a more direct way than in the methodologies based on response spectra, in general the dynamic analyses are able to provide more accurate results. In particular, the comparison between the nonlinear static methods (push-over) and the nonlinear dynamic methods is clearly favorable to them because, besides being more accurate in general, they have two important advantages: (i) by considering the cyclical behavior they are able to reproduce the accumulated plastic damage and (ii) the consideration of the effect of damping (both the present in the undamaged structure and the generated for increasing damage) is more direct.

The considered inputs are selected from the available information on the seismicity in the intended location and may consist in either records of historical earthquakes or in accelerograms generated artificially. Given the considerable uncertainty about the characteristics of the expected input, one must consider several accelerograms and then determine the average of the responses of the structure to each of them; in fact, in the earthquake-resistant design methodologies based on spectra equivalent operations have been done since the design spectra are smoothed, in other words, have been obtained as averaged envelopes of a group of spectra corresponding to individual accelerograms, as shown in Figure 2-3, Figure 2-4 and Figure 2-5. These figures show that the maximum response to each record is highly sensitive to the fundamental period of the building, particularly for low values of damping; therefore, considering an excessively low number of accelerograms generate a false information since the fit (or proximity) between the fundamental period of the building and any spectral peak will predict a structural response that is abnormally large. To avoid such problems the seismic design codes generally require considering at least five [NCSE-02 2002] or seven [ASCE 7-05 2005; NBCC 2005; NSR-10 2010] accelerograms; the response that is used for the earthquake-resistant design of the structure is determined as an average of the corresponding responses to each of such accelerograms. Some codes [ASCE 7-05 2005; NSR-10 2010] allow using only three accelerograms, but in that case the maximum response to them has to be considered.

The registers from historic events should be scaled to adjust its characteristics to the seismicity of the zone; since only the ordinates (acceleration) but not the abscissa (time) are changed, the frequency content is not modified. Usually this operation is done by comparing the design spectrum (specified in the regulations of the zone) with the response spectrum of the considered register, in the codes [EN-1998 2004; ASCE 7-05 2005] the comparison criteria is often described. These criteria usually indicate sets of minimum values for the spectral ordinates at periods near to the fundamental period of the structure. Furthermore, the synthetic accelerograms are generated so that its frequency content corresponds to the design spectrum and that its duration and other temporal characteristics match those of the expected records.

In zones of medium or high seismicity, buildings are often designed by accepting a given level of structural damage under the design earthquake (see Table 2-2). Accordingly, in these cases the dynamic analyses should be nonlinear, in other words, must be able to reproduce the behavior of the structure when it been damaged and therefore has experienced significant reductions in its strength and rigidity. Moreover, second-order analyses may be necessary because of the significant relative horizontal displacements, this being another source of complexity and increased computational cost. Although the nonlinear dynamic analyses are increasingly used in the earthquake-resistant design of important structures, this procedure is rarely used in the design of ordinary structures, this is due to the high computational cost involved and to the effort required to properly interpret the large amount of generated information.

The results of dynamic and push-over analyses can be compared. If the dynamic analyses are performed with accelerograms, either actual or synthetic, whose response spectra fits the one considered in the push-over analysis, the conclusions of both formulations should be similar. In [Powell 2007] the similarities and differences to be expected are discussed.

2.1.8 Incremental dynamic analyses

With the main purpose of alleviating the problem derived from the fact that the push-over analysis cannot take into account the accumulated plastic strain, the so-called incremental dynamic analysis (IDA, Incremental Dynamic Analysis) has been proposed [Vamvatsikos, Cornell 2001; Vamvatsikos, Cornell 2002; Vamvatsikos 2002]. The reference [Vega del Rey, Alarcón 2009] proposes a method to investigate the impact of bridge decks against the abutments. This strategy consists of determining the dynamic response of the structure to one or more inputs scaled with increasing factors; in this way, capacity curves are obtained similarly to the push-over analyses. If the incremental dynamic analysis is performed for a single record, such analysis is usually called *dynamic push-over analyses* (DPO, Dynamic Push-Over). It is remarkable that the incremental dynamic analyses require making several nonlinear dynamical calculations, which are expensive in computational time; on the other hand, it may be necessary to perform second-order analyses. However, the incremental dynamic analyses, especially when applied to several earthquakes, constitute powerful formulations, which may provide greater and more useful information than the rest of approaches that have been described in this section.

The results of these procedures are usually represented by the so-called IDA curves. These representations consist of capacity curves similar to the result of the push-over analyses; on the horizontal axis, an index related to the magnitude of the response is usually represented and the vertical axis usually contains an index related to the severity of excitation. Figure 2-24 shows the results of this kind; Figure 2-24 (a) corresponds to a single record and Figure 2-24 (b) corresponds to multiple (30) records. In both representations the severity of the seismic action is quantified by the ordinate of acceleration response spectrum for the first mode $S_a(T_1, 0.05)$ and the magnitude of the response is quantified by the maximum value (along the duration of the earthquake) of the relative displacement between floors (inter-story drift). Figure 2-24 (a) shows both increases and decreases of the damage on the upper floors with increasing severity of excitation, this effect is obviously due to the "protection" provided by the lower floors. None of the other methods described in this section are able to predict this phenomenon so clearly. Figure 2-24 (b) shows the remarkable variability in the response of a determined structure to records that have, in first approximation, a comparable level of severity

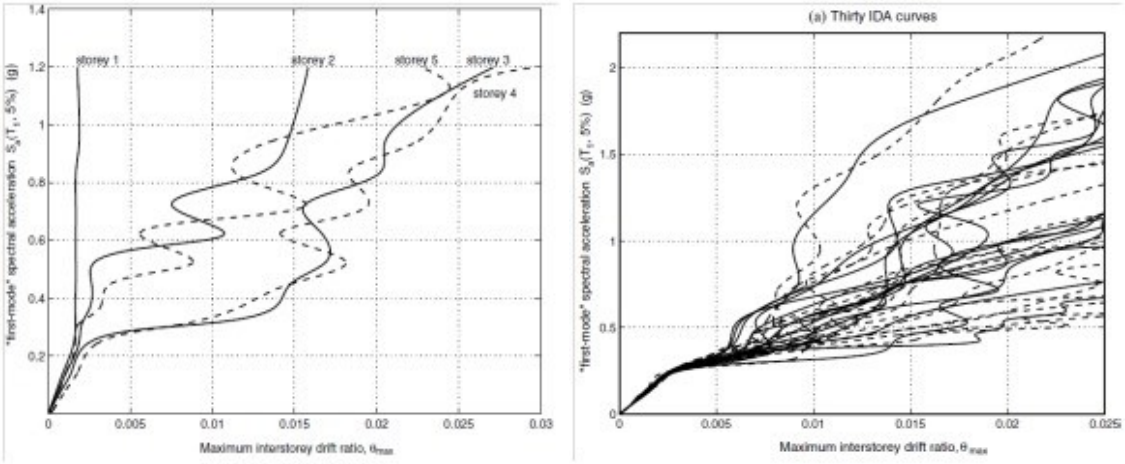

(a) Single Register (b) Thirty Registers

Figure 2-24. Examples of IDA curves [Vamvatsikos, Cornell 2002]

Usually the damage thresholds IO, LS and CP are related with certain values of the index that quantify the magnitude of the excitation (ordinate in Figure 2-24); in this way performance-based analyses can be made from incremental dynamic calculations.

It is remarkable that FEMA [FEMA 350 2000] has recently adopted these strategies as the reference method for assessing the earthquake-resistant capacity of structures.

2.2 Seismic design of steel buildings

2.2.1 Structural steel

Steel is a metal alloy, composed basically of iron and carbon, where the carbon percentage is comprised in between 0.008% and 2%; for lower percentages, the alloy is termed "mild iron" and for higher percentages, it is termed "cast iron". The carbon is providing both strength (elasticity, in terms of the yielding point) and fragility; for this reason mild and cast iron cannot be used as a construction structural material because of its low yielding point and poor weldability, respectively. In the current steel technology, the weldability is not only influenced by the carbon percentage but also by other metals, namely Mn, Cr, Mo, V, Ni and Cu; in this sense, instead of "carbon percentage", the steel weldability is rather characterized by the "carbon equivalent content" (CE). As well, the steel alloy contains also a number of impurities (mainly P, S, N and H).

For structural use, steel is used in two major applications: reinforcement bars for concrete members and main structural members (steel profiles for beams, columns and other members); given that this Thesis deals with steel building structures, only this last case is considered here.

Depending mainly on the chemical composition of the alloy, a number of steel types exist; for all of them the main common parameters are: unit weight γ = 78.50 kN/m^3, thermal expansion coefficient $\alpha = 1.2 \times 10^{-5}$ ºC^{-1}, modulus of elasticity E_s = 200/210 GPa, and Poisson's ratio ν = 0.29/0.3; the other major parameters are different for each type of steel. Yet there is a wide variety of steels in the market, in the construction world the steel is classified only through grade. The grade deals with the yielding point (f_y) and the ultimate strength (f_u). Figure 2-25 depicts uniaxial stress-strain plots for steel; noticeably, it is commonly assumed than the tensile and compressive behaviors are alike. Figure 2-25 shows that the initial elastic branch is linear (slope E_s) and the first segment of the plastic branch beyond the yielding point is roughly horizontal (zero slope, then), thus indicating a "perfect" plastic behavior (without strain hardening); for bigger strain values, further strain hardening rises the stress until the final failure (ultimate strength f_u).

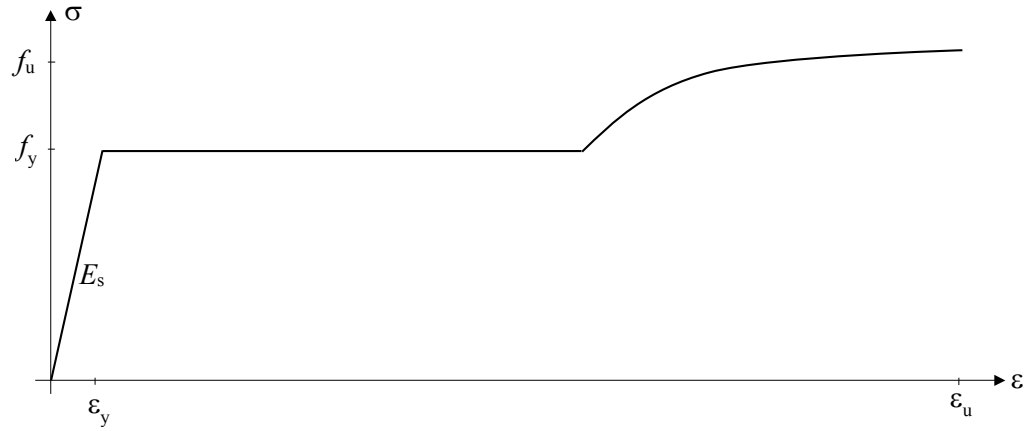

Figure 2-25. Uniaxial steel constitutive law

Figure 2-25 depicts the loading branch of the uniaxial elastic and plastic steel behavior; the unloading branches are linear with slope equal to the one of the elastic loading branch (E_s). For multiaxial stresses, the Von Mises yielding criterion is considered; this criterion consists of assuming than yielding arises when the Von Mises stress $\sqrt{\frac{1}{2}\left[(\sigma_x-\sigma_y)^2+(\sigma_y-\sigma_z)^2+(\sigma_z-\sigma_x)^2+6(\tau_{xy}^2+\tau_{xz}^2+\tau_{yz}^2)\right]}$ reaches the steel yielding point f_y. In terms of the principal stresses, the Von Mises stress can be written as

$\sqrt{\frac{1}{2}\left[(\sigma_I-\sigma_{II})^2+(\sigma_{II}-\sigma_{III})^2+(\sigma_I-\sigma_{III})^2\right]}$; this shows that the Von Mises stress depends only on the differences among the principal stresses and not on their values (in other words, the Von Mises stress depends only on the deviatory component of the stress tensor). As an exception, for triple tension stresses, the Von Mises stress is $\frac{1}{2}\sigma_I$. In structures composed of rod members undergoing bending there are only normal (σ) and shear stresses (τ); in that case the Von Mises stress is $\sqrt{\sigma^2+3\tau^2}$.

Next two paragraphs describe the most common steel grades used in Europe and in America, respectively.

Europe. Most steels used throughout Europe are specified to comply with the European standard [EN 10025 2004]. However, many national standards also remain in force. Typical grades are described as S275J2 or S355K2W. In these examples, S denotes structural rather than engineering steel; 275 or 355 denotes the yield strength (f_y) in N/mm^2 (MPa); J2 or K2 denotes the materials toughness by reference to Charpy impact test values and the W denotes weathering steel. The normal yield strength grades available are 235, 275 and 355. Noticeably, the yielding point drops slightly for thickness higher than 40 mm.

America. Steels used for building construction in the USA use standard alloys identified and specified by ASTM International. These steels have an alloy identification beginning with A and then two, three, or four numbers. The four-number AISI steel grades commonly used for mechanical engineering, machines, and vehicles are a completely different specification series. The standard commonly used structural steels are: carbon steels (A36 and A529, for structural shapes and plates), high strength low alloy steels (A441, A572, A992, A270 for structural shapes and plates). The yielding point (f_y) of A36 and A572 steels are 36 and 50 ksi, respectively (250 and 348 MPa). Similarly to the European steel, the yielding point drops slightly for thick members.

Apart from these major steel grades, other more corrosion-resistant types of steel are also employed. Among them, weathering and stainless steel. Weathering steel, best known under the trademark COR-TEN steel, is a group of steel alloys that were developed to eliminate the need for painting, and form a stable rust-like appearance if exposed to the weather for several years. Stainless steel differs from carbon steel by the amount of chromium present; stainless steels contain sufficient chromium to form a passive film of chromium oxide, which prevents further surface corrosion.

2.2.2 Steel structural products

For steel members, the aforementioned steel grades and types can be found in the market in form of plates, hot-rolled open profile sections, thin-gauge cold-formed open profile sections and closed profiles (rectangular and circular tubes). Apart from these major structural elements, minor parts, such as bolts and welding electrodes, are also available. Next four paragraphs describe the hot-rolled profiles, the cold-formed profiles, the plates and the closed profiles, respectively.

Hot-rolled sections. The available hot-rolled steel profiles are different in Europe and America. In Europe the offered profiles are IPN, UPN, IPE, HE, HL, HD, L (angle, either with equal or different sides), Z and T. In these names the first letter represents the shape: I sections are roughly shaped as a capital I, U are shaped as a channel (capital C), and so on; I and H profiles are similar yet H are wider than I. Figure 2-26 represents typical European steel profiles. The commercial designation of a profile is the series name followed by a number that represents the depth in mm: IPE 300 is an IPE profile that is 300 mm deep; the other dimensions are given. The available sizes

range between about 80 mm to 400 mm (for channel sections) or to 750 mm (for I and H sections). The horizontal elements of the I, U, H or L sections are termed “flanges”, while the vertical element is termed “web”; this notation is universal, even for other profiles, such as rectangular closed sections. In Europe, nowadays beams are made with IPE profiles and columns are made with HEB profiles; HEB is a subseries of the HE series, other major subseries are HEA (thin flanges) and HEB (thick flanges). L profiles are mostly used for trusses, mainly for diagonal and vertical members. Diagonal or chevron braces either with HEB profiles or with closed sections. In America, the offered profiles are similar to those in Europe; yet the main difference is constituted by the W (“wide”) profiles. W sections are I or H shaped and are characterized not only by the depth (inches) but also by the unit weight (pounds per foot): W36×256 means an H section being 36 inches deep and weighing 256 pounds per foot. Other common sections in America are M, S, HP, C, MC, L, WT, MT, ST, and 2L (double L). Figure 2-27 represents typical American steel profiles.

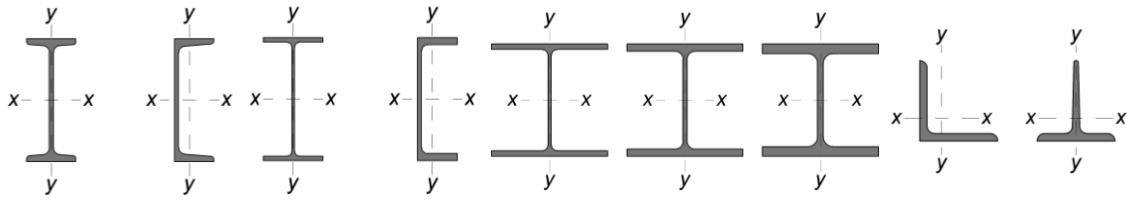

(a) IPN / UPN (b) IPE / UPE (c) HEA / HEB / HEM (d) L / T

Figure 2-26 Typical hot-rolled steel profiles used in Europe

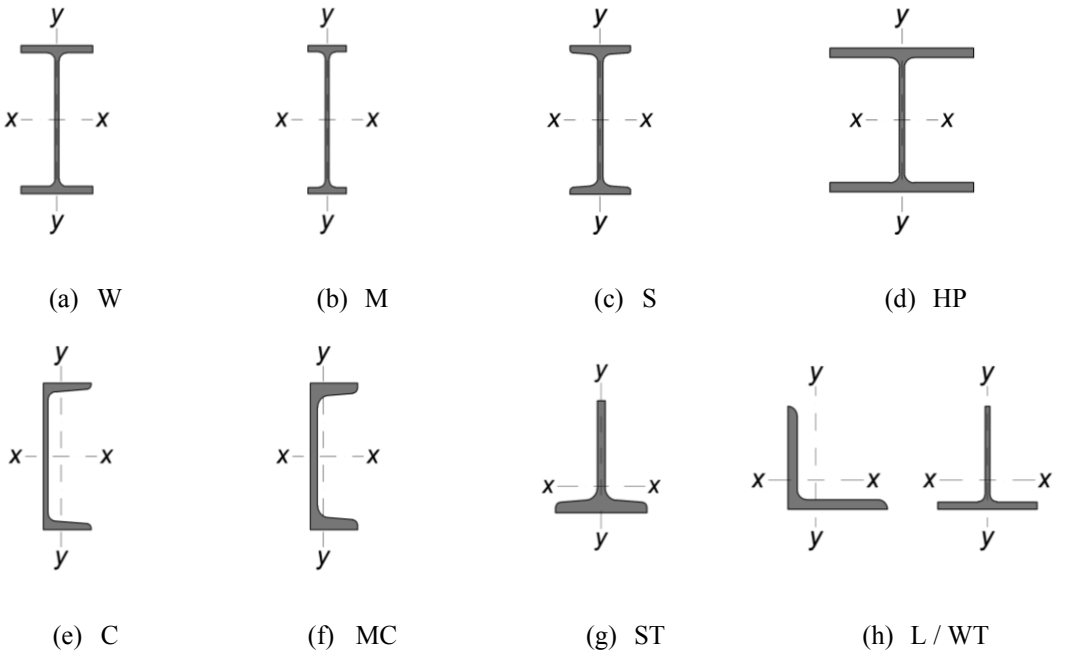

(a) W (b) M (c) S (d) HP

(e) C (f) MC (g) ST (h) L / WT

Figure 2-27. Typical hot-rolled steel profiles used in America

Plates. Steel plates are supplied in rectangular elements (“sheets”). The commonly available ranges of dimensions are approximately: width 1-4 m, thickness 3-20 mm (even 60 mm), length

3-18 m. Plates are mainly used for two purposes: small detailing elements (gusset plates, tapered members) and (plate) welded girders.

Thin-gauge cold-formed sections. These open profiles are obtained by folding at room temperature thin plates. Common sections are: Z, U (channel), hat (Omega), steel deck (folded plates), among others. Those shapes are similar to those of hot-rolled profiles yet the ends of the plates are frequently "lipped" to provide stiffening effect against distortional buckling (i.e. transverse buckling of the unstiffened flanges or webs.

Closed sections. Closed profiles are similar to the cold-formed sections; are obtained by folding at room temperature thin plates and then welding the seam to generate closed sections. There are two types of sections: circular and rectangular; are commonly termed as CHS (Circular Hollow Section) and RHS (Rectangular Hollow Section), respectively.

Given the roughness of the production system, the dimensions and shapes of the cross-sections and of the members are not accurate; therefore, the regulations [ASTM A6 2013; EN-10034 2013] establish the acceptable mill sectional, straightness, and length tolerances. In the hot rolled members, the thermal-origin initial (residual) stresses can be relevant, thus affecting significantly the buckling behavior. In the cold-formed sections, folding generates local large strains; this makes that in the corners of the sections the steel exhibits a higher yielding point.

2.2.3 Structural behavior of steel

The bases of the structural behavior of steel have been roughly described in subsection 2.2.1; this subsection addresses this issue in more depth.

Figure 2-25 depicts the uniaxial behavior of steel. Traditional design approaches consisted of limiting the stress to f_y; in other words, the steel was constrained to behave elastically (and linearly, then). This limitation seems reasonable since plastic excursions carry damage and permanent deformations; however, more recently, it was concluded that this approach can be over conservative since the safety factors (both for loads and for strengths) widely guarantee that in actual situations the yielding limit will be never exceeded even if limited plastic excursions are permitted for ultimate limit states. Therefore, the current design codes allow surpassing the elastic domain under certain conditions; namely, both local (sectional) and global (structural) plastic analyses are permitted and even encouraged. About local plastic analysis, the plastification (yielding) can be generated by any combination of the demanding internal forces: axial force (N), shear force (V), bending moment (M) and torque (T). Summarized descriptions of the plastic local behavior for N, V and M are described next; as well, the plastic interaction among such internal forces is also discussed. In steel structures the consideration of instability is of paramount importance, both for member buckling and for local buckling; local buckling caused by normal compressive stresses generated by N and M is used next (in this subsection) for the classification of sections. In overall terms, buckling can be considered in two opposite ways: (i) traditional formulation where the sectional strength is reduced by a dimensionless factor (termed as χ by the European regulations) which is obtained by empirical expressions in terms of the slenderness, geometrical unevenness, steel yielding point and other related magnitudes and (ii) a more advanced formulation where global second-order analyses are performed, taking into account the geometrical imperfections. About that, the Eurocode 3 [EN-1993 2005] states the minimum values to be taken into account for ordinary constructions; three types of imperfections are considered: (i) global initial sway imperfections of frames, (ii) lateral initial bow imperfection of bracing systems, and (iii) local bow imperfections of compressed members, mainly columns and chord members; noticeably, the geometrical imperfections cover also the effects of residual stresses.

Plastic local behavior for axial force. Since the normal stresses generated by the axial force are uniformly distributed in the section ($\sigma = N / A$), the values of the axial force that initiate and that

complete the yielding of the section are the same; they are commonly termed as N_{pl} (plastic axial force): $N_{pl} = A f_y$. Figure 2-28 describes this situation.

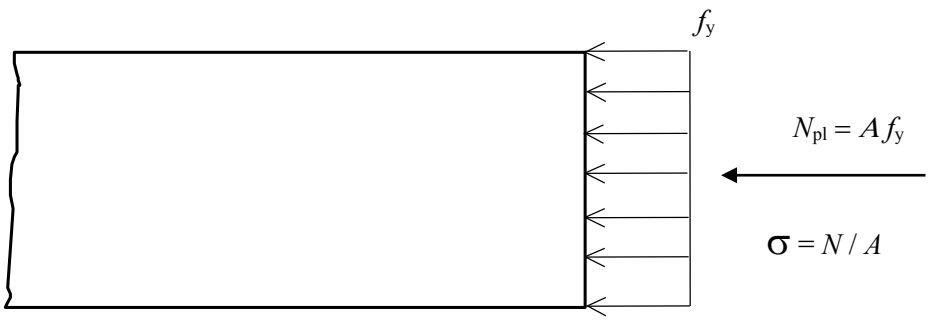

Figure 2-28. Sectional plastic behavior for axial forces

Plastic local behavior for shear force. Since in I, H, RHS or similar sections the shear stresses generated by the shear force are rather uniformly distributed in the so-called shear area A_v (A_v is roughly constituted by the webs and adjacent parts of the flanges; $\tau = V / A_v$), the values of the shear force that initiate and that complete the yielding of the section are nearly the same; they are commonly termed as V_{pl} (plastic axial force): $V_{pl} = A_v f_y / \sqrt{3}$ where A_v is the shear area ($\sqrt{3}$ factor arises from the Von Mises criterion, subsection 2.2.1). Figure 2-29 describes this situation.

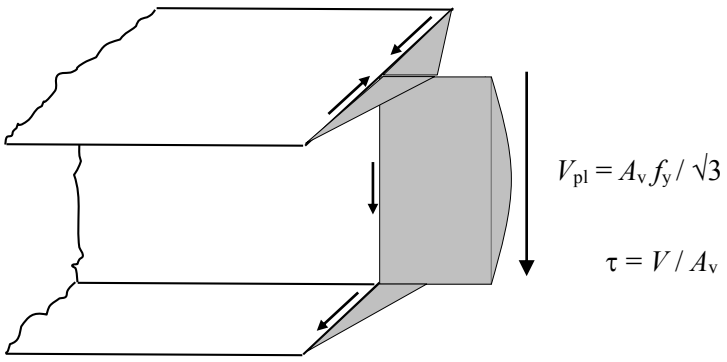

Figure 2-29. Sectional plastic behavior for shear forces

Plastic local behavior for bending moment. In linear elastic analysis, in any section the normal stresses generated by the bending moment are linearly distributed, being zero in the centroid and being compressive/tensile at both sides of such neutral axis (Figure 2-25 and Figure 2-30.a). Therefore, the maximum compressive/tensile stresses appear always at the extreme fibers, i.e. those situated farther from the centroid; consequently, the yielding will initiate at such ends and then will propagate inwards (Figure 2-30.b) until invading the whole section (Figure 2-30.c). The moment that causes the onset of yielding is termed "elastic moment" (M_{el}, Figure 2-30.a) and the moment that generates full yielding (i.e. all the section is plastified) is termed "plastic moment" (M_{pl}, Figure 2-30.c). Figure 2-30.c shows that in such a case the stresses distribution, instead of being bi-triangular, is formed by two rectangles whose amplitude is the yielding point f_y. The section considered in Figure 2-30 is symmetric with respect to the strong axis, in such a case the centroid belongs to the plastic neutral axis. Noticeably, if the section is not symmetric, the

centroid does not belong to the plastic neutral axis; in such a case, such axis divides the section in two equal-area parts (Figure 2-30.c).

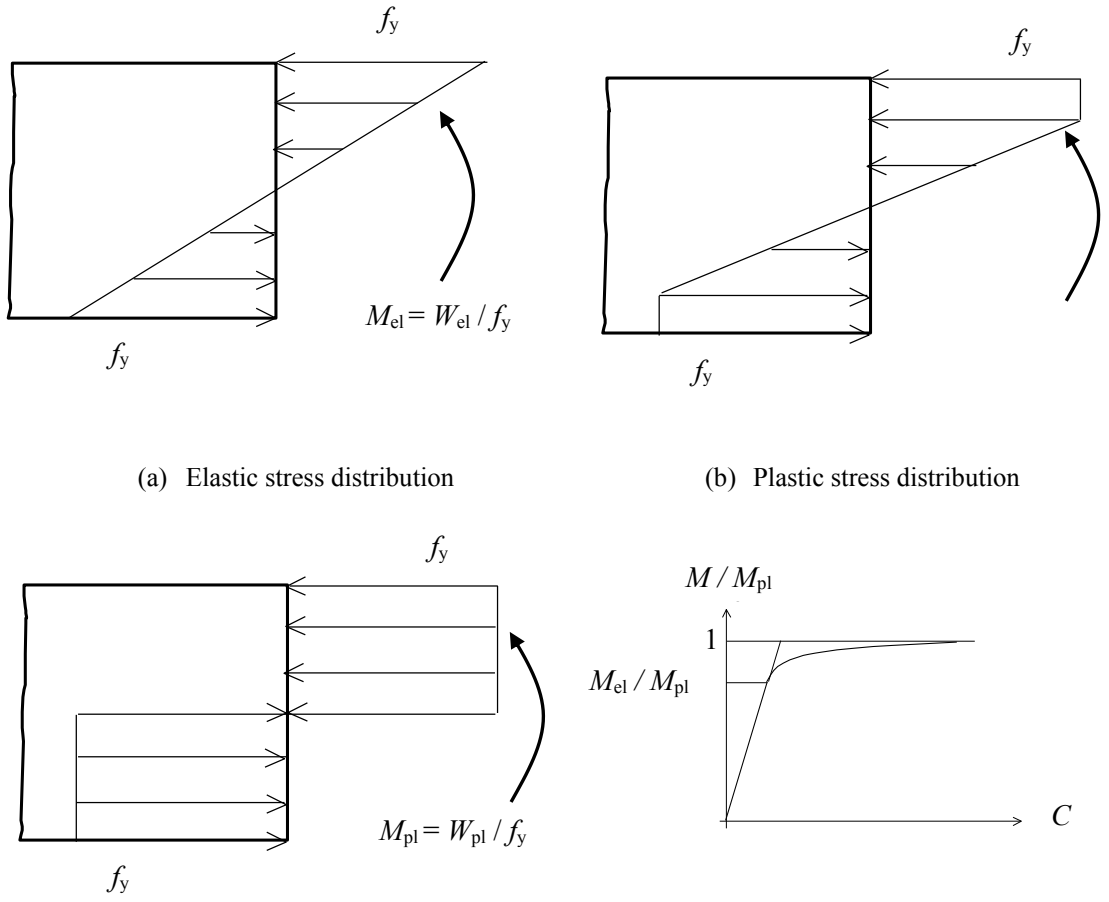

(a) Elastic stress distribution

(b) Plastic stress distribution

(c) Plastic resistance

(d) Moment-curvature law

Figure 2-30. Sectional plastic behavior for bending moments

Figure 2-30.d depicts the relationship between the bending moment (M) and the curvature of the section (C). Figure 2-30.d shows that the actual behavior of the section consists of a linear elastic branch until reaching the elastic moment M_{el} followed by a curved plastic branch that tends to converge to an idealized horizontal branch corresponding to $M = M_{pl}$; commonly this complex behavior is idealized to simpler multilinear laws. The behavior depicted by Figure 2-30.d is termed as "plastic hinge".

Figure 2-30 shows that, for sections that are symmetric with respect to the strong axis, the elastic and plastic moments and the corresponding section moduli (W_{el} and W_{pl}, respectively) fulfill the following relations:

$$M_{el} = f_y W_{el} \qquad M_{pl} = f_y W_{pl} \qquad W_{el} = 2I/h \qquad W_{pl} = 2S_y \tag{2-17}$$

I is the moment of inertia with respect to the neutral axis and S_y is the first moment of area of the part of the section that is situated above the neutral axis. The ratio ψ between the plastic and elastic section moduli ($\psi = W_{pl} / W_{el} = M_{pl} / M_{el}$) is termed as shape factor; for I and H sections ψ is approximately equal to 1.14 and 1.10, respectively.

Classification of sections. Regarding local plastic analysis, the sections (mainly the hot-rolled ones and the welded girders) are grouped in classes with respect to the onset of local buckling (generated by longitudinal normal stresses, i.e. those produced by axial forces and bending moments) compared to the inception and the full development of the plastification of the section generated by a bending moment alone (e.g. pure bending). The Eurocode 3 [EN 1993 2005] considers four classes of sections; they are termed 1, 2, 3 and 4, respectively. In section class 4, the moment that generates local buckling is lower than the elastic moment (M_{pl}); therefore, both the global and local analyses must be elastic and the strength of the section is given in terms of the effective parameters (A_{eff} and W_{eff}) that correspond to the initial section minus the buckled parts. In section class 3, the moment that generates local buckling is located in between the elastic and plastic moments (M_{el} and M_{pl}); therefore, both the global and local analyses must be elastic and the strength of the section is given in terms of the elastic parameters (A and W_{el}). In section classes 2 and 1, the local buckling arises after the total plastification of the section; the difference between classes 2 and 1 lies in that in class 1 the onset of buckling is far (in terms of rotation of the plastic hinge) from the total yielding of the section as to allow the bending moments law redistribution needed for global plastic analysis. In other words, for class section 1 the global and the local analyses can be plastic while for class section 2 the local analysis can be plastic but the global analysis has to be elastic. The American code [AISC 2010; AISC 360-10 2010] classifies the section in three groups: compact, semi-compact and slender; slender sections are approximately equivalent to class 4, semi-compact correspond roughly to class 3 and compact can be identified with classes 1 and 2. As discussed previously, reliable inelastic deformation requires that width-thickness ratios of compression elements be limited to a range that provides a cross section resistant to local buckling into the inelastic range. [AISC 2010; AISC 360-10 2010], uses the term "compact" for steel cross sections that are expected to be able to achieve the full plastic section capacity; in [AISC-327 2010], a higher level of compactness (termed "seismically compact") is required of beams and columns. Seismically compact sections are expected to be able to achieve a level of deformation ductility of at least 4. To be seismically compact, [AISC-327 2010] requires member flanges to be continuously connected to the web(s) and the width-thickness ratios of the compression elements must be less than or equal to those that are resistant to local buckling when stressed into the inelastic range. Limiting width-thickness ratios for compression elements are provided.

The class of a section depends on the steel grade (the yielding point f_y), the internal force (principally axial force or pure bending) and, mainly, the slenderness of the compressed parts of the section (webs and flanges). Obviously, the class of a section is the highest of those of their parts. The design codes [EN 1993 2005; AISC 2010; AISC 360-10 2010; AISC-327 2010] contain Tables for the classification of sections.

Interaction between shear force and bending moment. In an I or H section, the shear force is basically resisted by the web and the bending moment is principally resisted by the flanges. Therefore, the plastic interaction of a section undergoing simultaneously a shear force and a bending moment consists of maintaining the resistance to the shear force and of reducing the resistance to the bending moment by deducting the web contribution. Figure 2-31 describes the interaction criteria contained in the European and American major design codes.

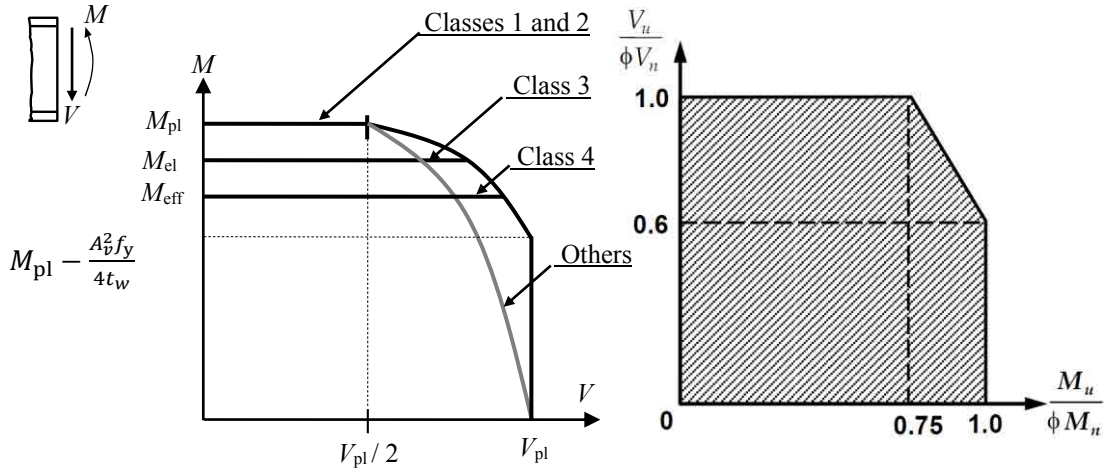

(a) European regulation [EN-1993 2005]

(b) American regulation [AISC 2010; AISC 360-10 2010]

Figure 2-31. Plastic interaction between a shear force and a bending moment

Figure 2-31.a shows that the Eurocode 3 [EN 1993 2005] states that if the demanding shear force does not reach half of the resistance of the section (V_{pl}), the interaction can be neglected. The term $M_{pl} - \frac{A_v^2 f_y}{4t_w}$ represents the bending moment that can be resisted by the flanges alone; t_w is the web thickness. In Figure 2-31.a M_{eff} is the moment resisted by the effective section ($M_{eff} = W_{eff} f_y$). The interaction represented in Figure 2-31.a is parabolic. Figure 2-31.b displays the shear force-bending moment interaction diagram by the AISC regulation [AISC 2010; AISC 360-10 2010].

Interaction between axial force and bending moment. Since the axial force and the bending moment generate axial stresses (σ), it is expected that their interaction is more severe than the one between the shear force and the bending moment; in fact, in elastic analysis that interaction is linear, i.e. the most severe that can exist. Figure 2-32 describes the interaction criteria contained in the European and American major design codes. Figure 2-32.a shows that, for bending along the strong (major) axis and classes 1 and 2, the Eurocode 3 [EN 1993 2005] states that if the demanding axial force does not reach one fourth of the resistance of the section (0.25 N_{pl}) and half of the resistance of the web (0.5 h_w t_w f_y), the interaction can be neglected. The Eurocode 3 considers the dimensionless coefficients n and a; n is the ratio between the demanding axial force and the plastic resistance ($n = N / N_{pl}$) and a is the ratio between the web area and the total section area ($a = [A - 2\ b\ t_f] / A$; $A \leq 0.5$). For I and H sections experiencing bending along the strong axis, the interaction criterion is linear, for class 1 and 2 sections it is given by $M = M_{pl} (1 - n) / (1 - 0.25\ a)$. For bending along the weak axis, the interaction can be neglected if $n \leq a$ (the demanding force does not exceed the capacity of the web); if $n > a$, the interaction is parabolic. For classes 3 and 4 the interaction is linear. In the Eurocode 3, for bi-axial bending the interaction criterion between the moments along both axes is basically quadratic. Conversely, in the American regulations [AISC 2010; AISC 360-10 2010] all the interactions are basically linear, as shown by Figure 2-32.b. Figure 2-32.b displays the 3-D interaction criterion for bi-axial composed bending.

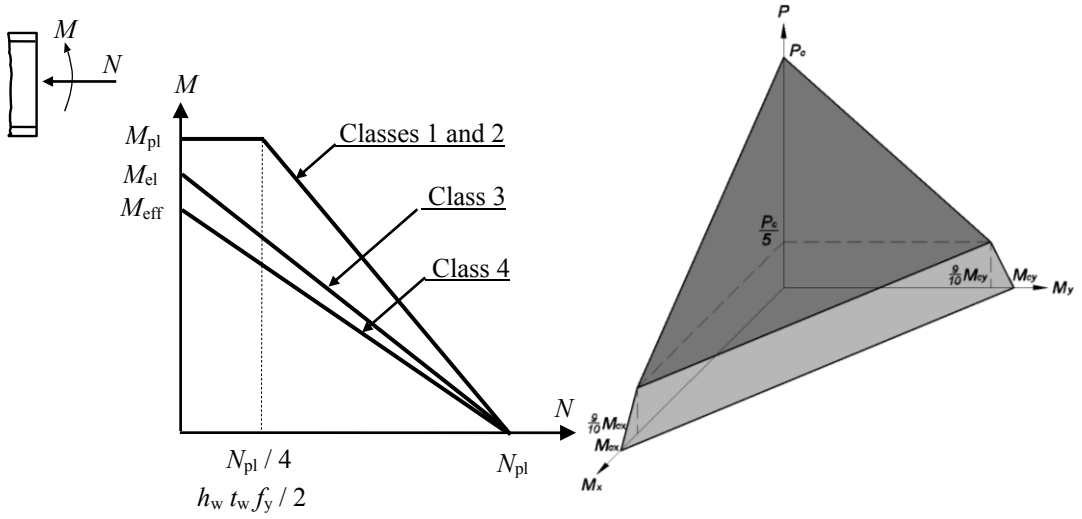

(a) European regulation [EN-1993 2005]

(b) American regulation [AISC 2010; AISC 360-10 2010]

Figure 2-32. Interaction between an axial force and bending moments for I or H sections

Figure 2-32.b shows that in double-symmetry sections if $P_r \geq P_c / 5$ then the interaction criterion is $\frac{P_r}{P_c} + \frac{8}{9}\left(\frac{M_{rx}}{M_{cx}} + \frac{M_{ry}}{M_{cy}}\right) \leq 1$ and if $P_r < P_c / 5$ then the interaction criterion is $\frac{P_r}{2P_c} + \left(\frac{M_{rx}}{M_{cx}} + \frac{M_{ry}}{M_{cy}}\right) \leq 1$. P_r and P_c are the demand and strength values of the compressive force, M_r and M_c have similar meanings referred to bending moment; sub-indexes x and y refer to bending with respect to the strong (major) and weak (minor) axes, respectively.

Interaction between shear force, axial force and bending moment. The Eurocode 3 [EN-1993 2005] states that if the demanding shear force does not reach half of the resistance of the section, then the interaction with the shear force can be neglected and only the interaction between the axial force and the bending moment has to be considered. If the demanding shear force exceeds half of the resistance of the section, also only the interaction between the axial force and the bending moment has to be considered but the shear area (A_v) is reduced by factor $1 - \rho$, where $\rho = (2\, V / V_{pl} - 1)^2$. V is the demanding shear force.

2.2.4 Steel structures

The available steel products previously described are used to form a wide variety of steel structures; among them: buildings, multipurpose buildings, stadiums, hangars, bridges (car, railway and pedestrian), warehouses, industrial facilities, stacks (chimneys), communication towers, antennae, traffic control towers, oil towers, stations, railways, electric power transmission towers, wind mills, silos, tanks, containers, pipes, offshore structures, piles, sheet piles, cable cars, chairlifts, monuments, sculptures, observation platforms, etc. As well, steel members can be used for structural retrofit. Virtually any structural or constructional need can be fulfilled with steel; moreover, even if other solutions are preferred (concrete, timber), the use of steel in mandatory (reinforcement bars, connexion elements, etc.). Remarkably, steel is also widely employed in other sectors, such as tools, machinery, mining, naval, aerial, military, automotive, sanitary, rail industry, bike, among many others. Since this Thesis deals with conventional steel buildings, next subsection focusses on them.

2.2.5 Steel buildings

This work deals with multistory steel buildings; their structure is composed of columns, slabs and, eventually, bracing members. The columns are made of ordinary hot-rolled steel I-shaped profiles and the slabs consist of an orthogonal network of (main) beams and joists also made of I-shaped hot-rolled steel profiles; the upper flanges of beams and joists form a flat surface that supports a

steel deck (folded plate) topped with a (reinforced) concrete layer. Figure 2-33 depicts sketches and images of steel structures of multistory buildings.

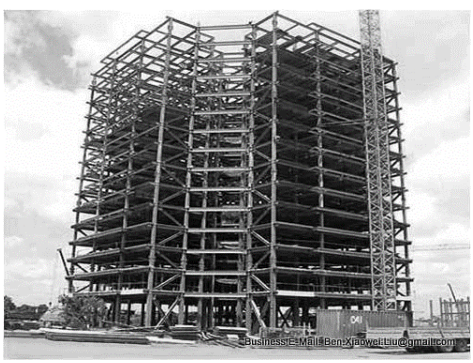

(a) Midrise steel frame

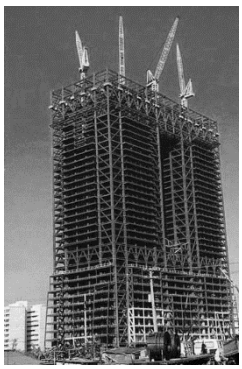

(b) High rise steel frame

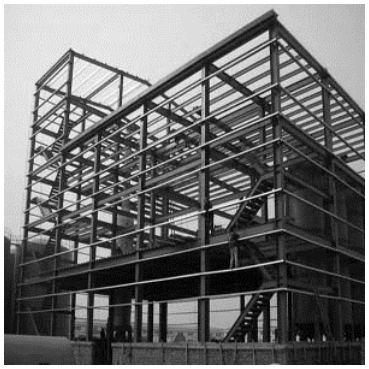

(c) Low rise steel frame

(d) Unbraced steel frame

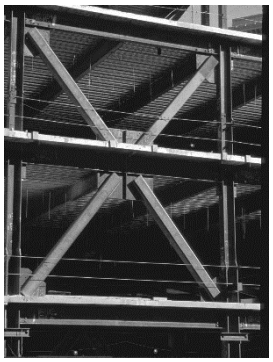

(e) Braced steel frame (concentric)

(f) Braced steel frame (eccentric)

Figure 2-33. Steel structures of multistory buildings

In the concrete-steel composite slabs, shear connectors (studs) can be installed between the top concrete layer and the lower steel members to avoid sliding along the contact; such connectors are intended to absorb the shear stress thus guaranteeing a joint work of concrete and steel. Figure 2-34 depicts sketches and images of shear studs.

(a) Installation of shear connectors (studs)

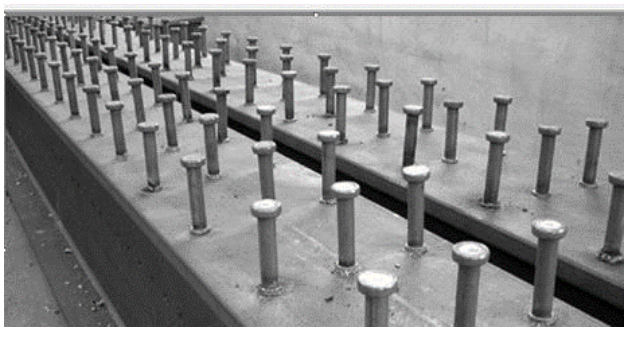

(b) Installed shear connectors

Figure 2-34. Shear connectors

The steel bracing elements, if any, are usually made of I-shaped, L-shaped, channel, HSS (Hollow Square Section) or CSS (Circular Square Section). Such braces can be installed either as diagonal

or chevron members. Figure 2-35 depicts sketches and images of braced steel structures of multistory buildings.

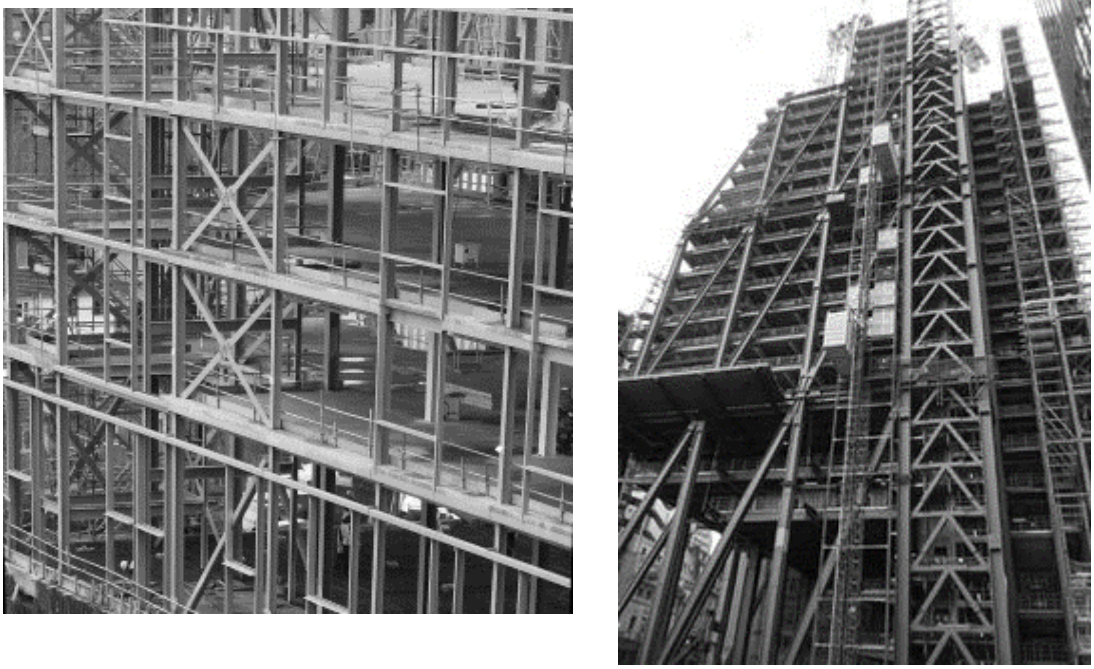

(a) Diagonal (X) braces (b) Chevron (V) braces

Figure 2-35. Braced steel structures of multistory buildings

Remarkably, in Figure 2-33 the lateral resistance is contributed merely by the rigidity of the beam-column connections while in Figure 2-35 it relies mainly in the bracing elements.

If the columns, instead of being merely steel members, are made either of hollow steel profiles filled with concrete or of concrete section reinforced with steel profiles, the buildings' structure is commonly termed as composite concrete-steel. This Thesis deals only with steel buildings.

In any steel construction, particular attention must be paid to the structural connections among different members. As is well known, two major types of joints exist: bolted and welded; globally speaking, satisfactory performance can be obtained with any of them. Figure 2-36 and Figure 2-37 depict sketches and images of bolted and welded connections, respectively.

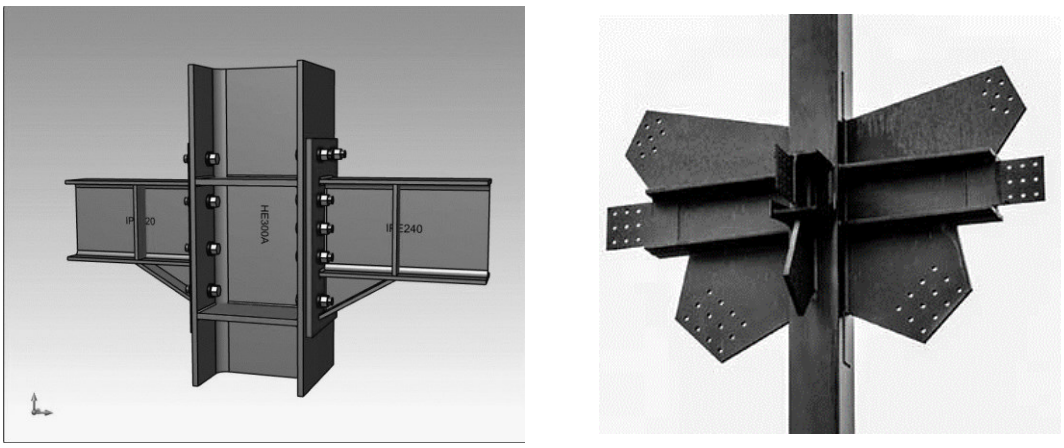

(a) Beam-column (b) Beam-column-brace

Figure 2-36. Bolted connections

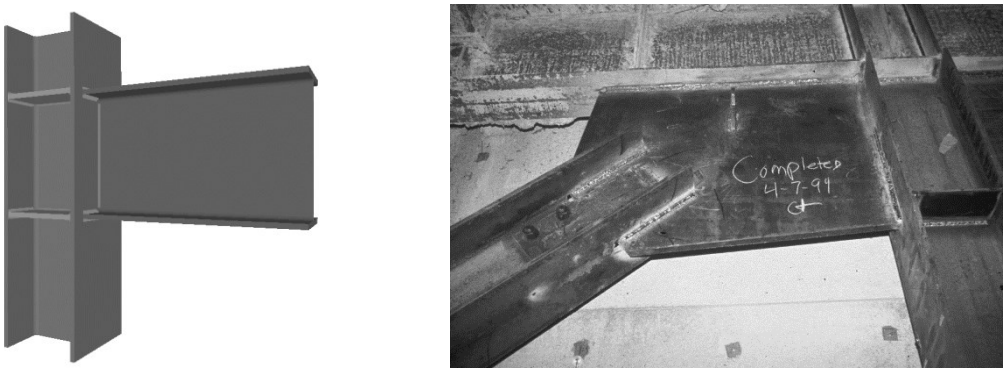

(a) Beam-column (b) Beam-column-brace

Figure 2-37. Welded connections

Figure 2-36 and Figure 2-37 represent basically connections between different structural members, either columns, beams or braces; however, it should be kept on mind that also splices joining several segments of a single member are commonly required, mainly for constructional reasons.

The connections can be classified with respect to their rigidity in three major groups: hinged, rigid and semi-rigid. Hinged connections are those whose moments have only residual importance in the overall structural behavior. Rigid connections are those effectively preventing relative connections among the connected members. Semi-rigid connections behave intermediately between hinged and rigid ones. Recently, the use of semi-rigid connections has been promoted because of their lower cost (compared to rigid connections) and of the beneficial effect on the bending moment laws redistribution. Globally speaking, semi-rigid connections are not recommended for earthquake-resistant buildings; however, some studies [Kumar, Rao 2004; Abolmaali et al. 2009] have pointed out their important energy dissipation capacity and how this quality might be convenient for seismic use.

The comparison between bolted and welded connections shows advantages and drawbacks of each of them. Advantages of bolted connections: less need for specialized workers, lack of induced fragility (because of thermal initial stresses), no energy consumption, more uniform and easily verifiable quality, easier dismantling. Advantages of welded connections: less voluminous unions, easier solutions for geometrically complex connections, tolerance with geometrical irregularities, no previous damage in the connected members (e.g. piercing, squashing). Therefore, different solutions are commonly preferred for different situations.

Given the current limited structural use of timber and of other materials, the only serious competitor of steel buildings are concrete buildings; compared to concrete, steel possesses the following major advantages:

- High strength-weight ratio.
- Tensile strength.
- Weldability. Moreover, bolted connections are also possible
- Isotropy.
- Uniformity.
- Simple and reliable structural behavior. The structural behavior is rather simple because of the equal compressive and tensile behavior, the isotropy, the linearity (in the elastic range), and the absence of any relevant rheology effect.
- Construction. Several advantages: rapidity, insensitivity to cold weather conditions, neither molds no shores are required, less possibility for human errors, and high prefabricability.

Conversely, steel exhibit other less desirable characteristics:

- Higher cost.
- Corrodibility.
- Controversial sustainability.
- Insufficient fire resistance.
- Higher vibrations. The inherent low damping and mass of steel building structures mainly generate this effect. One main consequence are stronger resonance effects, with higher vibration amplitudes. This applies to most of the feasible excitations such as wind gusts, human excitation, nearby traffic and vibrating machinery.

Moreover, for earthquake-resistant design, steel provides other relevant qualities:

- High ductility.
- Lightweight.

Given the abovementioned circumstances, steel construction is preferred when their advantages prevail; globally speaking, this happens for high span-length and for mid-height to tall buildings, mainly located in developed countries. As discussed in the next subsection, high seismicity also encourages the use of steel construction.

2.2.6 Earthquake-resistant steel buildings

In the previous subsection it has been preliminary pointed out that steel construction possesses two major earthquake-resistant qualities: lightweight and ductility. Conversely, steel structures exhibit a rather low inherent damping; this being extremely harmful for a proper seismic performance. Globally speaking, the earthquake-resistant design of steel buildings tries to take profit of both advantages while attempting to compensate this drawback. This subsection discusses more deeply the global earthquake-resistant qualities and shows how the design of steel buildings is oriented to collect such characteristics.

For any building, the overall quality of the seismic resistance can be formulated in terms of the following major features:

1. **Lateral resistance**. Since the buildings are more vulnerable to the horizontal components of the seismic ground motion than to the vertical ones, it is obvious that buildings should possess enough lateral resistance. In steel buildings, moment-resisting frames or braced frames are the only structural configurations that can provide enough lateral strength; frames whose beams are hinged to the columns are not a valid option since the horizontal stiffness would be provided only by the columns working as cantilevers.
2. **Plan symmetry**. Plan symmetry means that, at every story, the centers of mass and of rigidity are near coincident; remarkably, the center of mass refers to the upper part of the building and not to the considered floor only. The major advantage of designing symmetric buildings is that twisting motion (torsion) is minimized and, thus, the risk of collapse of any column (or any supporting member) that is far from the center of rotation is low. Obviously, the exact match between the centers of gravity and of rigidity is virtually impossible; consequently, if their eccentricity is lower than 5% of the building plan dimension, the building is commonly considered as symmetric. Conversely, given the sensitivity of the center of gravity to any irregular load distribution, even if a given building would result exactly symmetric, accidental eccentricity has to be considered to cope with such uncertainty; about that, the earthquake-resistant regulations state that 5% of the building size is enough.
3. **Uniformity in elevation**. As discussed in the previous section, the destructive effect of the ground motion can be more faithfully represented in terms of input (or hysteretic) energy; therefore, the uniformity in elevation is crucial, mainly in terms of energy dissipation capacity. Certainly, uniformity is more critical in the lowest floors, thus avoiding the risk of premature (brittle) collapse mechanisms. The requirement of uniformity does not prevent buildings with irregular elevation but the changes must be gradual and rather uniformly distributed.
4. **Diaphragm effect**. This quality means that each floor slab should be virtually infinitely rigid in its own plane; in other words, the plan configuration of each slab remains unchanged during the motion duration. Obviously, this quality is reached thanks to the high in-plane stiffness of the slab. Under normal conditions, most of the ordinary slabs of concrete or steel buildings guarantee the diaphragm effect because of the topping concrete layer; only exceptions are timber slabs (they do not have any concrete layer) of slabs with exceptionally high aspect ratio. Moreover, light steel roofs or prefabricated slabs or roofs without top concrete layer might not possess enough in-plane stiffness to assure the diaphragm effect. The main benefits of the diaphragm effect are: a complete monolithic structure, a lack of risk of slab failure, and an even distribution of the seismic forces among the vertical resisting members (e.g. without premature local collapses).
5. **Plan compactness**. This quality is strongly linked to the diaphragm effect since slabs with exceptionally high aspect ratio might not possess enough in-plane stiffness and strength. As well, plan layouts with deep inbounds might exhibit unsatisfactory performance.
6. **Lightweight**. Since the equivalent earthquake forces are proportional to the weight of the building, it is obvious that any mass increase is obnoxious; moreover, in general, the effect of the top masses is higher than the one of the bottom ones. Apart from timber buildings, steel structures provide less self-weight among all the concrete-based competing construction techniques.
7. **Torsion resistance**. Twisting motion (e.g. rotation with respect the vertical axis) is extremely harmful for the columns, mainly for those that are located at the opposite corners from the center of rotation; moreover, columns are exceptionally important for preventing the collapse of the building. Therefore, torsion strength is a highly relevant quality. Remarkably, torsion resistance is not only necessary for asymmetric buildings but also for symmetric ones since twisting motion can be generated both by accidental eccentricities (between the centers of mass and of rigidity) and by the rotational components of the seismic input. Typically, stair and elevator cases are situated commonly near the center of the building and frequently the supporting shear walls provide supplemental lateral stiffness and strength; however, the torsion resistance might be insufficient and additional elements should be provided in the perimeter of the building.

8. **Ductility**. Ductility can be defined as the reserve of strength after the onset of damage; in other words ductility is the margin between the yielding and ultimate values (see Figure 2-15 and Figure 2-22). Such margin can be either formulated in terms of displacement and of ductility. Subsection 2.1.6.3 describes the concept of ductility and its role in the determination of the response reduction factor. The benefit of ductility is the remoteness of the collapse; conversely, it should be kept on mind that taking profit of the ductility to reduce the input implies that important damage will arise under the design input. Globally speaking, the ductility depends on the type of lateral resisting system and of the quality of such system. About the first issue, the design codes incorporate empirical expressions of the response reduction factor for the most common structural types; the most relevant trend is that braced frames or shear walls are more ductile than bare frames. About the second issue, EC-8 [EN-1998 2004] defines three levels of quality termed as "ductility classes": L (low), M (medium) and H (high). Ductility class L corresponds to buildings that have been designed without accounting for any seismic provision, e.g. fulfilling only the prescriptions of Eurocode 2. To provide the appropriate amount of ductility in ductility classes M and H, specific provisions for all structural elements shall be satisfied in each class; namely the section class, even accounting for the rotation capacity (subsection 2.2.3). In correspondence with the different available ductility in the two ductility classes M and H, different values of the behavior factor q (subsection 2.1.2) are used for each class. Remarkably, for Moment-Resisting Frame Buildings the maximum value of q is 4 for ductility class M and 8 for ductility class H. The American regulations propose similar classifications.
9. **Damping**. The damping of a construction can be defined as its dynamic capacity of absorbing (or dissipating) energy without experiencing further damage. For the sake of simplicity damping is commonly described by linear viscous models (see equation (2-1)) being typically characterized by the critical damping factor ζ (equation (2-3)); by default it is usually assumed that $\zeta = 0.05$. Obviously, damping is always beneficial since, for highly damped structures, during the duration of the input the effect of the previous shaking is rapidly damped out. Therefore, one of the main objectives of any earthquake-resistant design is to provide as much damping as possible. Unfortunately, this task is highly cumbersome unless special techniques (e.g. seismic isolation, energy dissipators) are considered.
10. **Structural redundancy**. This quality refers to the duplicity (or even multiplicity) of the seismic protective systems. It means that, for example, at least two braced spans should exist in each of the façades of the building. The benefit of this quality arises from the reserve of safety in the event of failure of one of the duplicated (redundant) elements.
11. **Strong column-weak beam**. This quality is as widespread that "strong column-weak beam" (SCWB) has become a somewhat highly extended aphorism. It means that, under severity-growing inputs, in each joint the failure of the beams should precede the one of the columns. The benefit of this quality is obvious: since the columns are more vital to the structural safety than the beams, the risk of premature collapse mechanisms is minimized. Despite this condition should be fulfilled for all of the joints, it is more relevant for the lower stories than for the top ones. This requirement has one important practical consequence: globally speaking, the strengthening of the beams of a building can impair its seismic performance rather than improving it. Remarkably, for a given input intensity, the strengthening of the beams provides a better structural performance but for more severe inputs, this situation can be inverted.
12. **No "short columns"**. The short-columns mechanism consists of the shear failure of columns because of the restraining effect of partial-height infill masonry walls. Noticeably, this phenomenon can arise also for full-height infill masonry walls if they slide along horizontal courses. This issue is highly relevant for concrete framed structures but is not so important for steel frames since the steel columns are much stronger than the infill walls and are also more ductile.
13. **Subjection and strengthening of non-structural components**. Because of the absolute acceleration, the non- structural components can fall, thus causing extensive damage and even fatalities. This risk is particularly relevant for façade elements, such as balconies, cladding and curtain walls, panels, appendages, ornaments, railings, balustrades, among others. Inside

elements such as machines, appliances, tall bookshelves, racks, can be also dangerous. Obviously, this recommendation applies both to concrete and steel buildings.

14. **Monolithic foundations**. In buildings with isolated footing foundation (e.g. columns founded on unconnected footings), the horizontal relative displacements among aside bearings can be extremely harmful for the structural integrity. This effect can be avoided by connected the adjoining footings with tying beams, e.g. structural members that are capable of absorbing the arising axial forces thus guaranteeing the constant distance among the footings. This issue is relevant both for concrete and steel buildings; perhaps it is more crucial for concrete frames.
15. **Neither interrupted columns nor dared cantilevers**. It is widely accepted that most of the buildings are more vulnerable to the horizontal components of the seismic ground motion than to the vertical ones; however, this statement fails if strong irregularities occur. The highest risk appears mainly under two circumstances: (i) if some of the columns are not continuous down to foundation but their continuities are interrupted to allow for empty spaces or (ii) there are important cantilevers, both in terms of the cantilever length or supported weight. This recommendation applies both to concrete and steel buildings being perhaps more crucial for concrete constructions because of its biggest weight.
16. **Structural simplicity**. The structural earthquake-resistant design of buildings is a highly complicated task because of the important complexity of the nonlinear dynamic behavior of buildings and, mainly, because of the wide variety of collapse modes. Remarkably, the wide availability of advanced software codes for structural analysis and design does not reduce at all the need of a deep understanding of the structural behavior of the buildings. Therefore, the simpler the structure the less the risk of undetected failure modes. Obviously, this recommendation does not prevent the proposal of complex structures; but highly complicated buildings require a careful and juicy analysis (thinking). For this objective, the software codes are only of little use.
17. **Separation from aside buildings**. The lateral collisions among adjacent buildings ("pounding effect") are extremely dangerous, mostly if the slabs are unaligned (e.g. at different levels) because the columns of walls might collapse when receiving the impact of the nearby slabs. The easiest and most efficient solution is to provide enough gaps among the involved buildings; the use of seismic bumpers has been also suggested.

In a wide sense, the earthquake-resistant design of any building consists of seeking these qualities. With this aim, several structural solutions have been proposed: (i) MRF (Moment Resistant Frames), (ii) CBF (Concentrically Braced Frames), (iii) EBF (Eccentrically Braced Frames), (iv) Dual systems, (v) Special Truss Moment Frames, (vi) Outrigger walls, (vii) Base isolation and (viii) Energy dissipators. Each of these solutions is described and discussed next. The Eurocode 8 [EN-1998 2004] considers also "Inverted Pendulum Structures"; they are not discussed here given that this Thesis deals basically with steel multistory buildings.

MRF (Moment Resistant Frames). The Moment Resistant Frames consists of vertical and horizontal elements (beams and columns, respectively) which are rigidly connected among them. Figure 2-38 displays a sketch and an image of Moment Resistant Frames.

(a) Sketch of a Moment Resisting Frame (b) Image of a Moment Resisting Frame

Figure 2-38. Earthquake-resistant buildings. Moment Resisting Frames

Figure 2-38.b shows that, commonly, only some parts of the frames are earthquake-resistant (e.g. with rigid connections among beams and columns, indicated as "Seismic frame" in the Figure) while the other connections are merely hinged. This solution is adopted for simplicity and economy. The seismic parts of the frames should be distributed as ordinary bracings; it means that have to be continuous down to foundation and the plan layout need to be symmetric and as separated as possible (to provide torsion resistance).

In MRF the Eurocode 8 [EN-1998 2004] states that the dissipative zones should be mainly located in plastic hinges in the beams or the beam-column joints so that energy is dissipated by means of cyclic bending. However, the dissipative zones may also be located in columns in the following three cases: (i) at the base of the frame, (ii) at the top of the columns in the upper story of multi-story buildings and (iii) at the top and bottom of little compressed columns in single-story buildings. The Eurocode 8 specifies the behavior factors (q) to be considered for MRF buildings: for ductility class M is $q = 4$ and for ductility class H is $q = 5\ \alpha_u / \alpha_1$ where the ratio α_u / α_1 plays the role of the over-strength factor (Ω) discussed after Figure 2-22 and equation (2-16). Factor α_u / α_1 can be obtained either by push-over analysis or by empirical estimations; the Eurocode 8 suggests using 1.1 for single-story single-bay frames, 1.2 for multi-story single-bay frames and 1.3 for multi-story multi-bay frames. In any case, the maximum value of α_u / α_1 that may be used is 1.6.

The North-ridge earthquake (1994) showed a big number of brittle failures in the connections of many steel buildings; thus generating premature global collapse (or severe damage). After that seismic event, an important theoretical and experimental research activity was undertaken [FEMA 355D 2000] leading to the proposal of a number of pre-qualified connections; i.e. connections that exhibit highly ductile behavior. Such connections are comprehensively described in the [FEMA 350 2000]. The main design objective is that the inelastic drift is accommodated through the development of plastic flexural deformation (plastic hinges) within the beam span, remote from the face of the column, see Figure 2-39. Such behavior may be obtained by locally stiffening and strengthening fully restrained connections by using cover plates, haunches and similar detailing, such that the ratio of flexural demand to plastic section capacity is maximum at these interior span locations (see Figure 2-39.b). This condition can also be obtained by locally reducing

the section of the beam at desired locations for plastic hinging to obtain a condition of maximum flexural demand to plastic section capacity at these sections (see Figure 2-39.b).

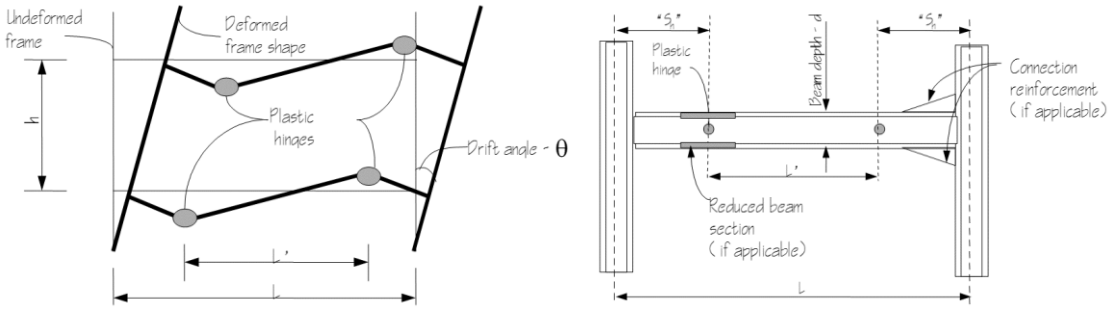

(a) Inelastic Behavior of Frames with Hinges in Beam Span

(b) Location of Plastic Hinge Formation

Figure 2-39. Desired locations of plastic hinges [FEMA 350 2000].

FEMA 350 present data on a series of prequalified connections, from which an appropriate connection type may be selected. Alternatively, if project-specific connection qualification can be performed, a connection of any configuration that provides the appropriate interstory drift capacity and meets the strength and stiffness demands for the structure may be selected.

Figure 2-40 displays a few examples of prequalified connections. Each of the connection prequalification is limited to specific conditions for which they are applicable, including member size ranges, grades of material and other details of the connection. The connections are grouped in the following categories: “Prequalified Welded Fully Restrained Connections”, “Prequalified Bolted Fully Restrained Connections”, and “Prequalified Partially Restrained Connections”. As well, some “Proprietary Connections” are also described, see Figure 2-41.

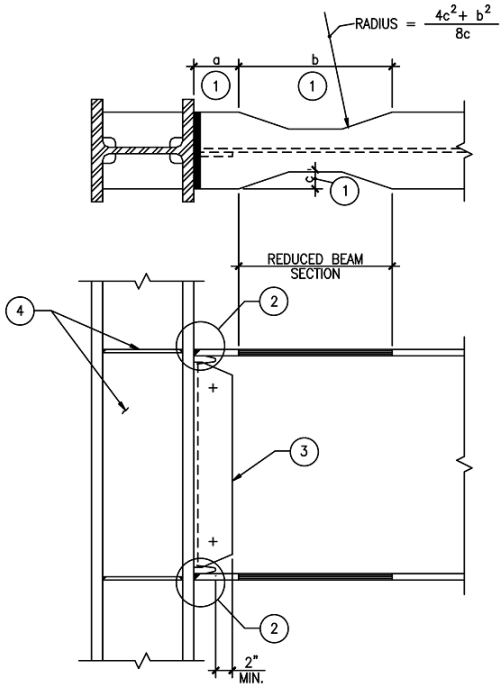

(a) Reduced Beam Section (RBS) Connection

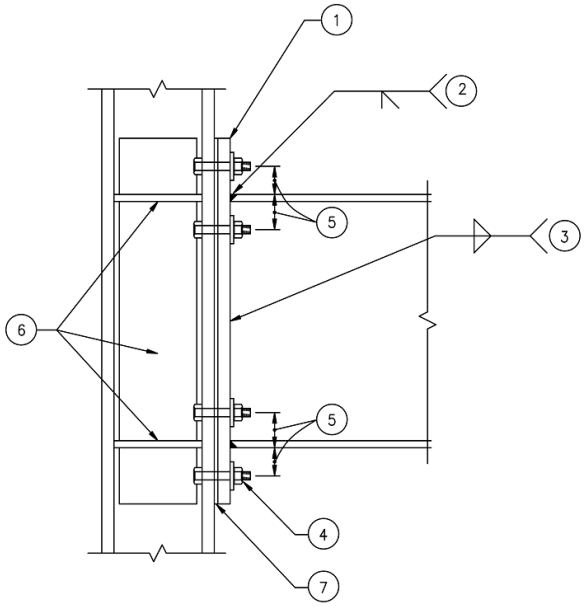

(b) Bolted Unstiffened End Plate (BUEP) Connection

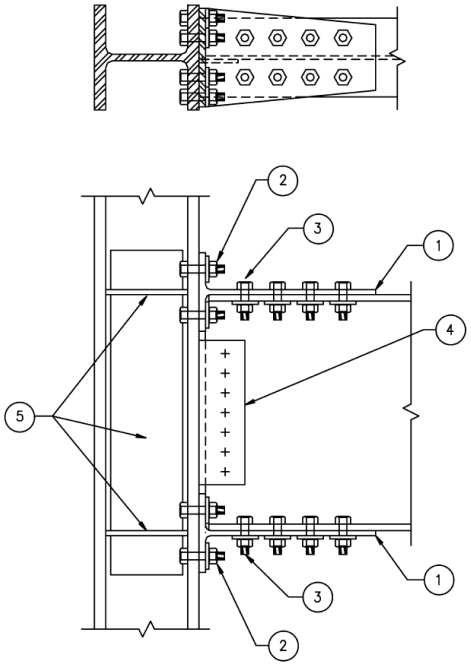

(c) Double Split Tee (DST) Connection

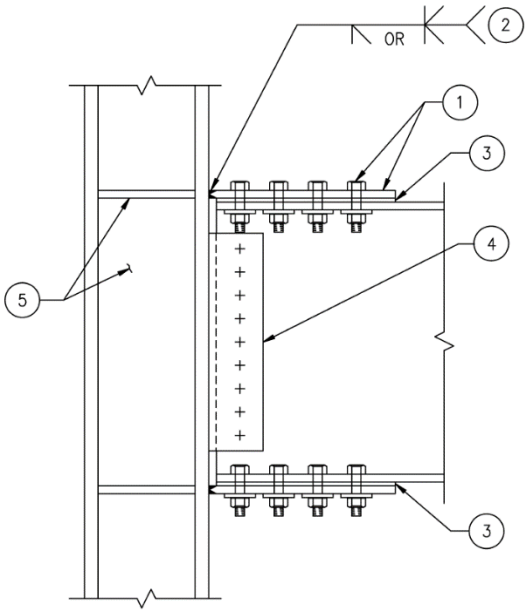

(d) Bolted Flange Plate (BFP) Connection

Figure 2-40. Pre-qualified steel connections [FEMA 350 2000]

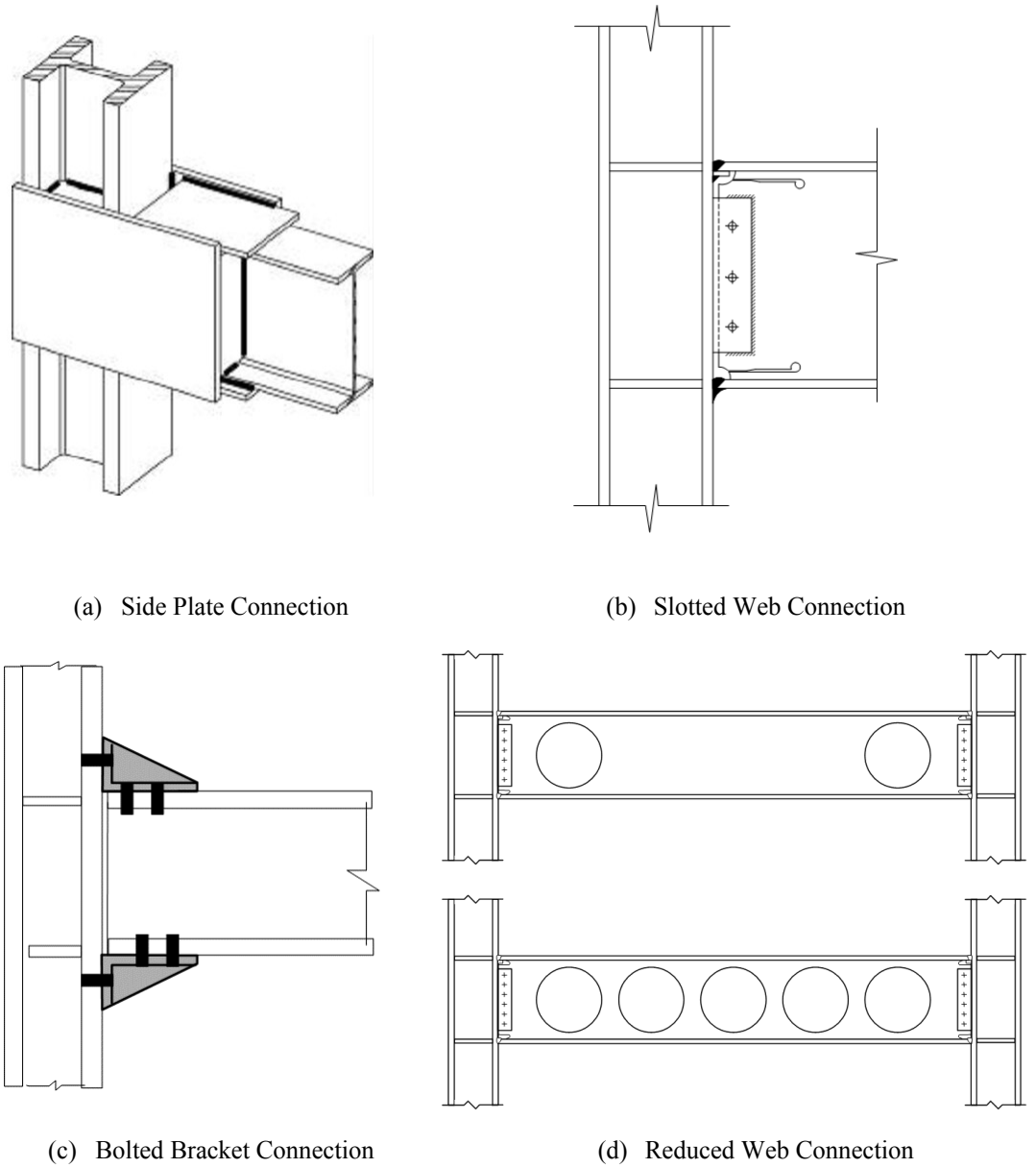

(a) Side Plate Connection

(b) Slotted Web Connection

(c) Bolted Bracket Connection

(d) Reduced Web Connection

Figure 2-41. Proprietary steel connections [FEMA 350 2000]

CBF (Concentrically Braced Frames). The Concentrically Braced Frames are frames stiffened by bracing members; "Concentrically" means that, in the connections between main members (e.g. beams and columns) and braces, all the axes of the members are intersected in a single point. Prior of describing the different types of bracing systems that have been proposed, it should be stated that the previously discussed qualities "Plan symmetry" and "Torsion resistance" require that at least four braces are installed per floor (one per façade, in fact). Moreover, accounting for the "Structural redundancy" quality, to duplicate those elements might be convenient. As well, the quality "Uniformity in elevation" demands that, globally, the same number of braces are considered along the height of the building. Figure 2-42 displays the most common bracing systems for building structures.

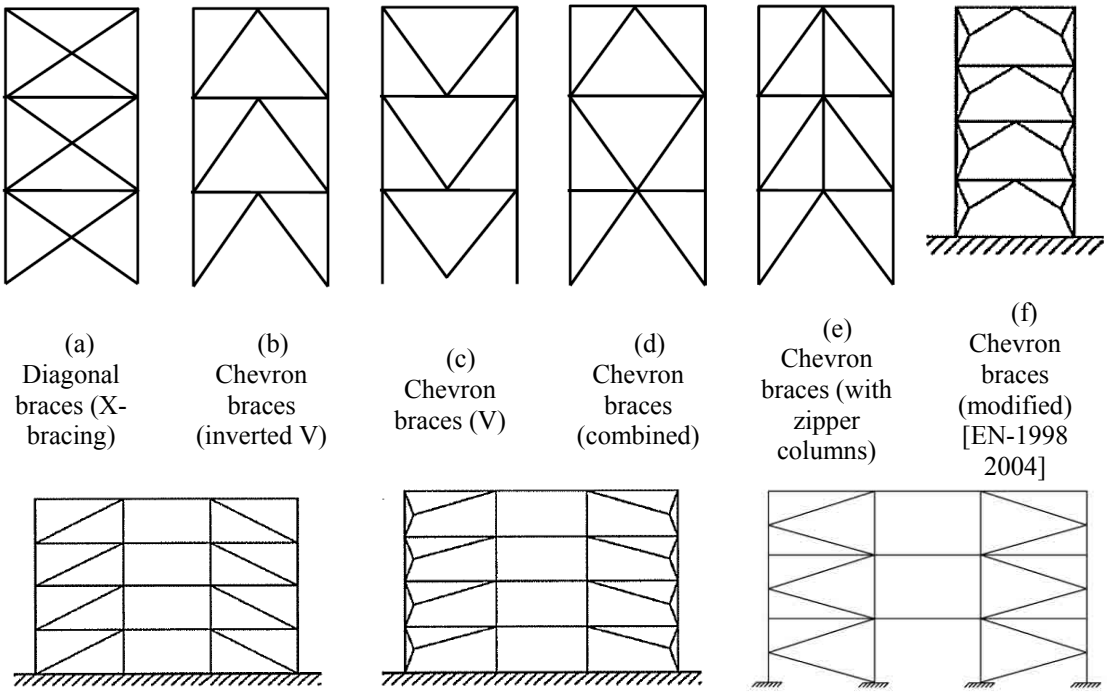

(a) Diagonal braces (X-bracing)

(b) Chevron braces (inverted V)

(c) Chevron braces (V)

(d) Chevron braces (combined)

(e) Chevron braces (with zipper columns)

(f) Chevron braces (modified) [EN-1998 2004]

(g) Diagonal braces (tension only)

(h) Diagonal braces (tension only-modified) [EN-1998 2004]

(i) K-bracing [Elghazouli 2009]

Figure 2-42. Bracing systems

Figure 2-42.a displays diagonal braces, i.e. bars that join opposing corners. When interstory drift appears, alternatively one brace is compressed while the other one is tensioned; given that, there are two design approaches: either the compressed brace is designed to resist the buckling or its contribution is neglected and then the tensioned brace is designed to resist the force alone. Figure 2-42.g depicts tension-only diagonal braces. The Eurocode 8 [EN-1998 2004] states that the horizontal forces can be resisted by the tension diagonals only, neglecting the compression diagonals, and that the slenderness of the diagonal members should be under and upper bounded: the non-dimensional slenderness should be comprised in between 1.3 and 2; the top bound means that the buckling is prevented and the lower bound aims to avoid overloading columns in the pre-buckling stage. Figure 2-42.h shows a bracing system based on tension-only diagonal braces (similarly to Figure 2-42.g) which have been modified to allow for more available space for openings.

Figure 2-42.b to Figure 2-42.d show chevron bracing; Figure 2-42.b corresponds to inverted V configuration, Figure 2-42.c reflects V configuration and in Figure 2-42.d both types are alternated along the height of the building. Similarly to diagonal bracing, when interstory drift appears, alternatively one brace is compressed while the other one is tensioned. Globally speaking, the performance of V and inverted V bracings are similar and the main difference lies in the availability of space for openings. Comparison between diagonal and chevron bracing shows that the performance of the diagonal braces is higher since the direction of the braces is closer to the horizontal and, therefore, the axial forces in the braces and in the involved columns are smaller. Moreover, in chevron bracing the buckling of the braces needs to be prevented since otherwise vertical forces would be introduced in the connected beam (see Figure 4-8.b). In fact, the only actual advantage provided by the chevron bracing is the higher availability of space for openings, either doors (Figure 2-42.b) or windows (Figure 2-42.c). Figure 2-42.f shows a bracing system based on chevron braces that have been modified to allow for more available space for openings. Finally, Figure 2-42.e depicts a chevron bracing that includes “zipper” columns; such members are intended to avoid the collapse mode consisting of premature buckling of the compressed braces, see Figure 4-8.b.

Figure 2-42.i displays a K bracing. Similarly, to diagonal and chevron bracing, when interstory drift appears, alternatively one brace is compressed while the other one is tensioned; however, if the compressed brace buckles, horizontal forces are applied to the columns. Because of this serious risk, the Eurocode 8 [EN-1998 2004] bans K bracing. Remarkably, some authors term as K bracing other configurations, such as chevron braces or alternated tension-only diagonal braces; this can lead to misunderstandings.

The failure modes of the frames represented in Figure 2-42 consist of the combination of yielding or buckling of the braces and the formation of plastic hinges in the main members. The Eurocode 8 [EN-1998 2004] states that, in frames with concentric bracings, the dissipative zones should be mainly located in the tensile diagonals. The Eurocode 8 specifies the behavior factors (q) to be considered for CBF buildings: for ductility class M is $q = 4$ for diagonal braces and $q = 2$ for chevron braces and for ductility class H is $q = 4$ for diagonal braces and $q = 2.5$ for chevron braces.

Noticeably, if the bracing members were located on the same bay (e.g. vertically superposed, as in all the cases depicted in Figure 2-42) the bottom supporting columns would experience strong tension/compression forces due to the cumulative effect of the axial forces generated by the braces; obviously, this result is more intense in tall buildings. To avoid this concentration of forces, an effective solution is to distribute the braces along all the bays, as shown by Figure 2-43. Comparison between Figure 2-43.a and Figure 2-43.b shows that the horizontal layout of the braces generates a higher lever arm (e.g. the horizontal distance between the vertical reaction forces), thus leading to smaller vertical forces. Frequently, the "empty" spaces are also filled with braces, thus providing a kind of a "complete" (or dense) network of diagonal members for the frame. Remarkably, even that Figure 2-43 depicts diagonal braces, the same consideration can be applied to chevron bracing.

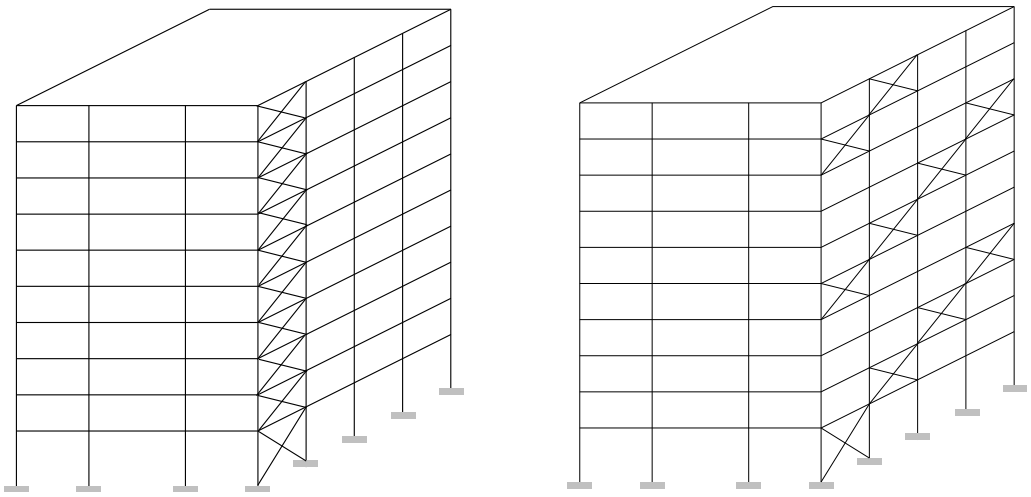

(a) Superposed braces (inconvenient) (b) Distributed braces (convenient)

Figure 2-43. Inconvenient and convenient layouts of braces

EBF (Eccentrically Braced Frames). This earthquake protective system consists of modifying the cases shown in Figure 2-42 (corresponding to Concentrically Braced Frames) in such a way that the axes of beams, columns and braces do not intersect in a single point. The purpose of this strategy is to shift the collapse modes to formation of hinges in the sections of the members where

the braces fall on; the segments comprised between such hinges constitute the dissipative parts of the structure and are commonly termed as "links". Given that the hinges are more dangerous for the overall structural stability in columns than in beams, the intersections between braces and main members should be located either in beams or in special-purpose members rather than in columns. Figure 2-44 depicts the proposed solutions, as described by the Eurocode 8 [EN-1998 2004].

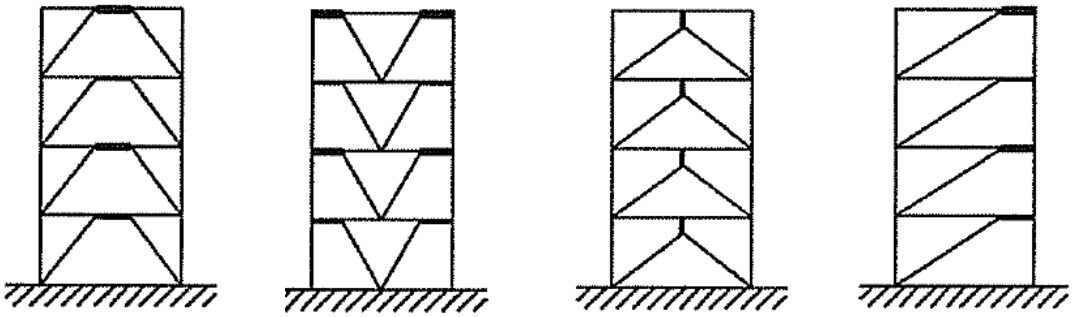

(a) Chevron braces (inverted V) | (b) Chevron braces (V) | (c) Chevron braces (inverted V with additional member) | (d) Tension-only diagonal braces

Figure 2-44. Eccentrically Braced Frames [EN-1998 2004]

In Figure 2-44.a, Figure 2-44.b and Figure 2-44.d the links are located in the beams while in Figure 2-44.c the link is constituted by the additional short vertical member joining the beam and the intersection between both braces. Figure 2-45 describes the collapse modes of the frames represented in Figure 2-44.a (left) and Figure 2-44.c (right).

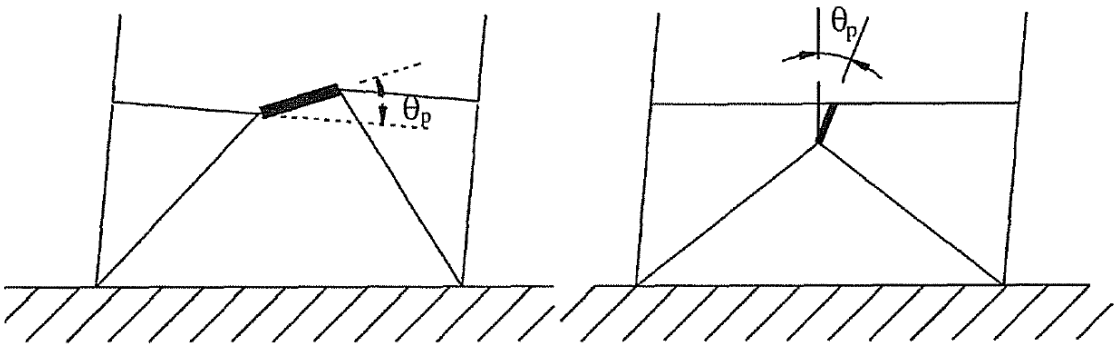

Figure 2-45. Collapse modes of eccentrically Braced Frames [EN-1998 2004]

The Eurocode 8 [EN-1998 2004] states design and detailing rules for frames with eccentric bracings. Seismic links are classified into three categories according to the type of plastic mechanism developed: short links yielding in shear, long links yielding in bending and intermediate links yielding in bending and shear. For I sections the Eurocode states the design resistances and limits of categories; as well the top bounds of angle θ_p (Figure 2-45) are specified, ranging in between 20 (long links) and 80 (short links) μrad. The Eurocode also stipulates the action effects to be considered in the design of the connections of the links or of the element containing the links. The members not containing seismic links, should be verified in compression considering the most unfavorable combination of the axial force and bending moments that is

indicated in the Eurocode. The Eurocode 8 specifies the behavior factors (q) to be considered for EBF buildings: for ductility class M is $q = 4$ and for ductility class H is $q = 5\ \alpha_u / \alpha_1$ where the ratio α_u / α_1 plays the role of the over-strength factor (Ω) discussed after Figure 2-22 and equation (2-16). Factor α_u / α_1 can be obtained either by push-over analysis or by empirical estimations; the Eurocode 8 suggests using 1.2.

To avoid the risk of premature failure by local buckling of the link segments, they should be conveniently stiffened, as shown by Figure 2-46. The Eurocode 8 [EN-1998 2004] states that links should be provided with intermediate web stiffeners and that lateral supports should be provided at both the top and bottom link flanges at the ends of the link.

Figure 2-46. Links of an eccentric braced frame

Dual systems. These solutions exhibit lateral behaviors intermediate between those of moment resisting frames and of braced frames. According to the classification of the Eurocode 8, these systems correspond to the following three categories: (e) Structures with concrete cores or concrete walls, (f) Moment resisting frames combined with concentric bracings, and (g) Moment resisting frames combined with infill walls. Remarkably, the cooperation of the non-structural components might be relevant and this mainly applies for concrete or masonry infill walls.

Special Truss Moment Frames. It is a seismic-resisting system that consists of trusses as horizontal members with specially designed segments that are expected to withstand large cyclic deformation during seismic events [Goel, Itani 1994]. This system allows detailing for controlled damage in the special segments of open web trusses, Figure 2-47. During lateral motion, the truss will be subjected to constant shear and varying axial forces in the chord members. The maximum axial forces in the chord members occur near the ends of the truss, while the minimum forces occur in the middle zone of the truss. Therefore, the special segment is located in the middle of the truss to minimize the adverse effect of the axial forces in the chord members, Figure 2-47.b and Figure 2-47.c. The shear in the special segment is resisted through axial forces in the diagonal members and flexural shear in the chord members. If the diagonal members are not present in the special segment, then the entire seismic shear is resisted by flexural shear of the top and bottom chord members, Figure 2-47.c.

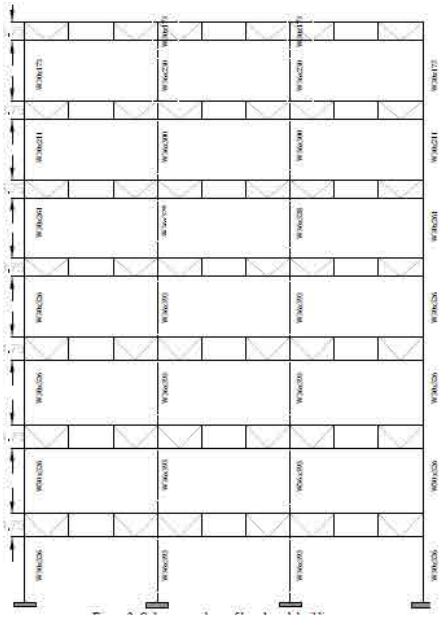

(a) Global layout

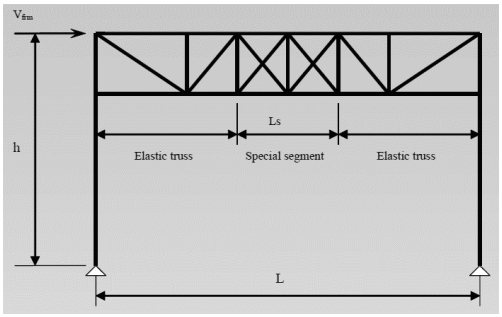

(b) Detail [The spectrus group 2013]

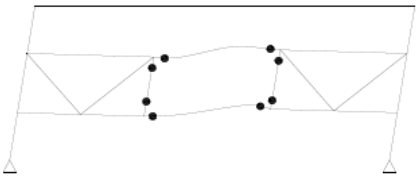

(c) Controlled damage

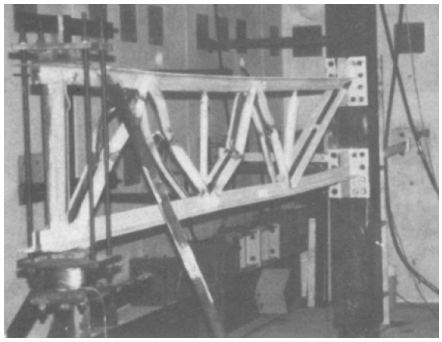

(d) Testing [Goel, Itani 1994]

Figure 2-47. Special Truss Moment Frames

Outrigger walls. In tall buildings, outrigger walls are stiff cantilever beams that join the rigid central core of the building (with stairs and elevators) and the external façades. In that way, the whole width of the building is involved in its lateral resistance and not only the inner kernel [Smith, Coull 1991].

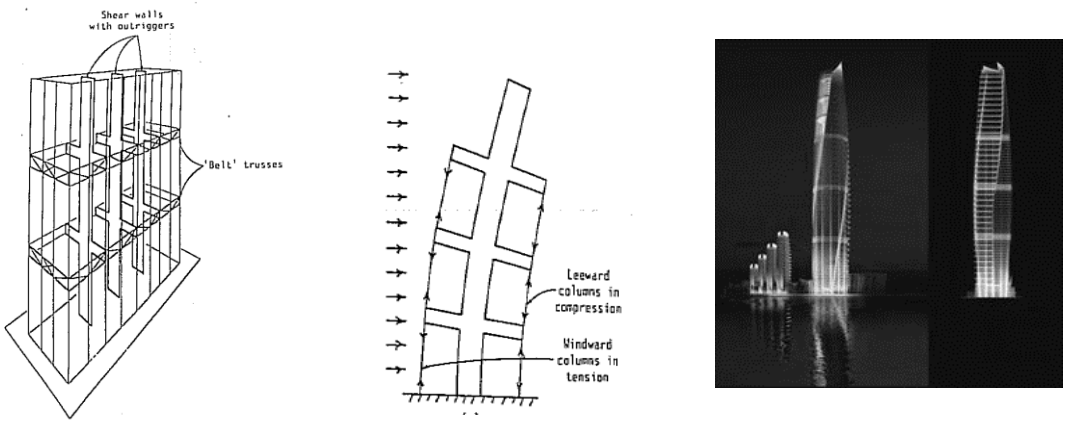

(a) Global layout [Smith, Coull 1991]

(b) Behavior during lateral motion [Smith, Coull 1991]

(c) Buildings with outrigger walls

Figure 2-48. Outrigger walls

Base isolation. The base, or seismic, isolation of buildings consists of adding flexible elements between the building structure and the foundation [Kelly 1993; Skinner et al. 1993; Naeim, Kelly 1999; Higashino, Okamoto 2006; Kelly, Konstantinidis 2011]. Those elements are commonly termed as isolators and are intended to uncouple the horizontal motion of the building and the soil, as depicted by Figure 2-49.b; the part of the building above the isolators is usually known as superstructure. The isolators are extremely flexible in the horizontal direction; this high flexibility elongates significantly the fundamental period of the building, common target values are close to 3 s. Figure 2-49.c points out, in terms of design spectra, the beneficial effect of base isolation; the top sketch corresponds to absolute acceleration spectra (Figure 2-5) and the bottom sketch corresponds to relative displacement spectra (Figure 2-3). Figure 2-49.c shows that the elongation of the period decreases importantly the equivalent seismic forces, yet increasing the design displacement, which has to be absorbed by the isolators; this displacement is commonly termed as seismic gap. Figure 2-49.c shows also that the increase of damping further reduces the design forces and the seismic gap; for this reason, the isolators are frequently series supplemented by additional dampers. Two major types of seismic isolators have been proposed: rubber bearings (Figure 2-49.a) and friction-based isolators (Figure 2-49.d). Despite the highly satisfactory performance of base isolation, this technology has two major limitations in its use: (i) tall buildings cannot be base-isolated because of the difficulties of withstanding the weight of the building and because of the high flexibility of such constructions, thus having long fundamental periods, and (ii) the foundation soil has to be at least reasonably firm since extremely soft soils constitute themselves a kind of "natural" isolators. Remarkably, base isolation can be used for any structural type, either concrete or steel-based, essentially in the same way.

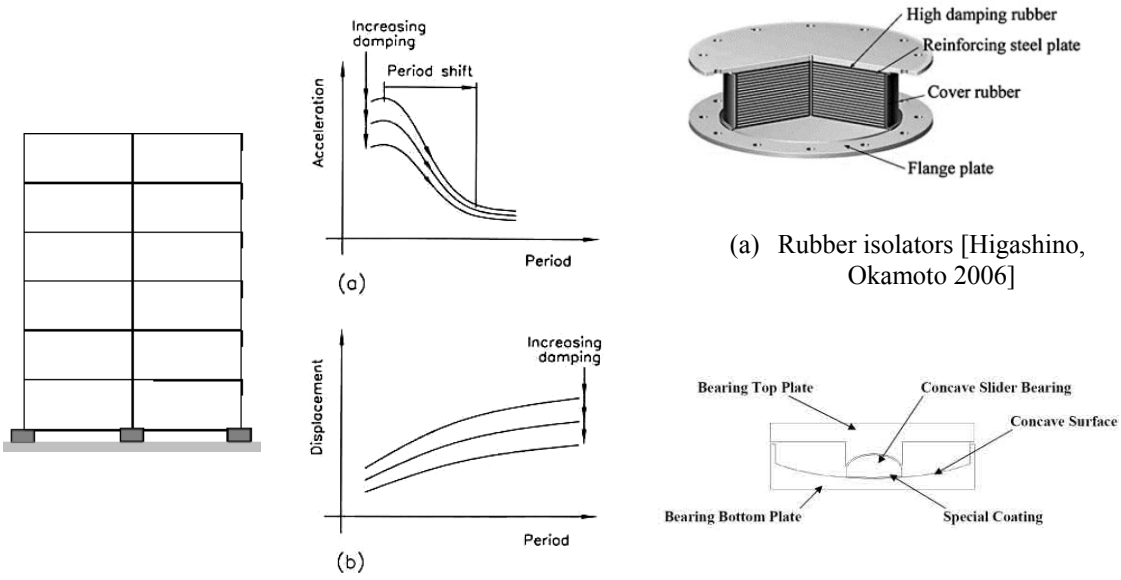

(a) Rubber isolators [Higashino, Okamoto 2006]

(b) Isolated building

(c) Design spectra

(d) Friction isolators

Figure 2-49. Base isolation of buildings

Energy dissipators. Energy dissipators are devices that are connected to the building structure in such a way as absorbing energy under strong drift motions, thus protecting the rest of the construction [Housner et al. 1997; Soong, Dargush 1997]. In other words, they are "structural fuses" that take most the input energy of the earthquake; therefore, they should constitute the "weakest link", in the sense that the yielding of the dissipators must be prior (in terms of drift displacement) to any structural damage. The dissipators respond to the philosophy of the "capacity-based design", because the collapse mode is extremely ductile. Since the dissipators are intended to yield under drift motion, are commonly connected to stiff bracing members, as shown by Figure 2-50. Figure 2-50.a represents devices linking chevron braces and the upper beam, Figure 2-50.b shows devices connected between two halves of diagonal braces, Figure 2-50.c displays devices connected to opposite diagonal braces (in that case the deformations are shear strains) and Figure 2-50.d depicts devices connected to infill walls and to the upper beam. Noticeably, in all the cases depicted in Figure 2-50 the dissipators take profit of the strains generated under drift displacements to yield and thus, to absorb energy. About the horizontal layout of the dissipators, they should be installed as any bracing system, i.e. looking for plan symmetry, torsion resistance and, if possible, structural redundancy. Remarkably, energy dissipators can be used for any structural type, either concrete or steel-based, essentially in the same way.

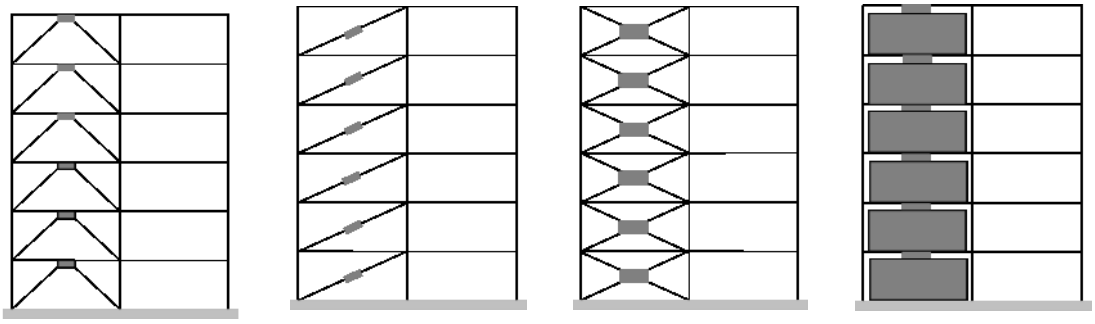

(a) Chevron braces (b) Diagonal braces (c) Diagonal braces (d) Infill walls

Figure 2-50. Energy dissipators

The energy dissipators are not a part of the main carrying load system and, therefore, can be easily replaced after being damaged by severe earthquakes. Compared to base isolation, energy dissipators exhibit several relevant advantages: (i) can be used even in soft soil and tall (flexible) buildings, (ii) can be also useful for wind gusts, (iii) the dissipators can be significantly simpler and easier to install than the isolators since do not need to resist the weight of the building. Conversely, it cannot be guaranteed that, under inputs more severe than expected, the structure does experience any damage. These qualities make the energy dissipators particularly suitable for mass use in developing countries [Palazzo et al. 2009].

Several types of devices have been proposed as energy dissipators; they can be broadly classified, with respect to their dissipative mechanism, into the following major groups: (i) plastification of metals (these elements are commonly termed as hysteretic), (ii) viscous dampers, (iii) viscoelastic materials, (iv) friction and (v) a wide variety of systems, such as shape-memory alloys, electro-inductive, among others. Obviously, these mechanisms can be combined to take better profit of their advantages. In global terms, the hysteretic devices are the simplest and most economic, reliable and robust; the other dissipators can provide, in general, better performance but the functioning of the hysteretic ones is fully satisfactory. In other words, the hysteretic devices exhibit the best price / performance ratio. Among them, the buckling-restrained braces are one of the dissipators that have been mostly used, mainly for seismic protection of building frames [Watanabe et al. 1988; Clark et al. 1999; Brown et al. 2001]; see Figure 2-51. They consist of slender steel bars connected usually to the frame to be protected either like concentric diagonal braces (Figure 2-50.b) or like concentric chevron braces (Figure 2-50.a). Under horizontal seismic excitations, the inter-story drift motion generates tensile and compressive axial strains in such steel bars beyond their yielding points. The buckling of these core bars is prevented by embedding them in a stockiest encasing (Figure 2-51.a); such casing is usually composed either of steel elements [Iwata 2004; Tsai et al. 2004] or of mortar coated with steel (see Figure 2-51.b, [Palazzo et al. 2009]). Some sliding interface between the steel core and the surrounding material is required to prevent excessive shear stress transfer, since it would reduce the longitudinal stress in the core thus impairing the energy dissipation capacity.

(a) Buckling-restrained braces with circular and rectangular cross-sections [Brown et al. 2001]

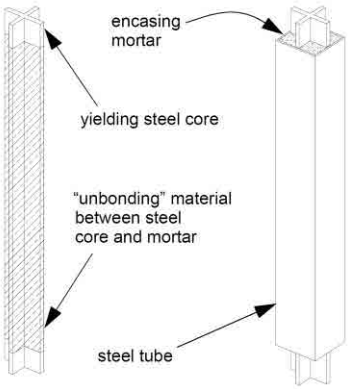

(b) Detail of a device [Brown et al. 2001]

Figure 2-51. Buckling-restrained braces

3 SEISMIC INFORMATION OF COLOMBIA

3.1 Seismicity of Colombia

Colombia is located in a zone with constant seismic activity, because of the convergence of the tectonic plates Nazca, South-America and Caribe, as shown by Figure 3-1.

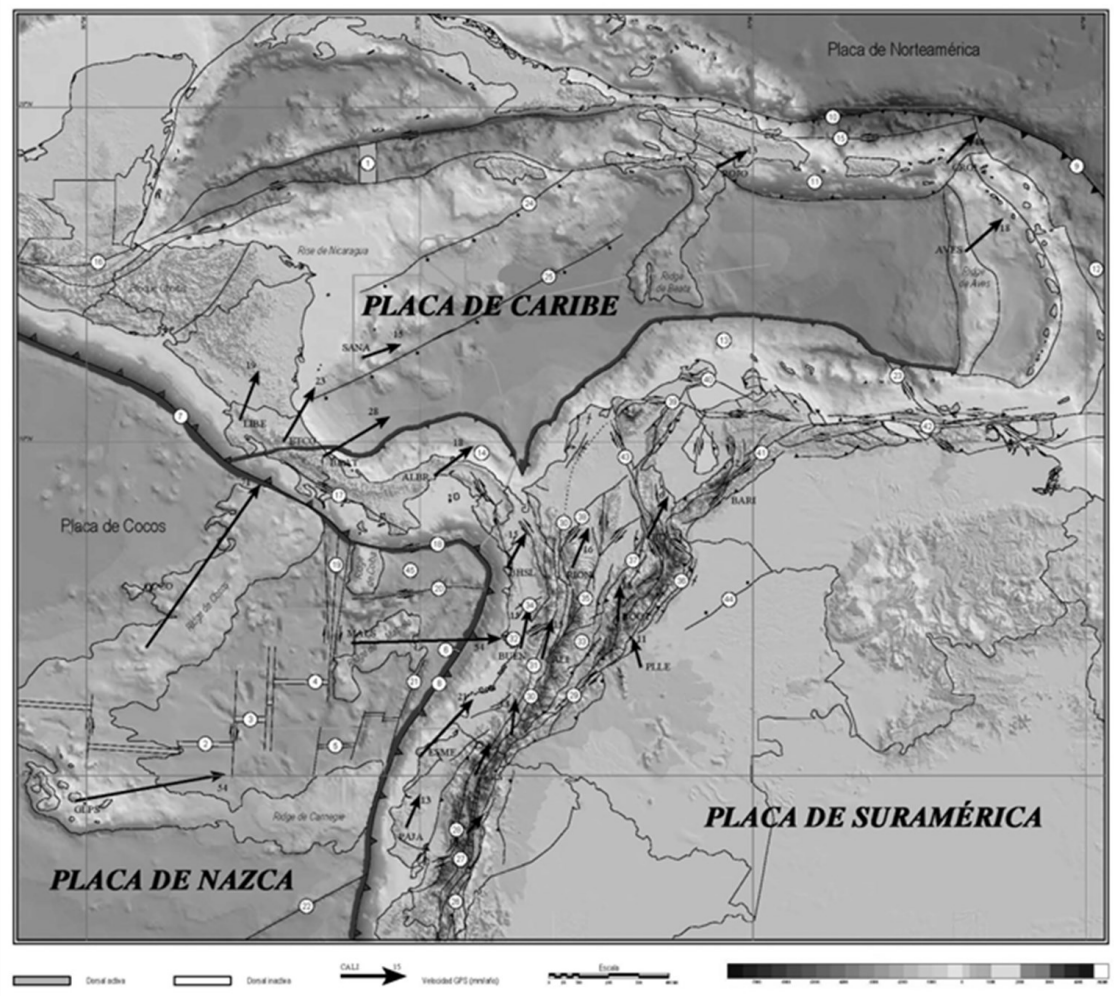

Figure 3-1. The major tectonic structures in Colombia [INGEOMINAS 2005]

Figure 3-1 displays the tectonic mechanism of the northern part of South-America and Caribe. The active ridges are: (1) Caimán, (2) Galápagos, (3) Ecuador and (4) Costa Rica. The inactive

ridges are: (5) Malpelo y (6) Buenaventura. The trenches with active subduction zones are: (7) Mesoamericana, (8) Colombo Ecuatoriana and (9) Caribe; the trenches with inactive subduction zones are: (10) Puerto Rico. The accretionary prisms - deformed belts are: (11) Los Muertos, (12) Antillas Menores, (13) Caribe and (14) Panamá. The zones of transform faults are: (15) Septentrional-Oriente, (16) Motagua-Swan, (17) Celmira-Ballena, (18) Jordán, (19) Panamá, (20) Hey, (21) Yaquina, (22) Grijalva and (23) Los Roques. The normal oceanic faults are: (24) Pedro Bank and (25) Hess. The faults in the continental plate are: (26) Cosanga, (27) Peltetec, (28) Pallatanga-Pujili, (29) Algeciras, (30) Cauca-Almaguer, (31) Cali-Patía, (32) Garrapatas, (33) Ibagué, (34) Zona de Falla de Itsmina, (35) Palestina, (36) Guaicaramo, (37) La Salina, (38) Espíritu Santo, (39) Oca, (40) Cuisa, (41) Boconó, (42) El Pilar, (43) Santa Marta Bucaramanga and (44) Meta. Lithospheric blocks are: (45) Microplatea of Coiba.

Figure 3-2.a displays the main faulting macro systems of Colombia. The mountain system of Colombia is rugged and consists basically of three mountain ranges (Andes) going roughly in the north-south direction. This is also the direction of the faults; the main seismotectonic accident being the subduction of the Nazca plate beneath the South-American plate in the Pacific Ocean. Figure 3-2.b displays the epicenters of the earthquakes with surface magnitude $M_s \geq 3$ in the period 1541-2009.

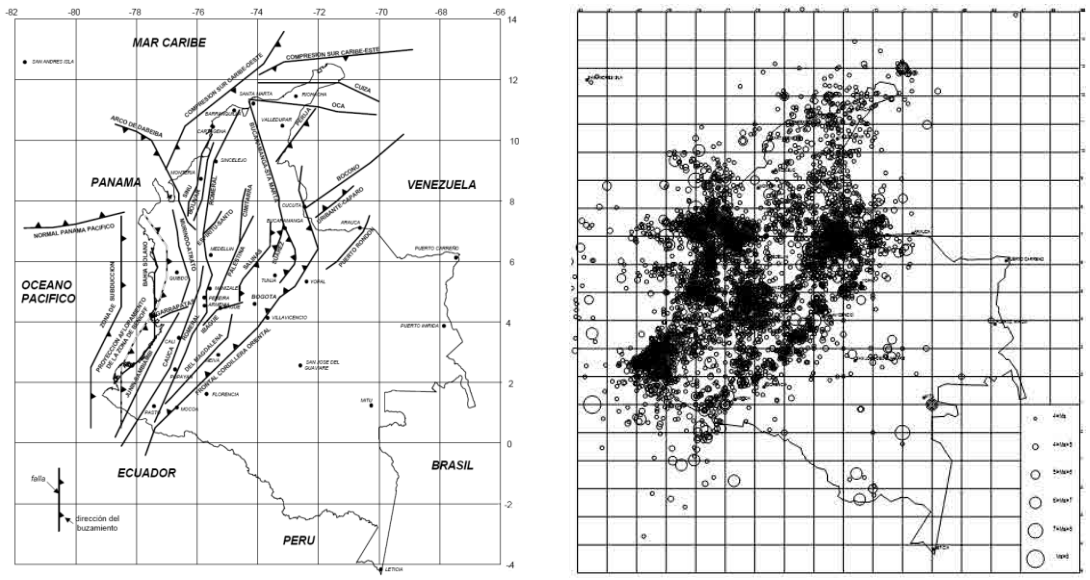

(a) Predominant faults [NSR-98 1998] (b) Epicenter location [NSR-10 2010]

Figure 3-2. Seismicity of Colombia [NSR-10 2010]

3.2 Colombian Earthquake-Resistant Design Regulations

The first draft of Colombian seismic building code was issued in 1976; it was based on the translation of the requirements of the "Structural Engineers Association of California" (SEAOC) basically describing the detailing of reinforced concrete structures required to mitigate the effects of seismic inputs. After two major earthquakes in 1979, the Colombian Association for Earthquake Engineering (AIS), issued the first seismic design requirements for buildings. After the earthquake of Popayan in 1983, many buildings with less than 5 floors collapsed, as well many as reinforced masonry buildings; in framed buildings, these failures appeared to be due to excessive permissiveness of the code in the horizontal flexibility of the and buildings to lack of reinforcement in the columns, among other issues. It was necessary to extend the scope of this code, so that AIS complements it by including an annex referred to buildings with one or two stories and another annex containing seismic hazard maps. In 1984, the code [Decreto 1400 1984] was issued; in 1998, it was superseded by the [NSR-98 1998] and, finally, in 2010 the current

code [NSR-10 2010] was issued. Globally speaking, the Colombian regulations are based in the American codes of SEAOC, ACI, AISC, FEMA, NEHRP, ATC and ASCE, among other institutions; the main specificities are constituted by the design spectra and by the zonation map. The current code [NSR-10 2010] describes the seismic hazard of Colombia by dividing the territory in three major seismic zones: low, intermediate and high seismic hazard, respectively. Such zones are depicted in Figure 3-3.a. Each seismic zone is subdivided in a number of sub-regions in terms of the horizontal PGA coefficient (A_a) whose values range between 0.05 to 0.50, as shown by Figure 3-3.b. Figure 3-3 shows that the most populated areas correspond to intermediate seismic hazard and that the higher seismicity occurs in less inhabited zones, such as the Pacific coast. Bogotá has an intermediate seismic hazard with $A_a = 0.15$.

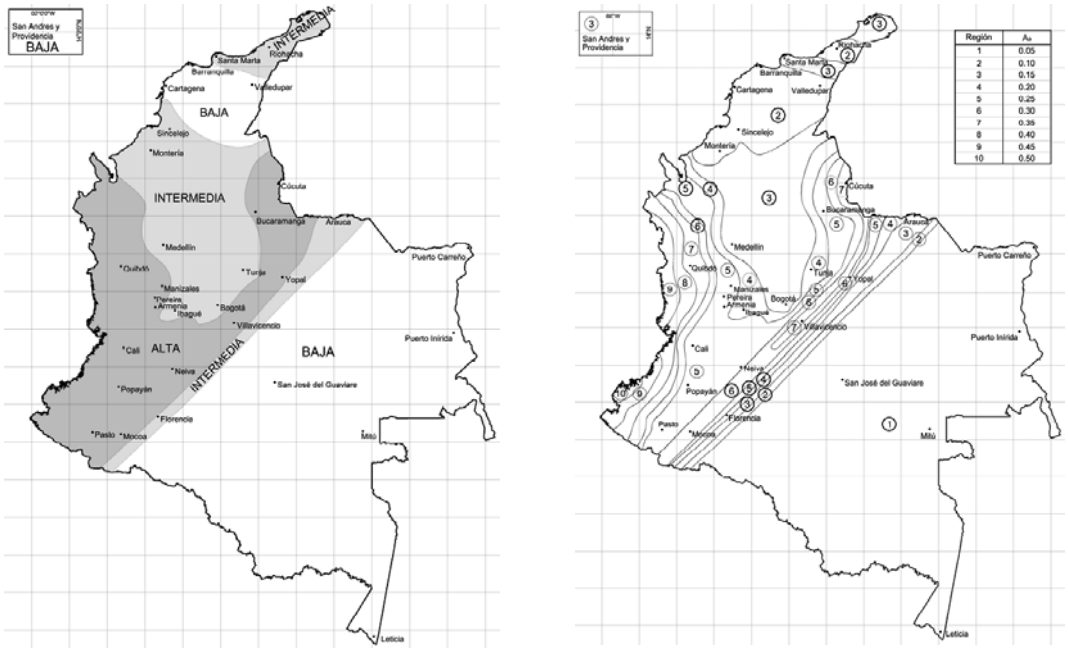

(a) Seismic zones (b) A_a factor

Figure 3-3. Design seismic hazard in Colombia [NSR-10 2010]

3.3 Seismicity of Bogotá

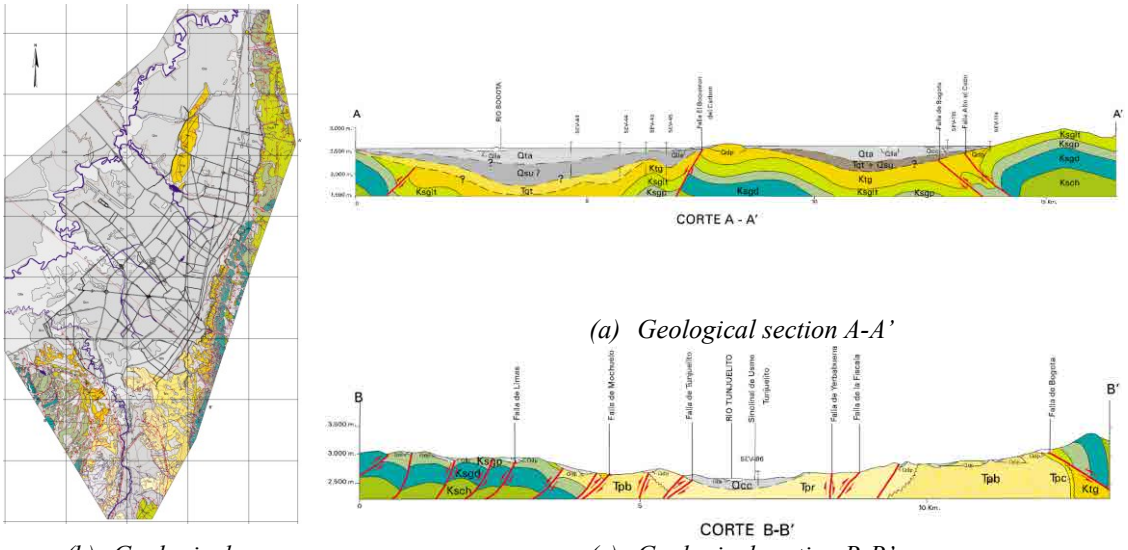

(a) Geological section A-A'

(b) Geological map *(c) Geological section B-B'*

Figure 3-4. Soil profile of Bogotá [INGEOMINAS 2005]

As discussed in the previous section, Bogotá possess only a moderate level of seismic hazard, namely the design PGA for the bedrock and return period 475 years is 0.15 g. However, Bogotá is founded on deep quaternary deposits, locally deeper than 500 m; this soil condition can generate important amplifications, as shown by Figure 3-4.

3.4 Seismic microzonation of Bogotá

This section describes the former and the current seismic microzonations that have been proposed for Bogotá.Figure 3-5 shows the former microzonation of Bogotá [Decreto 196 2006]. In Figure 3-5 "Cerros" corresponds to rock and stiff soil, "Piedemonte" refers to good quality colluvial soil and alluvial fans, and "Lacustre A" and "Lacustre B" correspond to soft clay deposits whose depth is higher and smaller than 50 m, respectively. "Terrazas y Conos" are terraces and alluvial fans, "Rondas de río y humedales" are river banks and swamps and "Rellenos de Basuras" and "Rellenos de Excavación" are rubbish and dig dumps, respectively. In this study, only zones "Piedemonte" and "Lacustre A" have been considered. The other seismic zones indicated in Figure 3-5 are not considered since they contain only small numbers of steel buildings. Figure 3-6 displays the design spectra of these two zones.

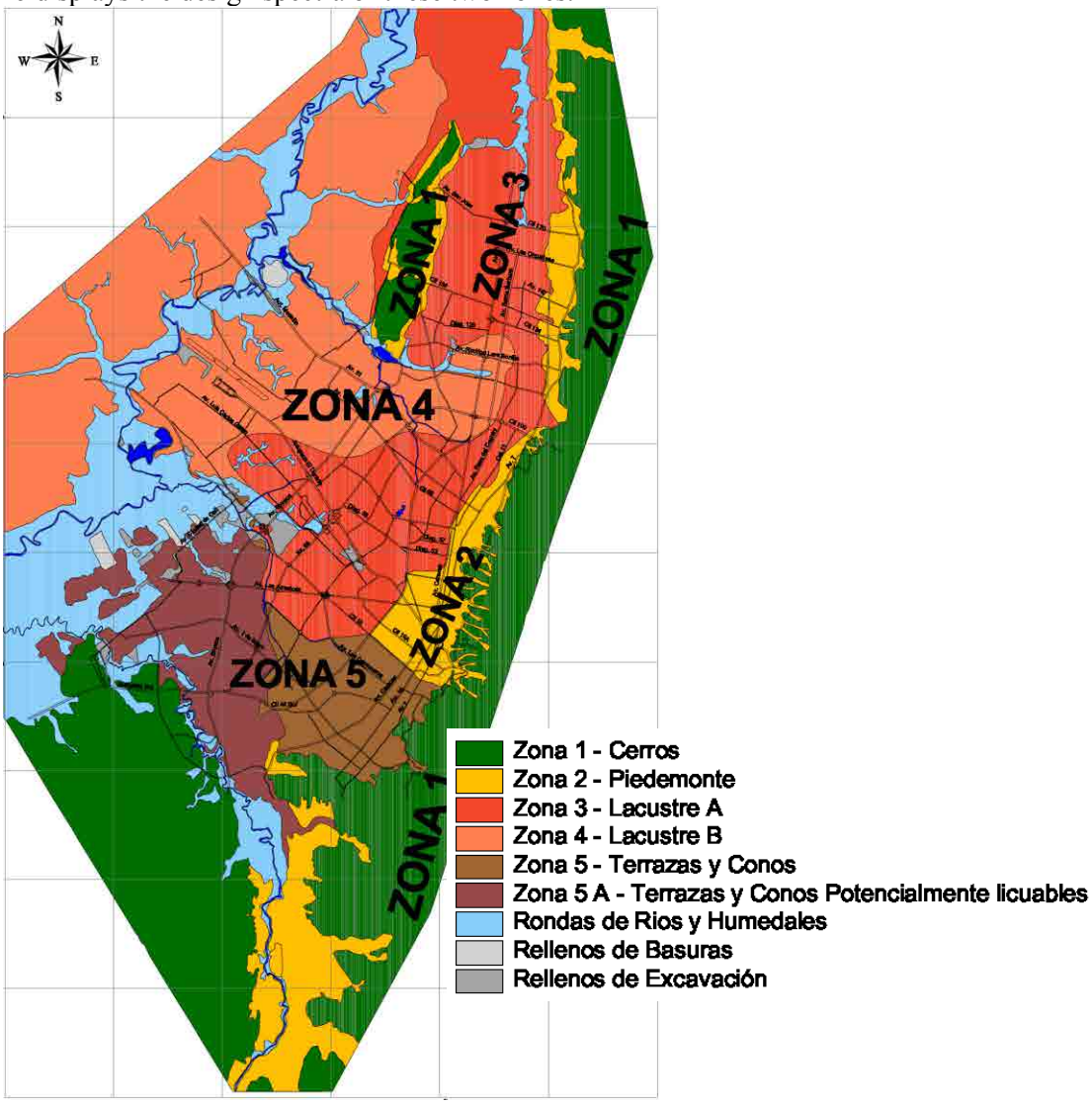

Figure 3-5. Former seismic microzonation of Bogotá [Decreto 196 2006]

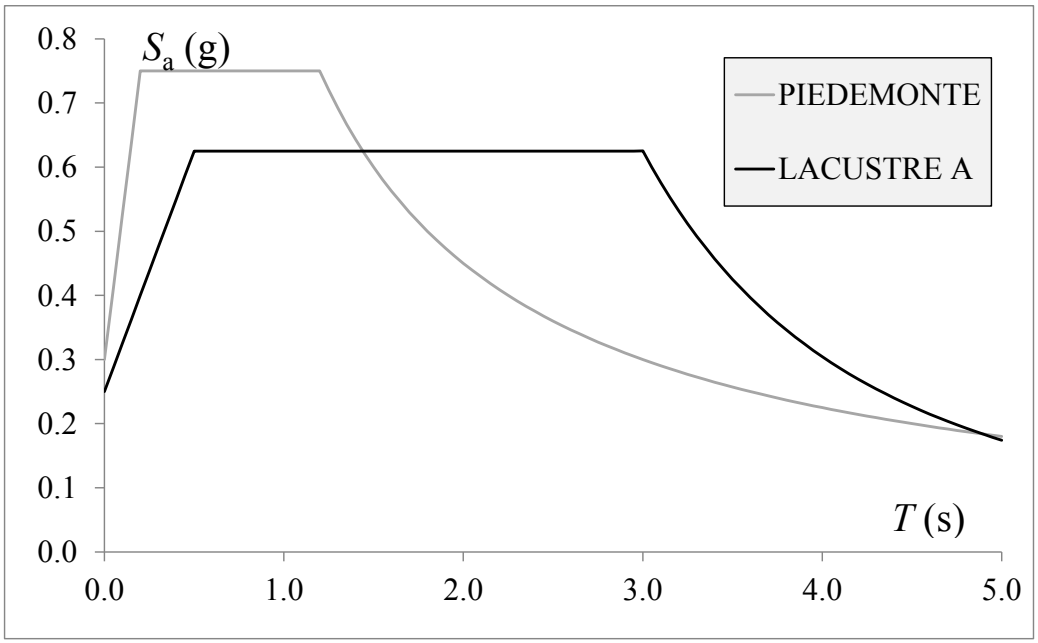

Figure 3-6. Design spectra according to the former seismic microzonation of Bogotá [Decreto 196 2006]

In Figure 3-6 the initial spectral ordinate (corresponding to $T = 0$) is termed as A_m (maximum acceleration); for Piedemonte, $A_m = 0.30$ g and for Lacustre A, $A_m = 0.25$ g. The plateau spectral ordinates are 2.50 $A_m F_a$ where F_a is an amplification factor; for Piedemonte and Lacustre A, $F_a = 1$. The left/right corner periods of the plateau are termed T_0/T_C; for Piedemonte, $T_0 = 0.2$ s and $T_C = 1.2$ s for Lacustre A, $T_0 = 0.5$ s and $T_C = 3$ s. For Piedemonte, the descending branch of the spectra are given by $S_a = A_n F_v / T$ where A_n is the nominal acceleration (0.4 g) and F_v is an amplification factor ($F_v = 2.25$). For Lacustre A, the descending branch of the spectra are given by $S_a = A_n F_v / T^{2.5}$ (faster decreasing) where $A_n = 0.3$ g and F_v 32.48).

Figure 3-7 displays the abovementioned current seismic microzonation of Bogotá [Decreto 523 2010]. In Figure 3-7 "Cerros" corresponds to rock and stiff soil with top soft layers not exceeding 6 m ($v_{s,30} > 750$ m/s, where $v_{s,30}$ accounts for the shear wave velocity in the top 30 m), "Piedemonte" refers to soft alluvial and colluvial soil (200 m/s < $v_{s,30}$ < 750 m/s) and "Lacustre" corresponds to very soft clay deposits ($v_{s,30} < 175$ m/s). As well "Aluvial" refers to mid-quality alluvial deposits (175 m/s < $v_{s,30}$ < 300 m/s) and "Lacustre Aluvial" shows intermediate characteristics in between "Aluvial" and "Lacustre". Finally, "Depósito ladera" are unstable high slope soils, with relevant risk of land-sliding; the construction is restricted. In the categories "Lacustre", "Aluvial" and "Lacustre Aluvial", the numbers indicate the depth (in m) of the soft deposit layers. In the category "Piedemonte", subcategories A, B and C do not differ deeply. In this study only zones "Piedemonte A, B and C" and "Lacustre-50, 100, 200, 300 and 500" have been considered. The other seismic zones indicated in Figure 3-7 are not considered since they contain only small numbers of steel buildings.

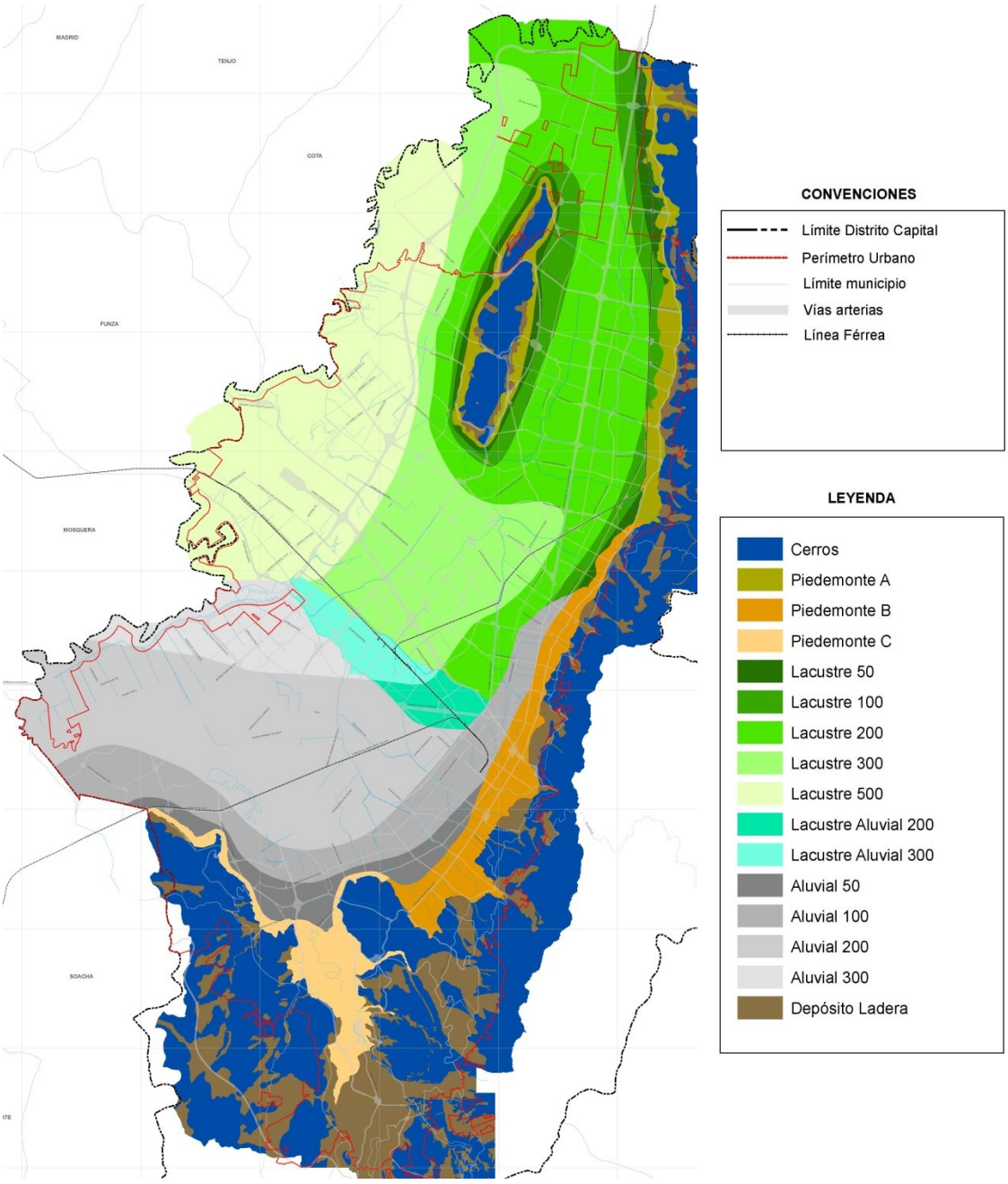

Figure 3-7. Current seismic microzonation of Bogotá [Decreto 523 2010]

Comparison between the two microzonations depicted in Figure 3-5 and in Figure 3-7 shows that the main difference is that the new microzonation consists basically in a refinement of the previous one. In the former microzonation (Figure 3-5) zones "Piedemonte" and "Lacustre A" have been considered; in the current microzonation (Figure 3-7) such zones are split in "Piedemonte A, B and C" and in "Lacustre-50, 100, 200, 300 and 500", respectively. Figure 3-8 displays the design spectra of these eight zones.

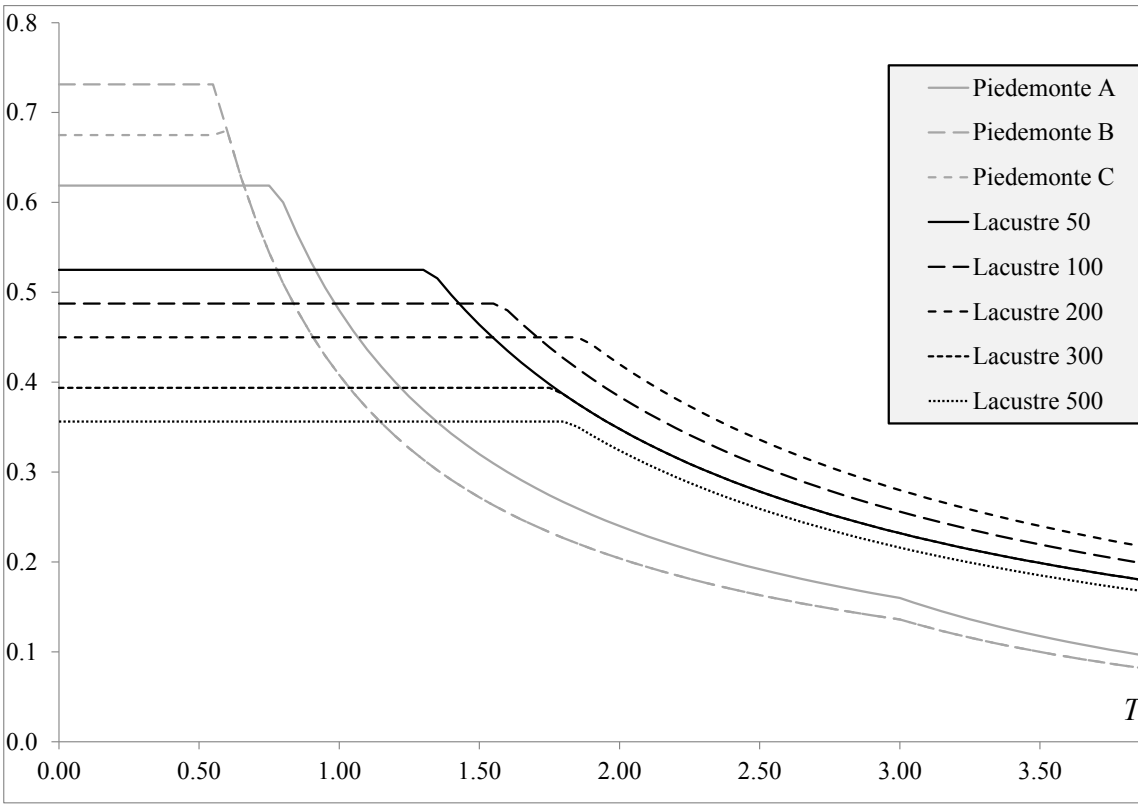

Figure 3-8. Design spectra according to the current seismic microzonation of Bogotá [Decreto 523 2010]

Comparison between Figure 3-6 and Figure 3-8 shows that in the former microzonation (Figure 3-6) the length of the plateau for soil "Lacustre A" is excessive; thus generating an over-conservative spectrum.

The spectra depicted in Figure 3-8 correspond to the overall formulation of the Colombian design code [NSR-10 2010]. Yet these spectra are three-branched, in the rank of periods of interest for this study (Table 4-21 through Table 4-30) only the initial (constant) and the second (decreasing) branches, are of interest. The ordinates of the initial branches are given by $S_a = 2.50\ A_a\ F_a\ I$ and the decreasing branches are given by $S_a = 1.20\ A_v\ F_v\ I\ /\ T$. A_v is an effective peak acceleration, F_a/F_v are the acceleration/velocity amplification factors for short/intermediate periods and I is the importance factor. Table 3-1 displays the values of such parameters for the considered zones.

Table 3-1. Parameters characterizing the spectra from the new microzonation of Bogotá [Decreto 523 2010]

Zone	A_a (g)	A_v (g)	F_a	F_v	T_C (s)
Piedemonte A	0.15	0.20	1.65	2.00	0.78
Piedemonte B	0.15	0.20	1.95	1.70	0.56
Piedemonte C	0.15	0.20	1.80	1.70	0.60
Lacustre-50	0.15	0.20	1.40	2.90	1.33
Lacustre-100	0.15	0.20	1.30	3.20	1.58
Lacustre-200	0.15	0.20	1.20	3.50	1.87
Lacustre-300	0.15	0.20	1.05	2.90	1.77
Lacustre-500	0.15	0.20	0.95	2.70	1.82

4 PROTOTYPE BUILDINGS

4.1 Steel buildings in Bogotá

4.1.1 Overall considerations

A number of mid-height steel buildings have been erected in Bogotá mainly after about 2000; before this date, only a limited number of steel buildings had been constructed, mainly as 3- to 5-story malls (commercial use). This boom was fuelled by big demand for commercial, housing and administrative uses; the number of stories ranges between three and twenty stories, while most of the buildings have 5 to 15 floors. The housing buildings usually tower 15 or more levels and usually this use is not shared with the commercial and administrative ones. The commercial and administrative uses are frequently mixed in a single building; commonly, the bottom two floors have commercial usage while the rest of the building is intended for administrative utility. The number of floors of the commercial and administrative buildings lies in between 5 and 10. In housing buildings, the span-length ranges usually between 4 and 6 m; in commercial and administrative buildings the span-length fluctuates usually between 6 and 8 m. The story height is established in terms of the required available height; it ranges between 2.20 m for housing use, 2.40 m for administrative use and 3 m for commercial use. Ordinarily, the first floor height is greater than 3 m for any use.

The overall shape of the buildings is constant-section prismatic, with rectangular plan configuration. The aspect ratio usually does not exceed two.

In general, the quality of the construction is rather good, in the sense that the design codes (both of Colombia [NSR-98 1998; NSR-10 2010] and of Bogotá [Decreto 196 2006; Decreto 523 2010]) are basically fulfilled, both in the design and construction phases. The quality of the steel (both for the main members and for the connections) and of the concrete is tightly supervised by testing.

Nowadays, it can be roughly estimated that more than 10000 buildings of this type exist, only in Bogotá D.C. ("Distrito Capital", with approximately 8 million of inhabitants). In other big and mid-sized cities of Colombia and of other close countries (Peru, Venezuela, Ecuador, among others), the situation is similar. This important abundance highlights the practical interest of this study.

The steel buildings have been fostered for their advantages, which are described in subsection 2.2.6. In particular, for commercial and administrative buildings, the construction rapidity is of specific interest. In areas of Bogotá with soft soil, the lightweight of the steel construction is a conclusive issue. In the last few years, the steel cost has comparatively decreased, thus making the steel construction more competitive; also, the construction of steel structures is becoming

more industrialized, therefore, the cost and the construction time are dropped, and the quality is improved, allowing more daring structural solutions.

4.1.2 Description of the buildings

Subsection 2.2.6 describes the most common structural solutions for multistory steel buildings, mainly MRF (Moment Resisting Frame, Figure 2-38), CBF (Concentrically Braced Frame, Figure 2-42) and EBF (Eccentrically Braced Frame, Figure 2-44). In many cases, those solutions are combined in different directions of a single building; mainly MRF with CBF. In virtually all the cases, the building have plan symmetry, e.g. the centers of mass and gravity are roughly coincident in all the floors.

The most usual steel grades are: for beams, joists and plates A36 [ASTM A36 2008], for columns and plates A572 [ASTM A572 2012], for braces A500 [ASTM A500 2009], for and for steel deck A1008 [ASTM A1008 2013]. Columns, beams and joists are made with W steel profiles; even in 15-story buildings, the depth of the columns usually does not exceed 14" (350 mm). The separation between adjoining joists ranges between 1.5 and 2.5 m; as a result, the depth of the steel deck ranges between 1.5" and 3" (38 and 76 mm) and the thickness ranges between 0.75 and 1.5 mm. The braces are made mainly with HSS profiles; in some cases, W profiles, pairs of channel sections and groups of four angle sections are also employed. Shear studs are employed in all the cases; both headed studs (Nelson-type) or segments of channel sections are used.

The particular characteristics of the MRF, CBF and EBF buildings are described in the next paragraphs.

- **MRF**. This solution has been considered mostly in commercial malls because of the availability of clear spaces between columns; in total, about 40% of the cases belong to this system. The pre-qualified steel beam-column connections [FEMA 350 2000] are widely popular (Figure 2-40 and Figure 2-41). In most of the situations, the connections are welded instead of bolted; this is because of its lowest cost (due to the relatively moderate workforce costs). The pre-qualified connections guarantee that the plastification of the joints occurs after the yielding of the connected bar members; in other words, the plastic hinges form in beams and columns and not in the panel zones. Therefore, the structural models do not consider the formation of plastic hinges in the beam-column connections.
- **CBF**. This solution has been considered in any use of the buildings; in total, about 40% of the cases belong to this system. In most of the occasions, the Chevron braces (inverted V, Figure 2-42.b) are utilized; only in few buildings, the Diagonal braces (X, Figure 2-42.a) are used.
- **EBF**. This solution has been considered in any use of the buildings; in total, about 20% of the cases belong to this system.

In virtually all the situations, the roof is not accessible (except for maintenance operations) and the roof slab consists of a steel deck without any topping concrete layer.

The stairs are commonly made with ordinary side beams (normally channel sections). The cooperation of the stairs in the lateral strength of the building can be neglected since the connections between the stair beams and the beams is designed to slide in the horizontal direction. The hoist way (hole for the elevators) is formed by four corner vertical steel profiles (either angle or HSS sections) and light cladding in the sides. The cooperation of these steel stacks in the lateral strength of the building can be neglected because of its high flexibility. Infill walls can be made either with unreinforced masonry or with light prefabricated wall elements ("dry-wall"). The masonry walls are detached from the main structure; therefore, the cooperation of the infill walls in the lateral strength of the building can be neglected. Different types of cladding are considered: unreinforced detached masonry, curtain walls, cement sheets, among others; in any case, the cooperation of the cladding in the lateral strength of the building can be neglected.

Figure 4-1 represents pictures of MRF, CBF and EBF steel buildings in Bogotá. Figure 4-1.a displays a 6-story MRF housing building; the building is known as "CVS" and has four apartments per floor. Figure 4-1.b displays an 8-story MRF building with commercial and administrative use; that building is located in the zone "Salitre". Figure 4-1.c displays a 3-story CBF building located in an industrial zone (known as "Zona Franca"). Figure 4-1.d displays a detail of a CBF building. Figure 4-1.e displays a 4-story EBF administrative building. Figure 4-1.f displays a detail of an EBF building; this building is known as "LTJ" and is located in the zone "Facatativá".

(a) 6-story MRF housing building

(b) 8-story MRF building with commercial and administrative use

(c) 3-story CBF building

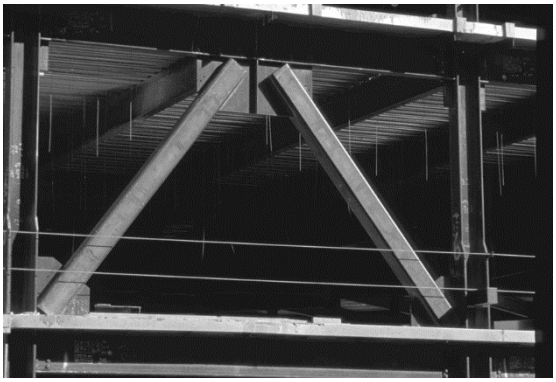

(d) Detail of a CBF building

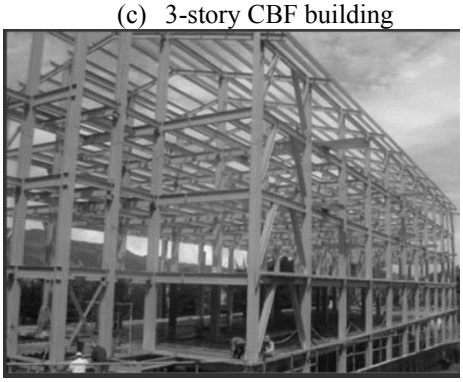

(e) 4-story EBF administrative building

(f) Detail of an EBF building

Figure 4-1. Multistory steel buildings in Bogotá

4.1.3 Prefabrication and erection

For MRF, CBF and EBF buildings, the construction process is essentially the same. In the factory, columns, beams, joists, decks and braces are prefabricated and then are transported unassembled to the construction site. Usually, columns are produced by segments of about 12 m each, involving three levels (group of levels) and two end segments either by their upper ends (for bottom columns), for both sides (for intermediate columns) or for their lower ends (for top columns). Beams and joists are produced by single-bay segments and braces are produced individually; therefore, there are no splices in such members. As many operations as possible are carried out in the factory. Columns and beams are prepared to be assembled to the other adjoining members; it includes drilling boltholes, welding base, stiffening and gusset plates and other similar operations. The preparation of joists, braces, and decks is similar, although less intense. The erection process is carried out (at the construction site) by ordinary means. The column splices are welded. Noticeably, the column splices correspond approximately to sections situated in the middle between consecutive floors. The column splices allow minor corrections of the verticality of columns, with the help of temporary steel wedges.

In CBF and EBF buildings, the braces corresponding to each group of levels are connected to the main frame prior to the erection of the next group. This strategy provides lateral strength during the erection process.

4.2 Selection criteria

As described in the first chapter, the main objective of this study is to analyze the seismic vulnerability of multi-story mid-height steel buildings in Bogotá; as well, the results of the research could be also generalized to the rest of the country and to other close or similar countries. Given the high number of buildings and their different characteristics (see the previous section), it is necessary to select a reasonable number of buildings that represent the bulk of the existing ones. One of the main concern of the selection is to take more care of the trends that are common to most of the buildings than of those issues that are only relevant to a limited number of buildings. For this reason, only buildings with plan symmetry and compactness and uniformity along their height are considered. As well, it is deemed that the separation from aside buildings is sufficient, the slabs guarantee the diaphragm effect and there are no short columns. Exceptions to these rules are infrequent and exhibit a wide variety of characteristics, which are hard to be described only by a limited number of models. The subsection 2.2.6 and the previous section have been taken into account along the selection process.

In the selection process, the main parameters have been: earthquake-resistant system, number of floors, span-length, and soil type. Other issues have been disregarded, as being considered less relevant to the seismic performance: number of bays, basement, cantilevers, cladding, partitioning, and plan configuration. The considered values of the relevant parameters are described in the next section.

4.3 Selected buildings

4.3.1 General description

Eighteen prototype buildings are selected to represent the vast majority of the mid-height steel edifices in Bogotá. As discussed in the previous section, all these buildings have plan symmetry and compactness and are uniform along their height, see subsection 2.2.6 and section 4.1; all the columns are continuous down to foundation and the influence of the basements is neglected. The main carrying-load system is composed of steel columns and of steel decks topped with a concrete layer. The plan floor of the buildings is square, with four equal-length bays in each direction; therefore, there are $5 \times 5 = 25$ columns, which are laid according to an orthogonal regular pattern. The prototype buildings are distinguished by the span-length in both directions, by the number of

floors and by the type of earthquake-resistant system (alike in both directions), see subsection 2.2.6 and section 4.1. Two span-lengths and three numbers of floors are considered: 6 – 8 m and 5 –10 – 15, respectively. Three earthquake-resistant systems have been considered: moment-resistant frames (MRF, see Figure 2-38, Figure 4-1.a and Figure 4-1.b), concentrically-braced frames (CBF, see Figure 2-42, Figure 4-1.c and Figure 4-1.d) and eccentrically-braced frames (EBF, see Figure 2-44, Figure 4-1.e and Figure 4-1.f); in these last two cases, chevron braces are contemplated (Figure 2-42.b and Figure 2-44.a). The diagonal braces (Figure 2-42.a) have not been considered in this study because they are not widely used in Bogotá (and in the rest of Colombia) for multistory buildings, despite their previously discussed advantages (subsection 2.2.6). The cooperation of the infill walls (cladding and partitioning) is neglected since, according to the common construction practices in Colombia, they are habitually separated from the main structure. Figure 4-2 shows overall views of the structures of the selected prototype buildings. The structures depicted in Figure 4-2 correspond to MRF; CBF and EBF are similar, yet incorporating the chevron braces.

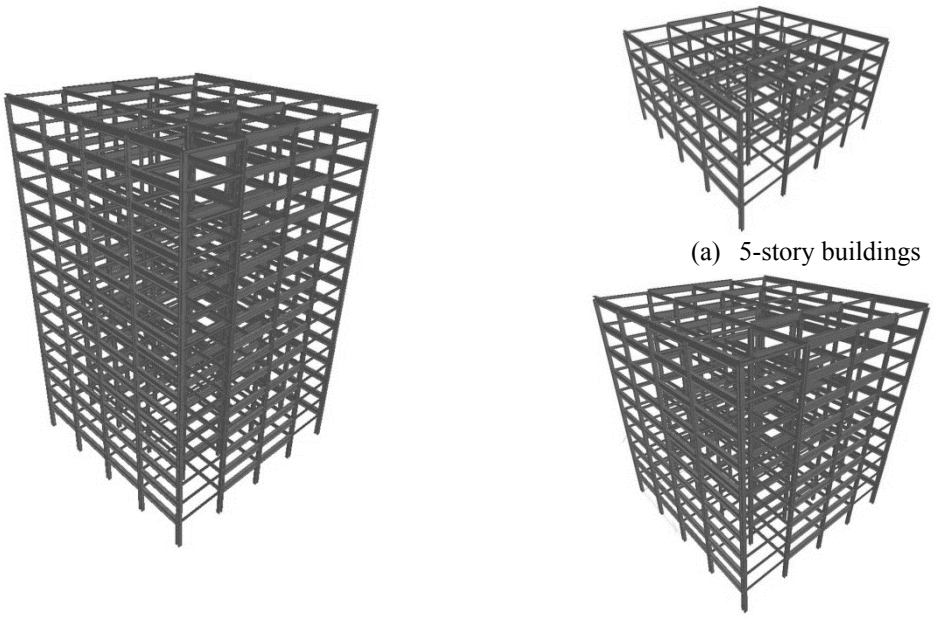

(a) 5-story buildings

(b) 15-story buildings

(c) 10-story buildings

Figure 4-2. Selected MRF representative prototype buildings

As discussed previously, the structure of each of the eighteen prototypes buildings is designed for ten seismic zones in Bogotá; two of them (Figure 3-5, "Piedemonte" and "Lacustre A") correspond to the former microzonation and the remaining eight correspond to the current microzonation (Figure 3-7, "Piedemonte A, B and C" and "Lacustre-50, 100, 200, 300 and 500"). Therefore, the number of analyzed structures is $18 \times 10 = 180$ (the number of prototypes buildings times the number of seismic zones in Bogotá).

To obtain representative results, the buildings in the two zones of the former microzonation have been designed according to the previous Colombian regulations [NSR-98 1998]; conversely, the buildings in the eight zones of the current microzonation have been designed according to the current Colombian regulations [NSR-10 2010]. The importance is "normal" (given their dwelling, administrative and commercial use). In Bogotá the design acceleration is $A_a = 0.15$ g. The dead load has been assumed as 2.5 kN / m^2 (slab self-weight) + 1.5 kN / m^2 (partitioning walls) + 1 kN / m^2 (facilities) + 1.5 kN / m^2 (cladding system, distributed along the whole surface of the façade). Live load is $L = 2$ kN / m^2 on the floors and $L_r = 0.5$ kN / m^2 on the roof. The wind forces have obtained according to the Colombian code [NSR-10 2010]; Bogotá corresponds to zone 2 (average wind speed 22 m/s). The effect of the wind forces has been disregarded since they are grossly smaller than the seismic horizontal forces. The design input spectra are obtained from the

former and current microzonations, Figure 3-6 and Figure 3-8, respectively. In spite that the buildings are symmetric, 5% accidental eccentricities established by the [NSR-98 1998] and the [NSR-10 2010] are considered. The damping factor has been assumed equal to 5%. The Colombian code states a design inter-story drift equal to 1%; this condition is the most restrictive in most of the MRF buildings, being comparatively less restrictive in the CBF and EBF. Noticeably, this drift limitation corresponds to the "whole" seismic input, i.e. without dividing by the R coefficient (response reduction factor). The seismic design has consisted of determining equivalent static forces in both directions and applying them to 3D models of the structures of the buildings. As suggested by both Colombian regulations, only compact sections are selected for columns and beams [AISC 2010; AISC 360-10 2010]. The carried out structural analyses are more deeply described in section 4.4.

The columns are made of A-572 steel (f_y = 342 MPa) [ASTM A572 2012] while the beams and joists are made of A-36 steel (f_y = 248 MPa) [ASTM A36 2008]; this difference attempts getting earlier failures in the beams than in the columns. The braces are made of A500 steel (f_y = 342 MPa) [ASTM A500 2009]. The steel deck is made of A1008 steel [ASTM A1008 2013] (f_y = 376 MPa). The compressive strength of the topping concrete is f_c' = 21 MPa; the depth of the steel deck is 50 + 70 mm (120 mm concrete depth) and its thickness is 0.75 mm. Figure 4-3 shows plan views of typical floor slabs of the selected buildings; Figure 4-3.a and Figure 4-3.b correspond to buildings with span-length equal to 6 m and to 8 m, respectively. Figure 4-3 shows that each building contains two seismic-resistant frames in the *y* direction (A and E frames) while in the *x* direction there are four seismic-resistant frames (inside 1, 2, 4 and 5 frames). As discussed previously, each of these resistant parts can be either a moment-resisting frame (MRF), a concentrically braced frame (CBF) or an eccentrically braced frame (EBF). In Bogotá (and in the rest of Colombia) the three solutions (MRF/CBF/EBF) are frequently combined in both directions of a given building; i.e. there are buildings without braces in the x direction and with concentric or eccentric braces in the y direction. Even those "mixed" buildings are not explicitly considered in this study, their conclusions are completely valid for them since they are formulated separately for each direction. Comparison between Figure 4-3 and Figure 2-43 shows that in the y direction the braces are extended along the four bays; therefore the axial forces in the columns do not strongly overload a single column, as in Figure 2-43.a. Conversely, in the x direction the situation is not so optimal since the braces are only installed in two bays. However, the layout depicted by Figure 4-3 provides another relevant advantage: the columns that are overloaded by the *x* and *y* components of the ground motion are different; in other words, none single column is simultaneously overloaded by both components.

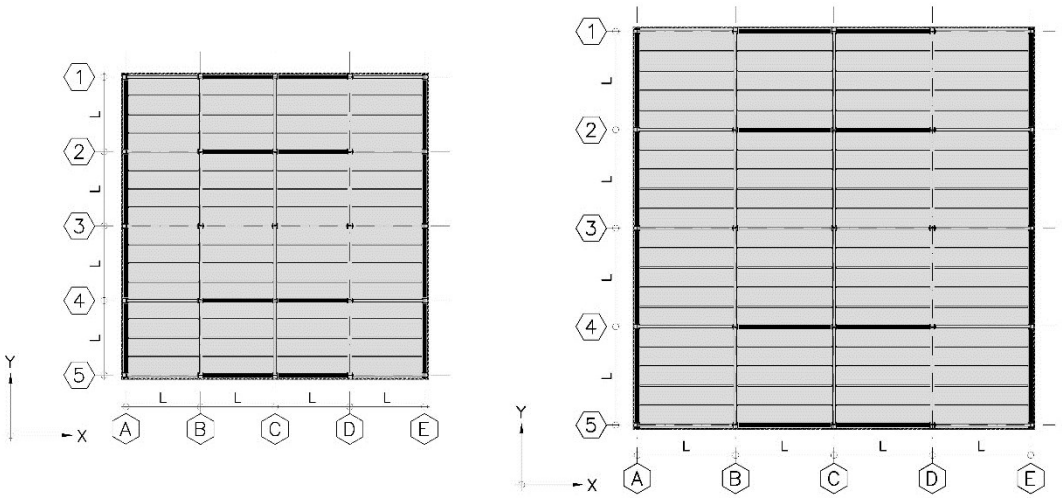

(a) 6 × 6 buildings (L = 6 m) (b) 8 × 8 buildings (L = 8 m)

Figure 4-3. Floor slab layout

In the 6 × 6 buildings the height of the first floor is 4 m and the one of the upper floors is 3 m; in the 8 × 8 buildings those heights are 4.50 m and 3.50 m, respectively (see section 4.1). As shown by Figure 4-3, the separation in between adjoining joists is 1.50 m (L / 4) for the 6 × 6 buildings and 1.60 m (L / 5) for the 8 × 8 buildings (see Figure 4-3.a and Figure 4-3.b, respectively). As described in section 4.1, the columns, beams and joists are made of W sections, and the braces are made with hollow square sections (HSS) [AISC 2010; AISC 360-10 2010]. All the joists are W10×15 and W12×19 for the 6 × 6 and 8 × 8 buildings, respectively. In the EBF buildings, the eccentricity between each pair of chevron braces (i.e. the length of the link segment, see Figure 2-44.a) is selected as to generate flexural-shear yielding failure in the link segment of the beam, prior to any other failure [Becker, Isler 1996; Hashemi 2011].

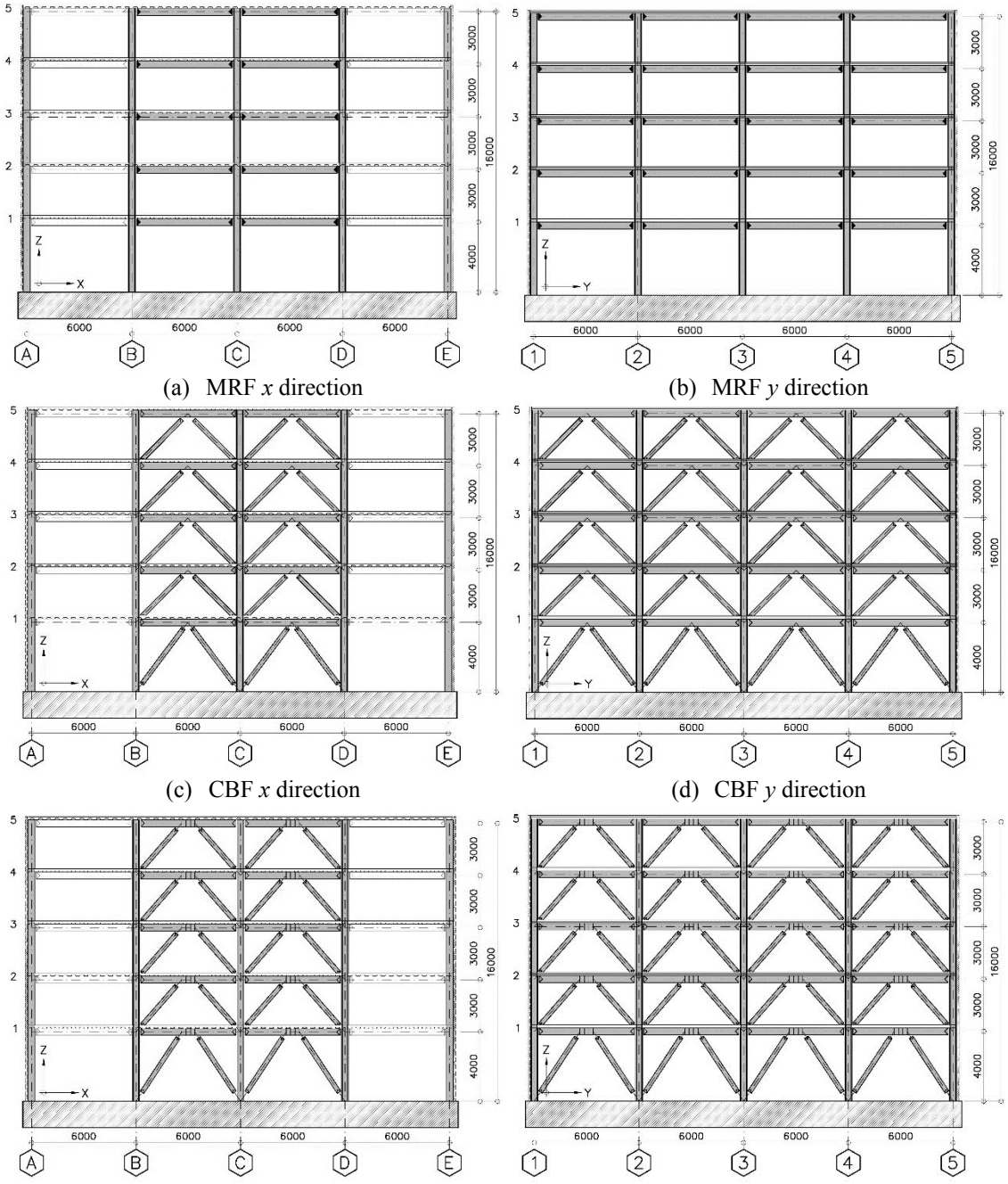

(a) MRF *x* direction (b) MRF *y* direction

(c) CBF *x* direction (d) CBF *y* direction

(e) EBF *x* direction (f) EBF *y* direction

Figure 4-4. Elevation views of the 5-story 6 × 6 buildings

Figure 4-4 shows overall elevation views of the selected 5-story buildings; the configurations of

the buildings with 10 and 15 floors are similar to these ones. Figure 4-3 and Figure 4-4 show that only some of the frames can be qualified as "seismic frames" (e.g. those designed to contribute to the lateral resistance, see Figure 2-38.b); Figure 4-3 shows that, in the *x* direction, there are four two-bay seismic frames (Figure 4-4.a, Figure 4-4.c and Figure 4-4.e) and, in the *y* direction, there are two four-bay seismic frames (Figure 4-4.b, Figure 4-4.d and Figure 4-4.f). In the seismic frames, the beam-column connections are pre-qualified according to [FEMA 350 2000] (see subsection 2.2.6 and Figure 2-40); the chosen type is "Welded Unreinforced Flange – Bolted Web" (WUF-B), commonly known as "California post-Northridge" connection, see Figure 4-6. Figure 4-6.a and Figure 4-6.b display a sketch and a picture of a connection, respectively. The connection in Figure 4-6 involves both welding and bolting; alternatively, a smaller number of bolts can be used, while in such a case the gusset plate is welded to the web of the beam. The weld access holes visible in Figure 4-6.b are designed to ease the welding operations (including the back-up plate) and to avoid brittle failure (mainly under cyclic loading) due to tensile stresses concentration.

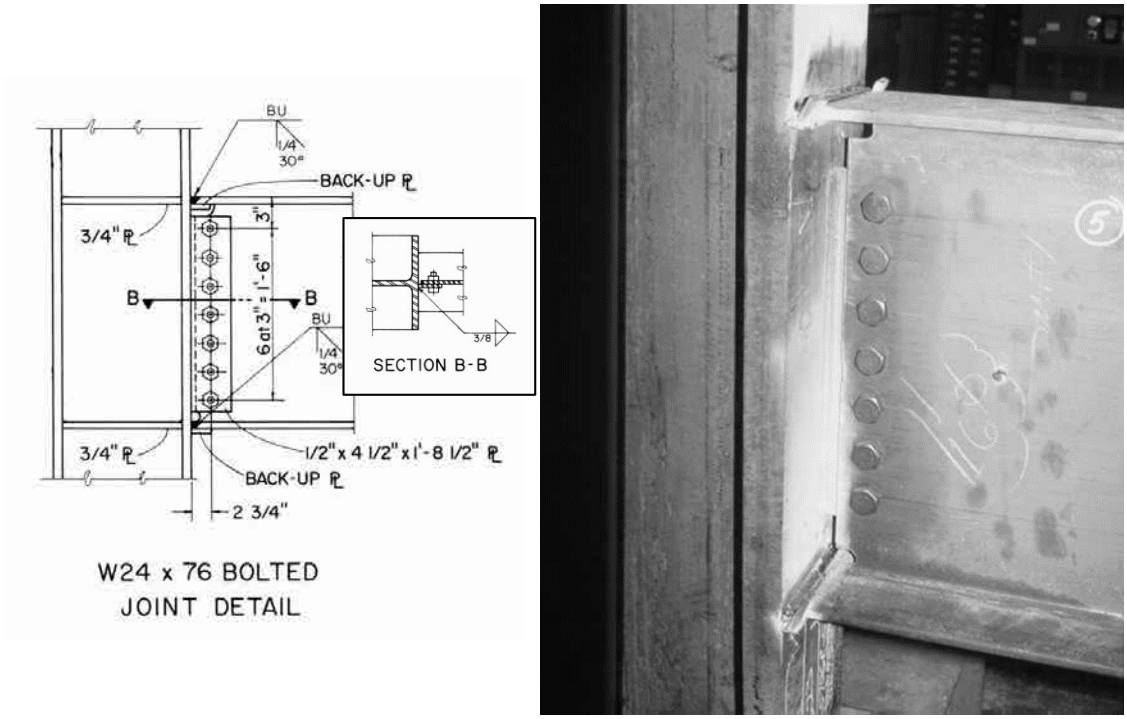

(a) Sketch of a connection (b) Picture of a connection

Figure 4-5. Prequalified "Welded Unreinforced Flange – Bolted Web" connection

In the non-seismic frames, the beam-column connections are mainly welded; they can be considered as hinged. In the CBF and in the EBF, the connections among the braces and the other members (through gusset plates) are also welded but can be considered as hinged. In the seismic frames, the columns can be considered as to be clamped to the foundation through welding to ordinary bolted base plates. In the non-seismic frames, the connections between the columns and the foundation can be considered as hinged since the columns are only partially welded to the base plates (by their web plates). Shear studs connecting the steel deck with the supporting horizontal members are placed only in the non-seismic elements, e.g. the joists (*y* direction) and those beams that do not belong to the seismic frames (both in *x* and *y* directions) [AISC-327 2005; Seek, Murray 2009]. This solution is customary in Bogotá; the studs are basically intended for guaranteeing the rigid diaphragm effect of the slabs (under lateral loading) rather than for increasing the bending stiffness and strength of beams and joists (as is common under gravity loads).

4.3.2 Detailed description

This subsection presents the sizes of the main members of the eighteen selected buildings. This information has been generated from the structural analysis described in section 4.4.

Table 4-1 to Table 4-10 display the main structural features of each of the eighteen selected buildings in each of the ten seismic zones. In the notation "5 – 6 × 6 – MRF", the digit "5" accounts for the number of stories, the set "6 × 6" refers to the span-length (in m) in both directions and the acronym "MRF" means Moment-Resisting Frame; analogously "CBF" and "EBF" relate to Concentric-Braced Frames and to Eccentric-Braced Frames, respectively. The steel profiles [AISC 2010; AISC 360-10 2010] belong to the seismic parts of the structure (see Figure 2-38.b; highlighted members in Figure 4-3 and Figure 4-4).

Table 4-1. Representative prototype buildings as designed for the "Piedemonte" zone (former microzonation)

Building	First floor beams	Top floor beams	First floor columns	Top floor columns	First floor braces	Top floor braces
5 – 6 × 6 – MRF	W24×146 / W24×162	W21×83 / W21×83	W14×257 / W14×283	W14×145 / W14×145	-	-
5 – 8 × 8 – MRF	W33×241 / W36×260	W24×146 / W24×146	W14×426 / W14×455	W14×257 / W14×257	-	-
5 – 6 × 6 – CBF	W27×178 / W30×191	W27×161 / W27×178	W14×193 / W14×145	W14×48 / W14×38	HSS6"×5/16"	HSS6"×3/16"
5 – 8 × 8 – CBF	W30×235 / W30×292	W30×191 / W30×191	W14×398 / W14×370	W14×193 / W14×176	HSS6"×⅝"	HSS6"×⅜"
5 – 6 × 6 – EBF	W12×50 / W12×53	W12×26 / W12×26	W12×96 / W12×58	W12×35 / W12×26	HSS5"×⅜"	HSS5"×½"
5 – 8 × 8 – EBF	W16×57 / W16×67	W16×36 / W16×40	W14×145 / W14×82	W14×53 / W14×34	HSS6"×½"	HSS6"× ¼"
10 – 6 × 6 – MRF	W33×241 / W33×241	W21×44 / W21×44	W14×426 / W14×455	W12×65 / W12×65	-	-
10 – 8 × 8 – MRF	W36×439 / W36×439	W24×131 / W24×131	W14×665 / W14×730	W12×230 / W12×230	-	-
10 – 6 × 6 – CBF	W33×263 / W33×263	W33×118 / W33×118	W14×455 / W14×370	W14×109 / W14×61	HSS7"×⅝"	HSS7"×¼"
10 – 8 × 8 – CBF	W36×527 / W36×527	W36×260 / W36×260	W14×550 / W14×455	W14×120 / W14×120	HSS12"×⅝"	HSS12"×½"
10 – 6 × 6 – EBF	W14×99 / W14×109	W14×22 / W14×22	W14×233 / W14×132	W14×26 / W14×22	HSS6"× ½"	HSS4½"×⅛"
10 – 8 × 8 – EBF	W18×106 / W18×106	W16×31 / W16×31	W14×398 / W14×257	W14×82 / W14×43	HSS7"×⅝"	HSS7"×3/16"
15 – 6 × 6 – MRF	W36×300 / W36×300	W30×191 / W30×191	W14×550 / W14×550	W14×342 / W14×342	-	-
15 – 8 × 8 – MRF	W36×650 / W36×650	W36×300 / W36×300	W14×730+P / W14×730+P	W14×500 / W14×500	-	-
15 – 6 × 6 – CBF	W36×393/ W36×328	W36×135 / W36×135	W14×730 / W14×665	W14×159 / W14×132	HSS14"×⅝"	HSS12"×5/16"
15 – 8 × 8 – CBF	W40×655 / W36×848	W36×527 / W36×393	W14×730+P / W14×730+P	W14×211 W14×211	HSS16"×⅝"	HSS12"×⅝"
15 – 6 × 6 – EBF	W14×348 / W14×193	W14×193 / W14×109	W14×455 / W14×283	W14×48 / W14×53	HSS8"× ½"	HSS7"×3/16"
15 – 8 × 8 – EBF	W21×201 / W21×166	W21×62 / W21×57	W14×730 / W14×550	W14×99 / W14×53	HSS9"×⅝"	HSS8"×3/16"

Table 4-2. Representative prototype buildings as designed for the "Lacustre A" zone (former microzonation)

Building	First floor beams	Top floor beams	First floor columns	Top floor columns	First floor braces	Top floor braces
5 – 6 × 6 – MRF	W21×147 / W21×147	W21×73 / W21×83	W14×233 / W14×257	W14×132 / W14×145	-	-
5 – 8 × 8 – MRF	W33×221 / W33×241	W24×117 / W24×131	W14×370 / W14×398	W14×193 / W14×233	-	-
5 – 6 × 6 – CBF	W27×161/ W30×173	W27×114 / W27×146	W14×176 / W14×132	W14×53 / W14×34	HSS5"×¼"	HSS5"×⅛"
5 – 8 × 8 – CBF	W30×191 / W30×211	W30×148 / W30×148	W14×311 / W14×283	W14×145 / W14×120	HSS6"×⅜"	HSS6"×¼"
5 – 6 × 6 – EBF	W12×35 / W12×40	W12×22 / W12×26	W12×87 / W12×50	W12×35 / W12×26	HSS5"×¼"	HSS5"×⅛"
5 – 8 × 8 – EBF	W16×45 / W16×57	W16×26 / W16×31	W14×145 / W14×82	W14×53 / W14×34	HSS6"×5/16"	HSS6"×3/16"
10 – 6 × 6 – MRF	W33×221 / W33×221	W21×44 / W21×44	W14×370 / W14×398	W12×65 / W12×65	-	-
10 – 8 × 8 – MRF	W36×393 / W36×439	W24×131 / W24×137	W14×665 / W14×665	W12×230 / W12×230	-	-
10 – 6 × 6 – CBF	W33×241 / W33×241	W33×118 / W33×118	W14×398 / W14×311	W14×90 / W14×48	HSS6"×⅜"	HSS6"×¼"
10 – 8 × 8 – CBF	W36×439 / W36×439	W36×245 / W36×235	W14×455 / W14×370	W14×90 / W14×90	HSS10"×⅝"	HSS10"×¼"
10 – 6 × 6 – EBF	W14×74 / W14×99	W14×22 / W14×22	W14×211 / W14×120	W14×26 / W14×22	HSS6"×⅜"	HSS4½"×⅛"
10 – 8 × 8 – EBF	W16×100 / W16×100	W16×31 / W16×310	W14×370 / W14×233	W14×74 / W14×38	HSS7"×½"	HSS7"×3/16"
15 – 6 × 6 – MRF	W36×330 / W36×330	W30×211 / W30×211	W14×605 / W14×605	W14×370 / W14×370	-	-
15 – 8 × 8 – MRF	W36×800 / W36×800	W36×359 / W36×359	W14×730+P / W14×730+P	W14×550 / W14×550	-	-
15 – 6 × 6 – CBF	W36×359/ W36×280	W36×135 / W36×135	W14×665 / W14×500	W14×120 / W14×99	HSS12"×⅝"	HSS10"×¼"
15 – 8 × 8 – CBF	W36×848 / W36×800	W36×393 / W36×359	W14×730+P / W14×730	W14×257/ W14×193	HSS14"×⅝"	HSS12"×¼"
15 – 6 × 6 – EBF	W14×257 / W14×145	W14×145 / W14×82	W14×398 / W14×257	W14×43 / W14×48	HSS7"×⅝"	HSS7"×⅛"
15 – 8 × 8 – EBF	W21×166 / W21×132	W21×50 / W21×50	W14×730 / W14×500	W14×99 / W14×48	HSS8"×⅝"	HSS7"×3/16"

Table 4-3. Representative prototype buildings as designed for the "Piedemonte A" zone (new microzonation)

Building	First floor beams	Top floor beams	First floor columns	Top floor columns	First floor braces	Top floor braces
5 – 6 × 6 – MRF	W21×132 / W21×147	W21×83 / W21×73	W14×233 / W14×257	W14×145 / W14×132	-	-
5 – 8 × 8 – MRF	W33×221 / W33×211	W21×147 / W21×132	W14×342 / W14×398	W14×233 / W14×233	-	-
5 – 6 × 6 – CBF	W27×146 / W30×146	W27×114 / W27×114	W14×211 / W14×159	W14×53 / W14×43	HSS4"×5/16"	HSS4"×3/16"
5 – 8 × 8 – CBF	W30×221 / W30×235	W30×173 / W30×148	W14×398 / W14×370	W14×193 / W14×176	HSS5"×½"	HSS5"×5/16"
5 – 6 × 6 – EBF	W12×35 / W12×45	W12×22 / W12×26	W12×79 / W12×50	W12×35 / W12×26	HSS5"×5/16"	HSS5"×¼"
5 – 8 × 8 – EBF	W16×50 / W16×57	W16×36 / W16×36	W12×136 / W12×65	W12×53 / W12×30	HSS6"×⅜"	HSS6"×3/16"
10 – 6 × 6 – MRF	W27×178 / W27×178	W18×35 / W18×35	W14×283 / W14×311	W10×60 / W10×60	-	-
10 – 8 × 8 – MRF	W36×260 / W36×280	W21×132 / W21×132	W14×426 / W14×455	W12×230 / W12×230	-	-
10 – 6 × 6 – CBF	W33×241 / W33×241	W33×118 / W33×118	W14×455 / W14×370	W14×109 / W14×61	HSS6"×½"	HSS6"×3/16"
10 – 8 × 8 – CBF	W36×393 / W36×393	W36×170 / W36×170	W14×550 / W14×455	W14×120 / W14×120	HSS10"×⅝"	HSS10"×¼"
10 – 6 × 6 – EBF	W14×48 / W14×53	W14×22 / W14×22	W14×193 / W14×109	W14×120 / W14×22	HSS5"×⅜"	HSS4½"×⅛"
10 – 8 × 8 – EBF	W16×57 / W16×77	W16×36 / W16×45	W14×311 / W14×159	W14×211 / W14×109	HSS6"×⅜"	HSS5"×3/16"
15 – 6 × 6 – MRF	W30×211 / W30×211	W24×104 / W24×104	W14×342 / W14×342	W14×193 / W14×193	-	-
15 – 8 × 8 – MRF	W36×300 / W36×300	W33×201 / W33×201	W14×550 / W14×550	W14×342 / W14×342	-	-
15 – 6 × 6 – CBF	W36×328/ W36×300	W36×210 / W36×194	W14×730 / W14×605	W14×257 / W14×211	HSS8"×⅝"	HSS7"×3/16"
15 – 8 × 8 – CBF	W36×848 / W36×720	W36×393 / W36×328	W14×730+ P / W14×730	W14×311/ W14×211	HSS9"×⅝"	HSS8"×¼"
15 – 6 × 6 – EBF	W14×68 / W14×68	W14×30 / W14×34	W14×283 / W14×174	W14×149 / W14×90	HSS6"×5/16"	HSS4½"×5/16"
15 – 8 × 8 – EBF	W16×77 / W16×100	W16×36 / W16×45	W14×455 / W14×257	W14×283 / W14×145	HSS7"×⅜"	HSS6"×3/16"

Table 4-4. Representative prototype buildings as designed for the "Piedemonte B" zone (new microzonation)

Building	First floor beams	Top floor beams	First floor columns	Top floor columns	First floor braces	Top floor braces
5 – 6 × 6 – MRF	W21×132 / W21×147	W21×83 / W21×73	W14×233 / W14×257	W14×145 / W14×132	-	-
5 – 8 × 8 – MRF	W30×191 / W30×211	W21×132 / W21×132	W14×342 / W14×370	W14×233 / W14×233	-	-
5 – 6 × 6 – CBF	W27×161 / W30×173	W27×146 / W27×161	W14×159 / W14×211	W14×53 / W14×43	HSS5"×½"	HSS4"×½"
5 – 8 × 8 – CBF	W30×261 / W30×292	W30×211 / W30×191	W14×398 / W14×370	W14×193 / W14×176	HSS6"×½"	HSS6"×⅜"
5 – 6 × 6 – EBF	W12×40 / W12×45	W12×26 / W12×26	W12×87 / W12×58	W12×35 / W12×26	HSS5"×½"	HSS4"×3/16"
5 – 8 × 8 – EBF	W16×50 / W16×57	W16×36 / W16×36	W12×136 / W12×65	W12×53 / W12×30	HSS6"×½"	HSS6"×⅜"
10 – 6 × 6 – MRF	W27×161 / W27×178	W18×35 / W18×35	W14×257 / W14×257	W10×54 / W10×54	-	-
10 – 8 × 8 – MRF	W33×241 / W33×241	W21×147 / W21×147	W14×398 / W14×426	W12×252 / W12×252	-	-
10 – 6 × 6 – CBF	W33×263 / W33×263	W33×118 / W33×118	W14×455 / W14×370	W14×109 / W14×61	HSS6"×½"	HSS6"×3/16"
10 – 8 × 8 – CBF	W36×328 / W36×328	W36×170 / W36×170	W14×550 / W14×455	W14×120 / W14×120	HSS10"×⅝"	HSS10"×¼"
10 – 6 × 6 – EBF	W14×38 / W14×48	W14×22 / W14×30	W14×176 / W14×109	W14×120 / W14×74	HSS5"×⅜"	HSS4½"×3/16"
10 – 8 × 8 – EBF	W16×50 / W16×67	W16×31 / W16×40	W14×283 / W14×145	W14×193 / W14×99	HSS6"×⅝"	HSS6"×¼"
15 – 6 × 6 – MRF	W30×191 / W30×191	W24×104 / W24×104	W14×311 / W14×311	W14×176 / W14×176	-	-
15 – 8 × 8 – MRF	W36×260 / W36×280	W27×161 / W30×173	W14×455 / W14×455	W14×283 / W14×283	-	-
15 – 6 × 6 – CBF	W36×280/ W36×260	W36×182 / W36×170	W14×605 / W14×500	W14×211 / W14×176	HSS7"×⅝"	HSS6"×3/16"
15 – 8 × 8 – CBF	W36×529 / W36×441	W36×328 / W36×280	W14×655 / W14×550	W14×311/ W14×211	HSS9"×⅝"	HSS8"×¼"
15 – 6 × 6 – EBF	W14×61 / W14×61	W14×26 / W14×30	W14×257 / W14×159	W14×145 / W14×90	HSS6"×⅜"	HSS5"×3/16"
15 – 8 × 8 – EBF	W16×67 / W16×89	W16×31 / W16×40	W14×426 / W14×233	W14×257 / W14×132	HSS7"×⅝"	HSS6"×5/16"

Table 4-5. Representative prototype buildings as designed for the "Piedemonte C" zone (new microzonation)

Building	First floor beams	Top floor beams	First floor columns	Top floor columns	First floor braces	Top floor braces
5 – 6 × 6 – MRF	W21×132 / W21×147	W21×83 / W21×73	W14×233 / W14×257	W14×145 / W14×132	-	-
5 – 8 × 8 – MRF	W30×191 / W30×211	W21×132 / W21×132	W14×342 / W14×370	W14×233 / W14×233	-	-
5 – 6 × 6 – CBF	W27×146 / W30×173	W27×114 / W27×146	W14×193 / W14×145	W14×48 / W14×38	HSS5"×5/16"	HSS5"×3/16"
5 – 8 × 8 – CBF	W30×261 / W30×292	W30×211 / W30×191	W14×398 / W14×370	W14×193 / W14×176	HSS6"× ⅜"	HSS46"×5/16"
5 – 6 × 6 – EBF	W12×40 / W12×45	W12×26 / W12×26	W12×87 / W12×50	W12×35 / W12×26	HSS5"×5/16"	HSS5"×¼"
5 – 8 × 8 – EBF	W16×50 / W16×57	W16×36 / W16×36	W12×136 / W12×65	W12×53 / W12×30	HSS6"×½"	HSS6"×⅜"
10 – 6 × 6 – MRF	W27×161 / W27×178	W18×35 / W18×35	W14×257 / W14×257	W10×54 / W10×54	-	-
10 – 8 × 8 – MRF	W33×241 / W33×241	W21×147 / W21×147	W14×398 / W14×426	W12×252 / W12×252	-	-
10 – 6 × 6 – CBF	W33×241 / W33×241	W33×118 / W33×118	W14×455 / W14×370	W14×109 / W14×61	HSS6"×½"	HSS6"×3/16"
10 – 8 × 8 – CBF	W36×328 / W36×328	W36×170 / W36×170	W14×550 / W14×455	W14×120 / W14×120	HSS10"×⅝"	HSS10"×¼"
10 – 6 × 6 – EBF	W14×38 / W14×48	W14×22 / W14×22	W14×176 / W14×109	W14×120 / W14×22	HSS5"×5/16"	HSS5"×¼"
10 – 8 × 8 – EBF	W16×50 / W16×67	W16×31 / W16×40	W14×283 / W14×145	W14×193 / W14×99	HSS6"×⅝"	HSS6"×¼"
15 – 6 × 6 – MRF	W30×191 / W30×191	W24×104 / W24×104	W14×311 / W14×311	W14×176 / W14×176	-	-
15 – 8 × 8 – MRF	W36×260 / W36×280	W27×161 / W30×173	W14×455 / W14×455	W14×283 / W14×283	-	-
15 – 6 × 6 – CBF	W36×280/ W36×260	W36×182 / W36×170	W14×605 / W14×500	W14×211 / W14×176	HSS7"×⅝"	HSS6"×3/16"
15 – 8 × 8 – CBF	W36×720 / W36×527	W36×328 / W36×280	W14×730+P / W14×730+P	W14×311/ W14×211	HSS8"×⅝"	HSS7"×¼"
15 – 6 × 6 – EBF	W14×53 / W14×61	W14×26 / W14×30	W14×257 / W14×159	W14×145 / W14×90	HSS6"×¼"	HSS4½"×¼"
15 – 8 × 8 – EBF	W16×67 / W16×89	W16×31 / W16×40	W14×426 / W14×233	W14×257 / W14×132	HSS7"×⅝"	HSS6"×5/16"

Table 4-6. Representative prototype buildings as designed for the "Lacustre-50" zone (new microzonation)

Building	First floor beams	Top floor beams	First floor columns	Top floor columns	First floor braces	Top floor braces
5 – 6 × 6 – MRF	W21×122 / W21×132	W21×62 / W21×57	W14×211 / W14×233	W14×109 / W14×99	-	-
5 – 8 × 8 – MRF	W33×201 / W33×201	W21×111 / W21×122	W14×311 / W14×342	W14×176 / W14×193	-	-
5 – 6 × 6 – CBF	W27×114 / W30×124	W27×102 / W27×114	W14×193 / W14×145	W14×48 / W14×38	HSS3½"×5/16"	HSS3½"×3/16"
5 – 8 × 8 – CBF	W30×191 / W30×211	W30×132 / W30×132	W14×398 / W14×370	W14×193 / W14×176	HSS4"×½"	HSS4"×5/16"
5 – 6 × 6 – EBF	W12×30 / W12×35	W12×19 / W12×22	W12×79 / W12×50	W12×35 / W12×26	HSS5"×¼"	HSS5"×⅛"
5 – 8 × 8 – EBF	W16×40 / W16×50	W16×26 / W16×31	W12×136 / W12×65	W12×53 / W12×30	HSS6"×¼"	HSS6"×3/16"
10 – 6 × 6 – MRF	W30×191 / W30×211	W18×40 / W18×40	W14×342 / W14×342	W10×68 / W10×68	-	-
10 – 8 × 8 – MRF	W36×330 / W36×330	W21×132 / W21×132	W14×605 / W14×605	W12×230 / W12×230	-	-
10 – 6 × 6 – CBF	W33×201 / W33×201	W33×118 / W33×118	W14×370 / W14×311	W14×109 / W14×61	HSS6"×½"	HSS6"×3/16"
10 – 8 × 8 – CBF	W36×300 / W36×300	W36×170 / W36×170	W14×550 / W14×455	W14×120 / W14×120	HSS10"×⅝"	HSS10"×¼"
10 – 6 × 6 – EBF	W14×48 / W14×61	W14×22 / W14×22	W14×193 / W14×120	W14×120 / W14×22	HSS5"×⅜"	HSS4½"×⅛"
10 – 8 × 8 – EBF	W16×67 / W16×89	W16×40 / W16×50	W14×342 / W14×174	W14×233 / W14×120	HSS6"×½"	HSS6"×3/16"
15 – 6 × 6 – MRF	W36×260 / W36×260	W27×161 / W27×161	W14×426 / W14×426	W14×257 / W14×257	-	-
15 – 8 × 8 – MRF	W36×439 / W36×439	W36×260 / W36×260	W14×730 / W14×730	W14×426 / W14×426	-	-
15 – 6 × 6 – CBF	W36×300/ W36×280	W36×194 / W36×182	W14×605 / W14×500	W14×233 / W14×193	HSS8"×⅝"	HSS6"×3/16"
15 – 8 × 8 – CBF	W40×655 / W36×798	W36×527 / W36×359	W14×730+P / W14×730+P	W14×370 / W14×211	HSS9"×⅝"	HSS8"×¼"
15 – 6 × 6 – EBF	W14×99 / W14×99	W14×48 / W14×48	W14×342 / W14×193	W14×193 / W14×90	HSS6"×½"	HSS4"×¼"
15 – 8 × 8 – EBF	W18×119 / W18×130	W16×50 / W16×57	W14×500 / W14×311	W14×311 / W14×176	HSS7"×½"	HSS6"×¼"

Table 4-7. Representative prototype buildings as designed for the "Lacustre-100" zone (new microzonation)

Building	First floor beams	Top floor beams	First floor columns	Top floor columns	First floor braces	Top floor braces
5 – 6 × 6 – MRF	W21×111 / W21×122	W21×62 / W21×57	W14×193 / W14×211	W14×109 / W14×99	-	-
5 – 8 × 8 – MRF	W30×173 / W30×191	W21×122 / W21×122	W14×311 / W14×342	W14×193 / W14×193	-	-
5 – 6 × 6 – CBF	W27×102 / W30×116	W27×94 / W27×114	W14×193 / W14×145	W14×48 / W14×38	HSS3½"×5/16"	HSS3½"×3/16"
5 – 8 × 8 – CBF	W30×173 / W30×191	W30×124 / W30×124	W14×398 / W14×370	W14×193 / W14×176	HSS4"×½"	HSS4"×5/16"
5 – 6 × 6 – EBF	W12×30 / W12×35	W12×19 / W12×22	W12×79 / W12×50	W12×35 / W12×26	HSS5"×¼"	HSS5"×⅛"
5 – 8 × 8 – EBF	W16×40 / W16×45	W16×26 / W16×36	W12×136 / W12×65	W12×53 / W12×30	HSS5"×½"	HSS5"×5/16"
10 – 6 × 6 – MRF	W30×191 / W30×191	W18×40 / W18×40	W14×311 / W14×342	W10×60 / W10×68	-	-
10 – 8 × 8 – MRF	W33×300 / W33×330	W21×132 / W21×132	W14×550 / W14×550	W12×230 / W14×230	-	-
10 – 6 × 6 – CBF	W33×201/ W33×201	W33×118 / W33×118	W14×370 / W14×311	W14×109 / W14×61	HSS5"×½"	HSS5"×3/16"
10 – 8 × 8 – CBF	W36×180 / W36×280	W36×170 / W36×170	W14×550 / W14×455	W14×120 / W14×120	HSS9"×⅝"	HSS9"×¼"
10 – 6 × 6 – EBF	W14×48 / W14×53	W14×22 / W14×22	W14×176 / W14×109	W14×109 / W14×22	HSS5"×⅜"	HSS4½"×⅛"
10 – 8 × 8 – EBF	W16×67 / W16×77	W16×40 / W16×45	W14×311 / W14×159	W14×211 / W14×109	HSS6"×½"	HSS6"×3/16"
15 – 6 × 6 – MRF	W36×260 / W36×260	W27×161 / W27×161	W14×455 / W14×455	W14×283 / W14×283	-	-
15 – 8 × 8 – MRF	W36×439 / W36×439	W36×280 / W30×280	W14×730+P / W14×730+P	W14×455 / W14×455	-	-
15 – 6 × 6 – CBF	W36×300/ W36×280	W36×194 / W36×182	W14×730 / W14×605	W14×257 / W14×211	HSS7"×⅝"	HSS6"×3/16"
15 – 8 × 8 – CBF	W36×798 / W36×650	W36×359 / W36×300	W14×730+P / W14×730+P	W14×370 / W14×257	HSS9"×⅝"	HSS8"×¼"
15 – 6 × 6 – EBF	W14×90 / W14×82	W14×43 / W14×43	W14×305 / W14×176	W14×176 / W14×82	HSS6"×½"	HSS4"×3/16"
15 – 8 × 8 – EBF	W18×119 / W18×130	W16×50 / W16×57	W14×500 / W14×311	W14×311 / W14×176	HSS7"×½"	HSS6"×¼"

Table 4-8. Representative prototype buildings as designed for the "Lacustre-200" zone (new microzonation)

Building	First floor beams	Top floor beams	First floor columns	Top floor columns	First floor braces	Top floor braces
5 – 6 × 6 – MRF	W21×111 / W21×122	W21×44 / W21×44	W14×193 / W14×211	W12×87 / W12×87	-	-
5 – 8 × 8 – MRF	W27×178 / W30×191	W21×111 / W21×101	W14×311 / W14×311	W14×193 / W14×178	-	-
5 – 6 × 6 – CBF	W27×102 / W30×108	W27×84 / W27×102	W14×193 / W14×145	W14×48 / W14×38	HSS3½"×5/16"	HSS3½"×3/16"
5 – 8 × 8 – CBF	W30×191 / W30×211	W30×132 / W30×132	W14×398 / W14×370	W14×193 / W14×176	HSS3½"×⅜"	HSS3½"×5/16"
5 – 6 × 6 – EBF	W12×26 / W12×30	W12×19 / W12×22	W12×79 / W12×50	W12×35 / W12×26	HSS5"×3/16"	HSS4½"×⅛"
5 – 8 × 8 – EBF	W16×36 / W16×45	W16×22 / W16×31	W12×136 / W12×65	W12×53 / W12×30	HSS5"×½"	HSS5"×3/16"
10 – 6 × 6 – MRF	W27×178 / W30×173	W18×40 / W18×40	W14×311 / W14×311	W10×60 / W10×68	-	-
10 – 8 × 8 – MRF	W36×300 / W36×300	W21×132 / W21×132	W14×500 / W14×550	W12×230 / W12×230	-	-
10 – 6 × 6 – CBF	W33×152 / W33×152	W30×99/ W30×99	W14×370 / W14×311	W14×109 / W14×61	HSS5"×½"	HSS5"×3/16"
10 – 8 × 8 – CBF	W36×260 / W36×260	W36×170 / W36×170	W14×550 / W14×455	W14×120 / W14×120	HSS8"×⅝"	HSS8"×¼"
10 – 6 × 6 – EBF	W14×43 / W14×48	W14×22 / W14×22	W14×176 / W14×109	W14×120 / W14×22	HSS5"×⅜"	HSS4½"×⅛"
10 – 8 × 8 – EBF	W16×67 / W16×77	W16×40 / W16×45	W14×311 / W14×159	W14×211 / W14×109	HSS6"×½"	HSS6"×3/16"
15 – 6 × 6 – MRF	W36×260 / W36×260	W27×161 / W27×161	W14×426 / W14×426	W14×257 / W14×257	-	-
15 – 8 × 8 – MRF	W36×439 / W36×439	W36×280 / W36×280	W14×730+P / W14×730+P	W14×455 / W14×455	-	-
15 – 6 × 6 – CBF	W36×260/ W36×245	W36×170 / W36×160	W14×605 / W14×426	W14×233 / W14×176	HSS7"×⅝"	HSS6"×3/16"
15 – 8 × 8 – CBF	W36×650 / W36×527	W36×300 / W36×280	W14×730+P / W14×730+P	W14×370 / W14×257	HSS9"×⅝"	HSS8"×¼"
15 – 6 × 6 – EBF	W14×82/ W14×82	W14×38 / W14×43	W14×283 / W14×176	W14×159 / W14×74	HSS6"×½"	HSS4"×¼"
15 – 8 × 8 – EBF	W16×100 / W18×119	W16×45 / W16×50	W14×500 / W14×311	W14×311 / W14×176	HSS7"×½"	HSS6"×¼"

Table 4-9. Representative prototype buildings as designed for the "Lacustre-300" zone (new microzonation)

Building	First floor beams	Top floor beams	First floor columns	Top floor columns	First floor braces	Top floor braces
5 – 6 × 6 – MRF	W21×93 / W21×101	W21×50 / W21×44	W14×159 / W14×176	W14×90 / W14×82	-	-
5 – 8 × 8 – MRF	W27×161 / W30×173	W21×93 / W21×93	W14×283 / W14×283	W14×159 / W14×159	-	-
5 – 6 × 6 – CBF	W27×94 / W30×99	W27×84 / W27×94	W14×176 / W14×132	W14×43 / W14×34	HSS3"×5/16"	HSS3"×3/16"
5 – 8 × 8 – CBF	W30×173 / W30×191	W30×124 / W30×124	W14×398 / W14×370	W14×193 / W14×176	HSS3"×⅜"	HSS3"×5/16"
5 – 6 × 6 – EBF	W12×26 / W12×26	W12×19 / W12×19	W12×79 / W12×50	W12×35 / W12×26	HSS5"×3/16"	HSS4½"×⅛"
5 – 8 × 8 – EBF	W16×31 / W16×40	W14×22 / W16×26	W12×136 / W12×65	W12×53 / W12×30	HSS5"×⅜"	HSS5"×3/16"
10 – 6 × 6 – MRF	W27×161 / W30×173	W21×101 / W21×101	W14×283 / W14×283	W12×170 / W12×170	-	-
10 – 8 × 8 – MRF	W36×260 / W36×280	W21×132 / W21×132	W14×455 / W14×500	W12×230 / W12×230	-	-
10 – 6 × 6 – CBF	W33×141 / W33×141	W30×99 / W30×99	W14×370 / W14×311	W14×99 / W14×61	HSS5"×⅜"	HSS5"×⅛"
10 – 8 × 8 – CBF	W36×245 / W36×245	W36×170 / W36×170	W14×398 / W14×342	W14×99 / W14×99	HSS7"×⅝"	HSS7"×¼"
10 – 6 × 6 – EBF	W14×38 / W14×43	W14×22 / W14×22	W14×159 / W14×99	W14×109 / W14×22	HSS5"×5/16"	HSS4"×3/16"
10 – 8 × 8 – EBF	W16×57 / W16×67	W16×36 / W16×40	W14×283 / W14×145	W14×193 / W14×99	HSS6"×⅜"	HSS6"×⅛"
15 – 6 × 6 – MRF	W33×241 / W33×241	W27×146/ W27×146	W14×398 / W14×398	W14×233 / W14×233	-	-
15 – 8 × 8 – MRF	W36×439 / W36×439	W36×260 / W36×260	W14×730 / W14×730	W14×426 / W14×426	-	-
15 – 6 × 6 – CBF	W36×245/ W36×230	W36×160 / W36×150	W14×605 / W14×426	W14×233 / W14×176	HSS6"×⅝"	HSS6"×⅛"
15 – 8 × 8 – CBF	W36×527 / W36×439	W36×380 / W36×260	W14×730+P / W14×730+P	W14×370 / W14×257	HSS8"×⅝"	HSS7"×¼"
15 – 6 × 6 – EBF	W14×68 / W14×74	W14×34 / W14×38	W14×283 / W14×176	W14×145 / W14×68	HSS6"×⅜"	HSS4"×3/16"
15 – 8 × 8 – EBF	W16×89 / W18×119	W16×40 / W16×50	W14×455 / W14×283	W14×283 / W14×159	HSS7"×⅜"	HSS6"×3/16"

Table 4-10. Representative prototype buildings as designed for the "Lacustre-500" zone (new microzonation)

Building	First floor beams	Top floor beams	First floor columns	Top floor columns	First floor braces	Top floor braces
5 – 6 × 6 – MRF	W21×83 / W21×93	W21×57 / W21×44	W14×145 / W14×259	W12×87 / W12×87	-	-
5 – 8 × 8 – MRF	W27×146 / W27×161	W21×83 / W21×83	W14×257 / W14×283	W14×145 / W14×145	-	-
5 – 6 × 6 – CBF	W27×84 / W27×94	W24×46 / W27×4	W14×176 / W14×132	W14×43 / W14×34	HSS3"×5/16"	HSS3"×3/16"
5 – 8 × 8 – CBF	W30×132 / W30×148	W30×116 / W30×116	W14×398 / W14×370	W14×193 / W14×176	HSS3"×⅜"	HSS3"×5/16"
5 – 6 × 6 – EBF	W12×26 / W12×26	W12×16 / W12×19	W12×72 / W12×50	W12×35 / W12×26	HSS5"×3/16"	HSS4½"×⅛"
5 – 8 × 8 – EBF	W16×31 / W16×36	W14×22 / W16×26	W12×136 / W12×65	W12×53 / W12×30	HSS5"×⅜"	HSS5"×3/16"
10 – 6 × 6 – MRF	W27×146 / W27×161	W21×101 / W21×101	W14×257 / W14×257	W12×170 / W10×170	-	-
10 – 8 × 8 – MRF	W36×245 / W36×260	W21×132 / W21×132	W14×398 / W14×426	W12×230 / W12×230	-	-
10 – 6 × 6 – CBF	W33×130 / W33×130	W27×84 / W27×84	W14×311 / W14×257	W14×68 / W14×61	HSS5"×⅜"	HSS5"×⅛"
10 – 8 × 8 – CBF	W36×230 / W36×230	W36×170 / W36×170	W14×398 / W14×342	W14×99 / W14×99	HSS6"×⅝"	HSS6"×¼"
10 – 6 × 6 – EBF	W14×34 / W14×43	W12×19 / W14×22	W14×159 / W14×90	W14×82 / W14×22	HSS5"×5/16"	HSS4"×3/16"
10 – 8 × 8 – EBF	W16×50 / W16×67	W16×31 / W16×40	W14×283 / W14×145	W14×193 / W14×99	HSS6"×⅜"	HSS6"×⅛"
15 – 6 × 6 – MRF	W33×221 / W33×221	W24×117 / W24×117	W14×370 / W14×342	W14×211 / W14×211	-	-
15 – 8 × 8 – MRF	W36×393 / W36×393	W36×245 / W36×245	W14×665 / W14×665	W14×398 / W14×398	-	-
15 – 6 × 6 – CBF	W36×210/ W36×194	W36×135 / W33×118	W14×426 / W14×311	W14×193 / W14×145	HSS6"×⅝"	HSS6"×⅛"
15 – 8 × 8 – CBF	W36×393 / W36×328	W36×245 / W36×210	W14×730+P / W14×730+P	W14×370/ W14×257	HSS8"×⅝"	HSS7"×¼"
15 – 6 × 6 – EBF	W14×61 / W14×68	W14×30 / W14×34	W14×257 / W14×159	W14×132 / W14×61	HSS6"×⅜"	HSS4"×3/16"
15 – 8 × 8 – EBF	W16×89 / W16×100	W16×40 / W16×45	W14×455 / W14×257	W14×283 / W14×145	HSS6"×⅝"	HSS6"×3/16"

4.3.3 Link of the EBF buildings

This subsection describes the link segments (see Figure 2-44 and Figure 2-46) of the EBF buildings. Figure 4-6 represents, for an EBF building, the connection between the bracing members and the corresponding beam.

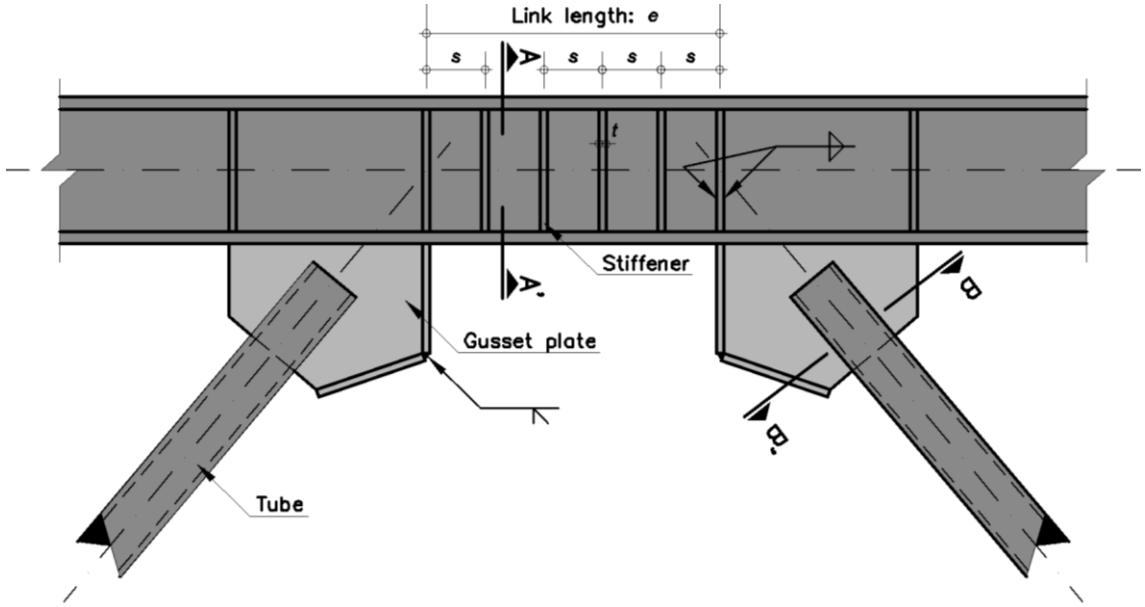

(a) Side view

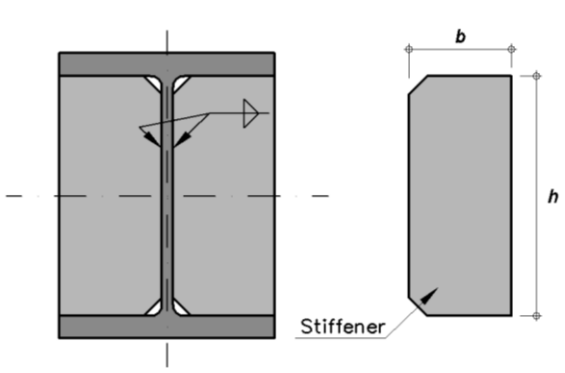

(b) Section by the link segment

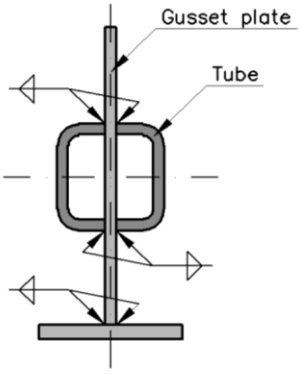

(c) Section by a gusset plate

Figure 4-6. Connection between two chevron braces and one beam of a EBF building

Table 4-11 through Table 4-20 present the main geometrical parameters of the stiffeners in the links of the EBF designed for the considered seismic zones, respectively. The connections (particularly, the stiffeners) have been designed according the code [AISC 2010; AISC 360-10 2010]. That regulation states that there are three types of links: predominantly shear yielding link (length less than 1.6 times the ratio between the resistant plastic moment and shear force), predominantly flexural yielding link (length greater than 2.6 times the ratio between the resistant plastic moment and shear force), and combined shear and flexural yielding link (length in between the two previous bounds). The type of failure is indicated in the fifth column of Table 4-11 through Table 4-20.

Table 4-11. Stiffeners for the EBF buildings. "Piedemonte" zone (former microzonation)

Building	Level	Direction	Length e (mm)	Failure mode	$b \times h \times t$ (mm)	Separation s (mm)
5 – 6 × 6 – EBF	First	x	1500	Shear and Flexural	93 × 277 × 10	233
		y	1500	Shear and Flexural	118 × 278 × 10	218
	Top	x	1500	Shear and Flexural	77 × 291 × 10	114
		y	1500	Shear and Flexural	77 × 291 × 10	114
5 – 8 × 8 – EBF	First	x	1600	Shear and Flexural	80 × 380 × 11	233
		y	1600	Shear and Flexural	120 × 380 × 10	218
	Top	x	1600	Flexural Yielding	81 × 382 × 10	309
		y	1600	Shear and Flexural	81 × 381 × 10	155
10 – 6 × 6 – EBF	First	x	1500	Shear Yielding	173 × 321 × 12	297
		y	1500	Shear Yielding	172 × 320 × 13	327
	Top	x	1500	Flexural Yielding	45 × 291 × 10	281
		y	1500	Flexural Yielding	45 × 291 × 10	281
10 – 8 × 8 – EBF	First	x	1600	Shear and Flexural	127 × 427 × 15	387
		y	1600	Shear and Flexural	127 × 427 × 15	387
	Top	x	1600	Flexural Yielding	63 × 382 × 10	282
		y	1600	Flexural Yielding	63 × 382 × 10	282
15 – 6 × 6 – EBF	First	x	1500	Shear Yielding	169 × 319 × 39	750
		y	1500	Shear Yielding	177 × 321 × 23	599
	Top	x	1500	Shear Yielding	177 × 321 × 23	599
		y	1500	Shear Yielding	172 × 320 × 13	327
15 – 8 × 8 – EBF	First	x	1600	Shear Yielding	137 × 501 × 23	577
		y	1600	Shear Yielding	138 × 502 × 19	457
	Top	x	1600	Shear and Flexural	94 × 502 × 10	210
		y	1600	Shear and Flexural	73 × 503 × 10	207

Table 4-12. Stiffeners for the EBF buildings. "Lacustre" zone (former microzonation)

Building	Level	Direction	Length e (mm)	Failure mode	$b \times h \times t$ (mm)	Separation s (mm)
5 – 6 × 6 – EBF	First	x	1500	Shear and Flexural	76 × 291 × 10	169
		y	1500	Shear and Flexural	94 × 276 × 10	174
	Top	x	1500	Flexural Yielding	45 × 291 × 10	281
		y	1500	Shear and Flexural	77 × 291 × 10	114
5 – 8 × 8 – EBF	First	x	1600	Shear and Flexural	81 × 380 × 10	186
		y	1600	Shear and Flexural	80 × 380 × 11	251
	Top	x	1600	Flexural Yielding	64 × 381 × 10	250
		y	1600	Flexural Yielding	63 × 382 × 10	282
10 – 6 × 6 – EBF	First	x	1500	Shear Yielding	117 × 321 × 11	271
		y	1500	Shear Yielding	173 × 321 × 12	297
	Top	x	1500	Flexural Yielding	58 × 331 × 10	234
		y	1500	Flexural Yielding	58 × 331 × 10	234
10 – 8 × 8 – EBF	First	x	1600	Shear and Flexural	117 × 382 × 15	390
		y	1600	Shear and Flexural	117 × 382 × 15	390
	Top	x	1600	Flexural Yielding	63 × 382 × 10	282
		y	1600	Flexural Yielding	63 × 382 × 10	282
15 – 6 × 6 – EBF	First	x	1500	Shear Yielding	173 × 321 × 30	816
		y	1500	Shear Yielding	180 × 321 × 17	443
	Top	x	1500	Shear Yielding	180 × 321 × 17	443
		y	1500	Shear and Flexural	115 × 320 × 13	343
15 – 8 × 8 – EBF	First	x	1600	Shear Yielding	138 × 502 × 19	457
		y	1600	Shear Yielding	141 × 501 × 17	385
	Top	x	1600	Shear and Flexural	73 × 501 × 10	184
		y	1600	Shear and Flexural	73 × 501 × 10	184

Table 4-13. Stiffeners for the EBF buildings. "Piedemonte A" zone (new microzonation)

Building	Level	Direction	Length e (mm)	Failure mode	$b \times h \times t$ (mm)	Separation s (mm)
5 – 6 × 6 – EBF	First	x	1500	Shear and Flexural	76 × 291 × 10	169
		y	1500	Shear and Flexural	94 × 278 × 10	205
	Top	x	1500	Flexural Yielding	45 × 291 × 10	281
		y	1500	Shear and Flexural	77 × 291 × 10	114
5 – 8 × 8 – EBF	First	x	1600	Shear and Flexural	80 × 382 × 10	212
		y	1600	Shear and Flexural	80 × 380 × 11	251
	Top	x	1600	Flexural Yielding	81 × 382 × 10	309
		y	1600	Flexural Yielding	81 × 382 × 10	309
10 – 6 × 6 – EBF	First	x	1500	Shear and Flexural	93 × 320 × 10	202
		y	1500	Shear and Flexural	93 × 320 × 10	226
	Top	x	1500	Flexural Yielding	58 × 331 × 10	234
		y	1500	Flexural Yielding	58 × 331 × 10	234
10 – 8 × 8 – EBF	First	x	1600	Shear and Flexural	80 × 380 × 11	251
		y	1600	Shear and Flexural	119 × 380 × 12	285
	Top	x	1600	Flexural Yielding	81 × 382 × 10	309
		y	1600	Shear and Flexural	81 × 380 × 10	186
15 – 6 × 6 – EBF	First	x	1500	Shear and Flexural	116 × 319 × 11	268
		y	1500	Shear and Flexural	116 × 319 × 11	268
	Top	x	1500	Flexural Yielding	79 × 331 × 10	287
		y	1500	Shear and Flexural	78 × 332 × 10	149
15 – 8 × 8 – EBF	First	x	1600	Shear and Flexural	119 × 380 × 12	285
		y	1600	Shear and Flexural	117 × 382 × 15	390
	Top	x	1600	Flexural Yielding	81 × 382 × 10	309
		y	1600	Shear and Flexural	81 × 380 × 10	186

Table 4-14. Stiffeners for the EBF buildings. "Piedemonte B" zone (new microzonation)

Building	Level	Direction	Length e (mm)	Failure mode	$b \times h \times t$ (mm)	Separation s (mm)
5 – 6 × 6 – EBF	First	x	1500	Shear and Flexural	94 × 276 × 10	174
		y	1500	Shear and Flexural	94 × 278 × 10	205
	Top	x	1500	Shear and Flexural	77 × 291 × 10	114
		y	1500	Shear and Flexural	77 × 291 × 10	114
5 – 8 × 8 – EBF	First	x	1600	Shear and Flexural	80 × 382 × 10	212
		y	1600	Shear and Flexural	80 × 380 × 11	251
	Top	x	1600	Flexural Yielding	81 × 382 × 10	309
		y	1600	Flexural Yielding	81 × 382 × 10	309
10 – 6 × 6 – EBF	First	x	1500	Shear and Flexural	78 × 332 × 10	169
		y	1500	Shear and Flexural	93 × 320 × 10	202
	Top	x	1500	Flexural Yielding	58 × 331 × 10	234
		y	1500	Flexural Yielding	79 × 331 × 10	287
10 – 8 × 8 – EBF	First	x	1600	Shear and Flexural	80 × 382 × 10	212
		y	1600	Shear and Flexural	120 × 380 × 10	238
	Top	x	1600	Flexural Yielding	63 × 382 × 10	282
		y	1600	Shear and Flexural	81 × 381 × 10	155
15 – 6 × 6 – EBF	First	x	1500	Shear and Flexural	117 × 320 × 10	235
		y	1500	Shear and Flexural	117 × 320 × 10	235
	Top	x	1500	Flexural Yielding	57 × 332 × 10	266
		y	1500	Flexural Yielding	79 × 331 × 10	287
15 – 8 × 8 – EBF	First	x	1600	Shear and Flexural	120 × 380 × 10	238
		y	1600	Shear and Flexural	119 × 382 × 13	341
	Top	x	1600	Flexural Yielding	63 × 382 × 10	282
		y	1600	Shear and Flexural	81 × 381 × 10	155

Table 4-15. Stiffeners for the EBF buildings. "Piedemonte C" zone (new microzonation)

Building	Level	Direction	Length e (mm)	Failure mode	$b \times h \times t$ (mm)	Separation s (mm)
5 – 6 × 6 – EBF	First	x	1500	Shear and Flexural	94 × 276 × 10	174
		y	1500	Shear and Flexural	94 × 278 × 10	205
	Top	x	1500	Shear and Flexural	77 × 291 × 10	114
		y	1500	Shear and Flexural	77 × 291 × 10	114
5 – 8 × 8 – EBF	First	x	1600	Shear and Flexural	80 × 382 × 10	212
		y	1600	Shear and Flexural	80 × 380 × 11	251
	Top	x	1600	Flexural Yielding	81 × 382 × 10	309
		y	1600	Flexural Yielding	81 × 382 × 10	309
10 – 6 × 6 – EBF	First	x	1500	Shear and Flexural	78 × 332 × 10	169
		y	1500	Shear and Flexural	93 × 320 × 10	202
	Top	x	1500	Flexural Yielding	58 × 331 × 10	234
		y	1500	Flexural Yielding	58 × 331 × 10	234
10 – 8 × 8 – EBF	First	x	1600	Shear and Flexural	80 × 382 × 10	212
		y	1600	Shear and Flexural	120 × 380 × 10	238
	Top	x	1600	Flexural Yielding	63 × 382 × 10	282
		y	1600	Shear and Flexural	81 × 381 × 10	155
15 – 6 × 6 – EBF	First	x	1500	Shear and Flexural	93 × 320 × 10	226
		y	1500	Shear and Flexural	117 × 320 × 10	235
	Top	x	1500	Flexural Yielding	57 × 332 × 10	266
		y	1500	Flexural Yielding	79 × 331 × 10	287
15 – 8 × 8 – EBF	First	x	1600	Shear and Flexural	120 × 380 × 10	238
		y	1600	Shear and Flexural	119 × 382 × 13	341
	Top	x	1600	Flexural Yielding	63 × 382 × 10	282
		y	1600	Shear and Flexural	81 × 381 × 10	155

Table 4-16. Stiffeners for the EBF buildings. "Lacustre-50" zone (new microzonation)

Building	Level	Direction	Length e (mm)	Failure mode	$b \times h \times t$ (mm)	Separation s (mm)
5 – 6 × 6 – EBF	First	x	1500	Shear and Flexural	76 × 290 × 10	138
		y	1500	Shear and Flexural	76 × 291 × 10	169
	Top	x	1500	Flexural Yielding	45 × 292 × 10	248
		y	1500	Flexural Yielding	45 × 291 × 10	281
5 – 8 × 8 – EBF	First	x	1600	Shear and Flexural	81 × 381 × 10	155
		y	1600	Shear and Flexural	80 × 382 × 10	212
	Top	x	1600	Flexural Yielding	64 × 381 × 10	250
		y	1600	Flexural Yielding	63 × 382 × 10	282
10 – 6 × 6 – EBF	First	x	1500	Shear and Flexural	93 × 320 × 10	202
		y	1500	Shear and Flexural	117 × 320 × 10	235
	Top	x	1500	Flexural Yielding	58 × 331 × 10	234
		y	1500	Flexural Yielding	58 × 331 × 10	234
10 – 8 × 8 – EBF	First	x	1600	Shear and Flexural	120 × 380 × 10	238
		y	1600	Shear and Flexural	119 × 382 × 13	341
	Top	x	1600	Shear and Flexural	81 × 381 × 10	155
		y	1600	Shear and Flexural	80 × 382 × 10	212
15 – 6 × 6 – EBF	First	x	1500	Shear Yielding	173 × 321 × 12	297
		y	1500	Shear Yielding	173 × 321 × 12	297
	Top	x	1500	Shear and Flexural	93 × 320 × 10	202
		y	1500	Shear and Flexural	93 × 320 × 10	202
15 – 8 × 8 – EBF	First	x	1600	Shear Yielding	127 × 429 × 17	403
		y	1600	Shear Yielding	125 × 429 × 17	412
	Top	x	1600	Shear and Flexural	80 × 382 × 10	212
		y	1600	Shear and Flexural	80 × 380 × 11	251

Table 4-17. Stiffeners for the EBF buildings. "Lacustre-100" zone (new microzonation)

Building	Level	Direction	Length e (mm)	Failure mode	$b \times h \times t$ (mm)	Separation s (mm)
5 – 6 × 6 – EBF	First	x	1500	Shear and Flexural	76 × 290 × 10	138
		y	1500	Shear and Flexural	76 × 291 × 10	169
	Top	x	1500	Flexural Yielding	45 × 292 × 10	248
		y	1500	Flexural Yielding	45 × 291 × 10	281
5 – 8 × 8 – EBF	First	x	1600	Shear and Flexural	81 × 381 × 10	155
		y	1600	Shear and Flexural	81 × 380 × 10	186
	Top	x	1600	Flexural Yielding	64 × 381 × 10	250
		y	1600	Flexural Yielding	81 × 382 × 10	309
10 – 6 × 6 – EBF	First	x	1500	Shear and Flexural	93 × 320 × 10	202
		y	1500	Shear and Flexural	93 × 320 × 10	226
	Top	x	1500	Flexural Yielding	58 × 331 × 10	234
		y	1500	Flexural Yielding	58 × 331 × 10	234
10 – 8 × 8 – EBF	First	x	1600	Shear and Flexural	120 × 380 × 10	238
		y	1600	Shear and Flexural	119 × 380 × 12	285
	Top	x	1600	Shear and Flexural	81 × 381 × 10	155
		y	1600	Shear and Flexural	81 × 380 × 10	186
15 – 6 × 6 – EBF	First	x	1500	Shear Yielding	173 × 320 × 11	264
		y	1500	Shear and Flexural	115 × 320 × 13	343
	Top	x	1500	Shear and Flexural	94 × 321 × 10	174
		y	1500	Shear and Flexural	94 × 321 × 10	174
15 – 8 × 8 – EBF	First	x	1600	Shear Yielding	127 × 429 × 17	403
		y	1600	Shear Yielding	125 × 429 × 17	412
	Top	x	1600	Shear and Flexural	80 × 382 × 10	212
		y	1600	Shear and Flexural	80 × 380 × 11	251

Table 4-18. Stiffeners for the EBF buildings. "Lacustre-200" zone (new microzonation)

Building	Level	Direction	Length e (mm)	Failure mode	$b \times h \times t$ (mm)	Separation s (mm)
5 – 6 × 6 – EBF	First	x	1500	Shear and Flexural	77 × 291 × 10	114
		y	1500	Shear and Flexural	76 × 290 × 10	138
	Top	x	1500	Flexural Yielding	45 × 292 × 10	248
		y	1500	Flexural Yielding	45 × 291 × 10	281
5 – 8 × 8 – EBF	First	x	1600	Flexural Yielding	81 × 382 × 10	309
		y	1600	Shear and Flexural	81 × 380 × 10	186
	Top	x	1600	Flexural Yielding	58 × 331 × 10	234
		y	1600	Flexural Yielding	63 × 382 × 10	282
10 – 6 × 6 – EBF	First	x	1500	Shear and Flexural	94 × 321 × 10	174
		y	1500	Shear and Flexural	93 × 320 × 10	202
	Top	x	1500	Flexural Yielding	45 × 291 × 10	281
		y	1500	Flexural Yielding	45 × 291 × 10	281
10 – 8 × 8 – EBF	First	x	1600	Shear and Flexural	120 × 380 × 10	238
		y	1600	Shear and Flexural	119 × 380 × 10	285
	Top	x	1600	Shear and Flexural	81 × 381 × 10	155
		y	1600	Shear and Flexural	81 × 380 × 10	186
15 – 6 × 6 – EBF	First	x	1500	Shear and Flexural	115 × 320 × 13	243
		y	1500	Shear and Flexural	115 × 320 × 13	243
	Top	x	1500	Shear and Flexural	78 × 332 × 10	169
		y	1500	Shear and Flexural	94 × 321 × 10	174
15 – 8 × 8 – EBF	First	x	1600	Shear and Flexural	117 × 382 × 10	390
		y	1600	Shear Yielding	127 × 429 × 10	403
	Top	x	1600	Shear and Flexural	81 × 380 × 10	186
		y	1600	Shear and Flexural	80 × 382 × 10	212

Table 4-19. Stiffeners for the EBF buildings. "Lacustre-300" zone (new microzonation)

Building	Level	Direction	Length e (mm)	Failure mode	$b \times h \times t$ (mm)	Separation s (mm)
5 – 6 × 6 – EBF	First	x	1500	Shear and Flexural	77 × 291 × 10	114
		y	1500	Shear and Flexural	77 × 291 × 10	114
	Top	x	1500	Flexural Yielding	45 × 292 × 10	248
		y	1500	Flexural Yielding	45 × 292 × 10	248
5 – 8 × 8 – EBF	First	x	1600	Flexural Yielding	63 × 382 × 10	282
		y	1600	Shear and Flexural	81 × 381 × 10	155
	Top	x	1600	Flexural Yielding	58 × 331 × 10	234
		y	1600	Flexural Yielding	64 × 381 × 10	250
10 – 6 × 6 – EBF	First	x	1500	Shear and Flexural	78 × 332 × 10	169
		y	1500	Shear and Flexural	94 × 321 × 10	174
	Top	x	1500	Flexural Yielding	58 × 331 × 10	234
		y	1500	Flexural Yielding	58 × 331 × 10	234
10 – 8 × 8 – EBF	First	x	1600	Shear and Flexural	80 × 380 × 10	251
		y	1600	Shear and Flexural	120 × 380 × 10	238
	Top	x	1600	Shear and Flexural	81 × 381 × 10	155
		y	1600	Shear and Flexural	81 × 381 × 10	155
15 – 6 × 6 – EBF	First	x	1500	Shear and Flexural	116 × 319 × 11	268
		y	1500	Shear Yielding	117 × 321 × 11	271
	Top	x	1500	Shear and Flexural	78 × 332 × 10	149
		y	1500	Shear and Flexural	78 × 332 × 10	169
15 – 8 × 8 – EBF	First	x	1600	Shear and Flexural	119 × 382 × 13	341
		y	1600	Shear Yielding	127 × 429 × 17	403
	Top	x	1600	Shear and Flexural	81 × 381 × 10	155
		y	1600	Shear and Flexural	80 × 382 × 10	212

Table 4-20. Stiffeners for the EBF buildings. "Lacustre-500" zone (new microzonation)

Building	Level	Direction	Length e (mm)	Failure mode	$b \times h \times t$ (mm)	Separation s (mm)
5 – 6 × 6 – EBF	First	x	1500	Shear and Flexural	77 × 291 × 10	114
		y	1500	Shear and Flexural	77 × 291 × 10	114
	Top	x	1500	Flexural Yielding	45 × 291 × 10	230
		y	1500	Flexural Yielding	45 × 292 × 10	248
5 – 8 × 8 – EBF	First	x	1600	Flexural Yielding	63 × 382 × 10	282
		y	1600	Flexural Yielding	81 × 382 × 10	309
	Top	x	1600	Flexural Yielding	58 × 331 × 10	234
		y	1600	Flexural Yielding	64 × 381 × 10	250
10 – 6 × 6 – EBF	First	x	1500	Shear Yielding	169 × 319 × 39	750
		y	1500	Shear and Flexural	118 × 278 × 10	174
	Top	x	1500	Flexural Yielding	45 × 291 × 10	248
		y	1500	Flexural Yielding	77 × 292 × 10	234
10 – 8 × 8 – EBF	First	x	1600	Shear and Flexural	80 × 382 × 10	212
		y	1600	Shear and Flexural	120 × 380 × 10	238
	Top	x	1600	Flexural Yielding	63 × 382 × 10	282
		y	1600	Shear and Flexural	81 × 381 × 10	155
15 – 6 × 6 – EBF	First	x	1500	Shear and Flexural	117 × 320 × 10	235
		y	1500	Shear and Flexural	116 × 319 × 11	268
	Top	x	1500	Flexural Yielding	79 × 331 × 10	287
		y	1500	Shear and Flexural	78 × 332 × 10	149
15 – 8 × 8 – EBF	First	x	1600	Shear and Flexural	119 × 382 × 13	341
		y	1600	Shear and Flexural	117 × 382 × 15	390
	Top	x	1600	Shear and Flexural	81 × 381 × 10	155
		y	1600	Shear and Flexural	81 × 380 × 10	186

4.4 Structural design of the selected buildings

The structures of the selected buildings are designed according to the Colombian regulations [NSR -98 1998; NSR-10 2010], which basically inspired in the American codes [Carrillo et al. 2013]. In the [NSR-98 1998], the following loading combinations are considered:

$$\begin{array}{cccc} 1.4\,D & 1.2\,D + 1.6\,L + 0.5\,L_r & 1.2\,D + 0.5\,L + 1.6\,L_r & 1.2\,D + 0.5\,L + 0.5\,L_r + 1.3\,W \\ 1.2\,D + 0.5\,L + E & 0.9\,D + 1.3\,W & 0.9\,D + E & \end{array} \quad (4\text{-}1)$$

In the [NSR-10 2010], the following loading combinations are considered:

$$\begin{array}{cccc} 1.4\,D & 1.2\,D + 1.6\,L + 0.5\,L_r & 1.2\,D + L + 1.6\,L_r & 1.2\,D + L + 0.5\,L_r + W \\ 1.2\,D + 0.5\,L + E & 0.9\,D + W & 0.9\,D + E & \end{array} \quad (4\text{-}2)$$

As discussed in section 4.3, the combinations involving wind forces (W) are not included in the analysis. The factor 0.5 of the live load in the combination $1.2\,D + 0.5\,L + E$, arises from the fact that L is lower than 4.8 kN/m^2. The thermal effects have not been considered.

The joists are not significantly affected by the seismic action. They are designed, for gravity loads only (equation (4-2)) jointly with the topping concrete layer as a composite section; i.e. assuming fully restraint of the sliding by the shear studs. The effective width has been determined as indicated by the Colombian codes [NSR-98 1998; NSR-10 2010]. For both the buildings spanning 6 and 8 m, the effective width is equal to the separation between adjoining joists; e.g. 1.50 and 1.60 m, respectively.

The seismic design is based in the simplified method stated in the code; among other common simplifications, it implies assuming the same fundamental period T in both directions (estimated from empirical expressions). Similarly to equation (2-9), the base shear force is given by

$$V = S_a(T)\,W / R \quad (4\text{-}3)$$

In this equation, the spectral ordinate S_A considers the importance (normal, section 4.3) of the buildings and the soil type. W is the weight of the building corresponding to the dead load alone. R is the response reduction factor ("energy dissipation coefficient"), which in the Colombian regulation is given by

NSR-98 1998: $$R = 0.9\,\phi_a\,\phi_p\,R_0 \quad (4\text{-}4)$$

NSR-10 2010: $$R = 0.9\,\phi_a\,\phi_p\,\phi_r\,R_0 \quad (4\text{-}5)$$

R_0 is the basic value of the response reduction factor; for MRF and CBF buildings is $R_0 = 5$ and for EBF buildings is $R_0 = 6$. Factor 0.9 is due to the additional uncertainty generated by the in-situ welded connections. ϕ_a, ϕ_p and ϕ_r are factors accounting for the lack of elevation uniformity, the plan asymmetry and the structural redundancy, respectively; given the satisfactory characteristics of the prototype buildings, in this study it is assumed that $\phi_a = \phi_p = \phi_r = 1$. The former Colombian code [NSR-98 1998] proposes the following modification of the response reduction factor in the short periods range:

$$R_c = 1 + (R - 1)\,(T / T_0) \quad (4\text{-}6)$$

In this expression, T_0 is the left corner period of the plateau (Figure 2-7 and Figure 3-6).

The base shear force V is distributed among all the stories proportional to their masses and their absolute heights, according to [NSR -98 1998; NSR-10 2010]:

$$F_j = \frac{m_j \, h_j^k}{\sum_{i=1}^{n} m_i \, h_i^k} \, V \tag{4-7}$$

In this expression, m_i and h_i are the mass and the height (with respect to the ground) of the i-th story, respectively, and exponent $k = 1$ if $T \leq 0.5$ s and $k = 0.75 + 0.5\ T$ if $T > 0.5$ s. If $T > 0.5$ s, $k > 1$ and, therefore, these values of the exponent k (equation (4-7)) show that, for high rise buildings (with long fundamental periods, then), the distribution of forces in the top levels tend to increase more than in low rise buildings. This a conservative assumption aiming to take into account in a simplified way the contribution of the higher modes.

Table 4-21 through Table 4-30 display the main seismic design parameters for the eighteen representative prototype buildings. As discussed previously (in this subsection), the weights correspond solely to the dead load. The fundamental periods T have been determined from the well-known empirical expressions suggested by both Colombian seismic design codes [NSR-98 1998; NSR-10 2010] (among many other regulations):

$$T_a = C_t \, h^{\alpha} \tag{4-8}$$

In this equation, h is the height of the building (m); noticeably, the heights of the 6 × 6 and 8 × 8 buildings are slightly different (section 4.3). According to the former Colombian code [NSR -98 1998], $\alpha = 0.75$, $C_t = 0.09$ for the MRF, $C_t = 0.05$ for the CBF, and $C_t = 0.08$ for the EBF. According to the current Colombian code [NSR-10 2010], $C_t = 0.072$ for the MRF, $C_t = 0.049$ for the CBF, and $C_t = 0.073$ for the EBF. For both Colombian codes, $\alpha = 0.8$ for the MRF and $\alpha = 0.75$ for the CBF and EBF. The value of exponent k in equation (4-7) is listed in the fourth column. The fundamental periods in both directions (T_x and T_y) have been also obtained from linear elastic modal analyses by using the same structural modeling than in the push-over analyses (chapter 5); since these modal analyses are linear, the obtained fundamental periods refer to initial (undamaged) conditions. The comparison among the values of T_a and T_x and T_y shows no huge differences among them; yet some discrepancies are relevant, the seismic equivalent forces have not been recalculated, for consistency with the common practice. The fundamental periods T_x and T_y listed in Table 4-21 through Table 4-30 show that, except few cases, the initial stiffness in both directions is similar. Comparison among the periods T_x and T_y for MRF, CBF and EBF cases shows that the stiffening generated by the concentric braces is important. The periods of the MRF and EBF buildings show that in most of the cases EBF buildings are stiffer, yet this rule has many exceptions, mainly in 10 and 15-story buildings. The MRF buildings spanning 6 m are stiffer than those spanning 8 m; about CBF and EBF buildings, this trend is clear, given the influence of the braces. The response reduction factor (R) is obtained as indicated previously by equation (4-4) [NSR-10 2010]. Columns seven and eight in Table 4-21 through Table 4-30 show the values of dimensionless spectral ordinates S_a / A_a, where $A_a = 0.15$ g, as discussed previously.

Figure 3-8 shows that, for the Piedemonte B zone (new microzonation [Decreto 523 2010] the constant-acceleration branch of the design spectrum ranges in between $T = 0$ and $T_C = 0.56$ s; therefore, for that zone, only buildings 5 – 6 × 6 – CBF, 5 – 8 × 8 – CBF and 5 – 6 × 6 – EBF lay inside the plateau (Table 4-24). The amplification factors accounting for the microzonation in this zone are $F_a = 1.95$ and $F_v = 1.70$ [NSR-10 2010; Decreto 523 2010].

The important values of S_a / A_a in the last two columns in Table 4-21 through Table 4-30 show that the input acceleration in the bedrock is significantly amplified in the top of the buildings; in the 5-story buildings, this effect is contributed by both the soft soil and the rather stiff building. Last two columns in Table 4-21 through Table 4-30 display the base shear coefficients (see equation (4-3)).

Table 4-21. Design parameters for the prototype buildings. "Piedemonte" zone (former microzonation)

Building	Weight (kN)	T_a (s)	k	T_x (s)	T_y (s)	R	S_a / A_a (x)	S_a / A_a (y)	S_a / R (x)	S_a / R (y)
5 – 6 × 6 – MRF	17285	0.720	1.11	0.761	0.754	4.5	5.000	5.000	0.167	0.167
5 – 8 × 8 – MRF	29429	0.803	1.15	0.818	0.812	4.5	5.000	5.000	0.167	0.167
5 – 6 × 6 – CBF	17285	0.400	1.00	0.388	0.376	4.5	5.000	5.000	0.167	0.167
5 – 8 × 8 – CBF	29429	0.446	1.00	0.390	0.382	4.5	5.000	5.000	0.167	0.167
5 – 6 × 6 – EBF	17285	0.640	1.07	0.706	0.685	5.4	5.000	5.000	0.139	0.139
5 – 8 × 8 – EBF	29429	0.714	1.11	0.706	0.683	5.4	5.000	5.000	0.139	0.139
10 – 6 × 6 – MRF	34496	1.182	1.34	1.008	1.005	4.5	5.000	5.000	0.167	0.167
10 – 8 × 8 – MRF	58760	1.323	1.41	1.157	1.146	4.5	5.000	5.000	0.167	0.167
10 – 6 × 6 – CBF	34496	0.657	1.08	0.552	0.548	4.5	5.000	5.000	0.167	0.167
10 – 8 × 8 – CBF	58760	0.735	1.12	0.615	0.573	4.5	5.000	5.000	0.167	0.167
10 – 6 × 6 – EBF	34496	1.051	1.28	1.172	0.955	5.4	5.000	5.000	0.139	0.139
10 – 8 × 8 – EBF	58760	1.176	1.34	1.040	0.998	5.4	5.000	5.000	0.139	0.139
15 – 6 × 6 – MRF	51707	1.590	1.55	1.388	1.372	4.5	4.320	4.373	0.144	0.146
15 – 8 × 8 – MRF	88091	1.780	1.64	1.560	1.563	4.5	3.847	3.840	0.128	0.128
15 – 6 × 6 – CBF	51707	0.883	1.19	0.780	0.661	4.5	5.000	5.000	0.167	0.167
15 – 8 × 8 – CBF	88091	0.989	1.24	0.897	0.805	4.5	5.000	5.000	0.167	0.167
15 – 6 × 6 – EBF	51707	1.413	1.46	1.172	1.178	5.4	5.000	5.000	0.139	0.139
15 – 8 × 8 – EBF	88091	1.583	1.54	1.257	1.219	5.4	4.773	4.920	0.133	0.137

Table 4-22. Design parameters for the prototype buildings. "Lacustre" zone (former microzonation)

Building	Weight (kN)	T_a (s)	k	T_x (s)	T_y (s)	R	S_a / A_a (x)	S_a / A_a (y)	S_a / R (x)	S_a / R (y)
5 – 6 × 6 – MRF	17285	0.720	1.11	0.820	0.822	4.5	4.167	4.167	0.139	0.139
5 – 8 × 8 – MRF	29429	0.803	1.15	0.888	0.878	4.5	4.167	4.167	0.139	0.139
5 – 6 × 6 – CBF	17285	0.400	1.00	0.487	0.486	4.8	4.100	4.100	0.128	0.128
5 – 8 × 8 – CBF	29429	0.446	1.00	0.473	0.470	4.1	4.033	4.020	0.148	0.147
5 – 6 × 6 – EBF	17285	0.640	1.07	0.823	0.768	5.4	4.167	4.167	0.116	0.116
5 – 8 × 8 – EBF	29429	0.714	1.11	0.817	0.719	5.4	4.167	4.167	0.116	0.116
10 – 6 × 6 – MRF	34496	1.182	1.34	1.098	1.092	4.5	4.167	4.167	0.139	0.139
10 – 8 × 8 – MRF	58760	1.323	1.41	1.182	1.186	4.5	4.167	4.167	0.139	0.139
10 – 6 × 6 – CBF	34496	0.657	1.08	0.624	0.593	4.5	4.167	4.167	0.139	0.139
10 – 8 × 8 – CBF	58760	0.735	1.12	0.673	0.629	4.5	4.167	4.167	0.139	0.139
10 – 6 × 6 – EBF	34496	1.051	1.28	1.080	1.036	5.4	4.167	4.167	0.116	0.116
10 – 8 × 8 – EBF	58760	1.176	1.34	1.132	1.091	5.4	4.167	4.167	0.116	0.116
15 – 6 × 6 – MRF	51707	1.590	1.55	1.321	1.303	4.5	4.167	4.167	0.139	0.139
15 – 8 × 8 – MRF	88091	1.780	1.64	1.428	1.429	4.5	4.167	4.167	0.139	0.139
15 – 6 × 6 – CBF	51707	0.883	1.19	0.851	0.725	4.5	4.167	4.167	0.139	0.139
15 – 8 × 8 – CBF	88091	0.989	1.24	0.947	0.853	4.5	4.167	4.167	0.139	0.139
15 – 6 × 6 – EBF	51707	1.413	1.46	1.172	1.178	5.4	4.167	4.167	0.116	0.116
15 – 8 × 8 – EBF	88091	1.583	1.54	1.257	1.219	5.4	4.167	4.167	0.116	0.116

Table 4-23. Design parameters for the prototype buildings. "Piedemonte A" zone (new microzonation)

Building	Weight (kN)	T_a (s)	k	T_x (s)	T_y (s)	R	S_a / A_a (x)	S_a / A_a (y)	S_a / R (x)	S_a / R (y)
5 – 6 × 6 – MRF	17285	0.627	1.06	0.834	0.830	4.5	3.840	3.853	0.128	0.129
5 – 8 × 8 – MRF	29429	0.726	1.11	0.900	0.902	4.5	3.553	3.547	0.118	0.118
5 – 6 × 6 – CBF	17285	0.362	1.00	0.490	0.489	4.5	4.127	4.127	0.138	0.138
5 – 8 × 8 – CBF	29429	0.421	1.00	0.454	0.455	4.5	4.127	4.127	0.138	0.138
5 – 6 × 6 – EBF	17285	0.523	1.01	0.804	0.744	5.4	3.980	4.127	0.111	0.115
5 – 8 × 8 – EBF	29429	0.621	1.06	0.769	0.709	5.4	4.127	4.127	0.115	0.115
10 – 6 × 6 – MRF	34496	1.215	1.36	1.316	1.313	4.5	2.433	2.440	0.081	0.081
10 – 8 × 8 – MRF	58760	1.211	1.36	1.503	1.494	4.5	2.127	2.140	0.071	0.071
10 – 6 × 6 – CBF	34496	0.635	1.07	0.665	0.641	4.5	4.127	4.127	0.138	0.138
10 – 8 × 8 – CBF	58760	0.717	1.11	0.654	0.616	4.5	4.127	4.127	0.138	0.138
10 – 6 × 6 – EBF	34496	1.001	1.25	1.269	1.201	5.4	2.520	2.667	0.070	0.074
10 – 8 × 8 – EBF	58760	1.173	1.34	1.414	1.218	5.4	2.260	2.667	0.063	0.074
15 – 6 × 6 – MRF	51707	1.525	1.51	1.840	1.832	4.5	1.740	1.740	0.058	0.058
15 – 8 × 8 – MRF	88091	1.726	1.61	2.085	2.103	4.5	1.533	1.520	0.051	0.051
15 – 6 × 6 – CBF	51707	0.816	1.16	0.905	0.834	4.5	3.533	3.840	0.118	0.128
15 – 8 × 8 – CBF	88091	0.972	1.24	1.070	0.954	4.5	2.993	3.353	0.100	0.112
15 – 6 × 6 – EBF	51707	1.287	1.39	1.807	1.684	5.4	1.733	1.900	0.048	0.053
15 – 8 × 8 – EBF	88091	1.424	1.46	1.950	1.697	5.4	1.640	1.887	0.046	0.052

Table 4-24. Design parameters for the prototype buildings. "Piedemonte B" zone (new microzonation)

Building	Weight (kN)	T_a (s)	k	T_x (s)	T_y (s)	R	S_a / A_a (x)	S_a / A_a (y)	S_a / R (x)	S_a / R (y)
5 – 6 × 6 – MRF	17285	0.627	1.06	0.662	0.629	4.5	4.109	4.324	0.137	0.144
5 – 8 × 8 – MRF	29429	0.726	1.11	0.743	0.706	4.5	3.660	3.853	0.122	0.128
5 – 6 × 6 – CBF	17285	0.362	1.00	0.392	0.372	4.5	4.873	4.873	0.162	0.162
5 – 8 × 8 – CBF	29429	0.421	1.00	0.437	0.415	4.5	4.873	4.873	0.162	0.162
5 – 6 × 6 – EBF	17285	0.523	1.01	0.584	0.555	5.4	4.658	4.873	0.129	0.135
5 – 8 × 8 – EBF	29429	0.621	1.06	0.651	0.618	5.4	4.178	4.401	0.116	0.122
10 – 6 × 6 – MRF	34496	1.215	1.36	1.123	1.067	4.5	2.422	2.549	0.081	0.085
10 – 8 × 8 – MRF	58760	1.211	1.36	1.266	1.203	4.5	2.148	2.261	0.072	0.075
10 – 6 × 6 – CBF	34496	0.635	1.07	0.644	0.611	4.5	4.224	4.452	0.141	0.148
10 – 8 × 8 – CBF	58760	0.717	1.11	0.720	0.684	4.5	3.778	3.977	0.126	0.133
10 – 6 × 6 – EBF	34496	1.001	1.25	0.959	0.911	5.4	2.836	2.986	0.079	0.083
10 – 8 × 8 – EBF	58760	1.173	1.34	1.073	1.019	5.4	2.608	2.669	0.072	0.074
15 – 6 × 6 – MRF	51707	1.525	1.51	1.540	1.463	4.5	1.763	1.859	0.059	0.062
15 – 8 × 8 – MRF	88091	1.726	1.61	1.738	1.651	4.5	1.565	1.647	0.052	0.055
15 – 6 × 6 – CBF	51707	0.816	1.16	0.865	0.822	4.5	3.145	3.309	0.105	0.110
15 – 8 × 8 – CBF	88091	0.972	1.24	0.969	0.921	4.5	2.807	2.953	0.094	0.098
15 – 6 × 6 – EBF	51707	1.287	1.39	1.289	1.222	5.4	2.110	2.226	0.059	0.062
15 – 8 × 8 – EBF	88091	1.424	1.46	1.444	1.372	5.4	1.884	1.983	0.052	0.055

Table 4-25. Design parameters for the prototype buildings. "Piedemonte C" zone (new microzonation)

Building	Weight (kN)	T_a (s)	k	T_x (s)	T_y (s)	R	S_a / A_a (x)	S_a / A_a (y)	S_a / R (x)	S_a / R (y)
5 – 6 × 6 – MRF	17285	0.627	1.06	0.834	0.830	4.5	3.260	3.280	0.109	0.109
5 – 8 × 8 – MRF	29429	0.726	1.11	0.956	0.953	4.5	2.847	2.853	0.095	0.095
5 – 6 × 6 – CBF	17285	0.362	1.00	0.441	0.439	4.5	4.500	4.500	0.150	0.150
5 – 8 × 8 – CBF	29429	0.421	1.00	0.465	0.458	4.5	4.500	4.500	0.150	0.150
5 – 6 × 6 – EBF	17285	0.523	1.01	0.783	0.722	5.4	3.473	3.767	0.096	0.105
5 – 8 × 8 – EBF	29429	0.621	1.06	0.817	0.801	5.4	3.326	3.393	0.092	0.094
10 – 6 × 6 – MRF	34496	1.215	1.36	1.417	1.415	4.5	1.920	1.920	0.064	0.064
10 – 8 × 8 – MRF	58760	1.211	1.36	1.633	1.605	4.5	1.667	1.693	0.056	0.56
10 – 6 × 6 – CBF	34496	0.635	1.07	0.644	0.611	4.5	4.227	4.453	0.141	0.148
10 – 8 × 8 – CBF	58760	0.717	1.11	0.720	0.684	4.5	3.780	3.973	0.126	0.132
10 – 6 × 6 – EBF	34496	1.001	1.25	1.380	1.232	5.4	1.913	2.207	0.053	0.061
10 – 8 × 8 – EBF	58760	1.173	1.34	1.424	1.301	5.4	1.913	2.093	0.053	0.058
15 – 6 × 6 – MRF	51707	1.525	1.51	1.978	1.972	4.5	1.373	1.380	0.046	0.046
15 – 8 × 8 – MRF	88091	1.726	1.61	2.281	2.279	4.5	1.193	1.933	0.040	0.064
15 – 6 × 6 – CBF	51707	0.816	1.16	0.865	0.822	4.5	3.147	3.307	0.105	0.110
15 – 8 × 8 – CBF	88091	0.972	1.24	1.112	0.990	4.5	2.447	2.747	0.082	0.092
15 – 6 × 6 – EBF	51707	1.287	1.39	1.897	1.786	5.4	1.433	1.520	0.040	0.042
15 – 8 × 8 – EBF	88091	1.424	1.46	1.954	1.903	5.4	1.393	1.427	0.039	0.040

Table 4-26. Design parameters for the prototype buildings. "Lacustre-50" zone (new microzonation)

Building	Weight (kN)	T_a (s)	k	T_x (s)	T_y (s)	R	S_a / A_a (x)	S_a / A_a (y)	S_a / R (x)	S_a / R (y)
5 – 6 × 6 – MRF	17285	0.627	1.06	0.886	0.890	4.5	3.500	3.500	0.117	0.117
5 – 8 × 8 – MRF	29429	0.726	1.11	0.965	0.971	4.5	3.500	3.500	0.117	0.117
5 – 6 × 6 – CBF	17285	0.362	1.00	0.521	0.521	4.5	3.500	3.500	0.117	0.117
5 – 8 × 8 – CBF	29429	0.421	1.00	0.519	0.511	4.5	3.500	3.500	0.117	0.117
5 – 6 × 6 – EBF	17285	0.523	1.01	0.868	0.787	5.4	3.500	3.500	0.097	0.097
5 – 8 × 8 – EBF	29429	0.621	1.06	0.874	0.777	5.4	3.500	3.500	0.097	0.097
10 – 6 × 6 – MRF	34496	1.215	1.36	1.195	1.190	4.5	3.500	3.500	0.117	0.117
10 – 8 × 8 – MRF	58760	1.211	1.36	1.262	1.297	4.5	3.500	3.500	0.117	0.117
10 – 6 × 6 – CBF	34496	0.635	1.07	0.679	0.644	4.5	3.500	3.500	0.117	0.117
10 – 8 × 8 – CBF	58760	0.717	1.11	0.666	0.618	4.5	3.500	3.500	0.117	0.117
10 – 6 × 6 – EBF	34496	1.001	1.25	1.269	1.166	5.4	3.500	3.500	0.097	0.097
10 – 8 × 8 – EBF	58760	1.173	1.34	1.302	1.147	5.4	3.500	3.500	0.097	0.097
15 – 6 × 6 – MRF	51707	1.525	1.51	1.558	1.545	4.5	2.980	3.000	0.099	0.100
15 – 8 × 8 – MRF	88091	1.726	1.61	1.771	1.780	4.5	2.620	2.607	0.087	0.087
15 – 6 × 6 – CBF	51707	0.816	1.16	0.930	0.844	4.5	3.500	3.500	0.117	0.117
15 – 8 × 8 – CBF	88091	0.972	1.24	1.066	0.969	4.5	3.500	3.500	0.117	0.117
15 – 6 × 6 – EBF	51707	1.287	1.39	1.531	1.520	5.4	3.033	3.053	0.084	0.085
15 – 8 × 8 – EBF	88091	1.424	1.46	1.679	1.518	5.4	2.767	3.053	0.077	0.085

Table 4-27. Design parameters for the prototype buildings. "Lacustre-100" zone (new microzonation)

Building	Weight (kN)	T_a (s)	k	T_x (s)	T_y (s)	R	S_a / A_a (x)	S_a / A_a (y)	S_a / R (x)	S_a / R (y)
5 – 6 × 6 – MRF	17285	0.627	1.06	0.924	0.927	4.5	3.253	3.253	0.108	0.108
5 – 8 × 8 – MRF	29429	0.726	1.11	0.988	1.006	4.5	3.253	3.253	0.108	0.108
5 – 6 × 6 – CBF	17285	0.362	1.00	0.517	0.517	4.5	3.253	3.253	0.108	0.108
5 – 8 × 8 – CBF	29429	0.421	1.00	0.523	0.511	4.5	3.253	3.253	0.108	0.108
5 – 6 × 6 – EBF	17285	0.523	1.01	0.868	0.804	5.4	3.253	3.253	0.090	0.090
5 – 8 × 8 – EBF	29429	0.621	1.06	0.827	0.761	5.4	3.253	3.253	0.090	0.090
10 – 6 × 6 – MRF	34496	1.215	1.36	1.231	1.243	4.5	3.253	3.253	0.108	0.108
10 – 8 × 8 – MRF	58760	1.211	1.36	1.336	1.239	4.5	3.253	3.253	0.108	0.108
10 – 6 × 6 – CBF	34496	0.635	1.07	0.717	0.703	4.5	3.253	3.253	0.108	0.108
10 – 8 × 8 – CBF	58760	0.717	1.11	0.692	0.647	4.5	3.253	3.253	0.108	0.108
10 – 6 × 6 – EBF	34496	1.001	1.25	1.292	1.200	5.4	3.253	3.253	0.090	0.090
10 – 8 × 8 – EBF	58760	1.173	1.34	1.303	1.210	5.4	3.253	3.253	0.090	0.090
15 – 6 × 6 – MRF	51707	1.525	1.51	1.500	1.486	4.5	3.253	3.253	0.108	0.108
15 – 8 × 8 – MRF	88091	1.726	1.61	1.691	1.698	4.5	3.027	3.013	0.101	0.100
15 – 6 × 6 – CBF	51707	0.816	1.16	0.955	0.890	4.5	3.253	3.253	0.108	0.108
15 – 8 × 8 – CBF	88091	0.972	1.24	1.047	0.941	4.5	3.253	3.253	0.108	0.108
15 – 6 × 6 – EBF	51707	1.287	1.39	1.574	1.558	5.4	3.253	3.253	0.090	0.090
15 – 8 × 8 – EBF	88091	1.424	1.46	1.679	1.518	5.4	3.047	3.253	0.085	0.090

Table 4-28. Design parameters for the prototype buildings. "Lacustre-200" zone (new microzonation)

Building	Weight (kN)	T_a (s)	k	T_x (s)	T_y (s)	R	S_a / A_a (x)	S_a / A_a (y)	S_a / R (x)	S_a / R (y)
5 – 6 × 6 – MRF	17285	0.627	1.06	0.958	0.956	4.5	3.000	3.000	0.100	0.100
5 – 8 × 8 – MRF	29429	0.726	1.11	1.043	1.047	4.5	3.000	3.000	0.100	0.100
5 – 6 × 6 – CBF	17285	0.362	1.00	0.514	0.515	4.5	3.000	3.000	0.100	0.100
5 – 8 × 8 – CBF	29429	0.421	1.00	0.605	0.606	4.5	3.000	3.000	0.100	0.100
5 – 6 × 6 – EBF	17285	0.523	1.01	0.935	0.864	5.4	3.000	3.000	0.083	0.083
5 – 8 × 8 – EBF	29429	0.621	1.06	0.873	0.799	5.4	3.000	3.000	0.083	0.083
10 – 6 × 6 – MRF	34496	1.215	1.36	1.287	1.294	4.5	3.000	3.000	0.100	0.100
10 – 8 × 8 – MRF	58760	1.211	1.36	1.377	1.368	4.5	3.000	3.000	0.100	0.100
10 – 6 × 6 – CBF	34496	0.635	1.07	0.732	0.701	4.5	3.000	3.000	0.100	0.100
10 – 8 × 8 – CBF	58760	0.717	1.11	0.723	0.681	4.5	3.000	3.000	0.100	0.100
10 – 6 × 6 – EBF	34496	1.001	1.25	1.313	1.232	5.4	3.000	3.000	0.083	0.083
10 – 8 × 8 – EBF	58760	1.173	1.34	1.303	1.219	5.4	3.000	3.000	0.083	0.083
15 – 6 × 6 – MRF	51707	1.525	1.51	1.560	1.547	4.5	3.000	3.000	0.100	0.100
15 – 8 × 8 – MRF	88091	1.726	1.61	1.691	1.698	4.5	3.000	3.000	0.100	0.100
15 – 6 × 6 – CBF	51707	0.816	1.16	0.974	0.911	4.5	3.000	3.000	0.100	0.100
15 – 8 × 8 – CBF	88091	0.972	1.24	1.039	0.934	4.5	3.000	3.000	0.100	1.100
15 – 6 × 6 – EBF	51707	1.287	1.39	1.615	1.595	5.4	3.000	3.000	0.083	0.083
15 – 8 × 8 – EBF	88091	1.424	1.46	1.747	1.573	5.4	3.000	3.000	0.083	0.083

Table 4-29. Design parameters for the prototype buildings. "Lacustre-300" zone (new microzonation)

Building	Weight (kN)	T_a (s)	k	T_x (s)	T_y (s)	R	S_a / A_a (x)	S_a / A_a (y)	S_a / R (x)	S_a / R (y)
5 – 6 × 6 – MRF	17285	0.627	1.06	1.034	1.026	4.5	2.538	2.538	0.085	0.085
5 – 8 × 8 – MRF	29429	0.726	1.11	1.110	1.106	4.5	2.538	2.538	0.085	0.085
5 – 6 × 6 – CBF	17285	0.362	1.00	0.558	0.558	4.5	2.538	2.538	0.085	0.085
5 – 8 × 8 – CBF	29429	0.421	1.00	0.655	0.657	4.5	2.538	2.538	0.085	0.085
5 – 6 × 6 – EBF	17285	0.523	1.01	0.935	0.915	5.4	2.538	2.538	0.071	0.071
5 – 8 × 8 – EBF	29429	0.621	1.06	0.936	0.832	5.4	2.538	2.538	0.071	0.071
10 – 6 × 6 – MRF	34496	1.215	1.36	1.369	1.361	4.5	2.538	2.538	0.085	0.085
10 – 8 × 8 – MRF	58760	1.211	1.36	1.469	1.438	4.5	2.538	2.538	0.085	0.085
10 – 6 × 6 – CBF	34496	0.635	1.07	0.796	0.769	4.5	2.538	2.538	0.085	0.085
10 – 8 × 8 – CBF	58760	0.717	1.11	0.778	0.733	4.5	2.538	2.538	0.085	0.085
10 – 6 × 6 – EBF	34496	1.001	1.25	1.397	1.274	5.4	2.538	2.538	0.071	0.071
10 – 8 × 8 – EBF	58760	1.173	1.34	1.420	1.320	5.4	2.538	2.538	0.071	0.071
15 – 6 × 6 – MRF	51707	1.525	1.51	1.652	1.640	4.5	2.538	2.538	0.085	0.085
15 – 8 × 8 – MRF	88091	1.726	1.61	1.771	1.780	4.5	2.538	2.607	0.085	0.087
15 – 6 × 6 – CBF	51707	0.816	1.16	1.042	0.985	4.5	2.538	2.538	0.085	0.085
15 – 8 × 8 – CBF	88091	0.972	1.24	1.090	0.978	4.5	2.538	2.538	0.085	0.085
15 – 6 × 6 – EBF	51707	1.287	1.39	1.736	1.642	5.4	2.538	2.538	0.071	0.071
15 – 8 × 8 – EBF	88091	1.424	1.46	1.858	1.634	5.4	2.500	2.538	0.069	0.071

Table 4-30. Design parameters for the prototype buildings. "Lacustre-500" zone (new microzonation)

Building	Weight (kN)	T_a (s)	k	T_x (s)	T_y (s)	R	S_a / A_a (x)	S_a / A_a (y)	S_a / R (x)	S_a / R (y)
5 – 6 × 6 – MRF	17285	0.627	1.06	1.085	1.087	4.5	2.373	2.373	0.079	0.079
5 – 8 × 8 – MRF	29429	0.726	1.11	1.172	1.165	4.5	2.373	2.373	0.079	0.079
5 – 6 × 6 – CBF	17285	0.362	1.00	0.555	0.555	4.5	2.373	2.373	0.079	0.079
5 – 8 × 8 – CBF	29429	0.421	1.00	0.653	0.655	4.5	2.373	2.373	0.079	0.079
5 – 6 × 6 – EBF	17285	0.523	1.01	0.949	0.915	5.4	2.373	2.373	0.066	0.066
5 – 8 × 8 – EBF	29429	0.621	1.06	0.936	0.860	5.4	2.373	2.373	0.066	0.066
10 – 6 × 6 – MRF	34496	1.215	1.36	1.449	1.421	4.5	2.373	2.373	0.079	0.079
10 – 8 × 8 – MRF	58760	1.211	1.36	1.558	1.553	4.5	2.373	2.373	0.079	0.079
10 – 6 × 6 – CBF	34496	0.635	1.07	0.808	0.776	4.5	2.373	2.373	0.079	0.079
10 – 8 × 8 – CBF	58760	0.717	1.11	0.829	0.788	4.5	2.373	2.373	0.079	0.079
10 – 6 × 6 – EBF	34496	1.001	1.25	1.447	1.344	5.4	2.373	2.373	0.066	0.066
10 – 8 × 8 – EBF	58760	1.173	1.34	1.465	1.320	5.4	2.373	2.373	0.066	0.066
15 – 6 × 6 – MRF	51707	1.525	1.51	1.727	1.738	4.5	2.373	2.373	0.079	0.079
15 – 8 × 8 – MRF	88091	1.726	1.61	1.864	1.877	4.5	2.373	2.373	0.079	0.079
15 – 6 × 6 – CBF	51707	0.816	1.16	1.092	1.011	4.5	2.373	2.373	0.079	0.079
15 – 8 × 8 – CBF	88091	0.972	1.24	1.083	0.971	4.5	2.373	2.373	0.079	0.079
15 – 6 × 6 – EBF	51707	1.287	1.39	1.796	1.696	5.4	2.373	2.373	0.066	0.066
15 – 8 × 8 – EBF	88091	1.424	1.46	1.827	1.697	5.4	2.367	2.373	0.066	0.066

As a continuation of the information provided by Table 4-21 through Table 4-30, Figure 4-7 displays the shapes (modal vectors, e.g. eigenvalues) of the fundamental modes of the buildings spanning 8 m (8 × 8 buildings) designed for the "Piedemonte-B" zone (new microzonation [Decreto 523 2010], Figure 3-7 and Table 4-24). These configurations have been obtained from ordinary linear eigenvalue analysis by using the numerical model mentioned earlier in this section and described in more detail in the next section (4.6); this model has been implemented in the software code described later in section 5.2. Each Figure (Figure 4-7.a through Figure 4-7.i) displays two companion modal shapes corresponding to the same building in the x and y directions; solid lines relate to x directions while dashed lines refer to y directions. For comparison purposes, both modal shapes have been normalized as having the same modal amplitude for the top floor.

The plots in Figure 4-7 correspond to regular and expected results, thus confirming the correctness of the structural design and the accuracy and reliability of the modelling. Figure 4-7 shows that all the modal shapes are rather similar, regardless of the number of floors (5/10/15), the direction (x/y) and the structural type (MRF/CBF/EBF); this information is relevant to a better understanding of the modal push-over analyses described in chapter 5. Comparison with the vertical distribution of the design forces given by equation (4-7) confirms that the actual increasing of the forces (and of displacements) in the top levels is less abrupt than as the design code.

In frame-type buildings (e.g. "shear buildings"), the first modal shape is rather close to a fourth of a sinusoidal wave (e.g. similar to the shear deformation of a vertical cantilever under any distribution of pushing horizontal forces). Conversely, in "shear-wall buildings", the first modal shape exhibits an opposite trend, being similar to the bending deformation of a vertical cantilever under any distribution of pushing horizontal forces. In our case, MRF buildings belong clearly to the first category, CBF buildings are closer to a shear behavior and EBF buildings exhibit an intermediate behavior (due to the bending deformations of the link caused by lateral forces, see Figure 2-44, Figure 2-45, Figure 2-46 and subsection 4.3.3). Therefore, as expected, the shape of the CBF buildings is slightly closer to a linear distribution than the one of the MRF and EBF buildings.

The modal vectors for the buildings designed for the other zones provide analogous conclusions than Figure 4-7.

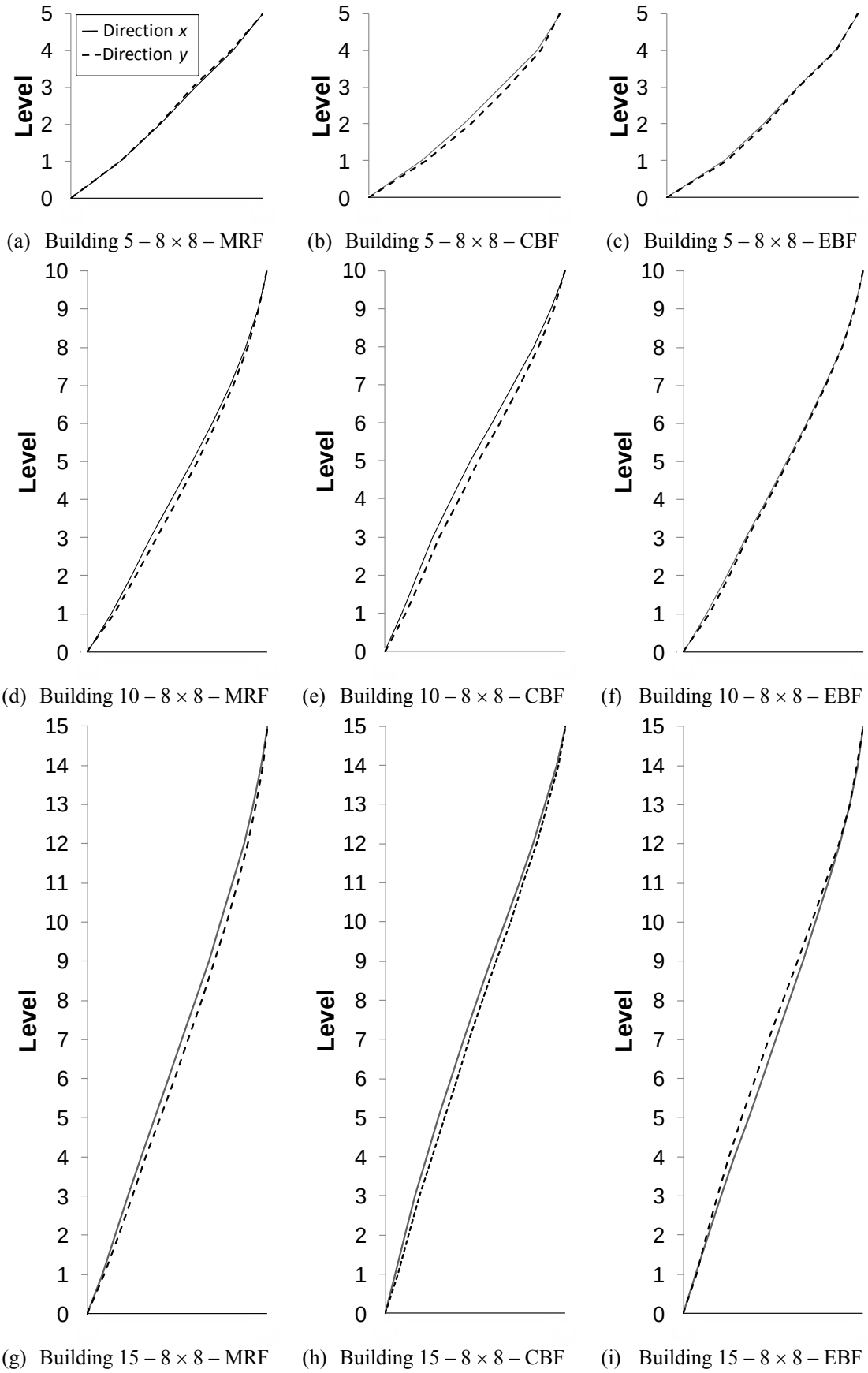

(a) Building 5 – 8 × 8 – MRF (b) Building 5 – 8 × 8 – CBF (c) Building 5 – 8 × 8 – EBF

(d) Building 10 – 8 × 8 – MRF (e) Building 10 – 8 × 8 – CBF (f) Building 10 – 8 × 8 – EBF

(g) Building 15 – 8 × 8 – MRF (h) Building 15 – 8 × 8 – CBF (i) Building 15 – 8 × 8 – EBF

Figure 4-7. Modal vectors of the first translational modes of 8 × 8 buildings. Zone "Piedemonte B" (new microzonation, Figure 3-7)

Table 4-31 to Table 4-40 display the equivalent modal masses (m_i*) normalized with respect to the total mass of the building (m); only translational modes are considered. Figures from Table 4-31 to Table 4-40 provide the following global conclusions regarding the relative importance of the first modes: (i) there are no highly relevant differences between the x and y directions and between the 6 × 6 and 8 × 8 buildings and (ii) the first modal masses of the lower modes are higher for shorter buildings. Results from Table 4-31 to Table 4-40 show that in many cases the modal masses of the first mode are higher than 75% of the mass of the building; in this case, the FEMA 356 Prestandard [FEMA 356 2000] indicates that, in the push-over analyses, the variation of the horizontal pushing forces along the height of the building is proportional to the coefficient given by equation 3-12 of that code. Such coefficient is proportional to the mass of each floor and to the height from the base of the building.

Table 4-31. Modal masses participation factors. "Piedemonte" zone (former microzonation)

Building	x direction					y direction				
	m_1*/m	m_2*/m	m_3*/m	m_4*/m	m_5*/m	m_1*/m	m_2*/m	m_3*/m	m_4*/m	m_5*/m
5 – 6 × 6 – MRF	**0.8499**	0.1105	0.0287	0.0081	0.0025	**0.8491**	0.1129	0.0274	0.0081	0.0024
5 – 8 × 8 – MRF	**0.8459**	0.1141	0.0290	0.0084	0.0025	**0.8461**	0.1164	0.0270	0.0081	0.0024
5 – 6 × 6 – CBF	**0.8597**	0.1033	0.0245	0.0091	0.0035	**0.8689**	0.0993	0.0210	0.0078	0.0030
5 – 8 × 8 – CBF	**0.8616**	0.1037	0.0226	0.0085	0.0035	**0.8743**	0.1040	0.0216	0.0083	0.0029
5 – 6 × 6 – EBF	**0.8778**	0.0945	0.0178	0.0072	0.0027	**0.8814**	0.0949	0.0150	0.0067	0.0021
5 – 8 × 8 – EBF	**0.8697**	0.1002	0.0188	0.0083	0.0030	**0.8767**	01015	0.0158	0.0053	0.0018
10 – 6 × 6 – MRF	**0.8165**	0.1011	0.0416	0.0223	0.0100	**0.8264**	0.0911	0.0429	0.0219	0.0095
10 – 8 × 8 – MRF	**0.8199**	0.1113	0.0330	0.0172	0.0092	**0.8261**	0.1052	0.0328	0.0176	0.0092
10 – 6 × 6 – CBF	**0.7523**	0.1684	0.0325	0.0225	0.0128	**0.7836**	0.1470	0.0375	0.0218	0.0151
10 – 8 × 8 – CBF	**0.7445**	0.1778	0.0425	0.0168	0.0073	**0.7733**	0.1543	0.0393	0.0157	0.0069
10 – 6 × 6 – EBF	**0.7994**	0.1248	0.0379	0.0178	0.0107	**0.7979**	0.1351	0.0360	0.0149	0.0072
10 – 8 × 8 – EBF	**0.7889**	0.1343	0.0375	0.0175	0.0094	**0.8033**	0.1292	0.0351	0.0150	0.0077
15 – 6 × 6 – MRF	**0.7742**	0.1420	0.0405	0.0188	0.0096	**0.7939**	0.1266	0.0389	0.0178	0.0091
15 – 8 × 8 – MRF	**0.7562**	0.1469	0.0461	0.0210	0.0112	**0.7708**	0.1365	0.0447	0.0201	0.0107
15 – 6 × 6 – CBF	**0.6691**	0.2134	0.0623	0.0255	0.0103	**0.7162**	0.1799	0.0533	0.0233	0.0093
15 – 8 × 8 – CBF	**0.7034**	0.1919	0.0514	0.0239	0.0107	**0.7339**	0.1678	0.0479	0.0226	0.0101
15 – 6 × 6 – EBF	**0.7119**	0.1898	0.0480	0.0199	0.0107	**0.7534**	0.1602	0.0440	0.0188	0.0090
15 – 8 × 8 – EBF	**0.7416**	0.1563	0.0441	0.0244	0.0121	**0.7633**	0.1450	0.0432	0.0212	0.0102

Table 4-32. Modal masses participation factors. "Lacustre A" zone (former microzonation)

Building	x direction					y direction				
	m_1*/m	m_2*/m	m_3*/m	m_4*/m	m_5*/m	m_1*/m	m_2*/m	m_3*/m	m_4*/m	m_5*/m
5 – 6 × 6 – MRF	**0.8505**	0.1098	0.0291	0.0081	0.0025	**0.8575**	0.1046	0.0276	0.0078	0.0025
5 – 8 × 8 – MRF	**0.8363**	0.1229	0.0288	0.0093	0.0027	**0.8506**	0.1125	0.0267	0.0079	0.0024
5 – 6 × 6 – CBF	**0.8516**	0.1123	0.0211	0.0110	0.0040	**0.8590**	0.1071	0.0194	0.0106	0.0039
5 – 8 × 8 – CBF	**0.8659**	0.0995	0.0227	0.0083	0.0036	**0.8725**	0.0944	0.0218	0.0078	0.0034
5 – 6 × 6 – EBF	**0.8720**	0.0978	0.0191	0.0082	0.0029	**0.8933**	0.0846	0.0152	0.0050	0.0019
5 – 8 × 8 – EBF	**0.8662**	0.1008	0.0203	0.0093	0.0034	**0.8719**	0.1011	0.0163	0.0082	0.0024
10 – 6 × 6 – MRF	**0.8050**	0.1151	0.0394	0.0216	0.0099	**0.8151**	0.1055	0.0400	0.0214	0.0096
10 – 8 × 8 – MRF	**0.8196**	0.1105	0.0333	0.0174	0.0094	**0.8291**	0.1053	0.0320	0.0164	0.0086
10 – 6 × 6 – CBF	**0.7612**	0.1653	0.0394	0.0161	0.0071	**0.7841**	0.1474	0.0369	0.0150	0.0065
10 – 8 × 8 – CBF	**0.7480**	0.1754	0.0418	0.0166	0.0072	**0.7749**	0.1533	0.0389	0.0157	0.0068
10 – 6 × 6 – EBF	**0.8063**	0.1248	0.0322	0.0168	0.0091	**0.7936**	0.1380	0.0383	0.0140	0.0067
10 – 8 × 8 – EBF	**0.7941**	0.1308	0.0375	0.0162	0.0089	**0.8083**	0.1256	0.0349	0.0142	0.0074
15 – 6 × 6 – MRF	**0.7713**	0.1432	0.0416	0.0188	0.0098	**0.7911**	0.1279	0.0399	0.0178	0.0093
15 – 8 × 8 – MRF	**0.7563**	0.1502	0.0440	0.0209	0.0011	**0.7730**	0.1377	0.0426	0.0199	0.0103
15 – 6 × 6 – CBF	**0.6539**	0.2191	0.0657	0.0256	0.0125	**0.7104**	0.1828	0.0550	0.0233	0.0102
15 – 8 × 8 – CBF	**0.6942**	0.1957	0.0516	0.0252	0.0123	**0.7275**	0.1694	0.0479	0.0239	0.0116
15 – 6 × 6 – EBF	**0.7119**	0.1898	0.0480	0.0199	0.0107	**0.7534**	0.1602	0.0440	0.0188	0.0090
15 – 8 × 8 – EBF	**0.7416**	0.1563	0.0441	0.0244	0.0121	**0.7633**	0.1450	0.0432	0.0212	0.0102

Table 4-33. Modal masses participation factors. "Piedemonte A" zone (new microzonation)

Building	*x* direction					*y* direction				
	m_1^*/m	m_2^*/m	m_3^*/m	m_4^*/m	m_5^*/m	m_1^*/m	m_2^*/m	m_3^*/m	m_4^*/m	m_5^*/m
5 – 6 × 6 – MRF	**0.8570**	0.1040	0.0286	0.0078	0.0026	**0.8503**	0.1105	0.0285	0.0083	0.0024
5 – 8 × 8 – MRF	**0.8549**	0.1084	0.0274	0.0071	0.0022	**0.8435**	0.1180	0.0281	0.0081	0.0023
5 – 6 × 6 – CBF	**0.8622**	0.1010	0.0229	0.0092	0.0047	**0.8703**	0.0958	0.0213	0.0083	0.0044
5 – 8 × 8 – CBF	**0.8635**	0.1015	0.0224	0.0101	0.0045	**0.8760**	0.0902	0.0226	0.0076	0.0035
5 – 6 × 6 – EBF	**0.8687**	0.1020	0.0184	0.0083	0.0027	**0.8833**	0.0890	0.0151	0.0056	0.0019
5 – 8 × 8 – EBF	**0.8762**	0.0953	0.0184	0.0074	0.0028	**0.8825**	0.0926	0.0167	0.0060	0.0022
10 – 6 × 6 – MRF	**0.8133**	0.1044	0.0414	0.0211	0.0104	**0.8164**	0.1005	0.0419	0.0215	0.0104
10 – 8 × 8 – MRF	**0.8251**	0.1103	0.0336	0.0152	0.0077	**0.8314**	0.1069	0.0321	0.0146	0.0074
10 – 6 × 6 – CBF	**0.7709**	0.1504	0.0414	0.0161	0.0082	**0.7886**	0.1372	0.0395	0.0151	0.0076
10 – 8 × 8 – CBF	**0.7550**	0.1680	0.0412	0.0167	0.0075	**0.7802**	0.1476	0.0384	0.0158	0.0070
10 – 6 × 6 – EBF	**0.8109**	0.1201	0.0350	0.0155	0.0083	**0.8311**	0.1145	0.0284	0.0131	0.0061
10 – 8 × 8 – EBF	**0.8098**	0.1199	0.0360	0.0155	0.0081	**0.8184**	0.1238	0.0323	0.0128	0.0057
15 – 6 × 6 – MRF	**0.7703**	0.1419	0.0418	0.0199	0.0100	**0.7876**	0.1290	0.0403	0.0189	0.0095
15 – 8 × 8 – MRF	**0.7884**	0.1274	0.0393	0.0184	0.0100	**0.8011**	0.1182	0.0383	0.0177	0.0095
15 – 6 × 6 – CBF	**0.7029**	0.1826	0.0522	0.0246	0.0133	**0.7280**	0.1640	0.0493	0.0233	0.0126
15 – 8 × 8 – CBF	**0.7237**	0.1674	0.0474	0.0246	0.0126	**0.7446**	0.1523	0.0453	0.0236	0.0118
15 – 6 × 6 – EBF	**0.7693**	0.1397	0.0414	0.0206	0.0101	**0.7795**	0.1383	0.0406	0.0183	0.0089
15 – 8 × 8 – EBF	**0.7747**	0.1319	0.0407	0.0213	0.0111	**0.7779**	0.1351	0.0448	0.0172	0.0097

Table 4-34. Modal masses participation factors. "Piedemonte B" zone (new microzonation)

Building	*x* direction					*y* direction				
	m_1^*/m	m_2^*/m	m_3^*/m	m_4^*/m	m_5^*/m	m_1^*/m	m_2^*/m	m_3^*/m	m_4^*/m	m_5^*/m
5 – 6 × 6 – MRF	**0.8570**	0.1040	0.0286	0.0078	0.0026	**0.8503**	0.1105	0.0285	0.0083	0.0024
5 – 8 × 8 – MRF	**0.8637**	0.1019	0.0307	0.0059	0.0019	**0.8812**	0.0897	0.0276	0.0076	0.0017
5 – 6 × 6 – CBF	**0.7664**	0.1117	0.0426	0.0211	0.0124	**0.7152**	0.1038	0.0424	0.0204	0.0112
5 – 8 × 8 – CBF	**0.7254**	0.1245	0.0503	0.0246	0.0115	**0.7343**	0.1124	0.0325	0.0223	0.0113
5 – 6 × 6 – EBF	**0.8723**	0.0984	0.0189	0.0077	0.0027	**0.8804**	0.0950	0.0157	0.0068	0.0021
5 – 8 × 8 – EBF	**0.8762**	0.0953	0.0184	0.0074	0.0028	**0.8867**	0.0905	0.0158	0.0053	0.0018
10 – 6 × 6 – MRF	**0.8042**	0.1117	0.0426	0.0021	0.0011	**0.8156**	0.1038	0.0424	0.0020	0.0010
10 – 8 × 8 – MRF	**0.8201**	0.1245	0.0503	0.0020	0.0007	**0.8347**	0.1124	0.0325	0.0016	0.0012
10 – 6 × 6 – CBF	**0.7723**	0.1684	0.0325	0.0225	0.0128	**0.7857**	0.1107	0.0540	0.0218	0.0122
10 – 8 × 8 – CBF	**0.7842**	0.1722	0.0364	0.0203	0.0118	**0.7962**	0.1134	0.0410	0.0254	0.0124
10 – 6 × 6 – EBF	**0.8132**	0.1224	0.0326	0.0153	0.0075	**0.8295**	0.1157	0.0315	0.0118	0.0054
10 – 8 × 8 – EBF	**0.8117**	0.1192	0.0354	0.0154	0.0080	**0.8199**	0.1229	0.0321	0.0126	0.0056
15 – 6 × 6 – MRF	**0.7625**	0.1283	0.0357	0.0022	0.0009	**0.7746**	0.1203	0.0540	0.0024	0.0007
15 – 8 × 8 – MRF	**0.7753**	0.1321	0.0420	0.0019	0.0011	**0.7881**	0.1229	0.0410	0.0018	0.0011
15 – 6 × 6 – CBF	**0.7373**	0.1626	0.0455	0.0217	0.0133	**0.7767**	0.1183	0.0513	0.0190	0.0127
15 – 8 × 8 – CBF	**0.7445**	0.1642	0.0459	0.0219	0.0112	**0.7840**	0.1195	0.0518	0.0192	0.0124
15 – 6 × 6 – EBF	**0.7659**	0.1381	0.0475	0.0184	0.0109	**0.7874**	0.1283	0.0436	0.0167	0.0094
15 – 8 × 8 – EBF	**0.7769**	0.1292	0.0421	0.0208	0.0106	**0.7607**	0.1480	0.0456	0.0195	0.0099

Table 4-35. Modal masses participation factors. "Piedemonte C" zone (new microzonation)

Building	*x* direction					*y* direction				
	m_1^*/m	m_2^*/m	m_3^*/m	m_4^*/m	m_5^*/m	m_1^*/m	m_2^*/m	m_3^*/m	m_4^*/m	m_5^*/m
5 – 6 × 6 – MRF	**0.8570**	0.1040	0.0286	0.0078	0.0026	**0.8503**	0.1105	0.0285	0.0083	0.0024
5 – 8 × 8 – MRF	**0.8511**	0.1093	0.0294	0.0078	0.0024	**0.8516**	0.1105	0.0280	0.0076	0.0022
5 – 6 × 6 – CBF	**0.8654**	0.1018	0.0209	0.0080	0.0039	**0.8640**	0.1108	0.0224	0.0074	0.0038
5 – 8 × 8 – CBF	**0.8739**	0.0918	0.0232	0.0076	0.0036	**0.8718**	0.1017	0.0225	0.0072	0.0034
5 – 6 × 6 – EBF	**0.8736**	0.0973	0.0185	0.0078	0.0028	**0.8827**	0.0940	0.0150	0.0064	0.0020
5 – 8 × 8 – EBF	**0.8762**	0.0953	0.0184	0.0074	0.0028	**0.8867**	0.0905	0.0158	0.0053	0.0018
10 – 6 × 6 – MRF	**0.8042**	0.1117	0.0426	0.0211	0.0107	**0.8156**	0.1038	0.0424	0.0199	0.0097
10 – 8 × 8 – MRF	**0.8155**	0.1174	0.0358	0.0152	0.0079	**0.8325**	0.1061	0.0321	0.0144	0.0073
10 – 6 × 6 – CBF	**0.7723**	0.1684	0.0325	0.0225	0.0128	**0.7857**	0.1107	0.0540	0.0218	0.0122
10 – 8 × 8 – CBF	**0.7842**	0.1722	0.0364	0.0203	0.0118	**0.7962**	0.1134	0.0410	0.0254	0.0124
10 – 6 × 6 – EBF	**0.8141**	0.1219	0.0321	0.0150	0.0074	**0.8248**	0.1173	0.0320	0.0124	0.0062
10 – 8 × 8 – EBF	**0.8117**	0.1192	0.0354	0.0154	0.0080	**0.8199**	0.1229	0.0321	0.0126	0.0056
15 – 6 × 6 – MRF	**0.7650**	0.1452	0.0429	0.0206	0.0101	**0.7815**	0.1333	0.0414	0.0195	0.0096
15 – 8 × 8 – MRF	**0.7893**	0.1260	0.0398	0.0187	0.0100	**0.8061**	0.1161	0.0374	0.0172	0.0091
15 – 6 × 6 – CBF	**0.7373**	0.1626	0.0455	0.0217	0.0133	**0.7767**	0.1183	0.0513	0.0190	0.0127
15 – 8 × 8 – CBF	**0.7264**	0.1632	0.0473	0.0246	0.0129	**0.7860**	0.1496	0.0453	0.0238	0.0120
15 – 6 × 6 – EBF	**0.7811**	0.1370	0.0371	0.0164	0.0099	**0.7895**	0.1297	0.0410	0.0167	0.0090
15 – 8 × 8 – EBF	**0.7769**	0.1292	0.0421	0.0208	0.0106	**0.7607**	0.1480	0.0456	0.0195	0.0099

Table 4-36. Modal masses participation factors. "Lacustre-50" zone (new microzonation)

Building	*x* direction					*y* direction				
	m_1^*/m	m_2^*/m	m_3^*/m	m_4^*/m	m_5^*/m	m_1^*/m	m_2^*/m	m_3^*/m	m_4^*/m	m_5^*/m
5 – 6 × 6 – MRF	**0.8453**	0.1125	0.0301	0.0090	0.0030	**0.8359**	0.1216	0.0296	0.0100	0.0029
5 – 8 × 8 – MRF	**0.8389**	0.1218	0.0284	0.0084	0.0025	**0.8461**	0.1164	0.0271	0.0081	0.0024
5 – 6 × 6 – CBF	**0.8623**	0.1003	0.0232	0.0093	0.0048	**0.8703**	0.0953	0.0215	0.0084	0.0045
5 – 8 × 8 – CBF	**0.8576**	0.1013	0.0263	0.0104	0.0045	**0.8726**	0.0909	0.0241	0.0084	0.0039
5 – 6 × 6 – EBF	**0.8725**	0.0974	0.0193	0.0080	0.0028	**0.8868**	0.0898	0.0154	0.0060	0.0020
5 – 8 × 8 – EBF	**0.8799**	0.0906	0.0193	0.0071	0.0031	**0.8874**	0.0893	0.0160	0.0054	0.0019
10 – 6 × 6 – MRF	**0.8069**	0.1074	0.0433	0.0221	0.0107	**0.8171**	0.1020	0.0412	0.0217	0.0096
10 – 8 × 8 – MRF	**0.8197**	0.1107	0.0336	0.0170	0.0093	**0.8284**	0.1054	0.0324	0.0162	0.0087
10 – 6 × 6 – CBF	**0.7626**	0.1603	0.0420	0.0156	0.0077	**0.7868**	0.1413	0.0393	0.0145	0.0072
10 – 8 × 8 – CBF	**0.7483**	0.1750	0.0418	0.0167	0.0073	**0.7773**	0.1509	0.0387	0.0157	0.0069
10 – 6 × 6 – EBF	**0.8107**	0.1203	0.0350	0.0155	0.0084	**0.8181**	0.1229	0.0312	0.0137	0.0065
10 – 8 × 8 – EBF	**0.8061**	0.1233	0.0366	0.0155	0.0080	**0.8281**	0.1168	0.0310	0.0122	0.0055
15 – 6 × 6 – MRF	**0.7753**	0.1421	0.0408	0.0181	0.0095	**0.7950**	0.1268	0.0391	0.0171	0.0090
15 – 8 × 8 – MRF	**0.7760**	0.1351	0.0416	0.0194	0.0104	**0.7895**	0.1253	0.0405	0.0186	0.0100
15 – 6 × 6 – CBF	**0.6983**	0.1868	0.0531	0.0251	0.0136	**0.7269**	0.1673	0.0494	0.0230	0.0123
15 – 8 × 8 – CBF	**0.7345**	0.1574	0.0457	0.0248	0.0127	**0.7483**	0.1493	0.0443	0.0237	0.0118
15 – 6 × 6 – EBF	**0.7699**	0.1369	0.0445	0.0192	0.0109	**0.7913**	0.1320	0.0382	0.0178	0.0077
15 – 8 × 8 – EBF	**0.7614**	0.1396	0.0444	0.0234	0.0115	**0.7611**	0.1455	0.0477	0.0185	0.0103

Table 4-37. Modal masses participation factors. "Lacustre-100" zone (new microzonation)

Building	*x* direction					*y* direction				
	m_1^*/m	m_2^*/m	m_3^*/m	m_4^*/m	m_5^*/m	m_1^*/m	m_2^*/m	m_3^*/m	m_4^*/m	m_5^*/m
5 – 6 × 6 – MRF	**0.8521**	0.1076	0.0292	0.0083	0.0028	**0.8453**	0.1145	0.0286	0.0089	0.0027
5 – 8 × 8 – MRF	**0.8488**	0.1110	0.0293	0.0083	0.0026	**0.8473**	0.1138	0.0281	0.0084	0.0025
5 – 6 × 6 – CBF	**0.8622**	0.1005	0.0231	0.0094	0.0048	**0.8702**	0.0955	0.0214	0.0085	0.0045
5 – 8 × 8 – CBF	**0.8633**	0.0992	0.0247	0.0091	0.0037	**0.8725**	0.0909	0.0241	0.0085	0.0039
5 – 6 × 6 – EBF	**0.8725**	0.0974	0.0192	0.0080	0.0028	**0.8902**	0.0868	0.0155	0.0055	0.0020
5 – 8 × 8 – EBF	**0.8621**	0.1054	0.0191	0.0101	0.0033	**0.8960**	0.0827	0.0154	0.0042	0.0017
10 – 6 × 6 – MRF	**0.8089**	0.1065	0.0435	0.0217	0.0103	**0.8063**	0.1098	0.0423	0.0222	0.0102
10 – 8 × 8 – MRF	**0.8219**	0.1090	0.0343	0.0165	0.0089	**0.8318**	0.1052	0.0315	0.0153	0.0081
10 – 6 × 6 – CBF	**0.7894**	0.1382	0.0394	0.0151	0.0077	**0.7901**	0.1367	0.0390	0.0149	0.0076
10 – 8 × 8 – CBF	**0.7534**	0.1700	0.0413	0.0166	0.0074	**0.7803**	0.1478	0.0385	0.0157	0.0070
10 – 6 × 6 – EBF	**0.8054**	0.1252	0.0358	0.0154	0.0081	**0.8311**	0.1146	0.0284	0.0130	0.0061
10 – 8 × 8 – EBF	**0.8043**	0.1246	0.0367	0.0155	0.0080	**0.8114**	0.1250	0.0339	0.0140	0.0065
15 – 6 × 6 – MRF	**0.7817**	0.1372	0.0398	0.0180	0.0093	**0.8016**	0.1214	0.0381	0.0171	0.0088
15 – 8 × 8 – MRF	**0.7779**	0.1332	0.0401	0.0193	0.0109	**0.7912**	0.1234	0.0392	0.0186	0.0104
15 – 6 × 6 – CBF	**0.7077**	0.1762	0.0520	0.0249	0.0137	**0.7304**	0.1596	0.0495	0.0237	0.0130
15 – 8 × 8 – CBF	**0.7292**	0.1611	0.0469	0.0250	0.0128	**0.7471**	0.1489	0.0450	0.0238	0.0119
15 – 6 × 6 – EBF	**0.7680**	0.1387	0.0442	0.0193	0.0111	**0.7843**	0.1330	0.0387	0.0190	0.0088
15 – 8 × 8 – EBF	**0.7614**	0.1396	0.0444	0.0234	0.0115	**0.7611**	0.1455	0.0477	0.0185	0.0103

Table 4-38. Modal masses participation factors. "Lacustre-200" zone (new microzonation)

Building	*x* direction					*y* direction				
	m_1^*/m	m_2^*/m	m_3^*/m	m_4^*/m	m_5^*/m	m_1^*/m	m_2^*/m	m_3^*/m	m_4^*/m	m_5^*/m
5 – 6 × 6 – MRF	**0.8191**	0.1330	0.0317	0.0126	0.0037	**0.8160**	0.1381	0.0295	0.0130	0.0035
5 – 8 × 8 – MRF	**0.8456**	0.1123	0.0306	0.0087	0.0028	**0.8444**	0.1172	0.0280	0.0081	0.0023
5 – 6 × 6 – CBF	**0.8622**	0.1006	0.0230	0.0095	0.0048	**0.8701**	0.0956	0.0213	0.0085	0.0045
5 – 8 × 8 – CBF	**0.8636**	0.0937	0.0278	0.0246	0.0100	**0.8689**	0.0906	0.0265	0.0095	0.0046
5 – 6 × 6 – EBF	**0.8797**	0.0903	0.0198	0.0073	0.0029	**0.8999**	0.0784	0.0153	0.0045	0.0020
5 – 8 × 8 – EBF	**0.8481**	0.1166	0.0193	0.0124	0.0036	**0.8919**	0.0856	0.0159	0.0048	0.0018
10 – 6 × 6 – MRF	**0.8087**	0.1081	0.0398	0.0229	0.0107	**0.8148**	0.1066	0.0388	0.0212	0.0097
10 – 8 × 8 – MRF	**0.8262**	0.1080	0.0334	0.0155	0.0083	**0.8317**	0.1036	0.0322	0.0156	0.0082
10 – 6 × 6 – CBF	**0.7702**	0.1517	0.0413	0.0160	0.0081	**0.7911**	0.1357	0.0389	0.0149	0.0075
10 – 8 × 8 – CBF	**0.7588**	0.1648	0.0406	0.0166	0.0075	**0.7835**	0.1445	0.0381	0.0158	0.0071
10 – 6 × 6 – EBF	**0.8117**	0.1205	0.0349	0.0152	0.0081	**0.8248**	0.1173	0.0320	0.0124	0.0062
10 – 8 × 8 – EBF	**0.8043**	0.1246	0.0367	0.0155	0.0080	**0.8183**	0.1239	0.0323	0.0128	0.0057
15 – 6 × 6 – MRF	**0.7754**	0.1417	0.0410	0.0182	0.0095	**0.7950**	0.1265	0.0393	0.0172	0.0089
15 – 8 × 8 – MRF	**0.7779**	0.1332	0.0401	0.0193	0.0109	**0.7912**	0.1234	0.0392	0.0186	0.0104
15 – 6 × 6 – CBF	**0.7054**	0.1816	0.0520	0.0245	0.0132	**0.7266**	0.1665	0.0498	0.0233	0.0124
15 – 8 × 8 – CBF	**0.7300**	0.1603	0.0438	0.0249	0.0128	**0.7478**	0.1483	0.0450	0.0238	0.0120
15 – 6 × 6 – EBF	**0.7651**	0.1424	0.0448	0.0190	0.0107	**0.7911**	0.1366	0.0362	0.0145	0.0085
15 – 8 × 8 – EBF	**0.7692**	0.1364	0.0420	0.0216	0.0111	**0.7608**	0.1415	0.0491	0.0206	0.0108

Table 4-39. Modal masses participation factors. "Lacustre-300" zone (new microzonation)

Building	*x* direction					*y* direction				
	m_1^*/m	m_2^*/m	m_3^*/m	m_4^*/m	m_5^*/m	m_1^*/m	m_2^*/m	m_3^*/m	m_4^*/m	m_5^*/m
5 – 6 × 6 – MRF	**0.8509**	0.1078	0.0297	0.0085	0.0032	**0.8436**	0.1160	0.0291	0.0087	0.0026
5 – 8 × 8 – MRF	**0.8374**	0.1190	0.0314	0.0094	0.0029	**0.8434**	0.1180	0.0280	0.0082	0.0024
5 – 6 × 6 – CBF	**0.8624**	0.0998	0.0233	0.0096	0.0049	**0.8696**	0.0953	0.0217	0.0088	0.0047
5 – 8 × 8 – CBF	**0.8594**	0.0948	0.0297	0.0109	0.0052	**0.8646**	0.0919	0.0282	0.0104	0.0049
5 – 6 × 6 – EBF	**0.8797**	0.0903	0.0198	0.0073	0.0029	**0.8903**	0.0854	0.0163	0.0058	0.0022
5 – 8 × 8 – EBF	**0.8644**	0.1023	0.0201	0.0098	0.0035	**0.8887**	0.0879	0.0161	0.0054	0.0019
10 – 6 × 6 – MRF	**0.8129**	0.1215	0.0352	0.0150	0.0076	**0.8148**	0.1231	0.0347	0.0136	0.0070
10 – 8 × 8 – MRF	**0.8253**	0.1097	0.0330	0.0155	0.0080	**0.8324**	0.1049	0.0317	0.0150	0.0078
10 – 6 × 6 – CBF	**0.7756**	0.1443	0.0398	0.0169	0.0097	**0.7939**	0.1305	0.0378	0.0159	0.0090
10 – 8 × 8 – CBF	**0.7598**	0.1644	0.0404	0.0165	0.0075	**0.7847**	0.1440	0.0378	0.0157	0.0070
10 – 6 × 6 – EBF	**0.8093**	0.1245	0.0342	0.0151	0.0075	**0.8272**	0.1165	0.0312	0.0121	0.0060
10 – 8 × 8 – EBF	**0.8100**	0.1205	0.0357	0.0154	0.0081	**0.8190**	0.1221	0.0332	0.0126	0.0059
15 – 6 × 6 – MRF	**0.7723**	0.1435	0.0411	0.0183	0.0099	**0.7910**	0.1292	0.0395	0.0174	0.0094
15 – 8 × 8 – MRF	**0.7760**	0.1351	0.0416	0.0194	0.0104	**0.7895**	0.1253	0.0405	0.0186	0.0100
15 – 6 × 6 – CBF	**0.7064**	0.1731	0.0554	0.0252	0.0138	**0.7250**	0.1603	0.0536	0.0241	0.0130
15 – 8 × 8 – CBF	**0.7332**	0.1560	0.0464	0.0248	0.0132	**0.7501**	0.1450	0.0446	0.0238	0.0123
15 – 6 × 6 – EBF	**0.7692**	0.1400	0.0404	0.0205	0.0107	**0.7722**	0.1437	0.0412	0.0188	0.0092
15 – 8 × 8 – EBF	**0.7695**	0.1421	0.0388	0.0185	0.0108	**0.7633**	0.1414	0.0451	0.0227	0.0108

Table 4-40. Modal masses participation factors. "Lacustre-500" zone (new microzonation)

Building	*x* direction					*y* direction				
	m_1^*/m	m_2^*/m	m_3^*/m	m_4^*/m	m_5^*/m	m_1^*/m	m_2^*/m	m_3^*/m	m_4^*/m	m_5^*/m
5 – 6 × 6 – MRF	**0.8553**	0.1046	0.0282	0.0088	0.0030	**0.8459**	0.1135	0.0284	0.0093	0.0029
5 – 8 × 8 – MRF	**0.8378**	0.1187	0.0313	0.0093	0.0029	**0.8356**	0.1223	0.0299	0.0094	0.0028
5 – 6 × 6 – CBF	**0.8623**	0.0999	0.0232	0.0097	0.0049	**0.8695**	0.0954	0.0216	0.0088	0.0047
5 – 8 × 8 – CBF	**0.8595**	0.0948	0.0296	0.0110	0.0052	**0.8646**	0.0919	0.0281	0.0104	0.0049
5 – 6 × 6 – EBF	**0.8726**	0.0967	0.0199	0.0080	0.0028	**0.8904**	0.0854	0.0163	0.0057	0.0022
5 – 8 × 8 – EBF	**0.8643**	0.1023	0.0201	0.0098	0.0035	**0.8938**	0.0837	0.0160	0.0047	0.0019
10 – 6 × 6 – MRF	**0.8112**	0.1223	0.0362	0.0151	0.0075	**0.8301**	0.1114	0.0319	0.0064	0.0036
10 – 8 × 8 – MRF	**0.8280**	0.1087	0.0333	0.0147	0.0074	**0.8339**	0.1056	0.0319	0.0140	0.0073
10 – 6 × 6 – CBF	**0.7736**	0.1490	0.0395	0.0162	0.0091	**0.7943**	0.1329	0.0374	0.0152	0.0084
10 – 8 × 8 – CBF	**0.7667**	0.1576	0.0397	0.0165	0.0076	**0.7888**	0.1398	0.0374	0.0157	0.0072
10 – 6 × 6 – EBF	**0.8043**	0.1255	0.0352	0.0159	0.0082	**0.8221**	0.1208	0.0317	0.0122	0.0057
10 – 8 × 8 – EBF	**0.8112**	0.1189	0.0355	0.0156	0.0082	**0.8190**	0.1221	0.0332	0.0126	0.0059
15 – 6 × 6 – MRF	**0.7709**	0.1433	0.0416	0.0187	0.0103	**0.7960**	0.1274	0.0377	0.0166	0.0092
15 – 8 × 8 – MRF	**0.7797**	0.1335	0.0405	0.0191	0.0102	**0.7929**	0.1239	0.0394	0.0183	0.0097
15 – 6 × 6 – CBF	**0.7019**	0.1829	0.0560	0.0245	0.0129	**0.7211**	0.1676	0.0535	0.0236	0.0125
15 – 8 × 8 – CBF	**0.7343**	0.1553	0.0460	0.0247	0.0132	**0.7511**	0.1444	0.0442	0.0237	0.0123
15 – 6 × 6 – EBF	**0.7699**	0.1401	0.0404	0.0204	0.0105	**0.7716**	0.1444	0.0415	0.0188	0.0092
15 – 8 × 8 – EBF	**0.7573**	0.1468	0.0429	0.0205	0.0115	**0.7679**	0.1459	0.0415	0.0186	0.0099

Table 4-41 displays the structural steel weight of the eighteen prototype buildings whose structure has been designed for the aforementioned ten seismic zones (Figure 3-5 and Figure 3-7). This weight comprises the main structural steel members: columns, beams, braces, base and gusset plates, stiffener plates, bolts and welds. Broadly speaking, that weight is proportional to the overall cost of the structure; however, the unit cost of the braced frames might be slightly higher than the one of the MRF due to the influence of the detailing of the connections (next subsection discusses more deeply this issue). Figures from Table 4-41 show that the concentrically braced frames have significantly less lightweight than the moment resisting frames, and that the eccentrically braced frames are significantly lighter than the concentrically braced ones; this last fact may be mainly due to the highest response reduction factor indicated by the design code (Table 4-11).

Table 4-41. Structural steel weight (kN)

Building	NSR-98		NSR-10							
	Pied.	Lac. A	Pied. A	Pied. B	Pied. C	Lac. 50	Lac. 100	Lac. 200	Lac. 300	Lac. 500
5 – 6 × 6 – MRF	2776	2628	2597	2597	2597	2335	2221	2140	1941	1858
5 – 8 × 8 – MRF	5584	5047	5042	4843	4843	4546	4475	4350	4020	3809
5 – 6 × 6 – CBF	4131	3451	2679	2841	2661	2365	2123	1960	1811	1653
5 – 8 × 8 – CBF	5992	4838	5517	6085	6012	5192	5043	5120	4940	4654
5 – 6 × 6 – EBF	1496	1338	1344	1408	1395	1288	1278	1235	1215	1196
5 – 8 × 8 – EBF	2680	2484	2498	2498	2498	2344	2406	2339	2276	2263
10 – 6 × 6 – MRF	8213	7363	5926	5533	5533	6696	6408	6145	5933	5533
10 – 8 × 8 – MRF	16719	16108	11687	10989	10989	14252	13489	13039	12163	11227
10 – 6 × 6 – CBF	7913	6938	7564	7937	7937	6359	6259	5902	5656	5121
10 – 8 × 8 – CBF	16503	14456	14391	13417	13417	12407	11922	11442	10527	10084
10 – 6 × 6 – EBF	4100	3698	3549	3546	3414	3593	3446	3449	3267	3041
10 – 8 × 8 – EBF	7710	7169	6857	6479	6479	7406	6987	6987	6464	6408
15 – 6 × 6 – MRF	14545	15619	9871	9187	9187	12162	12743	12195	11437	9837
15 – 8 × 8 – MRF	29697	34828	19357	17307	17307	24540	26291	26291	24540	22793
15 – 6 × 6 – CBF	16390	14236	16252	14108	14108	14701	15654	13446	12939	10830
15 – 8 × 8 – CBF	37651	33822	33112	26707	28988	35979	32774	29953	28217	26037
15 – 6 × 6 – EBF	10728	9079	6668	6262	6250	7812	7316	6954	6499	6128
15 – 8 × 8 – EBF	15565	13996	12455	11615	11615	14083	14083	13736	14895	12621

4.5 Steel structural cost of the selected buildings

This section presents a study about the cost of the steel construction of the selected prototype buildings. The considered amounts deal only with the steel; e.g. does not include the concrete-related structural operations, such as foundations and slab topping layer, among other issues.

The cost for each building has been obtained by multiplying the cost per unit weight by the steel weight (Table 4-41). The cost per unit weight is calculated as the sum of the price of materials (steel members, bolts, welding wire, etc.), construction equipment, transportation, manpower, and indirect costs. It has been assumed that the cost per unit weight does not depend neither on the seismic zone nor on the span-length. Table 4-42 displays the obtained figures. The prices corresponds to the present date (September 2014) in Bogotá and have been calculated in USD by assuming an exchange ratio 1 USD = 2028.5 COP. Figures from Table 4-42 show that the unit cost is higher for EBF than for CBF, and for CBF than for MRF. This difference is due to the bigger number and difficulty of the connections; in fact, in more developed countries, this difference would be higher, because of the biggest impact of the work force costs. Table 4-42 also shows that the unit cost is, as expected, higher for taller buildings.

Table 4-42. Structural steel cost per unit weight (USD/kg)

Building	NSR-98 / NSR-10
5 – 6 × 6 – MRF / 5 – 8 × 8 – MRF	3.34
5 – 6 × 6 – CBF / 5 – 8 × 8 – CBF	3.38
5 – 6 × 6 – EBF / 5 – 8 × 8 – EBF	3.40
10 – 6 × 6 – MRF / 10 – 8 × 8 – MRF	3.40
10 – 6 × 6 – CBF / 10 – 8 × 8 – CBF	3.45
10 – 6 × 6 – EBF / 10 – 8 × 8 – EBF	3.47
15 – 6 × 6 – MRF / 15 – 8 × 8 – MRF	3.47
15 – 6 × 6 – CBF / 15 – 8 × 8 – CBF	3.52
15 – 6 × 6 – EBF / 15 – 8 × 8 – EBF	3.54

Table 4-43 presents the costs of the steel construction and Table 4-44 presents the cost per unit surface area, i.e. the price for each building divided by its total plan area.

Table 4-43. Structural steel cost (× 1000 USD)

Building	NSR-98		NSR-10							
	Pied.	Lac. A	Pied. A	Pied. B	Pied. C	Lac. 50	Lac. 100	Lac. 200	Lac. 300	Lac. 500
5 – 6 × 6 – MRF	945	895	884	884	884	795	756	728	661	632
5 – 8 × 8 – MRF	1901	1718	1717	1649	1649	1547	1523	1481	1368	1297
5 – 6 × 6 – CBF	1426	1191	925	981	919	816	733	677	625	571
5 – 8 × 8 – CBF	2069	1670	1905	2101	2075	1792	1741	1768	1705	1607
5 – 6 × 6 – EBF	519	464	466	489	484	447	443	428	422	415
5 – 8 × 8 – EBF	930	869	867	867	867	813	835	812	790	785
10 – 6 × 6 – MRF	2852	2556	2058	1921	1921	2325	2225	2134	2060	1921
10 – 8 × 8 – MRF	5805	5593	4058	3815	3815	4948	4683	4527	4223	3898
10 – 6 × 6 – CBF	2786	2443	2664	2795	2795	2239	2204	2078	1992	1803
10 – 8 × 8 – CBF	5811	5090	5067	4725	4725	4369	4198	4029	3707	3551
10 – 6 × 6 – EBF	1451	1309	1256	1255	1208	1272	1219	1221	1156	1076
10 – 8 × 8 – EBF	2728	2537	2427	2293	2293	2621	2473	2473	2288	2268
15 – 6 × 6 – MRF	5151	5531	3496	3254	3254	4307	4513	4319	4050	3484
15 – 8 × 8 – MRF	10517	12334	6855	6129	6129	8691	9311	9311	8691	8072
15 – 6 × 6 – CBF	5887	5113	5837	5067	5067	5280	5622	4829	4647	3890
15 – 8 × 8 – CBF	13523	12148	11893	9592	10412	12923	11771	10758	10135	9352
15 – 6 × 6 – EBF	3872	3277	2407	2260	2256	2820	2641	2510	2346	2212
15 – 8 × 8 – EBF	5618	5052	4496	4193	4193	5083	5083	4958	5377	4556

Table 4-44. Structural steel cost per unit surface area (USD/m^2)

Building	NSR-98		NSR-10							
	Pied.	Lac. A	Pied. A	Pied. B	Pied. C	Lac. 50	Lac. 100	Lac. 200	Lac. 300	Lac. 500
5 – 6 × 6 – MRF	328.10	310.61	306.95	306.95	306.95	275.98	262.51	252.93	229.41	219.60
5 – 8 × 8 – MRF	371.24	335.54	335.21	321.98	321.98	302.23	297.51	289.20	267.26	253.23
5 – 6 × 6 – CBF	495.18	413.67	321.13	340.55	318.97	283.49	254.48	234.94	217.08	198.14
5 – 8 × 8 – CBF	404.02	326.21	371.99	410.29	405.37	350.08	340.03	345.22	333.09	313.80
5 – 6 × 6 – EBF	180.22	161.18	161.91	169.62	168.05	155.16	153.96	148.78	146.37	144.08
5 – 8 × 8 – EBF	181.60	168.32	169.27	169.27	169.27	158.84	163.04	158.50	154.23	153.35
10 – 6 × 6 – MRF	495.06	443.83	357.21	333.52	333.52	403.62	386.26	370.41	357.63	333.52
10 – 8 × 8 – MRF	566.88	546.16	396.26	372.60	372.60	483.23	457.36	442.11	412.40	380.67
10 – 6 × 6 – CBF	483.75	424.14	462.41	485.22	485.22	388.75	382.63	360.81	345.77	313.06
10 – 8 × 8 – CBF	567.50	497.11	494.87	461.38	461.38	426.65	409.97	393.46	362.00	346.76
10 – 6 × 6 – EBF	251.90	227.20	218.04	217.86	209.75	220.75	211.72	211.90	200.72	186.83
10 – 8 × 8 – EBF	266.45	247.75	236.97	223.91	223.91	255.94	241.46	241.46	223.39	221.45
15 – 6 × 6 – MRF	596.19	640.21	404.60	376.57	376.57	498.51	522.32	499.86	468.79	403.21
15 – 8 × 8 – MRF	684.71	803.01	446.30	399.04	399.04	565.80	606.18	606.18	565.80	525.52
15 – 6 × 6 – CBF	681.35	591.80	675.61	586.48	586.48	611.13	650.75	558.96	537.88	450.21
15 – 8 × 8 – CBF	880.42	790.88	774.28	624.51	677.84	841.32	766.37	700.41	659.81	608.84
15 – 6 × 6 – EBF	448.19	379.30	278.58	261.61	261.11	326.37	305.65	290.52	271.52	256.02
15 – 8 × 8 – EBF	365.78	328.91	292.69	272.95	272.95	330.95	330.95	322.80	350.03	296.59

The figures in Table 4-43 and Table 4-44 allow deriving the following general conclusions:

- **Seismic zone**. For the 5- and 10-story buildings, the construction cost in soft soil ("Lacustre") is lower than in stiff soil ("Piedemonte"). The softer the soil, the lower the price. This trend can be explained by the higher spectral amplitudes (Figure 3-6 and Figure 3-8) in the range of periods of interest (see the assumed fundamental periods in Table 4-21 through Table 4-30).
- **Building height**. With few exceptions, for any span-length and structural type (MRF, CBF and EBF), the unit cost grows significantly with the height of the buildings. This effect can be attributed to the higher price of the elevation machinery and operations and, mainly, to the heavier structural members.
- **Span-length**. Except for few cases (under the former microzonation) the unit cost for the 8 × 8 buildings is higher than for the 6 × 6 ones. This fact is mainly generated by the heavier beams and joists.

- **NSR-98/NSR-10**. For "Piedemonte" soil, in most of the cases, the construction cost with the new regulation is lower or slightly lower. For "Lacustre" soil, this trend holds but there are more exceptions. This trend can be explained by the higher spectral amplitudes in the formed code (Figure 3-6) than in the new one (Figure 3-8), in the range of periods of interest (Table 4-21 through Table 4-30).
- **Structural type**. In all the cases, the cost for EBF is significantly lower than for the other solutions; the price for EBF is about half the one for CBF. In general, the MRF option is cheaper than the CBF one. Noticeably, the differences are much higher than those in Table 4-42 are; therefore, they are not mainly generated by the bigger number and difficulty of the connections. The considerations issued after Table 4-41 apply here.

4.6 Numerical modeling of the selected buildings

4.6.1 Overall approach

For the push-over analyses, the structural behavior of the selected buildings is described with 2-D finite element models; the non-structural elements and the non-seismic members (joists, and also beams and columns of the non-seismic frames) are not modelled. Each model is a 2-D steel frame including all the columns that belong to the same plane; Figure 4-3 shows that there are four frames in *x* direction and two frames in *y* direction. These structures are discretized with 2-node Euler-Bernouilli frame elements. The shear deformation is taken into account with a simplified formulation that consists basically in obtaining the average shear strain at each section. Each frame element is assumed to span between the intersection points among the axes of the main structural members (beams, columns and braces); the stiffening effect of the panel zones (see Figure 2-40, Figure 2-41, and Figure 4-1) and of the gusset plates (see Figure 4-1.d) has been neglected. The beam-column connections are modelled either as completely rigid (in the seismic frames of the MRF, CBF and EBF buildings) or completely hinged (in the non-seismic frames of the MRF, CBF and EBF buildings). In the CBF and EBF buildings, the connections between the braces and the other members are taken as hinged. The first floor columns are assumed to be clamped to the foundation in the MRF building and hinged to the foundation in the CBF and EBF buildings. These distinctions are coherent both with the usual modelling recommendations [Becker 1995] and the construction practices [Becker, Ishler 1996].

As discussed in the previous paragraph, each push-over analysis is carried out on a single frame; the cooperation of the non-seismic frames is neglected, hence, as shown by Figure 4-3, there are four seismic frames in *x* direction and two in *y* direction. In the *x* direction, the outer and inner frames are considered to be alike, despite the minor differences among them, mainly because the inner frames support higher loads than the outer ones. Given the absence of shear studs in the seismic frames (section 4.3), the joint behavior of the steel beams and the topping concrete layers cannot be assumed. Since the stiffness of the top concrete is significantly smaller than the one of the steel beam, the cooperation of the concrete layer is neglected.

Next three paragraphs describe approximately the modelling of the nonlinear behavior for MRF, CBF and EBF buildings, respectively.

- **MRF buildings**. In the MRF buildings, the behavior of beams and columns is considered mostly linear, while the nonlinearities are concentrated in plastic hinges located inside them, near the beam-column connections [FEMA 356 2000]. Since the connections are pre-qualified [FEMA 350 2000], it can be assumed that the plastic hinges form earlier in beams and columns than in the connections themselves; therefore, the behavior of the panel zones is linear. The behavior of the plastic hinges is described by moment- rotation laws [FEMA 356 2000], without accounting for the influence of the shear forces. In the beams, the effect of the axial force in the behavior of the plastic hinges is neglected while in columns the reduction of the resistant moment due to the axial force is considered; that effect is analyzed according to the prescriptions of [AISC 2010; AISC 360-10 2010] (see Figure 2-32.b).

- **CBF buildings**. In the CBF buildings [FEMA 356 2000; Tapia, Tena 2008; Mahmoudi, Zaree 2011], the behavior of beams and columns is considered linear, while the nonlinearities are concentrated in the braces. In the tensioned braces, the nonlinear behavior is described by axial force-axial elongation laws. In the compressed braces, the nonlinear behavior is also described by axial force-axial elongation laws; given the relevant buckling effects, this behavior is less ductile than the one for the tensioned braces.
- **EBF buildings**. In the EBF buildings, the behavior of braces and columns is considered linear while the nonlinearities are concentrated in plastic hinges located in the link segments of the beams (Figure 2-44). The behavior of these plastic hinges is described by moment- rotation laws [FEMA 356 2000], accounting for the influence of the shear forces; that effect is analyzed according to the prescriptions of [AISC 2010; AISC 360-10 2010] (see Figure 2-31.b).

Figure 4-8 describes the aforementioned failure mechanisms for MRF, CBF and EBF.

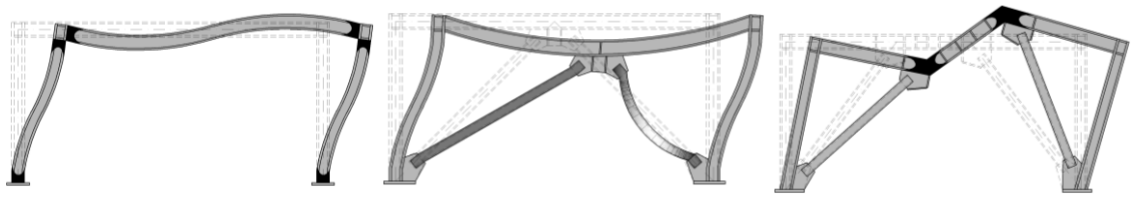

(a) MRF (b) CBF (c) EBF

Figure 4-8. Failure mechanisms for the considered building types

The hysteretic behavior of the plastic hinges is described by multi-linear moment-curvature laws, as the one displayed by Figure 4-9. The moment-curvature laws are derived from the structural parameters of the steel and the geometrical parameters of the members and of the connections, by following the recommendations of [FEMA 356 2000]. In Figure 4-9, Q accounts for any lateral force causing the moment in the joint and Q_y is the yielding value of Q; θ and Δ are deformation quantities (rotation angle and displacement, respectively).

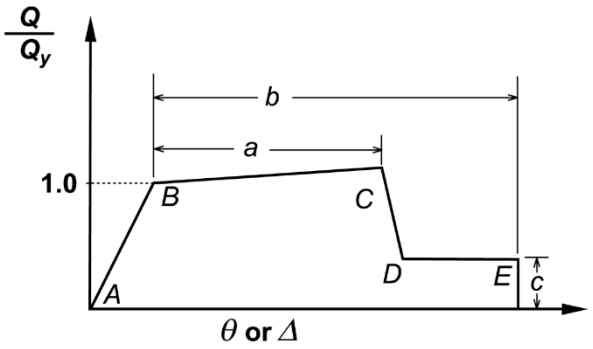

Figure 4-9. Model of the moment-rotation law of a plastic hinge [FEMA 356 2000]

The laws displayed in Figure 4-9 can be also used to represent the nonlinear axial behavior of the braces of the CBF buildings, see Figure 4-8.b.

Once two full hinges have developed at both ends of a column (i.e. points E in Figure 4-9 are reached), that element is considered as a truss member; once the buckling load [AISC 2010; AISC 360-10 2010] is reached, the axial stiffness of the column is ignored. In other words, this member is "inactive", i.e. it has disappeared form the structure. This applies for MRF, CBF and EBF buildings. This type of behaviour also applies for braces of CBF and EBF buildings.

4.6.2 Modelling of the MRF buildings

Following the global approach defined in Figure 4-9, the flexural plastic hinges are modelled as described in Figure 4-10.

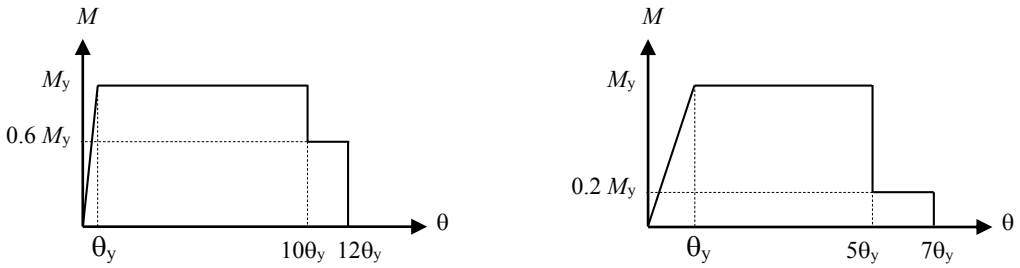

(a) Compact sections (b) Non compact sections

Figure 4-10. Moment-rotation law of a plastic hinge

Comparison between Figure 4-9 and Figure 4-10.a shows that $a = 9$, $b = 11$ and $c = 0.6$; for Figure 4-10.b such values are $a = 4$, $b = 6$ and $c = 0.6$. Figure 4-10.a and Figure 4-10.b depict the behavior for compact and non-compact sections, respectively. For beams, the bounds between both types of sections are:

compact sections: $$\frac{b_f}{2t_f} \leq \frac{52}{\sqrt{F_{ye}}} \quad \text{and} \quad \frac{h}{t_w} \leq \frac{418}{\sqrt{F_{ye}}} \tag{4-9}$$

non-compact sections: $$\frac{b_f}{2t_f} \leq \frac{65}{\sqrt{F_{ye}}} \quad \text{and} \quad \frac{h}{t_w} \leq \frac{640}{\sqrt{F_{ye}}} \tag{4-10}$$

In these equations, b_f is the flange width, t_f is the flange thickness, t_w is the web thickness, h is the section height and F_{ye} is the expected steel strength. $F_{ye} = F_y R_y$; where F_y is the steel yielding point and R_y is an increasing factor linking the lower value of the steel strength to the expected value. For intermediate situations, linear interpolation for the values of the flange and web parameters can be performed; the lowest resulting value shall be used.

For columns, if the demanding axial force does not exceed 20% of the critical value, the bounds between both types of sections are:

compact sections: $$\frac{b_f}{2t_f} \leq \frac{52}{\sqrt{F_{ye}}} \quad \text{and} \quad \frac{h}{t_w} \leq \frac{300}{\sqrt{F_{ye}}} \tag{4-11}$$

non-compact sections: $$\frac{b_f}{2t_f} \leq \frac{65}{\sqrt{F_{ye}}} \quad \text{and} \quad \frac{h}{t_w} \leq \frac{460}{\sqrt{F_{ye}}} \tag{4-12}$$

For columns, if the demanding axial force exceeds 20% of the critical value, the bounds between both types of sections are:

compact sections: $$\frac{b_f}{2t_f} \leq \frac{52}{\sqrt{F_{ye}}} \quad \text{and} \quad \frac{h}{t_w} \leq \frac{260}{\sqrt{F_{ye}}} \tag{4-13}$$

non-compact sections: $$\frac{b_f}{2t_f} \leq \frac{65}{\sqrt{F_{ye}}} \quad \text{and} \quad \frac{h}{t_w} \leq \frac{400}{\sqrt{F_{ye}}} \tag{4-14}$$

Verification of conditions (4-9) through (4-14) in Table 4-1 to Table 4-10 show that most of the sections are compact except for some columns in the top stories. Commonly, those members

remain mainly elastic during the push-over analysis.

4.6.3 Modelling of the CBF buildings

The model displayed in Figure 4-9 is also used to represent the axial failure of the braces of the CBF buildings. For tensioned braces, the values of parameters a, b and c are selected as indicated by [FEMA 356 2000] for "Braces in Tension": $a = 11\Delta_T$, $b = 14\Delta_T$ and $c = 0.8$. Δ_T is the axial deformation as the expected tensile yielding load. For compressed braces, parameters a, b and c depend also on the ratio between the width of the section and its thickness. If that ratio is smaller than $90/\sqrt{F_y}$, then $a = 0.5\Delta_C$, $b = 7\Delta_C$ and $c = 0.4$. If that ratio is greater than $190/\sqrt{F_y}$, then $a = 0.5\Delta_C$, $b = 3\Delta_C$ and $c = 0.2$. If that ratio lies between both bounds, then a, b and c can be obtained by linear interpolation. Δ_C is the axial deformation as the expected buckling load.

4.6.4 Modelling of the EBF buildings

The model displayed in Figure 4-9 is also used to represent the bending failure of the link of the EBF buildings. The values of parameters a, b and c are selected as indicated by [FEMA 356 2000] depending on the length of the link. If that length is smaller than $1.6\ M_{CE}/V_{CE}$, then $a = 0.15$, $b = 0.17$ and $c = 0.8$. If that length is greater than $2.6\ M_{CE}/V_{CE}$, then a, b and c can be taken as in the beams (subsection 4.6.2). If that ratio lies between both bounds, then a, b and c can be obtained by linear interpolation. M_{CE} and V_{CE} are the resistant bending moment and shear force, respectively.